Paleoecological and geochemical studies on sponge/microencruster -bearing communities contained in selected Cipit Boulders from the St. Cassian Formation (Lower Carnian, Upper Triassic) of the Dolomites, Northeastern Italy

Dissertation

zur Erlangung des Doktorgrades

der Mathemathisch-Naturwissenschaftlichen Fakultäten

der Georg-August-Universität-Göttingen

vorgelegt von

Juan Francisco Sánchez Beristain

aus Mexiko-Stadt, Mexiko

Göttingen 2010

D 7

Referent: Prof. Dr. Joachim Reitner

Korreferent: Prof. Dr. Volker Thiel

Tag der mündlichen Prüfung: 29.11.2010

Abstract

The Lower Carnian St. Cassian Formation (Dolomites, NE Italy) is well known for its very diverse and exceptionally well-preserved fauna. It dates from Middle to Late Triassic and comprises basin sediments deposited between carbonate buildups and local back reef areas. The degree of preservation is highest in the well-known "Cipit Boulders". These calcareous masses are mostly limestones derived from the Cassian carbonate platforms, which during emersion and karstification underwent complete lithification and extensive solution, and subsequently slid from the platform margins into the Cassian basin. They have been subject of diagenetic, paleogeographic, taxonomic, and most lately, geochemical studies. However, most works dealing with them focus on the taxonomy of reefal fauna. This unfortunately also applies to most publications concerning Triassic reef and reef-like environments.

Recent studies have shown that biofacies can differ considerably between different boulders. The outstanding preservation state of selected boulders allows taxonomical determination of most of their biomorpha. 112 thin sections from Cipit Boulders from the localities of Seelandalpe and Misurina were selected out of ca. 400 for microfacies and statistical analysis. Six species of microencrusters were found (*Koskinobullina socialis, Girvanella* sp., *Tubiphytes* cf. *obscurus, Terebella lapilloides, Reptonoditrypa cautica,* and *Baccanella floriformis*). These species represent an effective tool for paleoenvironmental intepretation due to their size and paleoecology.

In this study, I compiled a data matrix with all microfacies information from each thin section. Fourteen different phena were obtained through Cluster analysis in R-Mode using four algorithms and two indices. Each one of these phena is interpreted as a fossil association. Concurrently, three microencruster-pairs were determined in R-Mode cluster analysis as well. These pairs possess a high Jaccard Index value, thus supporting a strong ecological relationship.

Subsequently, Q-Mode Cluster analysis was performed with the microencruster data plus hexactinellid presence-absence in each one of the fourteen associations. Five communities were thus obtained. Each one of them can be assigned to a determined biotope.

Subsequently, selected element analyses were performed on well-preserved microbialite samples. All of them show a sign of siliciclastic input which hinders the possibility of finding a reliable Rare Earth Element + Yttrium (REY) pattern. Microbialites have high-Mg calcite mineralogy and are enriched in a variety of trace elements. Most of them are not in any way related to biological activity, albeit some of them provide important information on some vital effect.

This study reports geochemical profiles (Sr-Ca, stable C and O isotopes) from four samples, three coralline sponge skeletons and one stromatolite. All of them show variations in their $\delta^{13}C$ and $\delta^{18}O$

values. Carbon isotope values can be a consequence of of various environmental and biological effects, such as volcanic activity, sulphate reduction, and vital fractionation towards the uppermost growing zone, whereas oxygen isotopes provide information on variable temperature conditions and provide further evidence of a lack of diagenetical imprint.

Biogeochemical analyses have not shown any satisfactory result indicating presence of sponge biomarkers. Only relicts of bacterial activity can be seen.

Table of contents

Table of contents

Table of contents

Publications

Acknowledgements

Curriculum vitae

1. Introduction

The Dolomites are a region in Northeastern Italy which is bounded by Val Pusteria (from Pusteria River to St. Candid) to the N; by Valsugana (from Trento to Primolano) and Val Belluna (from Arsié to Feltre and Ponte) to the S; by Val di Sesto and Val Padola (from St. Candid to M.Croce di Comelico Pass) to the E, and by Valle Isarco and Val d'Adige to the W (Bosellini, 1991; Fig. 1). Gilbert & Churchill (1864) coined the term "Dolomitic Mountains" and since then it has been a valid name for this geologic complex, which is currently better known as "the Dolomites". Particularly the portion of the Dolomites in South Tyrol have been a very important locality for numerous studies, partly due to their imposing landscape, but mainly due to the impressive outcrops which generally allow precise stratigraphic correlations (Rech, 1998).
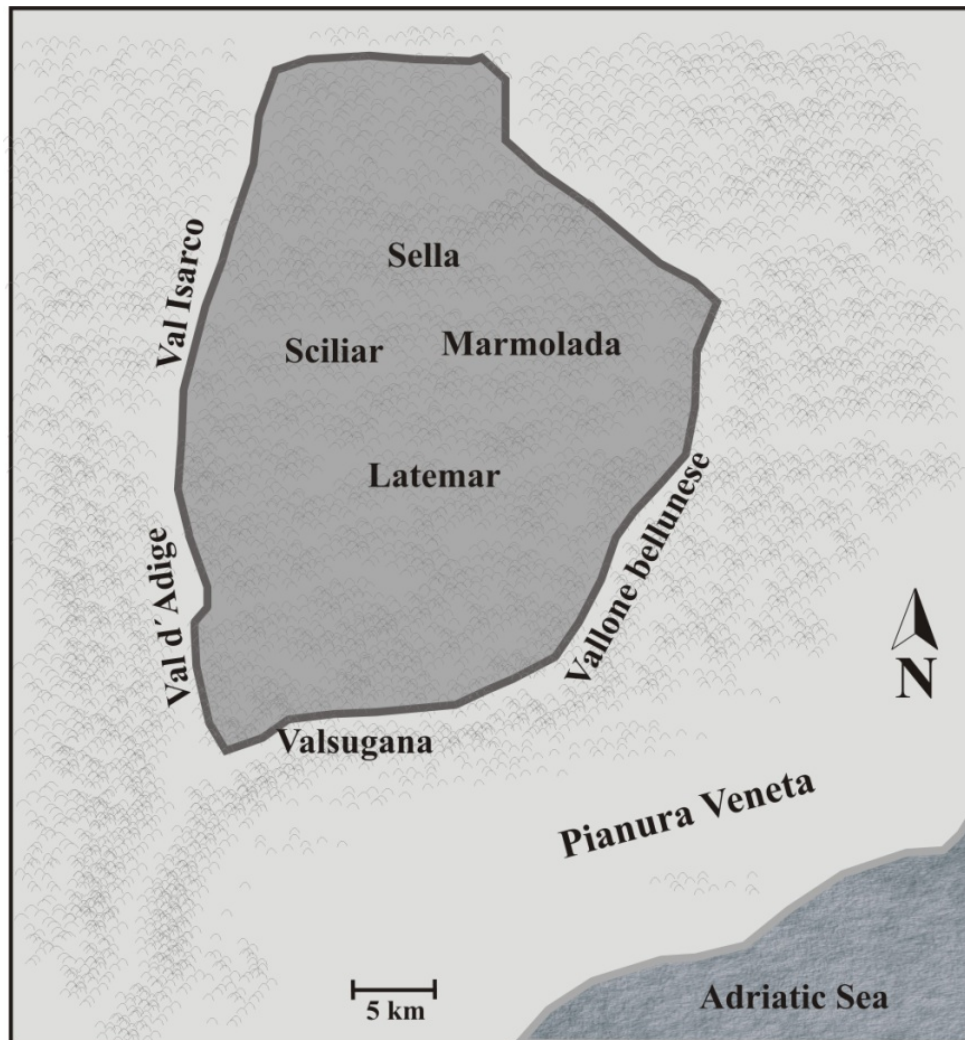
Figure 1: Geographical location of the Dolomites in Northeastern Italy. Modified from Bosellini (1991)

Introduction

1.1. Brief review of the history of research on the geology of the Dolomites, in particular the St. Cassian Formation.

The work of von Buch (1822) constitutes the first publication in the fields of "dolomite" and was seminal to a large amount of research on this topic. His contribution was especially important due to the genetic theories on this kind of mountains. According to him, dolomitic massives in South Tyrol formed as a result of vulcanism by changing the mineral composition of overlying carbonates to dolomite by means of magnesium steam (Magnesiumdämpfe) contained in the underlying volcanic rocks. Von Richthofen (1860) went further in the knowledge of the dolomitization process by rejecting the theory by von Buch due to chemical inconsistence. He also deepened the study of the Dolomites by assuming a biological origin for the Schlern Dolomite. This was, in turn, corroborated shortly afterward by the observations of von Mojsisovics (1879), who in addition introduced the term Heterotopy in order to reflect heterogeneity between synchronous and adjacent facies domains.

The end of the 19th century marks the beginning of continuous geological study in the Dolomites and a deepening of research on the St. Cassian Formation, which was only interrupted in the middle of 20th century. Ogilvie (1893) performed a geological characterization of the Wengen and St. Cassian Formations in seven districts of South Tyrol. She gave an outline to the St. Cassian Formation based on 11 sections from the Seisser Alm in the West to Misurina and the Seeland Alpe in the East, and defined its type section from several profiles obtained between the regions of Stuores Wiesen and Pralongia. Ogilvie-Gordon (1929) later defined the St. Cassian Formation as consisting of two subdivisions (see below for further details). This fact was also observed by Mutschlechner (1933), who studied the geology between the regions of Buchenstein and the town of St. Cassian, and by Pia (1937), who carried out complete tectono-stratigraphic work in the Pragser Dolomites and also pointed out the importance of the abundant fossil remains in the Plätzwiesen near Schluderbach.

A new stage of the research of the St. Cassian Formation started in the beginning of the 1960s. Leonardi (1961) recognized for the first time presence of lagunar facies within an atoll/barrier reef and listed a series of factors that contributed to the development, retrogression, and extinction of coralligenous formations in the Dolomites. Among them, he listed the presence of a sufficiently strong basis favoring the settlement of an embryonary colony, which could not have been located deeper than 90 m. Baccelle (1965) described four St. Cassian lithofacies (limestones and conglomerates) which she interpreted to have been deposited in shallow waters of narrow interrefal basins at the Sella Joch. Later, Leonardi (1967) summarized the main outcrops where the St. Cassian reef sediments can be found.

In an investigation on some carbonate buildups from the region between the Sciliar and Serla Dolomites, Bosellini & Rossi (1974) first provided the idea that some of them may not have been

ecological reefs in origin. According to them, these buildups represent the indented edge of a broad shallow-water carbonate platform which had grown in cyclically repeated subtidal, intertidal and supratidal conditions. This conclusion was shared by Leonardi (1979) concerning the Marmolada and Latemar buildups. His observations were corroborated much more recently by Russo et al. (1997), Keim & Schlager (2001) and Emmerich et al. (2005) who recognized the abundance of micrite produced in place (automicrite) for Punta Grohmann, the Sella Massif, and once again for the Latemar buildup, respectively. Regarding the variability of facies in carbonate buildups in the Dolomites, the most complete analyses ever performed at the St. Cassian Formation can be found in Fürsich & Wendt (1976) and Wendt & Fürsich (1980), where four depositional enviromnents in the St. Cassian Formation were recognized, mostly on the basis of their biofacies: deeper and shallow basinal, slope and shallow water facies. Diversity and complexity of facies can be concluded from these works, and among them, the Cipit boulders have been given special attention. (e.g. Russo et al., 1991; Russo et al., 1997; Rech, 1998; Sánchez Beristain & Reitner, 2008). For more detailed information on early investigations of the St. Cassian Formation, the reader is referred mainly to Leonardi (1967), Wendt & Fürsich (1980), Bosellini (1991), and Rech (1998).

1.2.   Stratigraphical considerations: the St. Cassian Formation.

The strata at present known as St. Cassian Formation have been widely studied and their denomination as Cassian Beds -"Cassianer Schichten"- appear first in Münster & Wissmann (1841), and were first cartographically recognized by Von Hauer (1858). The St. Cassian Formation is well known for its very diverse and exceptionally well preserved fauna. It dates from the Middle to Late Triassic and comprises basin sediments deposited between carbonate buildups and locally back reef areas (Wendt & Fürsich, 1980), and was named after the town of San Cassiano in the province of Bolzano.

Stratigraphically, the Cordevolian and Julian deposits of the Dolomites are represented by huge carbonate platform deposits (Lower and Upper Cassian Dolomite) and by their coeval basinal deposits, the St. Cassian Formation (Russo et al., 1991). Both formations have been widely studied and discussed. While the former apparently started growing at the end of the strong Ladinian volcanic phase and the subsequent erosion of the inherited reliefs (Bosellini, 1984), the St. Cassian Formation deposited on top of the Wengen Formation, a sequence of thick marly, tuffitic sandstone and calcareous strata (Leonardi, 1967). Rech (1998) also found mafic vulcanoclastic sediments in the Wengen section in a region located between Pralongia and Valparola Pass. This lithological unit can be divided in two members: the Lower and the Upper Cassian Formation. The Upper Cassian Formation houses the object of this dissertation, the Cipit Boulders, and has its type section (after Ulrichs, 1974) in Picolbach, near Pralongia, Piz Stuores and Stuores Wiesen. However, Bizzarini and Braga (1978) performed a division into three levels: a lower level comprising a pseudo-flysch facies,

which is superposed on the Wengen Formation, a middle, sandy-tuffaceous level poor in fossils, and an upper level consisting in marls and gray-brown marly limestones, where many fossiliferous beds ("Seelandschichten" sensu Pia, 1937) can be seen. It is also important to take into account that other authors (Stur, 1868; Mojsisovics; 1874) had assigned the marly and tuffitic Wengen Strata to the St. Cassian Formation. Müller-Wille & Reitner (1993) compiled a stratigraphical section of the Formation (Fig. 2) where they accept the original model from Ulrichs (1974), and place the St. Cassian Formation from the aon Zone in the Cordevolian to the Aonoides and Austriacum Zone in the Julian. For the present dissertation, the section of Müller-Wille & Reitner (1993) is taken as reference section.
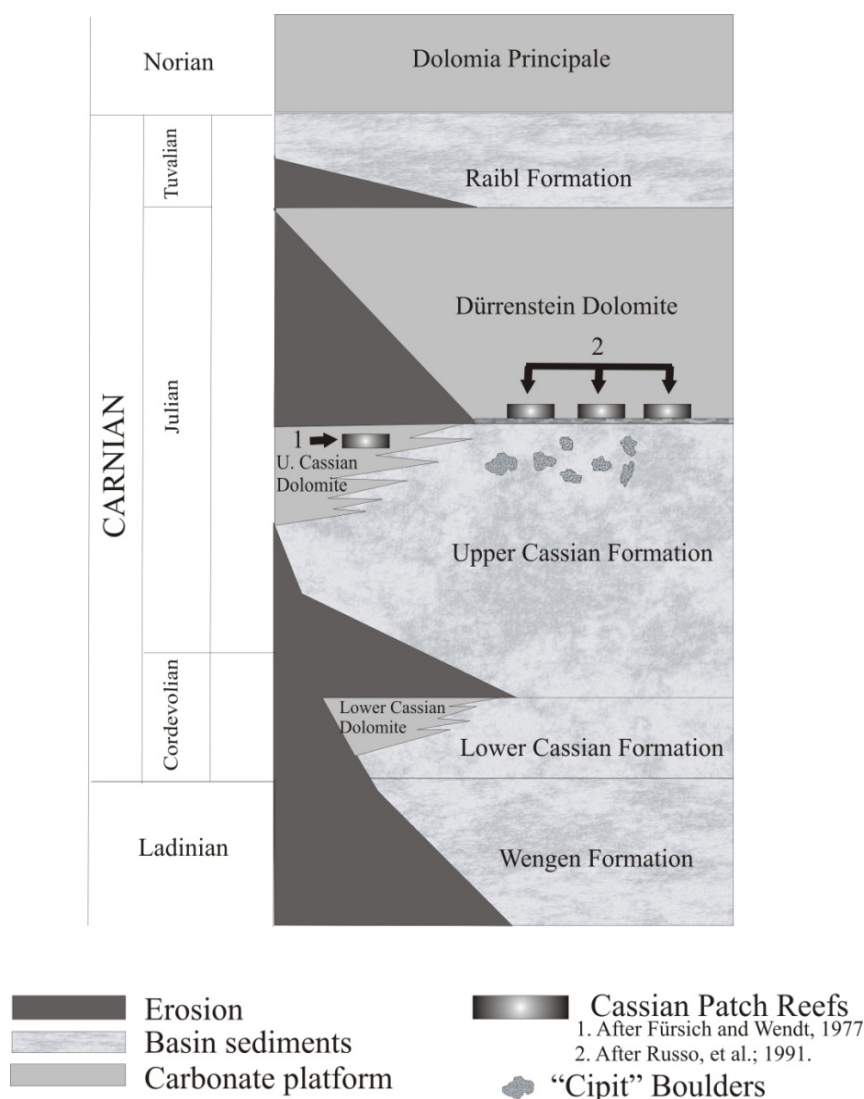
Figure 2: Stratigraphic section of the St. Cassian Formation, displaying the position of the Cipit Boulders. Modified from Müller-Wille & Reitner, (1993)

1.3. The Cipit Boulders from the St. Cassian Formation: In quest of a "valid" definition.

Due to the abundance of publications regarding the calcareous blocks that originated in the Cassian carbonate platforms, it is necessary to define and delineate the terms used in reference to these blocks.

The term "Kalkstein von Cipit" was first used by von Richhofen (1860) to name calcareous blocks deposited within tuffite in the Cassian Beds at the Seiser Alm. He described them as brown, partially crystallized bituminous limestones of an extraordinary tenaciousness, which he attributed to the abundant presence of celestine. The assignment of the name is toponymic, since the "type locality" for such masses is in the vicinity of the Tschipit Creek. He also pointed out that such blocks corresponded to the base of the St. Cassian Formation. Later, von Mojsisovics (1875) started to apply von Richthofen's definition to a wider assortment of limestones, including regularly deposited limestone strata (Kalkbänke) in the Cassian Beds as well as isolated blocks. However, he assigned the term "reefstone" (Riffstein) to most of the isolated blocks. Ogilvie (1893) and Salomon (1895) characterized Cipit Boulders as being autochthonous remains of small coral patch reefs in a shallow water zone. The same idea was presented by Nöth (1929), van Houten (1930), and Valduga (1962). However, as will be discussed later, it is nowadays accepted that most Cipit Boulders may be allochthonous in nature.

When Fürsich and Wendt (1977) published their biostratinomical analysis on the St. Cassian Formation, they also examined the microfacial features of Cipit Boulders collected from 50 localities. After identifying Fe-hydroxide crusts and solution cavities which cut primary textures, they concluded that these bodies were relics of the extensive carbonate platforms which slid down the slope into the basin after subaerial erosion, a phenomenon that had also been identified by Cros (1967, 1972, 1974). They also recognized early diagenetic cementation and a significant absence of dolomitization as main features. This conclusion was supported by Biddle (1981). Fürsich & Wendt (1977) gave the name "Cipit Boulder" to all limestones that derived from the Cassian carbonate platforms. These limestones underwent complete lithification and extensive solution during the emersion and karstification of the platforms, wherefrom they slid into the basin. They are predominantly composed of "algal biolithites" and "less commonly of coral limestones, which are associated with pelletal or micritic limestones". Fürsich & Wendt (1977) also recognize the existence of "erratic blocks" within the basin deposits of the St.Cassian Formation, at the Seelandalpe and Misurina, which may have originated from larger reef knolls. In a thorough study of the Cassian Patch Reefs, Wendt (1982) recognized four reef building/dwelling faunal associations, two of them found within these erratic blocks from the Seelandalpe/Alpe di Specie which he related also with the Cassian Platforms. Reitner (1987a) for the first time denominated as Cipit Boulder these erratic blocks, and the terminology was adopted by Keupp et al. (1989). Russo et al. (1991) included these erratic blocks while carrying out a detailed

characterization of selected Cassian sediments. They not only recognized their facial heterogeneity, but went beyond by identifying nodular limestones, calcarenite storm layers and others in addition to boundstone facies, and by proposing generally low taxonomic diversity for the olistholiths. They also performed a geochemical characterization of different carbonate phases present in selected erratic blocks, such as early vs. late cements, and skeletal organisms. However, they did not name these blocks Cipit Boulders.

In order to avoid confusion, stemming from the fact that some similar reef blocks originating from adjacent carbonate platforms had been discovered elsewhere (e.g. Engeser & Appold, 1988; Flügel & Link, 1996), the blocks which are the object of study of the present dissertation, will be termed "Cipit Boulders" in the following.

1.4. History of research on fossil Porifera in the St. Cassian Formation

The St. Cassian Formation has almost uninterruptedly been studied since the work of Münster (1834) who first mentioned it.

As long ago as in the first half of the 19th century, first reports on fossils found in the St. Cassian Formation come from Münster (1841). He described a vast number of specimens, which he found near the town of St. Cassian. It is, however, remarkable that terms like "plant-animals" ("Pflanzenthiere") or even "Polyparien" were still valid during that time, including taxa such as *Scyphia* (today the sponge *Celyphia*) and the coral *Lithodendron*. Münster described in total 79 genera and 422 species which comprise a taxonomical diversity ranging from corals to reptiles. Klipstein (1843) and Laube (1864) provided extremely complete monographs on poriferans, corals, echinoids, and crinoids. While both of them described several new species, the former reported the prevalence of some of the sponge and coral genera from the times when the Cassian Beds were deposited and until the Cretaceous, while the latter carried out the first study dedicated as a whole to the fauna of the St. Cassian Formation. Most of the poriferan taxonomical classifications both authors used are still valid.

Loretz (1875) pinpointed the fossil richness of the Seelandalpe, highlighting the poriferan content, and Zittel (1879) took substantially into account sponge material from this locality for his work. Nearly 40 new poriferan species were discovered by both of them. Steinmann (1882), who in an extensive work on "pharetronides" (including the also no longer valid taxa of "Inozoans" and "Sphinctozoans"), described also two new species in the Cassian Beds, *Thaumastocoelia cassiana* and *Cryptocoelia zitteli*.

Ogilvie-Gordon (1900) published an extensive list on Cassian specimens from Falzarego Valley along with their stratigraphical location. However she did not include any poriferan.

A notorious gap in Cassian poriferan paleontology is visible from the beginning of the last century until the end of the 1960s, when the first publication dedicated as a whole to this taxon in the Cassian Formation (Dieci et al., 1968) appeared. 40 species of "Inozoans" and "Sphinctozoans" are decribed here, ten of them for the first time. This publication represents a watershed for the investigation of Cassian poriferans. In this regard, further studies (e.g. Bizzarini & Braga, 1978; Russo, 1981) account for the recently discovered diversity, but also develop new trends. While Montanaro-Galitelli (1974) describes for the first time the microstructure of numerous Cassian corals, Dieci et al. (1974) perform a preliminary work on the microstructure of selected poriferans from the Seelandalpe identifying three types: micritic, penicillate (clinogonal), and spherulitic (Fig. 3) ones. Research on this field continued to expand and Cuif (1973, 1974) provided additional new descriptions and emphasized the role of the aragonitic sponges within the Triassic reefal fauna. However, some revolutionary issues emerged since Dieci et al (1977) first reported the occurrence of spicules in Cassian chaetetids and ceratoporellids, thus assigning them to the "Sclerospongia". Parallel to these investigations, Wendt (1974) identified a new type of microstructure for Cassian sponges: the orthogonal type (after Hudson, 1959; Figure 3). Moreover, he emphasized the extraordinary preservation of the aragonitic skeletons and included observations of spicules within their secondary skeletons, proposing for the first time the existence of such features within Cassian genera such as *Leiospongia*. He also determined the microstructural arrangement of Cassian stromatoporoids, identifying three types (the already mentioned ones with the exception of the sphaerulitic arangement) (Wendt, 1975). This topic was discussed in further publications that encompassed the distribution of the microstructural types in the time scale, their diagenetic patterns by means of microscopical/geochemical analyses, and by comparison with recent forms (Wendt, 1976, 1979, 1984; Veizer & Wendt, 1976). Scherer (1976, 1977) achieved important breakthroughs in the geochemical analysis of Cassian samples and exposed his results comparatively between corals, sponges, and specially cements. In addition, he provided the first insights into the isotopic $\delta^{13}C$ and $\delta^{18}O$ records for Cassian sponges.
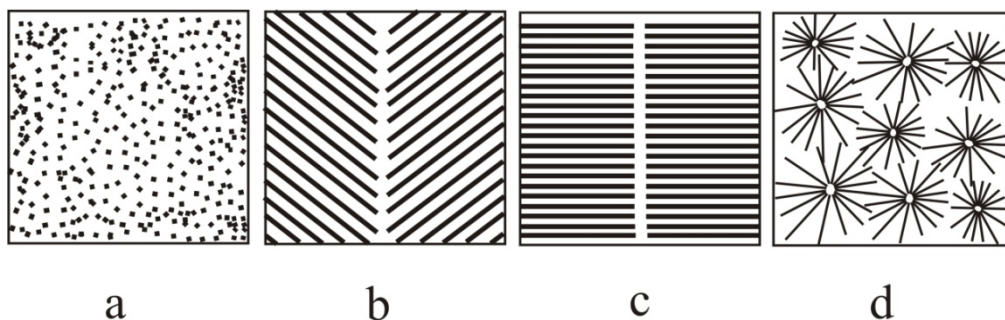
Figure 3: Microstructure types found in most "coralline" sponges. a) Micritic; b) Clinogonal (penicillate); c) Orthogonal; and d) Sphaerulitic. Modified from Wendt (1974)

Introduction

Fürsich & Wendt (1977) performed the first complete study on the biodiversity of the Cassian Formation. They described several associations and assemblages and characterized them paleoecologically. A particular feature of their study is that specific and proportional abundance for each taxon is given and each association is referred to different marine settings, ranging from shallow water to pelagic and basinal environments.

Keupp et al. (1989) obtained the first record of a Triassic hexactinellid and declared the fundamental need for work on the mega and microfacial features of these Cipit Boulders, concluding that gross facies heterogeneity exists among these masses. Reitner (1987a) described the first sphinctozoan with spicules in the Cipit Boulders from the Cassian Formation, *Cassianothalamia zardinii*, assigning it to the Hadromerida Topsent due to the presence of aster microscleres and occasional monoaxonid megascleres. Reitner & Engeser (1989a) also identified a "chaetetid" in the Cipit Boulders with sphaerulitic microstructure and style megascleres as primary skeleton thus assigning it to the Halichondrida Vosmaer sensu Levi. Such findings, amongst other works (e.g. Reitner, 1987b,c; Reitner, 1990; Reitner & Engeser, 1983, 1985, 1989b Reitner & Schlagintweit, 1990; Senowbari-Daryan, 1990) contributed in a crucial way to reassigning organisms which were formerly classified as "sphinctozoans", "chaetetids" and encrusting "sclerosponges" to different families within the class Demospongiae. It is remarkable that such terms are no longer valid since the taxonomical–phylogenetical approach from Reitner (1992), who with the help of cladistics (Hennig, 1966) and several microscopical, histological and geochemical procedures set a milestone in poriferan systematics. He also noted the presence of "microbial crusts" associated to some sclerosponges from the Cipit Boulders. These microbial crusts/organomicrites (sensu Reitner, 1993) are a very important part of many boulders, because they are often associated with the sponge communities. Due to the exceptional preservation of the material, it has even been possible to determine the presence of original organic matter in such organomicrites (Neuweiler & Reitner, 1995).

2.   **Study area**

The study area where the samples analyzed in this work were collected consists of two localities in the Dolomites, South Tyrol, in northeastern Italy: The most known, the Seelandalpe (Platzwiesen, Alpe di Specie) near the town of Schluderbach, and Misurina in the Rimbianco Valley (Fig. 4).
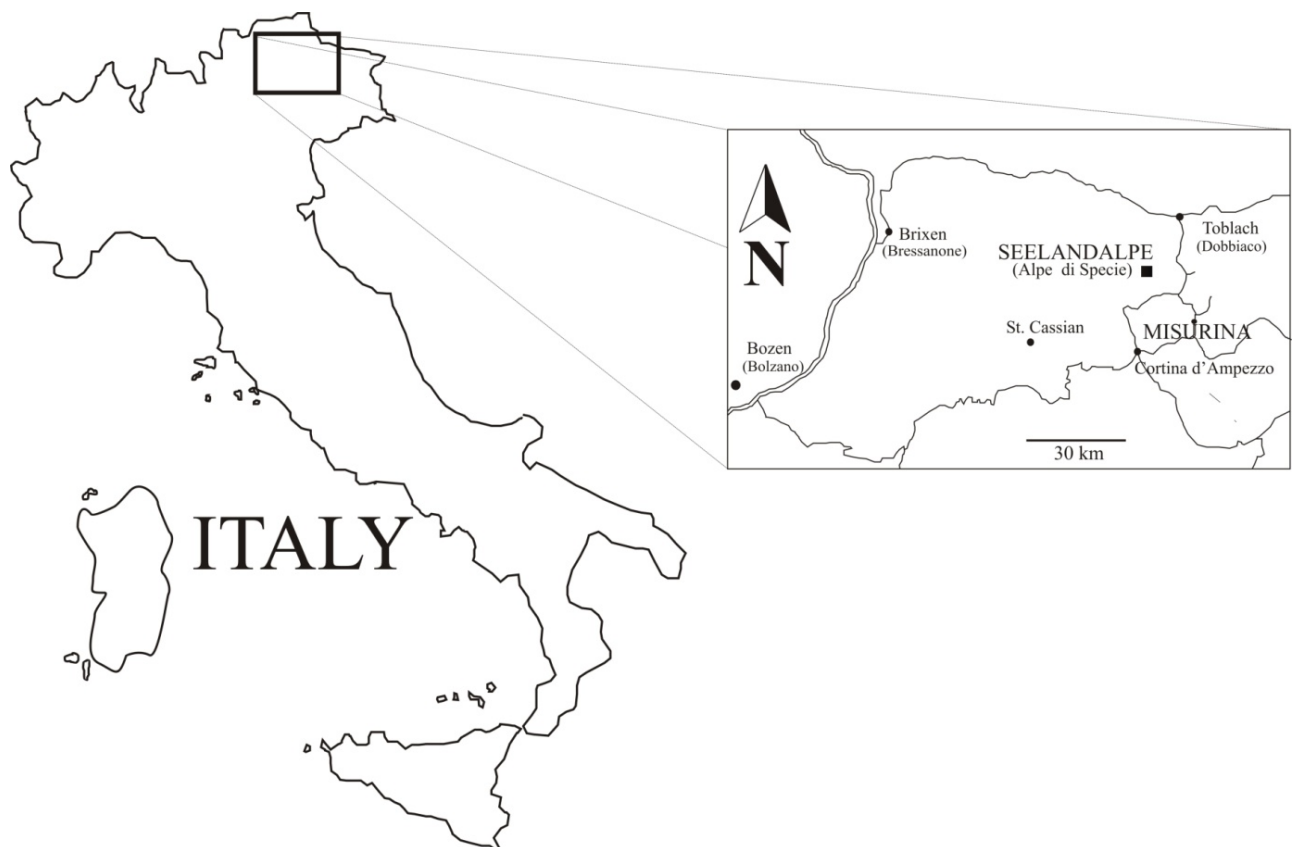
Figure 4: Location of the two collection areas (modified from Müller-Wille & Reitner, 1993).

3.   Aims of this work

Reconstructing the paleoecology of the Cipit Boulders was not an easy task. Since lithologically they do not correspond to the sediment they are deposited in and ammonites are rare, an exact stratigraphical correlation is difficult. As many of them display a boundstone lithology (Reitner, 1987a; Reitner & Engeser, 1989a; Russo et al., 1991), most of their paleoenvironmental determination relies on the assessing of biotopes on the basis of their organism associations (Frost, 1971; Reitner, 1984, 1987d; Fagerstrom, 1987). A considerable number of publications deal with systematic aspects of the Cassian fauna and almost none with paleoecological aspects (see above); therefore taxonomical research was excluded from this study. Biotope assessment was performed through paleosynecological determination.

As already indicated, the Cipit Boulders of the St. Cassian Formation, in particular those from the Seelandalpe /Alpe di Specie and Valle di Ribianco –Misurina, display a high biofacies diversity. However, neither degree of variability nor further paleoecological assessments have been established, mainly due to the lack of a deeper microfacial characterization. The most accepted theory states that these boulders may come from the Cassian Patch Reefs (e.g Fürsich & Wendt, 1977; Wendt & Fürsich, 1980; Russo, et al., 1991; Russo et al., 1997; Russo, 2005). Despite the apparent relationship between the biological communities found by Wendt (1982) in the shallow water Cassian Patch Reefs and their link to the Cipit boulders, it has also been proven that different biotopes may have been the place of origin for these masses. (Moussavian & Senowbari-Daryan, 1988; Keupp et al., 1989; Reitner & Engeser, 1989a). Furthermore, the lack of the knowledge of such communities was already stated a long time ago (Wendt, 1982).

The St. Cassian Formation has been considered a Fossillagerstätte due to its exceptional preservation (Fürsich, 2000) and has substantially contributed to the knowledge of Triassic reefs, even though an extensive number of publications regarding this topic exists, (for a detailed and extensive list see Flügel & Flügel-Kähler, 1992; Flügel, 2002; Flügel, 2004), few of them deal with the interactions between organisms ("fossil community" *sensu* Craig, 1953 and Dodd & Stanton, 1982). However, some constraints may be found regarding these interactions. Among them is variability in boulder size (Russo et al., 1991). This would considerably limit the feasibility of a successful and reliable paleoenvironmental analysis, since only winnowed communities (Fagerstrom, 1964) would be found. Furthermore, even organisms themselves can be found winnowed. However, a trend in paleoecology over the last decade has been to recognize the importance of microencrusters in paleoenvironmental reconstruction. This has proved to be useful in assessing some insights into the original environmental conditions, such as oxygenation, light dependence, water energy and depth in ancient carbonate settings (e.g. Leinfelder et al., 1993, 1994; Schmid, 1996; Shiraishi & Kano, 2004). This can be of

extreme help in determining paleoecological features on associated reef building organisms. In addition, the importance of microbial carbonates on the phanerozoic reef history has also been confirmed (Webb, 1996; Kiessling & Flügel, 2002) and must therefore been considered in order to perform a reliable paleoecological reconstruction, as it can also provide many insights into paleoenvironmental determination of ancient reef settings (e.g Leinfelder, et al., 1994).

Thus, the main questions arising from these statements are:

- Can the fossil assemblages define associations or communities?
- Can these communities define biotopes by themselves?
- How variable are the biofacies contained in the Cipit Boulders?
- Is there any indication for a different biotope that may not necessarily be related to the St. Cassian Patch Reefs?

A further objective of this work deals with the geochemistry of the Cassian microbialites. Although the excellent state of preservation in the Cipit Boulders from the St. Cassian Formation has been known for decades, only little geochemical research has been performed on its microbialitic deposits (e.g., Keupp et al., 1993). Geochemical research on microbialites can provide information on possible former impact of bacterial metabolism and terrigenous input into the sediments. In this regard, the following question arises:

- What information can be obtained from diverse geochemical signals in St. Cassian microbialites?

On other fields, some researchers (e.g. Reitner, 1992; Swart et al., 1998; Hasse-Schramm et al., 2003), have drawn conclusions on the potential impact of "sclerosponges" as paleoecological proxies. Since sponges have continuously been reported in the St. Cassian Formation and taking into account the extraordinary degree of preservation of their fossils, a geochemical archive can be opened for them. In a parallel scope, isotopic variations have been detected in subfossil stromatolites (Reitner, 1993). Stromatolites can be found, though seldomly, among St. Cassian microbialites. This leads to the next question:

- Which St. Cassian facies are good geochemical proxies for assessing climatic variations and how reliable are they?

The last scope of this research encompasses the assessment of sponge-related organic matter in selected St. Cassian deposits. Neuweiler and Reitner (1995) and then Russo et al., (1997) found indications for possible original organic matter in St. Cassian microbialites in selected Cipit Boulders,

Aims of this work

which can be confirmed by the presence of 2- and 3-methylalkanes (Thiel, 1997). The last question can be as follows:

- Which sponge biomarkers can be found in selected Cipits and what do they mean for the analyses of St. Cassian communities?

4. Material and Methods

4.1. Thin sections

Prof. Reitner's entire personal St. Cassian collection was revised, consisting of a total of ca. 400 thin sections; more than 300 of them in half-postcard format (7.5 x 10 cm) and the rest of them in postcard format (10 x 15 cm). In order to obtain a reliable paleoenvironmental interpretation, those originating from the Seelandalpe and Misurina were selected because they showed a better state of preservation and were dominated by boundstones were selected. Criteria of exclusion were a) samples without microencrusters and b) for most cases, samples with less than three reef guilds according to the model of Fagerstrom (1987). The last selection criterion was the number of thin sections per Cipit boulder. Since this study focuses on the paleoecology of the fossil associations contained in the Cipit Boulders, boulders represented by at least four thin sections (compare Russo et al., 1997) were selected, so consequently ca. 50 of them were taken in total for the final selection.

Furthermore, more than 150 new thin sections in half postcard format were newly made from 40 newly collected Cipit Boulders during a fieldtrip at the end of 2008 from the Seelandalpe and Misurina. After a selection according to the explained exclusion criteria, ca. 70 of them were analyzed. Their corresponding bulk material remained available for later biogeochemical analyses.

The processing of thin sections was performed as follows:

1. Rock samples were placed on a sawing machine equipped with a diamond saw and cut into slices of ca. 1.5 cm of thickness, placing a steel spacer in a way that the distance remained the same during the entire process and thus avoiding cuneiform slices. At this step, the size of the glass slide –the final step– must be considered.

2. After the slices were obtained, they were dried in an oven at 50°C for two hours, along with their corresponding glass subcarriers, which border must be previously preventatively polished.

3. A synthethic two-component epoxy glue of the brand Araldite was prepared in the proportion of 10 to 3. Hereafter, rock slices were glued to the glass subcarriers with the adhesive mixture and dried at 50°C for at least 12 hours and then removed from the oven.

4. After cooling for one hour and cleaning, a fretting machine with coarse disc was used for abrading the surface of the slide, so that the definitive glass slide could be placed on it, following the method described in number 3, and then be placed inside a screw clamp. The samples were removed from the oven and then cut in a vacuum saw, placing the glass slide (not the subcarrier) on the surface where the vacuum acts. Immediately, the resulting sample (approx. 1 mm in thickness) had to be abraded at the fretting machine first with a coarse disc and finally with a glossy disc in order to avoid scratches until reaching between 70 and 80 mm of thickness.

Material and Methods

Some methods described below can also be performed on these thin sections (Raman Spectroscopy, Epifluorescence microscopy).

Additionally, 20 petrographic thin sections, format 4.8 x 2 cm, were obtained by the same technique, for the purpose of performing Cathodoluminiscence (see below)

In addition, 20 petrographic thin sections, format 4.8 x 2 cm, were obtained by the same technique for the purpose of performing Cathodoluminiscence (see below).

In order to answer the questions posed under number 3. (Aims of this work), the following procedures were carried out, either on thin sections or on their corresponding polished slabs.

- Staining
- Microfacies analysis
- Transmitted light microscopy
- Cathodoluminiscence
- Microprobe analysis
- Epifluorescence microscopy
- Mass spectrometry (stable isotopes and LA-ICP-MS)
- Raman spectroscopy
- Biomarker analysis

4.2. Staining

Dickson (1965, 1966) developed a method to recognize different mineralogical phases in a carbonate sample in which the presence of Fe^{2+} is recognized through blue staining by means of the combined effect of potassium hexacyanoferride and alizarine red–S. This method proved to be useful for qualitatively recognizing the presence of diagenetic cements as well as for qualitatively determining the state of preservation of some samples (pink-staining of aragonite) and for distinguishing spicule pseudomorphs in coralline sponges (Reitner, 1992). It was performed as follows:

Solution I: 0.2 g Alizarin Red dissolved in 100 ml of 1.5% HCl.
Solution II: 2.0 g $K_3[Fe(CN)_6]$ (potassium hexacyanoferride) dissolved in 100 ml of 1.5% HCl.

1. Etching with 1.5 % HCl for 10 s.
2. From previously prepared solutions I and II, a mixture in a ratio of 3:2 must be obtained. This mixture can be used 2 days at most after its preparation. Etching for 30-45 seconds produces a differential staining, yielding pale pink/red for calcite, Turnbull's blue for ferran calcite, and colorless for dolomite.

3. Etching with Solution I yields further increase of all previous stainings.

After each stage, the sample must be washed thoroughly, but not roughly, with destilled water and at the end, the sample must be dried with an air pistol at a range of minimum 50 cm. Finally, thin sections must be covered with Bühler Spray. Stage 3 of the original method by Dickson (1965) was not carried out with most of the samples, because a distinct staining pattern was already recognizable after the first two steps.

4.3.   Microfacies Analysis

Microfacies analysis is a technique that deals with the determination of the different components found at microscopic scale in thin section. It can be successfully applied with carbonate rocks, where it yields valuable information on the deposition history of the sediments (Flügel, 2004). Considering previous results and observations which point out the importance of microbial deposits in the Cipit Boulders from the St. Cassian Formation (e.g. Reitner, 1987a; Neuweiler & Reitner, 1995; Russo et al., 1997; Russo et al., 2000; Russo, 2005), classification of reef carbonates according to the proportion of their micrite fraction will follow the outlines by Reitner & Neuweiler (1995) in this work. For the purpose of naming associated facial textures, facies classification is performed after Dunham (1962).

Qualitative methods for microfacies analysis include "free lance" visual estimation (Flügel, 2004). However, in order to assess a conclusion on the sedimentary history and paleoenvironmental conditions of a carbonate a semiquantitative to quantitative analysis is necessary. Semiquantitative methods include visual area estimations (Bacelle & Bosellini, 1965). Quantitative methods include Point, Ribbon and Area Counting (Flügel, 2004).

Point count analysis was performed on sixteen thin sections, using a 1mm transparent-film grid. However, it was decided not to continue with this method, because very similar or nearly identical results could be obtained through visual area estimations and area counting methods. These methods were performed on the rest of the selected material. In addition, point counting consumes much more time (compare Flügel, 2004) and it is not completely suitable here due to the heterogeneity of the samples, including drastic component variations in the same thin section.

Visual area semiquantitative estimation was performed in some thin sections in the following way: The contours of different facies were drawn upon a plastic film on the surface of the thin section under the stereoscope. Efficiency of this method was proved by matching the resulting sketch through light microscopy. The corresponding sketch was matched in the end with the estimation charts of Bacelle and Bosellini (1965).

Quantitative area counting was performed as follows: All analyzed thin sections were processed on an AGFA Snap Scan 1236 Scanner. Thin sections were analyzed microscopically alongside the scanned images, in order to distinguish difficult boundaries between facies and be able to establish a graphical on-screen classification. To achieve this goal, software utilities like Metamorph (licensed to the University of Göttingen) and VistaMetrix (licensed to the author) were used. Some representative samples were selected to perform a detailed thin section map, using the Corel Draw v.11 software. A similar procedure was used by Martínez-Rodríguez et al. (2010).

Comparison of different area counting methods, i.e. semiquantitative or quantitative, did not show significant differences between both of them.

For the determination of the proportional abundance of microencrusters, the scale of Dupraz & Strasser (1999) was followed.

4.4.   Cluster Analysis

Cluster analysis (e.g., Zar, 2009) is a method that permits hierarchical grouping of information in multivariate data sets. No assumptions are needed, and the only requirements are two or more rows of counted, measured, or presence/absence data in one or more variables or categories, or a symmetric similarity or distance matrix. In any given matrix, two modes of clustering can be performed: **R**, which renders phenograms with information from the rows of a matrix as phena, and **Q**, which basically consists in a transposition of the same matrix; that is, taking information from the columns as phena for the phenogram. This method can allow to help grouping thin sections (assemblages) into associations and furthermore of grouping these associations into communities.

Three main different algorithms can be used in paleontology in order to perform this task:

- UPGMA/WPGMA (Sneath & Sokal, 1963; Unweighted/Weighted Pair-Group Method with Arithmetic mean) join clusters based on the average distance between all members of both groups. The difference between them relies on the prerequisite that distances between groups in UPGMA do not contribute to the hierarchization of phena as it does at the WPGMA, thus being *weighted* in the latter. Furthermore, in UPGMA the cophenetic correlation coefficient of a cluster analysis is maximised, which produces results with minimum levels of distortion (Farris, 1969; Sokal & Rohlf, 1970). This is because it attempts to use a greater proportion of the information present in the similarity matrix. Since UPGMA algorithm has been used repeatedly in diverse fields of Paleontology (e.g. Tway, 1979; Martínez Hernández & Ramírez Arriaga, 2006), including the study of Triassic reef faunas (Yarnell, 2000), it was taken as the most reliable source of similarity in this work.

- Single Linkage (Sneath, 1957; Sokal & Sneath 1963; Saitou & Nei, 1987) (Nearest Neighbor) is a method that calculates distances between clusters. The distance between two clusters is calculated as the distance between the two closest elements in the two clusters.

- Ward's distance method (Ward, 1963) involves an agglomerative clustering algorithm. It starts out with *n* clusters of size 1 and continues until all the observations are included into one cluster. This method is most appropriate for multi-state variables.

While Ward´s method works with Euclidian distances exclusively, both UPGMA/WPGMA and Single Linkage methods can work with ca. 15 different indices. However, since most cluster analyses in Paleontology are performed based on the Jaccard coefficient (Cheetham & Hazel 1969; Schäfer, 1979; Stanton & Flügel, 1987), it was used with all clustering processes. This coefficient is defined as the value of the number of taxa common to two compared samples or the number of features common to two compared species (Schäfer, 1979) and has traditionally been used as a measure for comparison in diversity studies, because it has a wide array of applications especially due to its versatility. The last used index in community cluster analysis is the Bray-Curtis coefficient, which is interpreted as a measure of dissimilarity (Bray & Curtis, 1957). For low values, a high similarity is expected. (Michie, 1982)

R- and Q- Mode Cluster analyses were performed by means of the MVSP Software (1985-2009 by Kovach Computing Systems, trial version) on a set of 112 thin sections, including newly prepared material and also material from Prof. Reitner's personal collection.

4.5. Transmitted light microscopy

Stereoscopy was carried out in order to examine samples in low magnitudes without the need of distinguishing small-scale characteristics like skeletal microstructural traits, and also in order to obtain large-scale photographs, which proved to be very useful for community analyses. A Zeiss stereoscope with an attached Axioplan-series camera was used to perform this part of the study. By contrast, transmitted light microscopy proved to be helpful for recognizing microfacial and microstructural traits. The following equipment was used: Zeiss Axioplan Microscope with Plan Neofluar Objectives 2.5x, 5x, 10x and 20x with mounted photographic equipment VISICOL made by Visitron Systems GmbH, Germany. This method is required for Microfacies Analysis

4.6. Cathodoluminiscence

The principle of Cathodoluminiscence examination of carbonate rocks is based on the excitation and activation of bivalent cations such as Mn^{2+} by an electron beam, which results in a yellow to red luminiscence. (Tucker, 1996). This technique was previously used with St. Cassian samples by Reitner (1992) and by Müller-Wille & Reitner (1993).

This method was performed on polished petrographic sections using a Citl CCL (CCL 8200 MK- 3A)-Siemens (Pressure port M10 x1, Type KPY 42 MA) coupled system attached to a Zeiss Axiolab microscope. Working conditions were as follows: gun potential = 13 – 14 kV; current intensity = 300 – 350 mA. Photographs were taken with a SPOT-CCD camera.

A total of 20 petrographic thin sections, plus several half-postcard sized thin sections were analyzed by this technique.

4.7. Microprobe Analysis

The principle of microprobe analysis is based on the determination of the elemental composition of solid substances through the emission of electrons onto a sample, which produces X-rays upon the irradiation (Reed, 1996). The content of Ca, Mg, Si, Fe, Mn, and S was measured in three selected carbon-coated petrographic thin sections of microbialites. The measurements were carried out by Dr. Andreas Kronz at the Department of Geochemistry (Uni Göttingen), using a JEOL JXA– 900 RL microprobe using a gun potential of 15.0 kV and a current of 12 nA. The diameter of the exciting electon beam was 5 μm.

4.8. Epifluorescence microscopy

Fluorescence can be defined as the property of a given substance to emit visible light after stimulation by ultraviolet or visible light. (Dravies and Yurewicz, 1985). Although the phenomenon was observed by Stokes (1852) a long time ago, in the last decade it has had considerable implications in the field of geobiology. The main cause of fluorescence has been attributed to the presence of organic matter (Van Guzel, 1979) and it has abundantly been recognized in St. Cassian samples (e.g. Cuif et al., 1990; Müller-Wille & Reitner, 1993; Neuweiler & Reitner, 1995; Russo et al., 1997; Rech, 1998; and Sánchez-Beristain & Reitner, 2008). However, some other factors, such as the presence and activation of trace elements like Mn can produce similar results (Van Guzel, 1979, Dravies & Yurewicz, 1985).

Epifluorescence was conducted on each thin section sample, in order to assess the content of organic matter.

4.9.   Stable Isotopes

Sampling for these analyses was performed with a dental drill out of polished slabs mounted on a petrographic slide. For a reliable analysis, a quantitiy of 60 μg per sample is required. Sampling spots were allocated with the help of previous microscopic examination of the corresponding petrographical thin sections. Reproducibility of the experiments was assessed using laboratory standards. Maximum standard deviation (σ) value for further used data is 0.014 for $\delta^{13}C$ and 0.029 for $\delta^{18}O$.

However, despite careful drilling, the possibility of contamination by other facies cannot totally be excluded.

Measuring were done using a Kiel IV Spectrometer, at the Department of Geochemistry in the University of Göttingen under the direction of Prof. Andreas Pack. 79 drillings were performed; 55 in coralline sponge samples, 13 in a stromatolite, and 11 in accompanying facies. All values are expressed relative to PDB, except where indicated. Conversion from VSMOW to VPDB was performed after Wiedner (2004).

4.10.   LA-ICP-MS

Inductively Coupled Plasma Mass Spectrometry is a high-resolution method that allows detection of trace element concentrations in the ppm range (Schäfer, 2006). Coupling this equipment with a Laser-Ablation system makes it possible to analyze all samples without previously dissolving anything. It is of special importance that this method allows a high spatial resolution sampling, by permitting located ablations at determined places, which in turn render sublimates consisting of single phases, and it is therefore adequate for complex rock samples consisting of various phases of minute size.

Laser ablation was performed under the direction of Dr. Klaus Simon with an Excimer 193nm COMPEX 110 (Lambda Physik, Göttingen, Germany) equipped with an optical beam shape enhancer GEOLAS (MicroLas, Göttingen, Germany) at about 3 J/cm^2 with spot sizes and line width of 120 μm. The ablated material was carried into the ICP-MS DRC II (Perkin-Elmer, Canada) plasma using Argon carrier gas. Measurements were made using the method of Kamber & Webb (2007) on three polished slabs, with the following variations for the time-series: 28 isotopes (and separately the 13 REEs only for a "pilot" study) were analyzed at dwell times of 20 ms; time duration of measurements was 165 s, which comprised 402 Reading Points (RP). Measurements started after 30 seconds of pre-warming and ended 10 seconds prior to the macro end, but only measurements from 10 to 130 seconds (280 RPs in total) after the start of ablation were taken. Quantification of a single sweep, which has a dwell time of 20 ms for one isotope, is very erroneous. However, if 5 or more sweeps produce the

same results, the error of the mean average decreases dramatically. Standardization and quantification was done with NBS610; Internal Standard Isotope was Ca43, assumed to have variable concentrations in the carbonates as obtained by microprobe results (390,000 ppm for the aragonite and the late cement, 360,000 ppm for the microbialite, and 350,000 ppm for the allochthonous micrite/detritus). Absolute concentrations are prone to have rather large errors, especially for those elements that have the most near- background concentrations. However, ratios can be measured more precisely –with errors of less than 2%.

The procedure to obtain samples was to allow laser ablation to go deep into the sediment, which yields less variation among the values obtained at each count, in contrast to performing a continuous line along a given facies type. In a preliminary attempt to apply the line- method, it was seen that it provided a considerable value variation. Kamber & Webb (2007) attributed this to pollution from the polishing slab, and was the reason for which they recommend discontinuing its use. In addition, Schäffer (2006) also performed point-distributed measuring while applying LA- ICP-MS in a study of sediments from the Black Sea.

The visual result is a surface where ablation spots can be seen, instead of the mentioned line. Furthermore, two replicate measurements adjacent to each point were in order to assess reproducibility of the experiment. The displayed results in Appendices AVII and AIX are thus an average of three values.

On the other hand, line-ablation method proved to be useful while analyzing compositional variation along layered structures like stromatolithes and coralline sponges.

This technique was performed first with three polished slabs, in order to assess its suitability for further analyses. Subsequentely, it was conducted on five further polished slabs which included diverse carbonate facies. However, 24 isotopes were measured instead of the original 28 at this stage. Tantalium was not taken into account due to its low concentrations. Yttrium, as well as the reference Rare Earth Elements originally used, (La and Ce) were also removed since results yielded no satisfactory REE + Y pattern (see section 5.5.2.1.2).

Laser ablation has a higher resolution than than dilution methods, since the latter require much more material than the former, implying thus a mixture of facies (Delecat, 2005).

4.11. Raman Spectroscopy

Raman Spectroscopy is a light scattering technique where a photon of light interacts with a sample in order to produce scattered radiation of different wavelengths. It has the goal to qualitatively determine

the primary chemical composition of the given sample (Ferraro et al., 2003). Raman spectra were recorded using a Horiba Jobin Yvon LabRam-HR 800 UV microprobe with a focal length of 800 mm. As excitation wavelength the following was used: 1) the 244 nm line of a frequency-doubled Ion Laser (Coherent Innova 90C FreD) with a laser power of 30 mW; 2) the 488 nm line of an Argon Ion Laser (Melles Griot IMA 106020B0S) with a laser power of 25 mW. Regarding the 244 nm line the laser beam was dispersed by a 2,400 lines/mm grating on a liquid nitrogen cooled CCD detector with 2048x512 pixels, yielding a spectral resolution of 1.05 cm^{-1}.

An Olympus BX41 microscope equipped with an OFR LMV-40x-UVB objective with a numerical aperture of 0.5 focused the laser light onto the sample. In order to get a better signal-to-noise ratio, the diameter of the confocal hole was set to 200 μm. The typical acquisition time varied from 30 to 120 s for a spectral range of 500-2,500 cm^{-1}. For calibration of the spectrometer, a diamond standard with a major peak at 1,332.0 cm^{-1} was used. The 488 nm-line laser was dispersed by a 600 line/mm grating on a CCD detector with 1024x256 pixels, yielding a spectral resolution of 0.43 cm^{-1}.

In order to perform Raman spectroscopy, ca. 20 samples including diverse carbonate facies were selected.

4.12. Biomarker analysis

Five samples (FSSA) containing primarily hexactinellid and lithistid sponges were selected to undergo biogeochemical analyses in order to find sponge related-biomarkers, in the context of a Diploma Thesis (Germer, 2010). Subsequently they were sawn to remove all trace from visible weathering and diagenetical alteration, especially found at the rims of most Cipit Boulders. The remaining fragments were crushed into small pieces. To further remove organic contamination, the sample pieces were ultrasonicated with acetone before they were pulverized using a swing mill.

Further details regarding decalcification, extraction, chromatography, derivatization and desulfurization can be found in Germer (2010).

5.   Results

5.1.   Facies diversity in the Cipit boulders from the St. Cassian Formation.

Among the selected thin sections, following components and cements could be recognized: Biomorpha (Fossils), Microbialite, Allochthonous detritus/ allomicrite, cements and microsparite. These components had previously been identified by Rech (1998) in St. Cassian Cipit Boulders from Stuores Wiesen, the Seiser Alm and the Seelandalpe.

5.1.1. Biomorpha.

Although all the selected Cipit Boulders are rich in remains of biological "reef" building communities, the composition and variety of their biofacies is completely different. Fossils preserved in the selected thin sections are represented by a vast variety of taxa, which primarily include a vast diversity of sponges, especially of the encrusting type. However, *in situ* calcareous red algae, corals, brachiopods, and microencrusters (among them microproblematica) are also present and sometimes even so numerous that they define or represent the most significant element of the association. Nevertheless, as the main focus of this work are sponges, communities where they do not play a dominant role will be mentioned only in a comparative way.

5.1.2. Microbialite

The term microbialite was defined by Burne and Moore (1987) as "organosedimentary deposits that have accreted as a result of a benthic microbial community trapping and binding detrital sediment and/ or forming the locus of mineral precipitation". Reitner (1993) compiled the definition and problematics regarding microbialite origin and genesis based on a case study at Lizard Island, Australia. Microbialites are thus a type of automicrite, which is defined in principle as a microcrystalline carbonate formed at the sea floor or within the sediment (Wolf, 1965; Reitner, 1993). However, considering the semantic problems this would cause, Reitner et al (1995) defined a new type of automicrite, the organomicrite, which is automicrite genetically related to Ca-binding organic macromolecules. Microbialites are included in the term organominerals, reviewed by Defarge et al., (2009).

Neuweiler and Reitner (1995) first noticed epifluorescence properties in St. Cassian organomicritic samples from Cipit Boulders. In addition, since they also noted a peloidal matrix in some of them, they concluded a microbial origin for the samples. These criteria can be considered as strong enough to support a microbial origin for organomicrites (Rech, 1998), apart from the presence of specific biomarkers in them (Thiel, 1997). Furthermore, the importance of microbial sediments at more St.

Cassian localities has been steadily confirmed since the last decade, for instance at Punta Grohmann (Russo et al., 1997); Marmolada (Russo et al., 2000); Latemar (Emmerich et al., 2005; Keim & Schlager, 1998, 2001); and the Seelandalpe and Misurina (Sánchez-Beristain & Reitner, 2008).

In the present work, since most features belonging to microbialites can be seen only in thin sections, a classification mostly based on its microstructure is performed. Numerous classifications of microbialite fabrics according to their microstructure have been made. The first one, proposed by Kennard and James (1986), is based on microstructural features. Schmid (1996) resumed this classification and applied it to authochthonous micrite sediments associated to microencruster networks. Riding (2000) deepened and expanded the classification by Kennard and James (1986) also giving a special importance to microbialite macrofabrics. Shapiro (2004) also developed a classification based on the microstructure of microbialites.

In the St. Cassian Formation, Russo et al. (1997) identified five microfabric types for microbial carbonates: peloidal thrombolytic, peloidal stromatolitic, peloidal structureless, microcrystalline stromatolitic and microcrystalline structureless.

Following types of fabrics could be identified in this work:

Microbialite Fabric Type 1 (M1) consists of a distantly separated and cloudy arrangement of peloids, ("wolkig" according to Rech, 1998) and is represented only by thrombolites. Size of clots ranges from 50 to 200 μm. Its distribution is poor in all samples.

Microbialite Fabric Type 2 (M2) which can also be seen within thrombolites and consists of densely clotted peloids. This type is by far the most abundant in the analyzed samples. (Pl. IV, Fig. 5; Sánchez Beristain et al., accepted; Figs. 1a-b).

Microbialite Fabric Type 3 consists of an aphanitic micrite (~ leiolite from Braga et al., 1995; Schmid, 1996; Riding, 2000) which is characterized by a very fine arrangement of carbonate grains. No clear peloidal structure can be seen within the fabric, although sometimes the fabric itself can be found strongly associated to M2-type fabrics. This type is undoubtedly the one which displays the most intense fluorescence. (Pl.II, Fig. 4-5).

Microbialite Type 4 (M4) is a peloidal stromatolite, in which the dimension of the peloids is more uniform, ranging from 70 to 90 μm. The space between the layers is filled by interstitial

microcrystalline cements. It appears only in few samples, and is not associated with microencrusters. (Pl.XIX, Fig. 5)

Although traditionally microbialites and automicrites respectively, are not categorized within biofacies, in this work it was decided to include them both in biofacies in order to pursue a paleoecological approach in the investigation of reef communities.

5.1.3. Allomicrite and associated allochthonous components.

In addition to automicrites, allomicrite and a very diverse assortment of allochthonous components can be found in the analyzed samples. The most notorious difference between automicrites and allomicrites is that the former displays generally high levels of epifluorescence when excited with UV beam, whereas in the latter epifluorescence is minimal or nonexistent. An additional contrast is defined by the homogeneity of the matrices. While automicrite normally does not have allochthonous components associated with it, allomicrite is rich in these as a general rule. Among these components –consisting mostly of bioclasts-, foraminifers, fragments of bivalves, brachiopods, gastropods, reef builders (sponges, corals, calcareous algae) could be identified. These allochthonous micrites can be found mainly in the primary vugs created by means of microbialite growing. Their composition and proportions among thin sections and thus can only give a general indication of the remains of an associated fauna of the implied biofacies type , if any. However, in some cases allochthonous components may be useful for defining certain biological communities, especially due to the scarcity of some bioclasts in all the array of samples. (See *Cryptocoelia- Mesophylum* community).

5.1.4. Cements.

Although cements have been considered to have had an important role in reef building in some localities in the Dolomites (Russo et al., 2000) and even in many geological time settings (Riding, 2002; Flügel, 2002), they do not play a predominant role in most of the analyzed thin sections. They seldom constitute more than 5% of rock volume and are represented by primary and secondary types. Primary cements appear mostly in form of fibrous threadlike structures or botryoids within microbialites. Their synsedimentary identity was proven by microscopic features, a red to pink color after staining, and by high contents of Mg (2 – 3% Mol) determined by microprobe and LA-ICP-MS measurements (Russo et al., 1997).

Secondary cements are mainly represented by granular sparry low Mg- calcite which can be found as a general rule in secondary cavities or veins within fossils or microbialites; however most of the primary reef builder pores are filled with them. They generally display a blue color after staining with Potassium Hexacyanoferride and Alizarin Red. Occasionally these sparry calcites can be found in the

middle of various cement generations, many of them primary, forming stromatactis or stromatactoid cavities.

5.1.5. Microsparite

Microsparite was considered by Folk (1958) as a neomorphic texture. It is represented by a dense arrangement of crystals in the size range of 5 -15 μm, which are strongly associated to allochthonous micrite, but never to microbialitic matrices. Its importance in the analyzed thin sections is also minimal, since it is present in a very small fraction of the samples.

5.2. Fossil associations contained in selected Cipit Boulders.

5.2.1. Determination of fossil "reef" associations

Reefs are one of the most diverse marine ecosystems (Sheppard et al., 2009) containing a vast range of well-defined communities (Jaap, 1984; Fagerstrom, 1987), the floristical and faunistical composition of which can sometimes change over distances of a few centimeters (Jackson, 1991). These considerations are extremely important taking into account that some of the Cipit boulders may originate from reef settings (Fürsich & Wendt, 1977; Wendt & Fürsich, 1980; Wendt, 1982; Russo, 2005). Therefore the biotic composition can vary from boulder to boulder (Russo et al., 1991) and even sometimes from thin section to thin section. It must furthermore be stressed that Cipit boulders potentially represent partly winnowed or trimmed associations/communities due to the following factors: a) the fact that they are considered allochthonous and therefore isolated from their source depositional environment, and b) the consequences of the "cutting" effect, present in all studies based on thin sections (Flügel, 2004).

All fossils found in a single thin section should be considered as assemblages, since they are mere observational units (Brenchley & Harper, 1998). Criteria for considering fossil assemblages contained in each one of the thin sections from Cipit boulders as remains of true biological associations or communities (Craig, 1953; Dodd & Stanton, 1990; Brenchley & Harper, 1998) are in principle hard to assess. Due to their allochthonous nature, the Cipit Boulders are prone to recolonization and multiple rotation prior to their final deposition. In addition, it is hard to assess whether all biomorpha included in each boulder had a syn-vivo relationship with each other and whether they lived in a geologically insignificant time span, respectively; yet this can be assumed in most cases by observing either characteristic encrusting patterns between organisms (Reitner, 1987 a,d) or the same growth orientation of different microbialite generations.

25

Results

The solution thus relies on grouping fossil assemblages into fossil associations. However, all assemblages can be grouped in order to obtain fossil associations. In order to pursue this aim, it is necessary to use a method which eliminates subjectiveness of plain observation by eye and estimation. Cluster Analyses (see above) proved to be a functional method for achieving this aim.

Taking into account these considerations, the term "fossil association" or simply "association" will be used in all descriptions reported in this section, prior to the clustering process aimed at obtaining fossil communities (see section 5.4.1).

5.2.2.   Results from Cluster Analysis

A matrix was constructed containing all identified taxa in each thin section, microbial carbonates, cements, allochtnonous sediments and undetermined taxa (Appendix AI). Data from either point or area count are shown as percentages in this matrix. A key is assigned to each taxon/feature (Appendix AII)

Fourteen different fossil associations were identified in the selected thin sections from Cipit Boulders. They could be recognized thanks to high Jaccard coefficient values (averaging > 0.50, Appendix AIII - V). UPGMA, WPGMA, and Nearest Neighbour analyses performed with the Jaccard coefficient provided similar phenograms (Appendix AIII - V) Almost all assumed associations prior to the analysis (samples originating from the same boulder or displaying a similar estimated microfacial composition) proved solid after clustering. Furthermore, phenograms from these analyses showed that most microbialite-rich samples ("mud mound" associations) belong to the same phenon .Moreover, communities having *Cassianothalamia zardinii* (C-G and C-G II) are also grouped in an additional single phenon.

In UPGMA analysis (Appendix AIII), 11 associations appear clearly recognizable through branches separated from each other by distant nodes from their initial nodes with low-Jaccard values. Only the three Patch Reef associations are all grouped in a single phenon within a node with a medium to low Jaccard value of 0.31. This phenon encompasses two further nodes, a smaller phenon of five samples assigned to P-R-II with a Jaccard value of 0.70 and a further phenon with four samples which is assigned to P-R-III with J = 0.87 . Thus, 14 samples remain without resolutive grouping in different phena. However, because the two nodes including P-R II and P-R III are closely clustered, these remaining 14 samples were interpreted as being part of a single association (P-R-I), which in addition to P-R-II and P-R-III and the 11 associations mentioned before, constitute the 14 associations to be described.

WPGMA clustering yields a very similar phenogram, with only small variations (Appendix AIV). The most dissimilar phenogram of the three is the one obtained by Nearest Neighbour clustering, (Appendix AV). Equal Jaccard values thus occur very frequently. Nonetheless, most associations persist.

WPGMA algorithm performed with Bray-Curtis coefficient was carried out on the sample array in order to determine if abundance data influence clustering (Appendix AVI). Most associations remain stable. Nonetheless, all samples from the four associations with the lowest metazoan content in area counting appear as a single phenon with a low Jaccard value (0.25), which altogether would support similarity; yet this can be explained by means of a high microbialite percentage, which would suppose *a priori* an overall high degree of similarity.

Associations were named after their most representative element (s).
A color key to the facial maps of some selected thin sections can be found in figure 11.
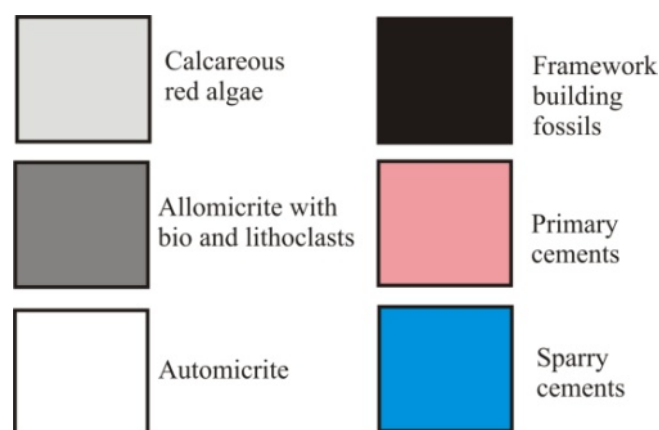
Figure 5: Color chart for the selected microfacial maps. Except where indicated, all microfacial featrures will follow the guidelines of this chart.

5.2.2.1. *Dendronella*–Hexactinellida association (D-H; Misurina)

5.2.2.1.1 Biomorpha (Figs. 6, 7a-b)

This association comprises around 58% of the total area of the analyzed thin sections from the boulders where it can be found. Its abundance is readily detectable due to the conspicuousness of *Dendronella articulata,* which constitutes in average 37% of the total area examined. It displays its typical branching growth form according to the original description by Moussavian & Senowbari-Daryan (1988) and the redescription by Barattolo et al (1993) **(Figs. 6, 7a-b; Pl. I, Fig. 1)**. An

Results

important fraction of microencrusters is associated with the alga and includes serpulid worms and the microproblematica *Plexoramea cerebriformis*, *"Tubiphytes" obscurus* and *Ladinella porata*. While the former two can well be seen within the algal branches settling only in semi-cryptic microenvironments **(Pl. I, Figs. 2-4)**, the latter can only be found on the top of them **(Pl. I, Fig. 5).** Further encrusters include bryozoans which, although they do not constitute a volumetricly important fraction due to their size, are relatively abundant. Taxonomically they belong to one single species, *Reptonoditrypa cautica* Schäfer & Fois, 1987. It can be preferentially found settling on microbialitic crusts **(Pl. I, Fig. 6)**, yet it can also be found attached to brachiopod?-bioclasts **(Pl. I, Fig. 7)**. It could not be found dwelling on the branches of *Dendronella.*
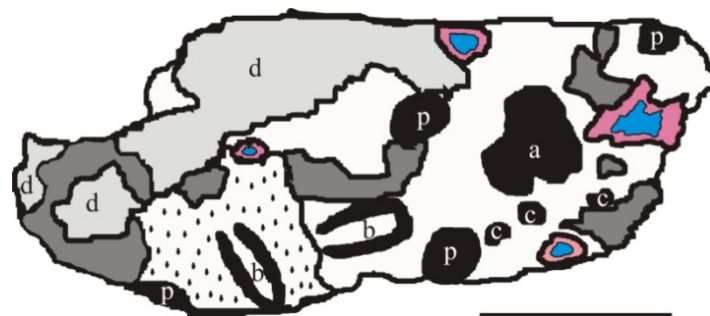
Figure 6. Microfacial map of sample JR III- 58, containing part of the *Dendronella* – Hexactinellida association. Key: d= *Dendronella*; b= bivalve shells; a= *Atrochaetetes medius*; p = *Petrosistroma stearni*; c = undetermined coralline sponges. Note the considerable amount of microbialite and the bivalve shell encased within a hexactinellid mummy. Scale bar = 2 cm.

Typical skeletal frame-builders do not constitute an important part of the association, yet they are not completely absent as in some others (see below). They are represented only by *Atrochatetes medius* **(Pl. I, Fig. 8)** and by forms lacking a clearly recognizable microstructure which show some borings of unknown origin. These forms are possibly related to *Petrosistroma stearni* **(Pl. II, Fig. 1)**.

Although lychniscose Hexactinellid sponges could also be determined due to the presence of spicule pseudomorphs preserved *in situ* **(Pl. II, Fig. 2, 3)**, it was decided to number them among the microbialitic component due to the mode of preservation (e.g. Keupp et al., 1993, Neuweiler; 1993), consisting of Type 2 microbial deposits, with peloids ranging from 30 to 70 μm (average = 40 μm). Associated to this sponge, unrecognizable, autochthonous bivalve shells can be found. Two types of shells were identified. One of them, although not found in life position, does not display significant evidence of reworking, which can mean that it was only slightly transported **(Pl. II, Fig. 4).** However, it shows poor preservation. The other type, also poorly preserved, can be found inside the osculum of this "sponge mummy" (sensu Keupp et al., 1993) **(Pl. II, Figs. 2,3)**. Unfortunately, the state of preservation of the latter shell does not allow a further, deeper classification, which would help in an assertive paleoecological inference on the interaction of the organisms.

The hexactinellid sponge is assumed to have had a vase-shaped skeleton with a central oscular channel, since there are not hexactine pseudomorphs in the middle of it, where one of the shells lies. The micritic grains surrounding the shell constitute a more purly dense, Type 3 leiolitic fabric, and thus, sedimentologically they do not correspond with the pelloidal matrix of the sponge mummy. Some inclusions can be seen in this leiolite. The organic nature of this micrite can be confirmed by its intense fluorescence (**Pl. II, Fig. 5**).

Apart from the presence of hexactinellids (4%), microbialite percentage reaching only 10% at most is negligible in comparison to other associations contained in thin sections. Microbialite mainly grows as Type 2- crusts on the surface of "coralline" sponges, but occasionally, also on *Dendronella.* Numerous diverse microencrusters dwell in these crusts, like *Microtubus communis* (**Pl. II, Fig. 6**) but also abundant *Tubiphytes* cf *obscurus* (**Pl. II, Figs. 7,8; Pl. III, Figs. 1,2**) and *Terebella* cf. *lapilloides* (**Pl. II, Fig. 6, Pl. III, Figs. 1,3**) can be found associated with these microbialitic crusts. Occcassionaly, some encrusting thalamides, which could be assigned to *Uvanella irregularis* are also seen (**Pl. III, Fig. 4**).

5.2.2.1.2. Associated facies

Allochthonous detritus accounts for at most 28% of the analyzed sections. It is mainly composed of non-fluorescent, poorly sorted mudstones-wackestones, often with peloid aggregates, sparse bioclasts which mainly comprise bivalve and thalamid sponge fragments and rare uniseriate foraminifers (**Pl. III, Fig. 5**). It is important to say that most of this mud-wackestones can be found in primary cavities in direct contact with the fossils, but also within primary vugs of the thrombolites. Cements constitute no more than 6% and are mostly represented by granular textures and a late diagenetic ferroan calcitic mineralogy, as revealed by staining with K-Hexacyanoferride . However, sometimes such cements are surrounded by bladed cements. These are interpreted as primary-synsedimentary. Altogether, they tend to form stromatactis or stromatactoid structures with various cement generations, including baroque dolomite. (**Pl. III, Fig. 6**).
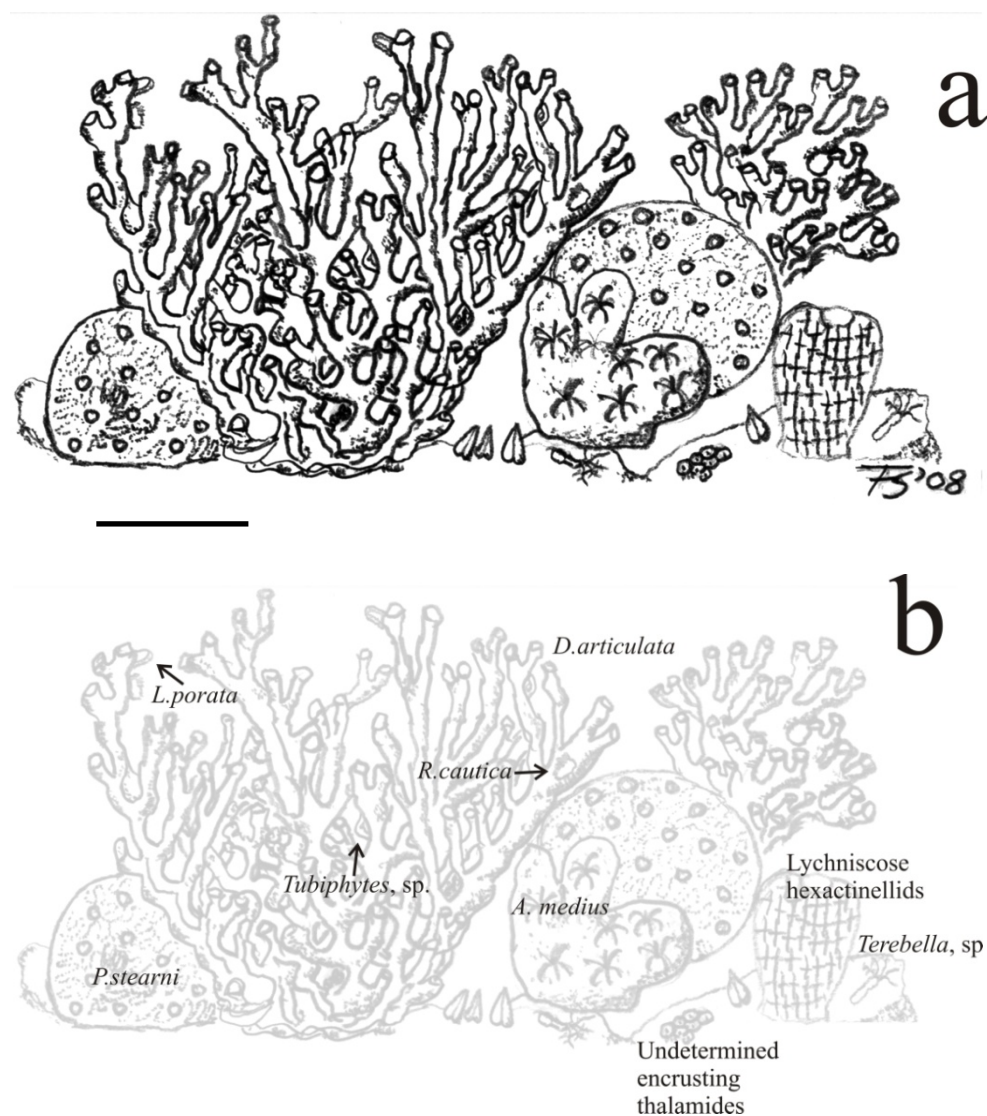
Figure 7: a) Reconstruction of the *Dendronella*- Hexactinellida association. Note the absence of a metazoan dominated framework. Scale bar equals approximately 3 cm. b) Taxonomic explanation for a).

5.2.2.1.3. Discussion

Keupp et al. (1989) made the first description of the hexactinellids from the St. Cassian Formation. Although they profoundly studied the paleoecology of such fauna in the context of the "*Cassianothalamia* Gemeinschaft" (see below) they did not explain the ecological features of the remaining hexactinellids, which are sparsely present (Keupp et al., 1989). Today hexactinellid sponges preferentially settle in deep waters, far below the "normal" wave base. Since red algae may dwell in depths ranging of up to 300 m (Riding, 1975; Round, 1981) and diagnostic organic indications of shallow waters were not found –i.e. green algae- the hypothetic depth of this association is between 100 and 150 m. Further support for this assessment is provided by a similar association of microencrusters (i.e., the *Terebella–Tubiphytes* association) which was also described by Schmid (1996) for the deep water siliceous sponge facies from the Upper Jurassic of Portugal.

The number of fossils is relatively high; however most of them correspond to a branched, non metazoan reef-building organism. On the one hand, Russo (2005) assigned *Dendronella* to have a "not important role" in framework formation. However, Fürsich (2000) conferred *Dendronella* on the other hand to have a reef-building potential, yet he did not give any further explanation in this regard. Nevertheless, his thesis can be confirmed tosome degree by the presence of peloids between the branches, which would eventually lead to framework stabilization. Wendt (1982) found this phenomenon valid for *Cladogirvanella cipitensis*.

As the amount of reef-building organisms is not significant and the most predominant microbialite type is related to a hexactinellid sponge, boulders containing this association most probably originate from a moderately deep carbonate mound under low energy conditions. Unfortunately, some features typical of these mud mounds (e.g. a considerable amount of primary cements and an abundant fraction of automicrite) are not found.

Schmid (1996) found leiolitic microbialite types to be restricted to the siliceous sponge facies. However, because they appear only restricted to a microenvironment within the osculum of the sponge and because they can also be found in shallower settings (Dupraz & Strasser, 1999) no conclusion can be drawn from their presence.

5.2.2.2.   *Ceratoporella breviacanthostyla-Tubiphytes* association (C-T; Seelandalpe)

5.2.2.2.1. Biomorpha (Figs. 8a-b; 9a-b)

Fossil content in this association represents the most abundant facies, which reaches up to 44% of the area/point counting. (Pl. 4) Sponges are the most abundant fraction, reaching almost 30%. Bulbous-domical "chaetetids" with a clinogonal microstructure and *Colospongia* are the most dominant builders among them, yet some specimens ascribed to *Petrosistroma* (compare Reitner, 1992) can also be seen. Above all, the most significant feature is *Ceratoporella breviacanthostyla*, which has a very important role in framework-building and binding. A minor component is *Dendronella articulata.* (**Figs. 8a-b, 9a-b; Pl. III, Figs 7-8**).

Results
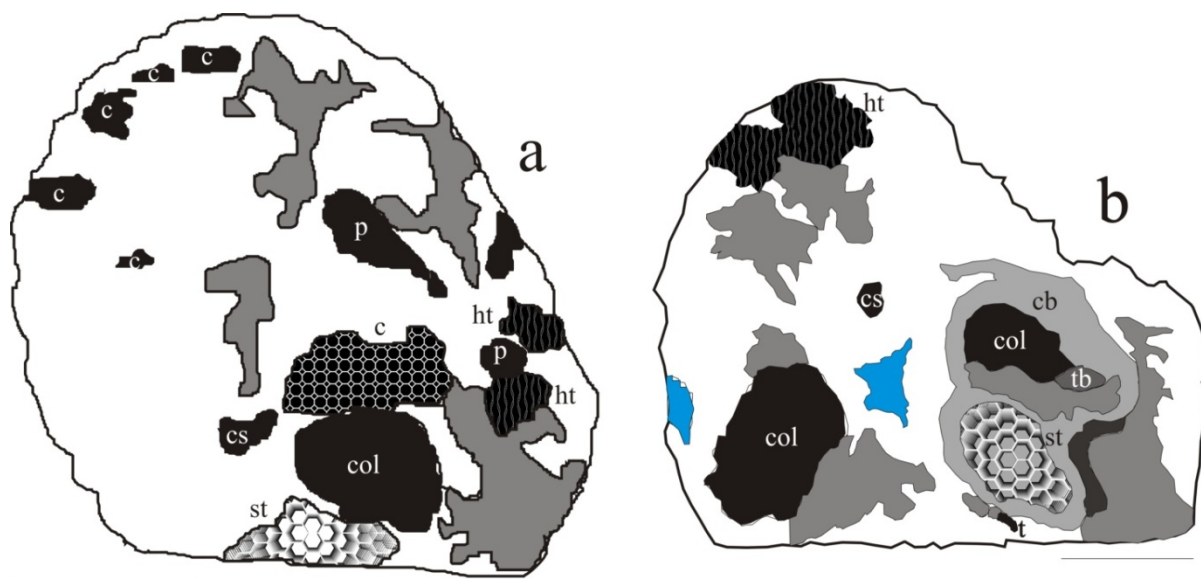
Figure 8: Microfacial maps of samples a) JR III- 19 and b) JR III- 33, containing the *Ceratoporella breviacanthostyla-Tubiphytes* association. Key: cb = *Ceratoporella breviacanthostyla;* col = *Colospongia,* sp., ht = *Hispidopetra triassica*; p = *Petrosistroma stearni;* tb= thecideid brachiopods; c = undetermined chaetetids; cs = undetermined chaetetid sponges; t = undetermined encrusting thalamides. In blue, secondary cements. A relatively massive microencruster framework is represented in 7b in dark grey. Scale bar = 2 cm.

A moderately diverse encrusting guild mainly composed by microencrusters can be detected in this association. While *Tubiphytes* (**Pl. IV , Fig. 1**) and some serpulid tubes and sponges (such as several *Uvanella* –like and other undeterminable thalamides (**Pl. IV, Figs. 2-4**)) can only be found on and sometimes even within the skeleton of *Ceratoporella breviacanthostyla*, others like *Koskinobullina socialis* and *Girvanella* may also be located on other substrates, such as chaetetides and even on thrombolites (**Pl. IV, Fig. 5-8**). Due to the small size of the microencrusters, it is noteworthy that their abundance can be as high as 4%. Identification of *Ceratoporella breviacanthostyla* was possible due to the typical ceratoporellid microstructure and to the presence of short acanthostyles. (**Pl. V, Figs. 1-2**; compare Reitner, 1992). Further sponges in the association are *Hispidopetra triassica*, which encrusts on *Petrosistroma*? (**Pl. V, Fig. 3**). All observations within this work confirm that when *Hispidopetra triassica* is found *in situ*, it is always found encrusted on hard skeletal substrates – sponges- and never on microbial carbonates.

Microbialites are represented by thrombolitical growth forms (Types 1 and 2), but never by stromatolites. Together they constitute 45% of the area counting fraction. Type 2 thrombolite is by far the most abundant type. Type 3 leiolitical fabrics can occasionally be observed only as crusts on builders developing into, or mixed with a thrombolitical growth pattern (**Pl. V, Figs. 4-5**; compare Schmid, 1996). It is noticeable that *Microtubus communis* borings can only be found at such leiolitic

fabrics, which are directly bound to skeletal frameworks (**Pl. V, Fig. 6**), but they are completely absent in thrombolitic formations

5.2.2.2.2. Associated facies

Allochthonous components are present in low quantity, reaching no more than 26%. They are represented mainly by poorly sorted mud- to wackstones lying within primary vugs (**Pl. V, Figs. 7-8**). among the automicrite/microbialite. Unrecognizable gastropod and bivalve fragments can also be found there. Sparse foraminifer oncoids can be found within this detritus as well as free foraminifers, peloid aggregates, and very few siliciclastic remains Clasts are subrounded to subangular. The presence of ammonoid remains is however remarkable. A sphaerulitic microstructure can still be found (**Pl. VI, Figs. 1-2**). Sphaerulites range in size from 40 to 60 μm in diameter.

Microsparite, with 1.5% of the total area counting, does not seem to have played an important role in the microfacial interpretation/composition of the association.
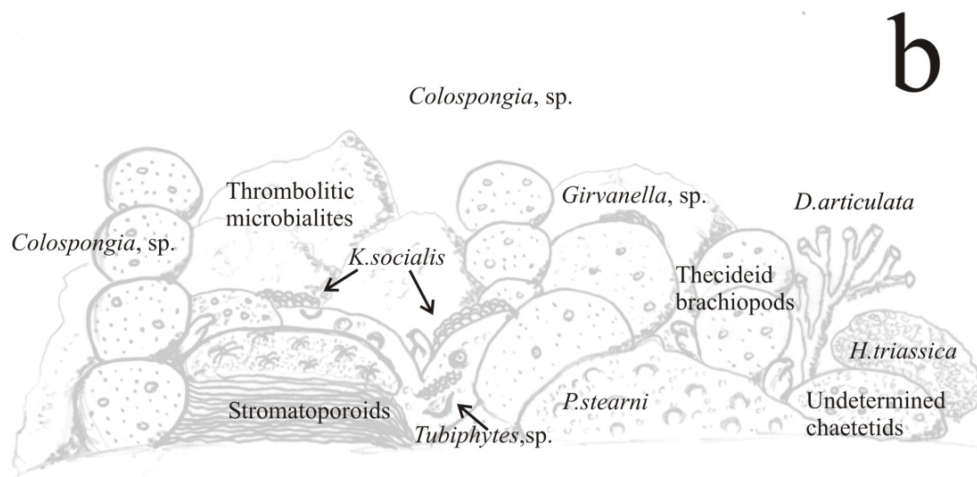
Figure 9: a) Reconstruction of the *Ceratoporella breviacanthostyla- Tubiphytes* association.Note the proportional similarities between microbialites and metazoans. Scale bar equals approximately 1 cm. In circle: Reconstruction of *Microtubus communis* in leiolitic substrate. Scale bar equals approximately 200 μm. b) Taxonomic explanation for a).

5.2.2.2.3. Discussion

It is difficult to assess particular paleoenvironmental conditions for this association, since none of the facies present here provide sufficiently deep diagnostic criteria. Different microbialitic fabrics – leiolitic and thrombolytic - may point to differential conditions either in the sedimentation or in the bacterial associations producing biomineralization. However, Schmid (1996) noted a strong relationship of thrombolites and leiolites and concluded genetic reasons as the cause for their similarities. The presence of both mudstone-wackstone and packstone-grainstone facies within the allochthonous material supports both low- and high-energy depositional events. In this respect, it must be stressed that encrusting skeletal organisms are generally more adapted to high energy conditions than erect ones (James & Bourque, 1992; Flügel, 2004), being sponges specially sensitive to this factor (Turón et al, 1998; Tanaka, 2002). However, this statement is only applicable to "massive" skeletal builders and not to microencrusters (Schmid, 1996; Schlagintweit & Gawlick, 2008, Reolid et al., 2009). Furthermore, this does not mean that sponges with an encrusting skeleton -such as *Ceratoporella breviacanthostyla*- belong exclusively to high energy-environments (Schumacher & Plewka, 1981; Bell & Barnes, 2003). Since a considerable part of the fossil area in thin section is represented by encrusting organisms and no branched / baffling organism was found, middle- to high-

energy level episodes can be concluded. Further indications of these conditions are the morphology and degree of sorting of the clasts within the allochthonous micrite.

The depth from which this association comes is indeterminate, since neither *Girvanella* nor any other algae present here are diagnostic for depth. Yet their abundance is lower than in other associations. A similar association was described by Schmid (1996), which he assigned to middle- to high-energy environments within the upper part of a ramp above the storm wave base. However, because some microencrusters that are diagnostic of light-influenced environments, such as *Baccinella* or *Lithocodium* (Leinfelder et al., 1996; Koch et al, 2002; Götz et al., 2005; Conrad & Clavel, 2008) are missing, a deeper position may be suggested.

Another possible scenario would be an environment under sub cryptic/low light conditions at the entrance of a reefal cave (compare Reitner, 1993). Recent associations (Hartman & Goreau, 1970; Goreau et al., 1971; Jackson et al; 1971; Lüter et al., 2003; Logan, 2008) as well as fossil associations (Keupp et al., 1989) have been widely described in the literature as containing similar faunal components that dwell either in reef crevices or caves, where organisms dependent on light experience harsher living conditions. Conditions of total darkness can be excluded due to the abundant presence of *Koskinobullina socialis*, since it can dwell in both semi cryptic environments as well as in environments rich in light (Schmid, 1996; Schlagintweit & Gawlick, 2008).

Whether *Microtubus* had dwelled better on hard microbial carbonates or in mud leiolitical fabrics, remains unknown. The fact that neither synsedimentary cements nor any other feature described in Neuweiler (1993) which assesses previous lithification of a microbialite, can be found in the leiolitic fabrics of this association, suggests that this fabric may be interpreted as the original sediment to have been soft at the time of the colonization by *Microtubus* (Schlagintweit & Gawlick, 2009).

5.2.2.3.   Cryptocoelia zitteli–Mesophylum association (C-M; Misurina)

5.2.2.3.1. Biomorpha (Figs. 10, 11 a-b)

Fossils in this association reach up to 40 % (36% in average) area abundance. The most prominent features are the patches of the corallinacean algae attributed to *Mesophyllum*, which normally constitute more than half of the total content of fossils. Thus *Dendronella articulata* is here not the primary algal component, yet it is also present and it can be found in patches. **(Figs. 10, 11a-b)**

Results

Sponges are also an important fraction of this association. *Cryptocoelia zitteli* (**Pl. VI, Fig. 3**) appears as the dominant type, yet also *Corynella* is also abundant (**Pl. VI, Fig 4**). Branched chatetids with a ceratoporellid structural growth (occasionally without tabulae - **Pl. VI, Fig 5**) are present in smaller quantity. Encrusting thalamides are a common feature of the association and mainly settle on *Cryptocoelia* (**Pl. VI, Fig 6**) but also within the cryptic voids of *Mesophylum* (**Pl. VI, Fig.7**).

In the case of the whole association, the highest frequency of encrusters corresponds to bryozoans, especially of *Reptonodytrypa cautica*, which dwells in the opposite way of thalamid encrusters, that is, they settle primarily in the vugs of *Mesophyllum* and not so frequently on the surface of *Cryptocoelia*. A further encruster of this thalamid sponge is *"Tubiphytes"* cf. *obscurus*, which can only seldom be seen (**Pl. VI, Fig 8**)

Microbialite fraction is represented by Type 2 thrombolitic structures, <5% of the total. The almost complete absence of *Microtubus* within microbialites is remarkable, in comparison to other associations where its presence is a distinctive feature. In contrast, serpulid worm tubes (**Pl. VII, Fig. 1**) and *Baccanella floriformis* (**Pl. VII, Fig 2**) can be located dwelling in microbialite. Just as in the *Dendronella*- Hexactinellida Association, lychniscosid spicules contained on a peloidal- matrix (possible relicts of another "sponge mummy") can also be seen. (**Pl. VII, Fig. 3**).
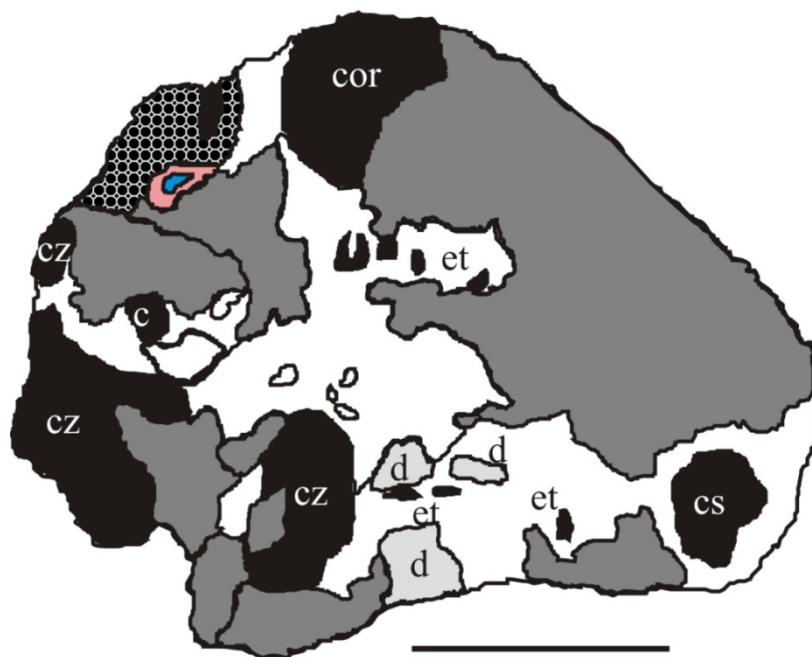
Figure 10: Microfacial maps of sample JR III- 43 containing the *Criptocoelia zitteli - Mesophylum* association. Key: cz = *Cryptocoelia ziteli;* cor = *Corynella* sp.; c = undetermined chaetetid sponges; cs = undetermined coralline sponges; d= *Dendronella articulata;* et = encrusting thalamide sponges. Microbialite content in this association is represented by net-patterned black surface, whereas white corresponds to the suface covered by *Mesophyllum*, sp. Scale bar = 3 cm.

5.2.2.3.2. Associated facies.

Allochthonous materials in these thin sections are abundant (up to 50% of the total area) and possess a rich component variation. They are primarily characterized by wack-packstones rich in bioclasts which primarily include *Mesophylum* fragments, undeterminable gastropods, serpullids, echinoid spines, bivalves, bryozoans (including *Reptonoditrypa* and a further, undeterminable type), *Tubiphytes* cf. *obscurus*, fragments of thecideid brachiopods and also relatively abundant siliciclastics and very diverse foraminifera, including miliolids like *Lameliconus* cf. *cordevolicus* and seldom oncoids (**Pl. VII, Fig 4, 5**). These allochtonous components can be found in immediate contact to *Mesophylum* and "coralline" sponges, but also as fillings within primary microbialite vugs, where the clast diversity is not so high. Pyrite framboids can occasionally be seen.

Cements are relatively widespread (7%), and mainly consist of blocky late diagenetic calcite, within the microbialite and inside the conceptacles of the coralline algae. However some primary cement microcrystalline high Mg-calcite crusts can occasionally be found. Neomorphic microsparite accounts for <1% of the total and is not supposed to have played an important role in the total environmental determination of the association.

Results
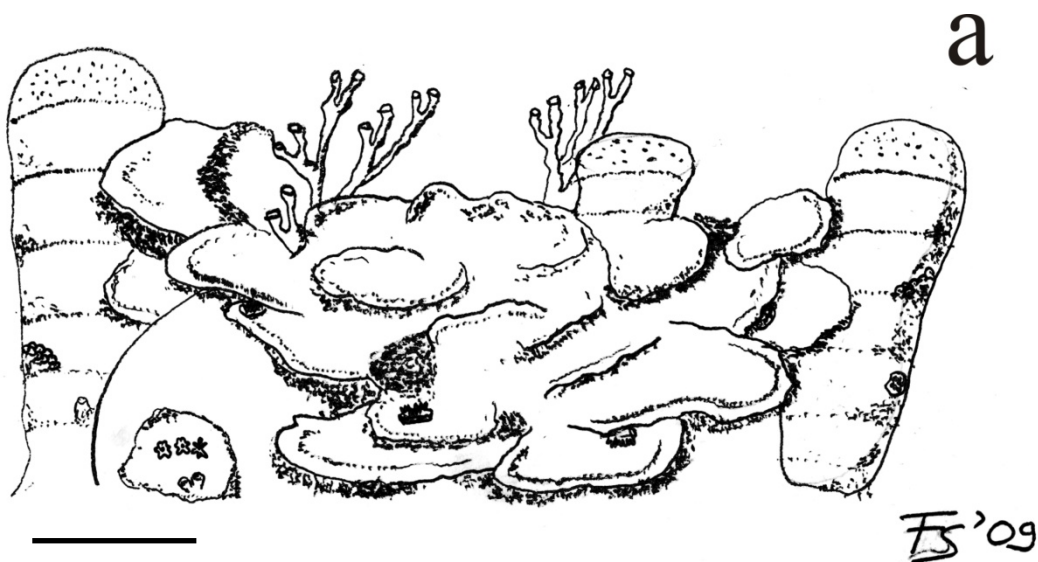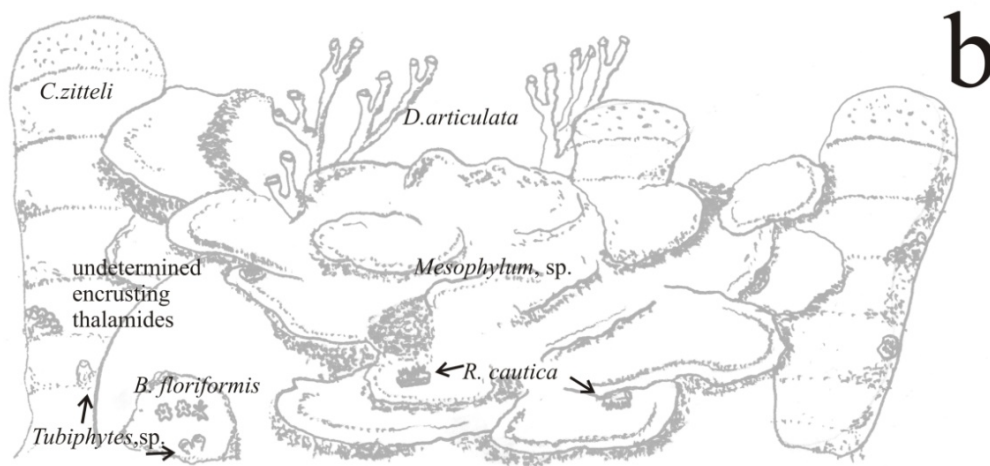
Figure 11: a) Reconstruction of the *Cryptocolia zitteli Mesophyllum* association. Note that a microbialite framework is almost absent and the algal component predominates. Scale bar equals approximately 2 cm. b) Taxonomic explanation for a).

5.2.2.3.3. Discussion

The presence and abundance of crustose algae may support the interpretation of an environment which could withstand high energy conditions (e.g. Flügel, 2004). This can be confirmed by the heterogeneity regarding the size and nature of the grains within the allochems, and by the presence of microcrystalline cements (Flügel, 2004). Although no evidence of boring organisms could be found, all other variables permit such an interpretation. Microencruster associations are noteworthy, since thalamides and *Reptonoditrypa* predominate. Another diagnostic microencruster for high energy environments is *Baccanella floriformis* (Riedel, 1988; Brandner et al., 1991; Martini et al., 2004). Otherwise, no microencruster occurs significantly, or any at all. *Tubiphytes* occurs only associated to *Cryptocoelia zitteli*, a feature already observed by Müller Wille & Reitner (1993), who interpreted it as a commensalistic relation.

All this could mean that this association is related to medium- to high-energy levels. The shape of the bryozoans, being unilaminar, (Smith, 1995) further supports this assumption.

However, the presence of hexactinellid sponge spicules in peloidal matrix would support low energy conditions, since no evidence of adaptation to a high energy environment in hexactinellids (Reif & Robinson, 1976) could be found within the spicules. This could be explained in context of changing conditions, in the following way: An association represented by *Baccanella floriformis,* patches of *Mesophyllum* and *Dendronella articulata* could have settled under the onset of high-energy conditions and then on the last step, a mid-depth to deep-water association (~ 100 m) of hexactinellids was preserved in, as peloidal microbialite. This could have happened by means of sea level change, continouously reported in the literature in St. Cassian platforms. (e.g. Biddle, 1984; Bosellini, 1984).

Nonetheless, some hexactinellids can withstand continuous high energy conditions, adopting very dense compact forms. (Austin et al, 2007). This could be applied also for other sponges, like *Cryptocoelia zitteli,* though maybe due to the lack of morphological plasticity of most thalamides, such conditions have never been reported. However, energy conditions could have been different without a sea level change. In this way, temporary low-energy events would have allowed the establishment of hexactinellids, which then would have died during high-energy events. Unfortunately, more specificy conditions cannot be obtained from the hexactinellid, since the body of the sponge cannot be reconstructed due to the scarcity of the spicules found.

5.2.2.4. *Cladogirvanella*–**stromatolite association (C-S; Pralongia)**

5.2.2.4.1. Biomorpha (Fig. 12)

In this association, fossil content is neither so abundant, nor so diverse as in others. Area Counting average percentage covered by fossils reaches no more than 22 % and it is widely dominated by algae, particularly by *D.articulata*. However, huge and conspicuous patches of *Cladogirvanella cipitensis* can also be seen (**Pl. VII, Fig. 6**). Peloid binding potential can be seen for both species. (see also *Dendronella* – Hexactinellida association). Sponges are the other significant fraction among the fossils. However, in comparison to other associations, their diversity and porportional abundance is much lower.   They are represented by additional undeterminable chaetetids with a ceratoporellid structure (**Pl. VII, Fig. 7**). Otherwise they are scarce (**Figure 21**).

Also serpulids can be found in an encrusting complex composed of aragonitic synsedimentary cements/*Murania* (**Pl. VII, Fig. 8**). Reitner & Keupp (1989) argue that encrusting coralline sponges have usually a cementing role in reef frameworks and can never be found on primary vugs. Crusts found in this association are always found in a tight relationship to microbialite Type 3 crusts and are never in direct contact with primary vugs. However, no spicules could be found. Nevertheless, the fact that spicules are absent, does not constrain the cementing role of these crusts. Additional encrusters include a *Terebella /Tubiphytes* close association, which dwells exclusively in thrombolites. (**Pl. VIII, Figs. 1-2**). *Terebella* cf. *lapilloides* binds exclusively peloids (**Pl. VIII, Fig. 3**).

Results
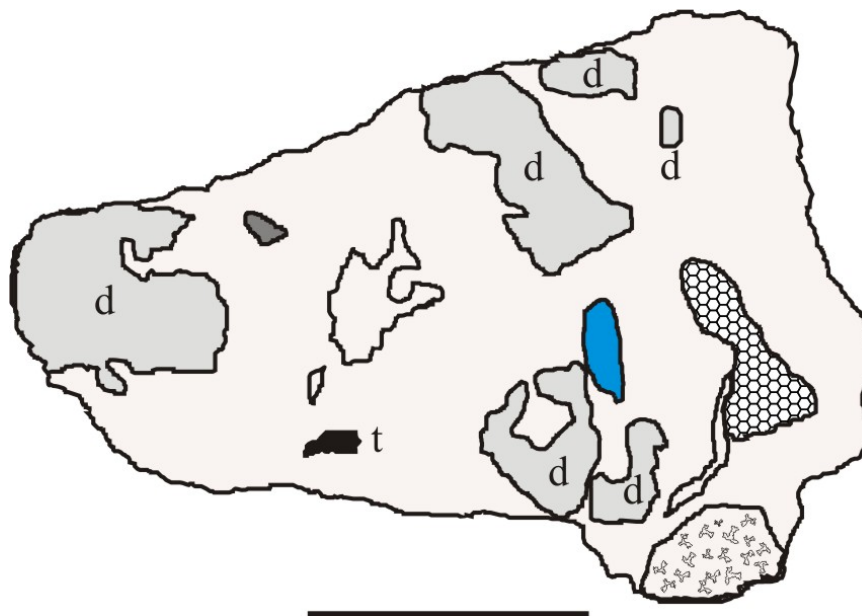
Figure 12: Microfacial map of sample JR III- 88 containing the *Cladogirvanella cipitensis* - stromatolite association. Key: d = *Dendronella articulata.* t = encrusting thalamides. In a hexagonally patterned filling: undetermined ceratoporellid chaetetids. Note lithistid sponge at lower right. Microbialite content in this association is represented mostly by peloidal stromatolites. Scale bar = 3 cm.

Microbialite however, is very abundant. Three types can be identified. The most abundant of them is a Type 4 stromatolite which can be found growing both as crusts on framework builders and associated to *Dendronella.* Peloids have a size of 30 – 80 μm (mean = 40 μm). An alternation of peloid layers and microcrystalline cements can be seen. Type 2 thrombolites are often associated to *Cladogirvanella cipitensis* and sometimes also to indeterminate bacterial? filaments that have a mean length of 120 μm and mean width of 10 μm. (**Pl. VIII, Fig 4**). The additional microbialites are the Type 3 leiolitic fabrics that are parts of the encrusting complexes above lithistids. Altogether, microbialitesand automicrites, respectively, reach ca. 70% of the component analysis.

5.2.2.4.2. Associated facies

The percental fraction consisting of cements, allocthtnonous components and microsparite (<7%) is much smaller in comparison to most facies types. Regarding the cements, late diagenetic sparry calcite infillings present inside geopetal cavities are the most abundant, while primary synsedimentary cements may be seen at the encrusting complexes described above. Allochthonous detritus are thought to have undergone neomorphic processes described by Folk (1958) and reviewed by Rech (1998) for samples from Pralongia at the Cassian Beds, and thus to have transmuted into microsparite. Most of the vugs containing microsparite still have allocththonous components, mainly loose peloids and *Tubiphytes* cf. *obscurus* fragments (**Pl. VIII, Fig. 5)** as well as sparse coralline sponge debris.

5.2.2.4.3. Discussion

Although some algae could be found, none of them are diagnostic of shallow depths. Hence the interpretation of the paleoenvironment of this association is somewhat difficult. Not all stromatolites exclusively depend on light. (Keupp & Arp, 1990; Böhm & Brachert, 1993; Maliva et al., 2000). The presence of some microencrusters associated to thrombolites (*Terebella-Tubiphytes*) have been repeatedly found in deep settings. (Leinfelder et al.,1993, 1994; Schmid, 1996; Dupraz & Strasser, 1999; Olóriz et al., 2003). However, this is not so exclusive for these microencrusters as low energy conditions are (Pratt, 1995; Schmid, 1996; Olóriz, 2006).

Similar stromatolite and algae-dominated biofacies have been studied for the Triassic of the Dolomites, in particular those found at the Mahlknecht Cliff by Brandner et al. (1991) and Russo (2006), where *Cladogirvanella* and *Tubiphytes* associations are common. However, no indication for the depth is specified in these studies. On the contrary, Brachert & Dullo (1991, 1994) found similar crusts in triassic as well as in recent deep (150– 50 m) marine settings. Since red algae can thrive up to a depth of 360 m, (Riding, 1975, Round, 1981), a deep setting between 100 and 200 m would in principle be inferred for this association.

The growth orientation of the stromatolites, as well as of *Cladogirvanella* and unknown filaments among the microbialites and the erected thallus of *Dendronella* nevertheless support light–influenced conditions. Similar associations have been described by Senowbari- Daryan et al. (1983) for the Norian in Sicily.

Thus, either achieved by temporary emersion or by constant shallowness, the *Terebella-Tubiphytes* association would easily be attributed to a quiet shallow setting, which would not contradict its described thriving environment (Schmid, 1996; Dupraz & Strasser, 1999; Olivier et al., 2008). Modern terebellids can also thrive in shallow settings. (Garaffoni & Lana, 2003). The scarcity of metazoans would, in this case, point to a back reef setting, due to the scarcity of metazoans and the abundance of porostromate algae (Chablais et al., 2010).

5.2.2.5.   Thrombolite-microencruster association (T-M; Misurina)

5.2.2.5.1. Biomorpha (Figs. 13, 14a-b)

Dominant facies in the boulders where this association appears is microbialite, averaging 71%. Type 2 is the most frequent type. Peloids range from 20 to 100 mm in size (average = 50 mm) Occasionally *Tubiphytes* and *Planiinvoluta* (**Pl. VIII, Figs. 6-7**), sparse nubeculariids and *Terebella* cf. *lapilloides* can only be seen in this kind of microbialite. Microbialite Type 4 also appears, yet very rarely. While

Results

Alpinophragmium and *Koskinobullina socialis* encrustations can only be seen associated with microbialite Type 2 (**Pl. VIII, Fig. 8; Pl. IX, Figs. 1-2**), Type 3 leiolitic fabrics appear only associated with frequent *Microtubus* borings (**Pl. IX, Fig 3**). Pyrite framboids are very common. (**Pl. IX, Fig 4**). (**Figs. 13, 14 a-b**).

Apart from the mentioned microproblematica and foraminifera, fossils are rare. They comprise only 15% of the analyzed thin sections and are represented only by the coralline sponge *Praecorynella* as well as by few fragments of the alga *Dendronella articulata*. It is, however, not clear if these fragments grow *in situ* or rather are allochthonously incorporated in the framework.
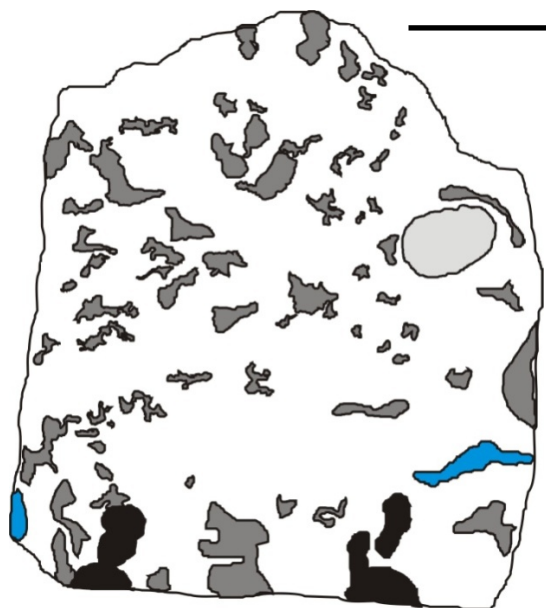
Figure 13: Microfacial map of sample FS-MI 6, which contains the Thrombolite – microencruster association. Ceratoporellid chaetetid sponges are represented by hexagonal-patterned filling. Scale bar = 2 cm.

5.2.2.5.2. Associated facies

All microbialite is frequently embossed with fibrous and botryoid cements, presumably of aragonitic origin (**Pl. IX, Fig. 5**). However, the most frequent type is blocky spar cement. Nevertheless, content of cements is altogether < 1%.

Allochthonous material consists almost entirely of micrite, peloids and peloidal aggregates. In general, it proved difficult to distinguish allochthonous detritus from microbialite, especially due to the epifluorescence properties it exhibited. However, fluorescence displayed by microbialite was higher.
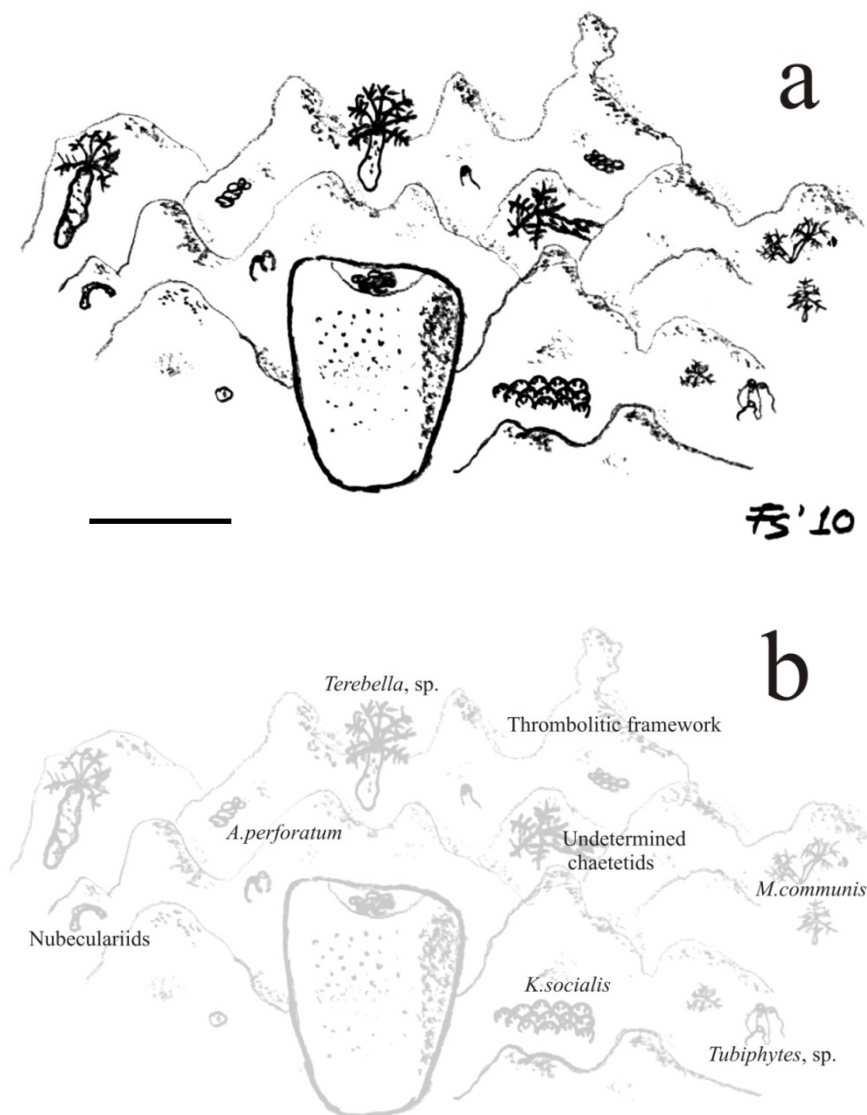
Figure 14: a) Reconstruction of the Thrombolite–microencruster association. Note the diversity of microencrusters and that a metazoan framework is almost absent – except rare *Precorynella* appearances, here depicted once. Scale bar equals approximately 3 cm. Microencrusters not to scale. b) Taxonomic explanation for a).

5.2.2.5.3. Discussion

Since no considerable skeletal framework could be assessed, algae could seldom be found and microbialite is the most conspicuous facies, in principle this association could have originated at a deep, low energy «mud-mound» setting (Reitner & Neuweiler, 1995). However, stromatactis/stromatactoid cavities, which are often characteristic of these settings, are completely absent. Neuweiler et al. (2001) described mud mounds from the Basque Country in northern Spain that are poor in stromatactis or completely devoid of them, arguing that geopetal cavities resulting from

internal sediment could be their equivalents. Nevertheless, stromatactoid or geopetal cavities are also absent.

Neuweiler (1993) described a reef setting from the Albian in northern Spain, where microbialites acted as main builders, making baffling and binding subordinate. Therefore, this possibility also remains plausible for the origin of this association.

Similar associations were described by Aurell & Bádenas (2004) for the Kimmeridgian of NE Spain, which were interpreted as shallow reef settings in principle. Nevertheless, they noticed a high abundance of *Tubiphytes* and *Terebella* as the depth increased. Nicol (1987) found shallow coral-based reef communities containing *Alpinophragmium* strongly associated to *Tubiphytes* and abundant calcareous algae in the Norian of the Northern Calcareous Alps. Regarding *Alpinophragmium,* it should however not be considered as an encruster which is diagnostic for depth conditions, since it appears to have had a broad paleoecological distribution in reef facies (Senowbari-Daryan et al, 1983), though it is often associated to particular coral genera (Stanton & Flügel, 1987). Nevertheless, the presence and abundance of these encrusters associated to the few *Koskinobullina socialis* and on the other side, to the scarcity of algae suggests that the boulders containing this association would have originated at a mid- to deep ramp low-energy microbialite- reef setting, perhaps also poor in oxygen.

5.2.2.6. Cassianothalamia Gemeinschaft II (C-G II; Misurina)

5.2.2.6.1. Biomorpha (Figs. 15, 16a-b)

The most abundant facies in the samples where this association can be found is microbialite (53%). Microbialite is almost solely represented by Type 2, which is encrusted to a great extent by a diverse microencruster association (**Pl. IX, Figs. 6-8; Pl. X, Fig 1-3**), which includes *Baccanella floriformis,* some *Tubiphytes, Ladinella porata, Alpinophragmium perforatum, Reptonoditrypa cautica, Terebella* cf. *lapilloides, Girvanella*–like porostromate filaments and undetermined thalamides. Small amounts of microbialite Type 4 can however be found closely associated to the remains of a hexactinosid sponge mummy (**Pl. X, Fig. 4**), which encrusts the metazoan framework, and Microbialite Type 1 fabric is exclusively linked to lithistid spicules. (**Pl. X, Fig. 5**). This framework apparently belongs altogether to the association originally described as the "*Cassianotalamia* Gemeinschaft" (Keupp et al., 1989) and is further described as being represented by ceratoporellid chaetetids, *Reptonoditrypa,* unidentifiable coralline sponges, *Uvanella*- like encrusting thalamides and tetraclone lithistids. A small proportion (10%) of these organisms belongs to *Cassianothalamia zardinii* and the coral *Thecosmilia*. A vase-formed structure made of pelloids can also be seen. However, related spicules

could not be found in this structure, yet they could have belonged to a hexactinellid? sponge (**Pl. X, Fig. 6**).

Remains of the activity of boring organisms can also be observed (**Pl. X, Fig. 7**), as well as some *Aka cassianensis* spicules (**Pl. X, Fig. 8**, compare Reitner & Keupp, 1991). Pyrite crystals can also be detected at some microbialite layers.
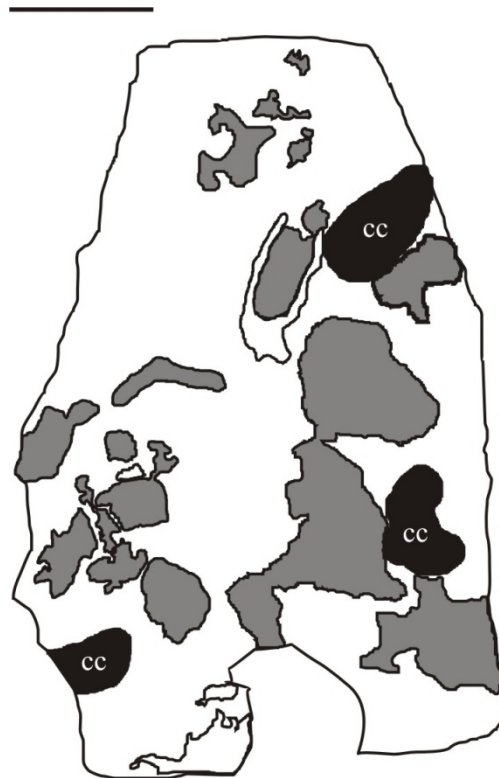
Figure 15: Microfacial map of sample FS-MIV-3, which contains the *Cassianothalamia* Gemeinschaft II . Legend: cc: ceratoporellid chaetetid sponges. Scale bar = 2 cm.

5.2.2.6.2. Associated facies.

Cements are represented by thread-like structures (Rech, 1998), aragonitic botryoids and sparry calcite crystals. Although they do not reach an important fraction of the boulder, some stromatactis and stromatactoid structures could be identified. (**Pl. XI, Fig. 1**)

Allochthonous components consist of mud-wackestone infillings of the primary and secondary vugs mainly left by the microbialite and they are composed of micrite, pelloid aggregates, scarce serpulid remains and isolated uniseriate foraminifers.

Microsparite, present at a content of 1% does not play an important role in the interpretation or the analysis of this association.
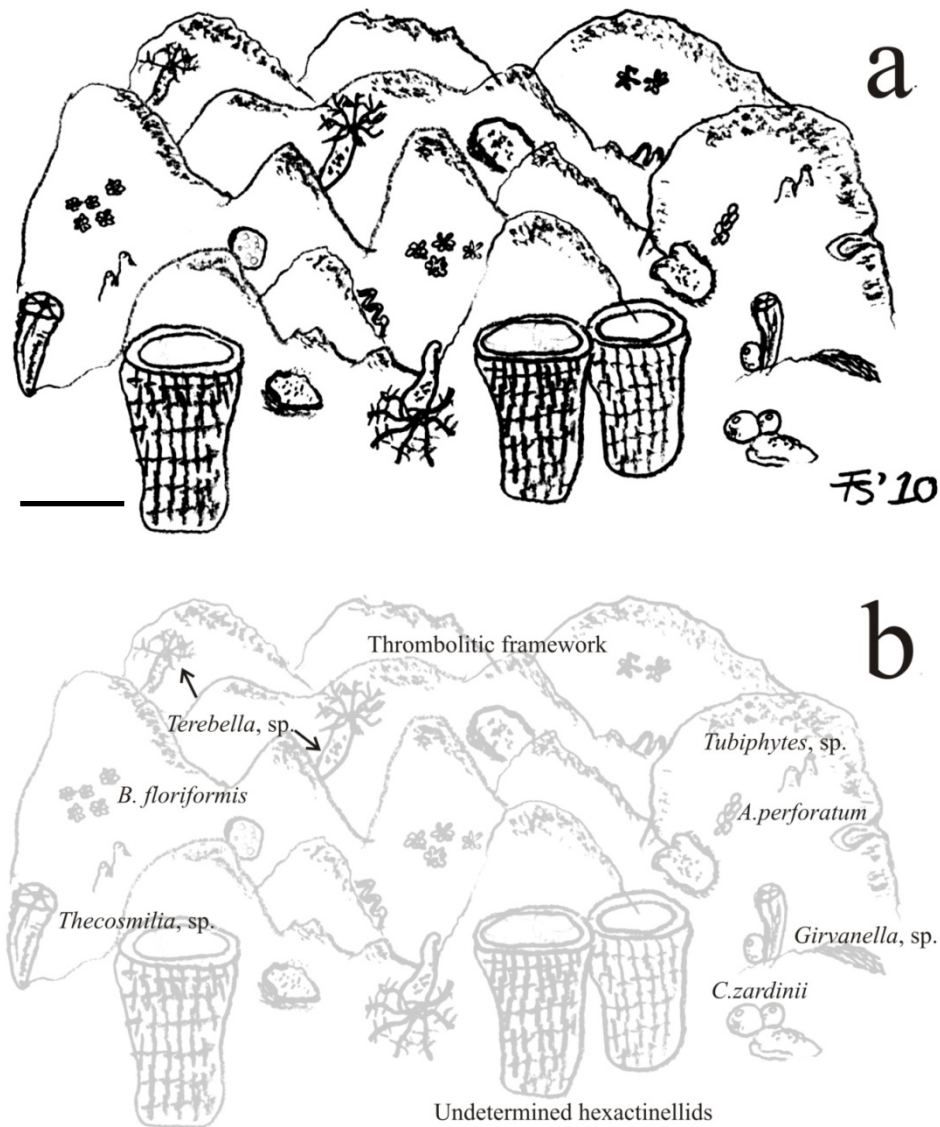
Figure 16: a) Reconstruction of the *Cassianothalamia* Gemeinschaft II. Note the predominance of a microbialitic framework as well as the diversity of microencrusters. Scale bar equals approximately 2 cm. Microencrusters not to scale. b) Taxonomic explanation for a).

5.2.2.6.3. Discussion

The *Cassianotalamia* Gemeinschaft has been assigned to cryptic or deep environments due to the scarcity of algae associated to it (Keupp et al., 1989). The presence of some microencrusters like *Terebella* and *Tubiphytes* in association with the hexactinellid sponge support the interpretation of a deep, low-energy setting as the original paleoenvironment. However, some criteria are inconsistent with the assumption of a constant low-energy environment, especially the presence of both *Baccanella floriformis* and *Reptonoditrypa cautica* which could be explained on the basis of sporadic conditions of moderate energy.

The proportional abundance of metazoans in this association must be compared with the original description of this *Gemeinschaft* from Keupp et al. (1989) who described it as a-framework dominated by metazoans. The proportion of microbialite is much higher here than in the one inferred from the original description by Keupp et al. (1989) and hexactinellid as well as lithistid spicules appear associated with this microbialite, so that this association can be characterized as having not originated in a shallow setting under low- to mid-energy conditions, but possibly from a bathymetrical zone where both lithistids and hexactinellids can be found (Krautter, 1997) and where light was still present (due to the diversity of *Girvanella*-like microencrusters and the presence of algae together). Since hexactinellids are scarcer in the material containing the *Cassianothalamia* Gemeinschaft s.s. than in this association, a direct proportion between both the abundance of microbialite framework and Hexactinellida –and therefore deep settings-, can be assumed.

Similar sponge-microbialite associations have been already identified in the Ladinian from Catalunya; Northeastern Spain (Calvet & Tucker, 1995).

5.2.2.7. Patch Reef Association I (P-R I; Misurina, Seelandalpe)

5.2.2.7.1. Biomorpha (Figs. 17, 18a-b)

Fossils constitute the dominating fraction in this association, occupying at most 62% of the area in thin sections and being represented by an extense diversity of builders. Bulbous and conical stromatoporoids assigned to *Balatonia* sp. are the most abundant among them (**Pl. XI, Fig. 2**), yet undeterminable branched chaetetid sponges and the thalamid *Eudea polymorpha* also account for the main reef –builders. The alga *Dendronella articulata* and scleractinians, represented by *Thecosmilia*, and *Margarophylia* (**Pl. XI, Fig. 3**)*,* only play a minor role. Striking here is, however, the abundance and diversity of encrusting sponges, which include *Murania kazmierczaki* and three different encrusting skeletons, possibly related to *Ceratoporella breviacanthostyla* (**Pl. XI, Fig. 3-6**)*.* Thalamid sponges other than *Eudea* are rare, and are only represented by *Vesicocaulis,* sp. and some unidentifiable encrusting forms.

Results
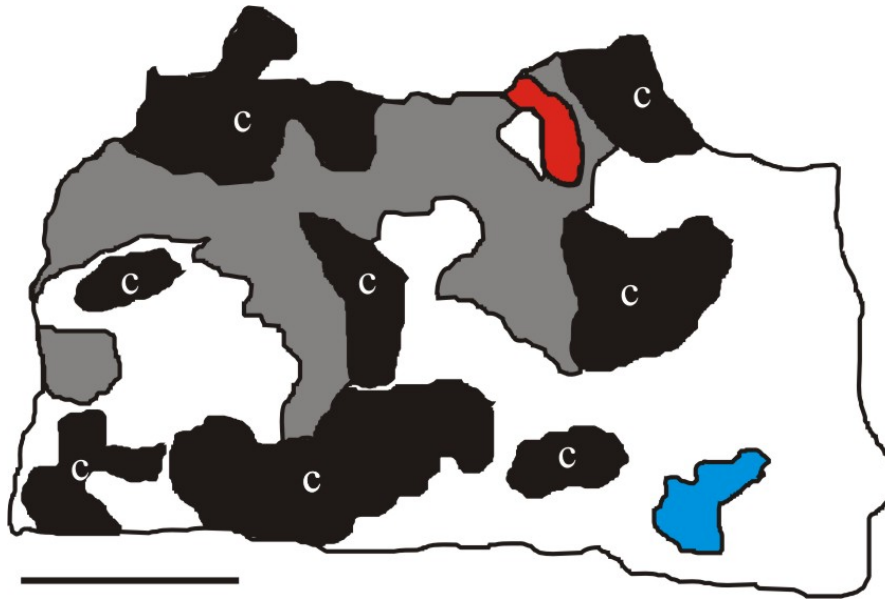
Figure 17: Microfacial map of sample M IX-2 containing part of the Patch Reef association II . Legend: c= undetermined chaetetid sponges. In red, an encrusting coralline sponge, possibly assignable to *Ceratoporella*. Note the prominent sponge fraction, which is a constant in all samples containing this association. Scale bar = 2 cm.

Microencrusters are also abundant, yet not so diverse, and enclose *Koskinobullina socialis*, *Planiinvoluta*, and two undeterminable types of porostromate filaments. *Planiinvoluta* is strongly associated to *Murania kazmierczak* – microbialite crusts (**Pl. XI, Figs. 3, 7-8**) while *K. socialis* takes only stromatoporoid skeletons and ceratoporellids as substrate (**Pl. XII, Fig. 1**)**.**

Microbialites are thus reduced (15%). They can be found as primary encrustations on main reef builders. Their texture can be assigned to Type 2 and is frequently bored by unknown tubes. (**Pl. XII; Fig. 2**). However, some Type 3 leiolites are strongly associated to the surface of some corallites. The occasional presence of s phylloid algae (**Pl. XII; Fig. 3**) encrusted onto a stromatoporoid along with microbialite is also noticeable.

5.2.2.7.2. Associated facies.

Allochthonous material is composed by packstone-wackestone infillings in primary vugs. It includes medium-sorted bioclasts (gastropod skeletons, bivalve fragments and crinoid stalks) as well as quartz fragments and several peloidal aggregates. It accounts for no more than 20% of the total area of the analyzed sections.

Cements are almost absent. Primary cements have a bladed morphology and can be found associated with microbialites. Secondary cements are more conspicuous and consist of blocky sparry calcite infillings mainly found in secondary vugs.

This sample has an overall poor preservation, which can be assessed especially in some diagenetically affected locations in stromatoporoids.
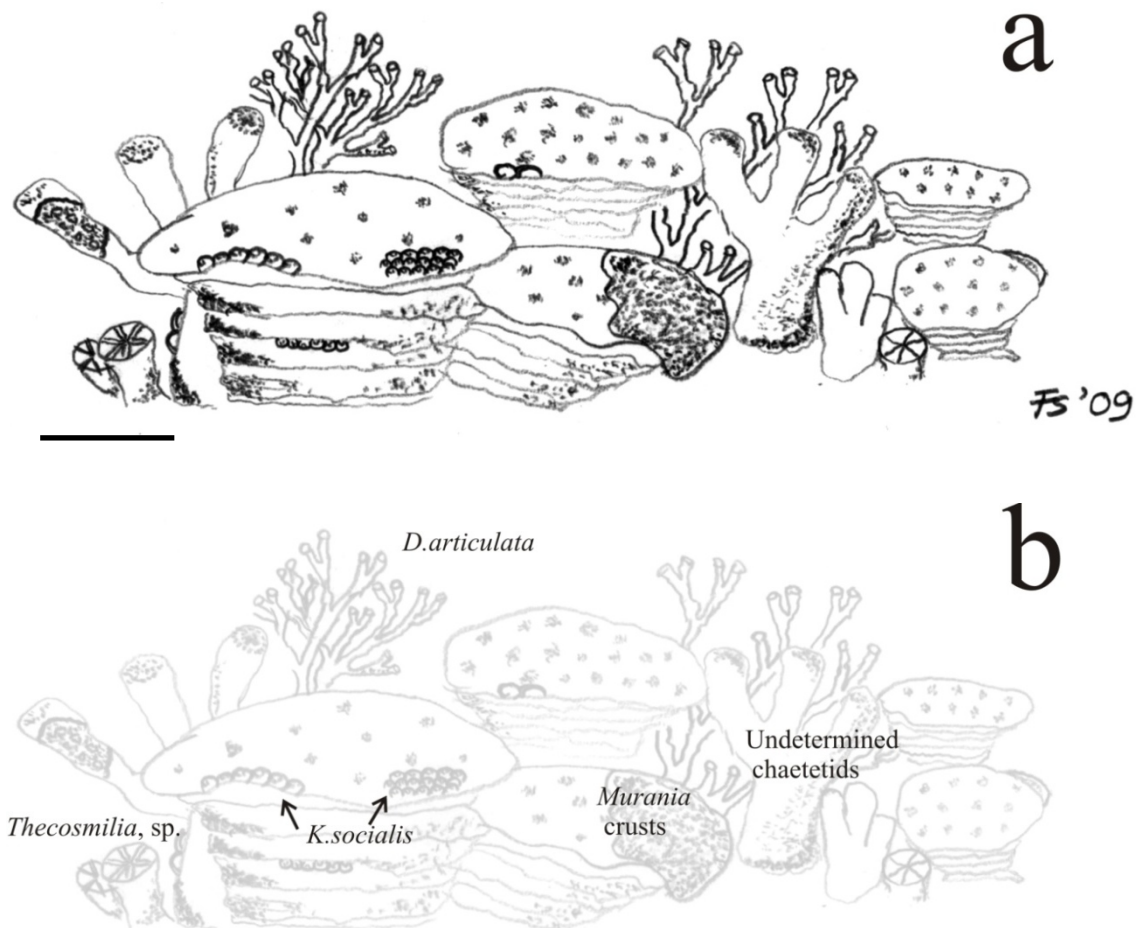
Figure 18: a) Reconstruction of a section from the Patch reef association based on stromatoporoids possibly assignable to *Balatonia*. Note that a microbialitic framework is almost absent and sponge and microencruster are abundant. Scale bar equals approximately 3 cm. Microencrusters not to scale. b) Taxonomic explanation for a).

5.2.2.7.3. Discussion

Due to the conspicuous skeletal material of this framework mainly represented by stromatoporoids and the relatively scarce microbialite proportion, an ecological reef environment is likely. The presence of *Dendronella articulata*, the fragment of phylloid alga and some microencrusters (*K. socialis*, porostromates) are evidence of light-dependance/light presence for the establishment of this association. The abundance of microencrusters and encrusting coralline sponges, in addition to the medium sorting of allochthonous materials may further support the occassional presence of mid- to high-energy conditions. On the other hand, the leiolitic encrustations would more likely validate a

medium to deep and thus, low-energy environment below the storm wave base and even under restricted oxic conditions. Pyrite crystals within leiolites would further corroborate this conclusion. However, the amount of leiolite is scarce, and it appears to be bored by unknown, undetermined microproblematica. Moreover, Dupraz & Strasser (1999) found leiolitic microbialite crusts associated with photoautotrophic microencrusters. Thus, an oxygen-deprived or oxygen-poor environment for this association must be discarded.

A likely paleoenvironmental setting for this association may be the so-called Cassian Patch Reefs (Wendt, 1982).

5.2.2.8. Mud Mound Association I (M-M I, Misurina)

5.2.2.8.1. Biomorpha (Fig. 19)

Skeletal fossils can only be assessed by seldom branching ceratoporellid chaetetids (**Pl. XII; Fig. 4**). Microencrusters are as absent, as are any algae. The predominant facies type in the boulders where this association appears, is microbialite (in average 75%), most of which is assessed to Type 2, yet Type 4 can also be observed. The former facies can be found growing as crusts on top of chaetetid sponges and consisting of peloids with a size of ~ 30 μm), whereas the latter facies can also be recognized due to the frequently associated stromatactis or rather stromatactoid cavities. In this facies, peloid size is also very uniform, but bigger, mostly ranging from 50 to 70 μm in diameter.

Notorious however is that stromatolitic facies can be located in a very different growth direction in comparison to the chaetetids and the encrusting thrombolites (**Pl. XII; Fig. 5**).
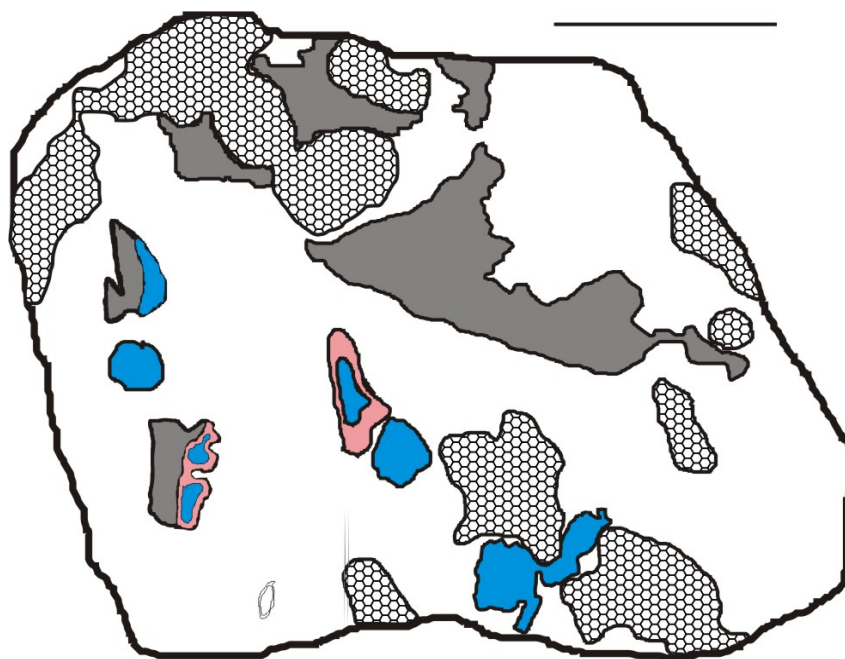
Figure 19: Microfacial map of sample FS-MX-2 , containing part of the Mud Mound Association I . Key: In hexagonal patterned filling, branched chaetetids with a ceratoporellid skeletal structure. Note the massive microbialite fraction and stromatactis cavities. Scale bar = 2 cm.

5.2.2.8.2.   Associated facies

Allochthonous sediments, which include peloid remains, are reduced to less than 5%, so they do not play an important role in the composition of this association. They are found in primary vugs in the thrombolitic facies, yet they can occasionally also be found in secondary cavities within this microbialites and contains some *Tubiphytes* cf. *obscurus* and gasteropod fragments**.**

Cements can mostly be found in stromatactis cavities. These include bladed calcite crystals, which are interpreted as primary on the basis of a pink-red staining, and up to several generations of sparry calcite. (**Pl. XII; Fig. 6**).Overall, cements account for up to 15% of the total estimated volume of the boulders containing this association, thus being one of the samples with a higher cement fraction. Other types are elsewise sparry granular calcites, which fill in stromatactis as the last generation of cements.

5.2.2.8.3.   Discussion

Since microbialite is the dominating facies, it can be concluded that fossils did not have an important role in the palaeoenvironmental implications of this association.Microencrusters can neither be found on the surface of the chaetetid skeletons nor in their associated thrombolitic crusts so that a deep setting can be inferred for these chaetetids.

It is moreover significant, that the orientation of the overlying layered leiolite is completely different from that of the chaetetids. This is supported by the presence of geopetal cavities with their respective infilling, which underlie this kind of microbialite. These microbialites are not colonized by any microencrusters, so that it can be inferred that they formed even at greater depths than the precursor chatetids, especially since an associated alga cannot be found. Furthermore, deep water stromatolites are known to exists from the Mississippian (Shen & Qing, 2008) until the Holocene (Brachert, 1999). Considering these criteria, along with the relative abundance of stromatactis, it is highly probable that the last depositional setting for this sample had been related to a deep water microbi alite-rich, mud mound–like environment. Therefore, a possible scenario would imply a further encrustation of an association based on chaetetids and thrombolites by means of stromatolites, after some boulders containing the association fell from the carbonate platform front and were deposited in a deeper setting of the slope.

5.2.2.9.   Patch Reef Association II: Dendronella-Solenopora-Association (P-R II; Seelandalpe)

5.2.2.9.1. Biomorpha (Figs. 20; 21 a-b)

The most significant feature in this association is the abundance of *Solenopora* cf. *cassiana,* **(Pl.XII, Fig. 7)** which is by far the most abundant species in it. It is also remarkable that corals or sponges are not present as important reef builders. These are only represented by undeterminable chaetetid sponges.

This alga encompasses almost the total of the whole fossil content which is sometimes even around 49% in area counting of single thin sections. A minor fraction corresponds to *Dendronella articulata.* As in previously described associations, the branches of *Dendronella* fix peloidal material. In these peloids, some hexactine spicule pseudomorphs can be seen **(Pl. XII, Fig. 8; Pl. XIII, Fig. 1)**.

There are a considerable amount of microencrusters present in this association. They settle mainly on the surface of *Solenopora* **(Pl.XIII, Fig. 2)** but never on *Dendronella.* Present are *Uvanella* cf. *irregularis, Koskinobullina socialis, Ladinella porata*, and undeterminable porostromate filaments, possibly related to *Girvanella* **(Pl.XIII, Figs. 2-6)**. *K. socialis* and porostromates are very abundant and are strongly associated with microbialites and constitute similar encrustating associations as in the *Ceratoporella breviacanthostyla-Tubiphytes* association, whereas *L.porata* and *U.irregularis* tend to encrust directly on *Solenopora* and are rather scarce.
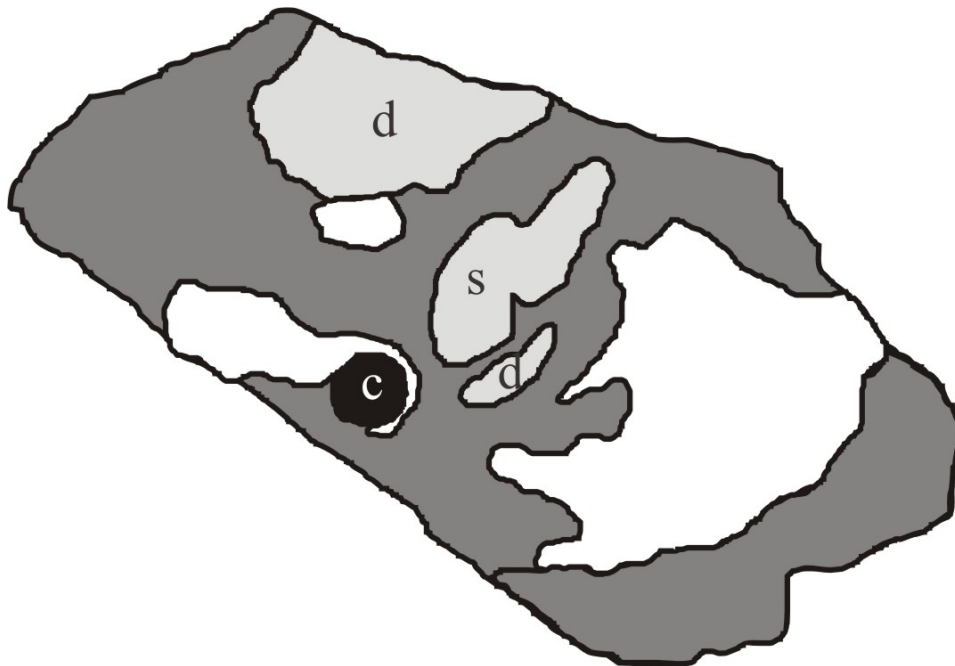
Figure 20: Microfacial map of sample JRIII-76 containing part of the *Dendronella-Solenopora* association. Key: d= *Dendronella articulata;* s= *Solenopora cassiana.* c = undetermined chaetetids. Note the abundance of allochthonous components, which may reach up to 40%.

Microbialite can be found in moderate proportions compared with fossil fraction, with an average of 23% in area counting. It is represented by Type 2 fabrics, which mainly settle on the surface of the algal builders. Occasionally, when two or more builders get united through the accretion of these microbialitic crusts, a building function can also be assumed for these microbialites. It is important to assess that most microencrusters associated with microbialite are found in direct contact with the surface of builders, and as in the case of the *C. breviacanthostyla-Tubiphytes* association, also the fabric of these microbialites tend to change to a Type 3 fabric. Some tubes which may be related to *Microtubus communis* **(Pl. XIII, Fig. 4-6)** can be found in these fabrics. However, some diagnostic features like an assiduous branching are lacking.

Results
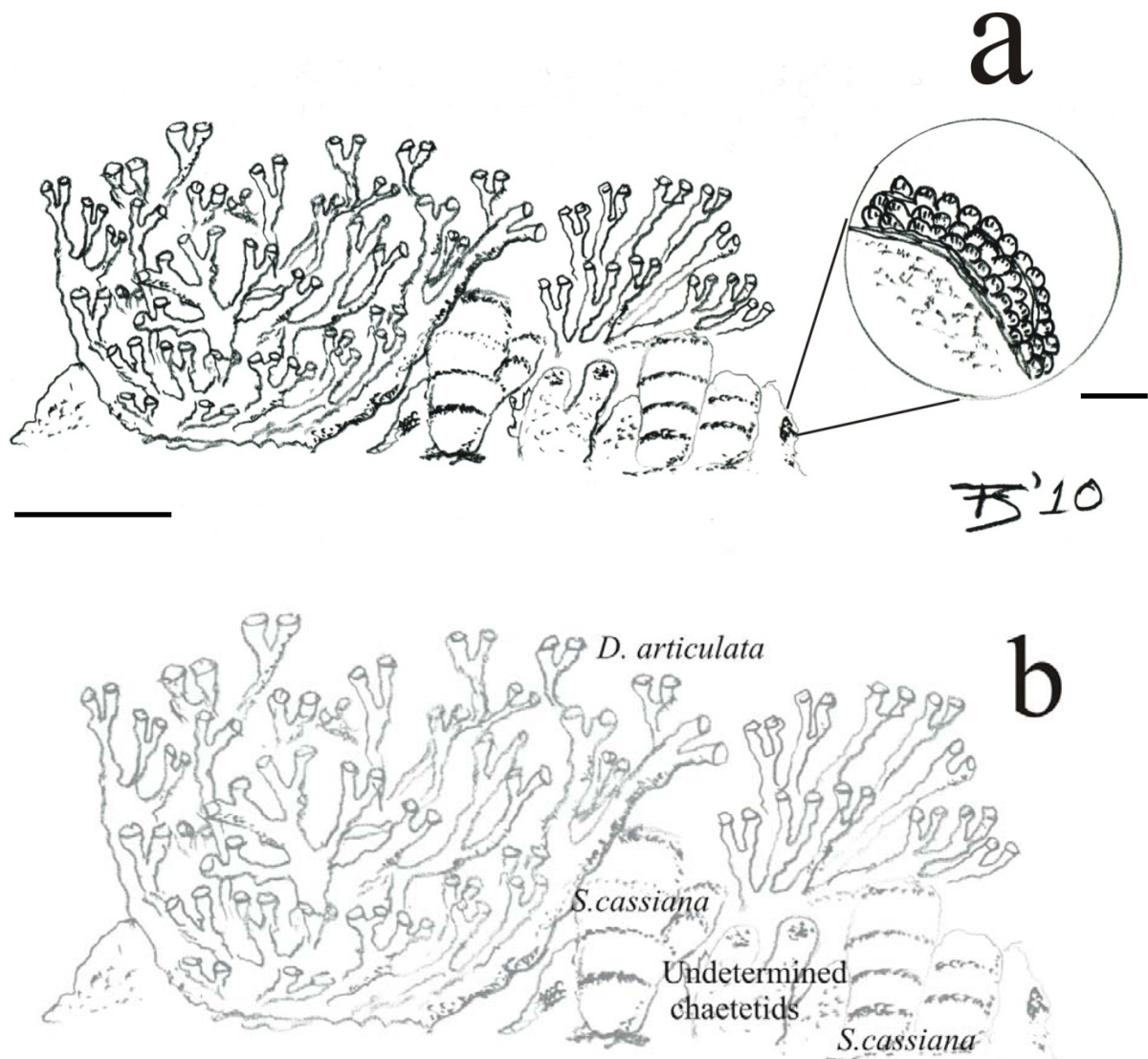
Figure 21. a) Reconstruction of a section from the *Dendronella-Solenopora* association. Note that a microbialitic framework is almost absent. Scale bar equals approximately 3 cm. In the circle: a *Koskinobullina-Girvanella* association dwelling on microbialitic substrate. Scale bar = 500 μm. b) Taxonomic explanation for a).

5.2.2.9.2. Associated facies.

Allochthonous components are represented in a considerable amount (up to 45%). They are represented by well-sorted mudstones and rarely wackestones inside primary vugs of microbialite/automicrite (**Pl. XIII, Figs. 7-8**). Unrecognizable bivalve fragments, as well as some *Lamelliconus cordevolicus* can also be found.there. Cements and microesparite, representing less than 1% of the total area counting, do not seem to have played an important role in the microfacial interpretation.

5.2.2.9.3. Discussion

Fossils cannot provide a definitive paleoenvironmental interpretation on their own. A significant metazoan framework is not present, which means most of the building function relies on the algae and less importantly on microbialite. Solenoporaceans may represent an important part in framework building at shallow depths (Dronov et al., 1982 ; Bernecker, 1996 ; Flügel, 2004). This alone would support shallow reef conditions as the original setting of this association. Furthermore, the association of microencrusters and the abundance of some of them corroborate this hypothesis. *Ladinella porata* is a microproblematicum which does not commonly appear in all studied samples, whereas porostromates are relatively abundant, and so is *Koskinobullina socialis*. In particular, *K. socialis* is found only directly on skeletal surfaces, contrary to the statement by Olivier et al., (2008), who did not find any difference in the substrate for this encruster. Furthermore, *Terebella* cf. *lapilloides* is missing. Conversely, encrusting thalamides are scarce. However, *Microtubus*–related tubes are abundant, but only in relation to Type 3 microbialite fabrics. This might be related with hardness of the substrate at the time of fossilization.

The fact that most microencrusters in this association are linked to one and not to another particular algal species may be of special significance and may be conjoined with the different growth form of both algae. This can be in turn confirmed by the fact that chaetetids, of which the growth form is more similar to that of *S. cassiana,* also bear a considerable amount of biogenic encrustations.

The presence of hexactine pseudomorphs trapped in microbialitic matrix within the branches of *Dendronella* would likely confirm the poriferan origin for some of the automicrites being part of this association. However, since they are only found in these conditions, an original deep setting in principle can be excluded for the paleoenvironmental interpretation.

5.2.2.10.   Patch Reef Association III: Spongiomorpha ramosa association (P-R III; Seelandalpe)

5.2.2.10.1. Biomorpha (Figs. 22; 23 a-b)

Sponges, mainly represented by *Spongiomorpha ramosa* constitute the most abundant part of the fossil fraction, which is collectively as high as 38 %. It shows its typical branched growth (Frech, 1890) Besides branched ceratoporellid chaetetids and *Eudea polymorpha* (**Pl. XIV, Fig. 1**) are also to be found. Macroscopic algae could not be identified. Altogether, fossil fraction contained in the samples containing this association reaches up to 50% in most thin sections.

Microencrusters are certainly diverse, yet they appear seldom. Some structures which may be related to porostromates are the most frequent among them. Possibly they belong to *Girvanella*, however they

are strongly diagenetized. (**Pl. XIV, Fig. 2**). Associated to these porostromate? crusts, *Koskinobulina socialis* can be found, the latter always crusting on the former. Occasionally, thalamide encrusters and the bryozoan *Reptonoditrypa cautica* can also be recognized (**Pl. XIV, Figs. 3-5**). The alga *Ladinella porata* (**Pl. XIV, Fig. 6**). is frequently found, specially encrusting directly on microbialites. No other microencruster could otherwise be found.
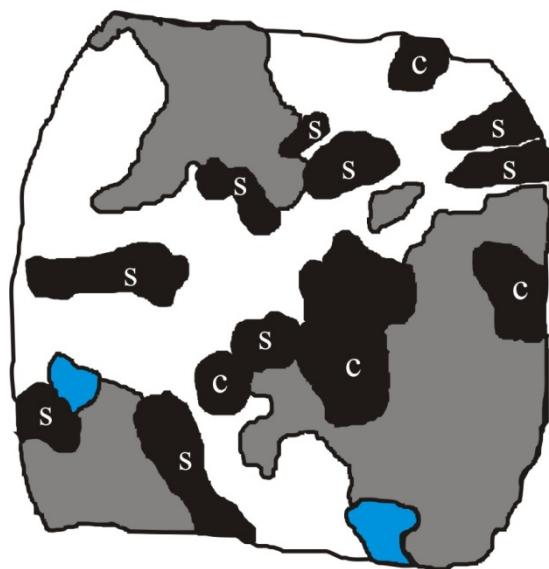
Figure 23: Microfacial map of sample JRIII-14 containing part of the *Spongiomorpha ramose* association. Key: s= *Spongiomorpha ramose;* c= undetermined chaetetids. Scale bar = 2 cm.

Microbialite does not constitute an important fraction of this association, as it only reaches at most 15% in point counting. It is represented by Type 2 fabrics growing on the surface of skeletal framework buildings and without forming a notorious framework by itself.
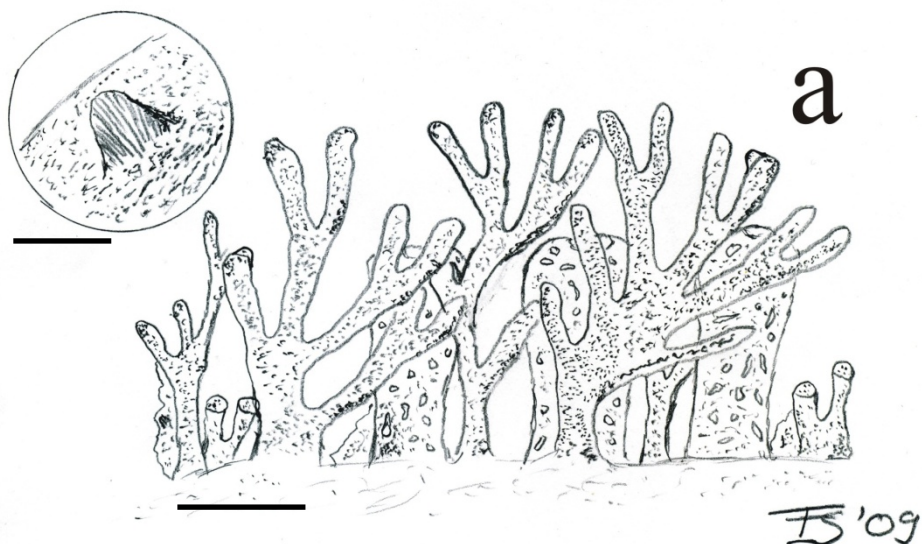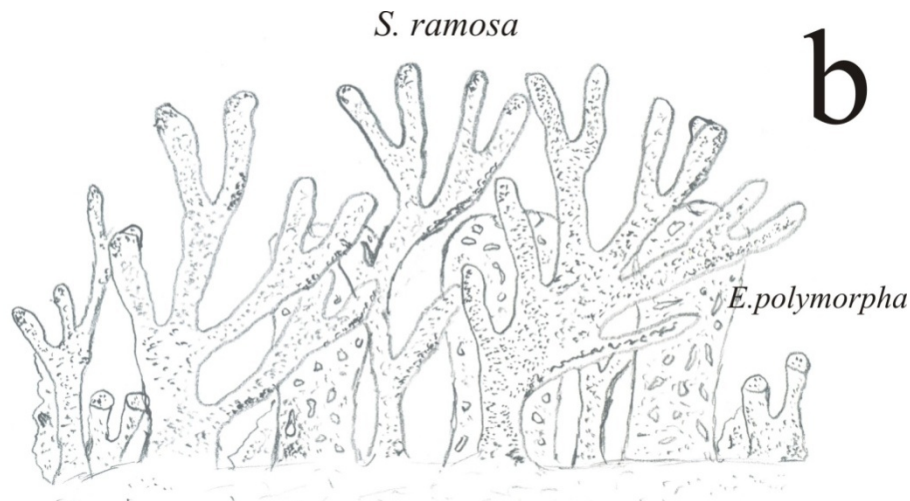
Figure 23: a) Reconstruction of a section from the *Spongiomorpha ramosa* association. Note that a microbialitic framework is almost absent. Scale bar equals approximately 3 cm. Detail in the circle: *Ladinella porata* is a common microencruster of framework builder associations dwelling on microbialitic substrate. Scale bar = 500 μm. b) Taxonomic explanation for a).

5.2.2.10.2. Associated facies.

Allochthonous micrite and its associated detritus represent an important part of the analyzed samples containing this association. Their amount reaches almost 30%. Loose peloids as well as microbialite clots can be found. It is notable that some clots contain spicule pseudomorphs (**Pl. XIV, Fig. 7**). However, since they are allochthonous, it is not possible to try a paleoecological interpretation with their aid. Some parts of the allochthonous micrite can be seen to have undergone transmutation to microsparite, thus reaching 5% (compare Rech, 1998). Nonetheless, this can be attributable to diagenesis, as this sample appears to be the less well-preserved.

Cements have negligible abundances, yet played an important role in binding. They are also interpreted to be primary, as they display Raman spectra for an original high-magnesium calcite.

5.2.2.10.3. Discussion

There are numerous sources in the literature that assign *Spongiomorpha ramosa* to shallow, low energy reef settings. (Fuchs et al., 1988 ; Stanley & Whalen, 1989 ; Stanley, 1994 ; Bernecker, 1996 ; Yancey & Stanley, 1999 ; Caruthers & Stanley,2008; Senowbari-Daryan et al., 2008) Moreover, Yancey & Stanley (2008) reported a coexistence of *S. ramosa* and the bivalve *Megalodon*, which has been repeatedly identified as a diagnostic fossil for shallow depths (Michalik, 1982; Bernecker, 1996, Weidlich & Bernecker, 2007, Nützel et al., 2009). This on its own would provide sufficient criteria to assign light-influenced shallow water conditions to this association. Although some light-depending

encrusters like *Koskinobulina socialis* are scarce, the finding of frequent *Ladinella porata* and also occasionally that of porostromates, further support this assumption.

The lack of a *Tubiphytes- Terebella* association furthermore supports an environment with changing energy, especially regarding *Terebella.* As this microencruster can dwell also in shallow settings (Schmid, 1996), its absence contrasted with the presence of *Reptonoditrypa* and the poorly sorted allochthonous sediments would thus mean that occasional high-energy events could have taken place.

5.2.2.11.   Chaetetid-microencruster association (C-m; Seelandalpe)

5.2.2.11.1. Biomorpha (Figs. 24; 25 a-b)

The most noteworthy feature of this association is represented by a colony of branched chaetetids with a sphaerulitic structure which performs a baffling function (**Pl. XIV, Fig. 8; Pl XV, Figs. 1-2)**. It is also noticeable that almost no other metazoan can be found in thin sections originating from boulders up to 40 cm in diameter. The coral *Margarosmilia* appears secondarily, not constituting an important fraction. Anyhow, these chaetetid colonies comprise up to 40% of area counting measurings. Thus, they provide the habitat for, and are part of the niche of a huge microencruster association.

Most branches are covered by Type 2 to Type 3 microbialitic crusts, which also has a consequence for the type of associated microencrusters. Altogether, however, microbialite does not reach more than 34% of area countings.
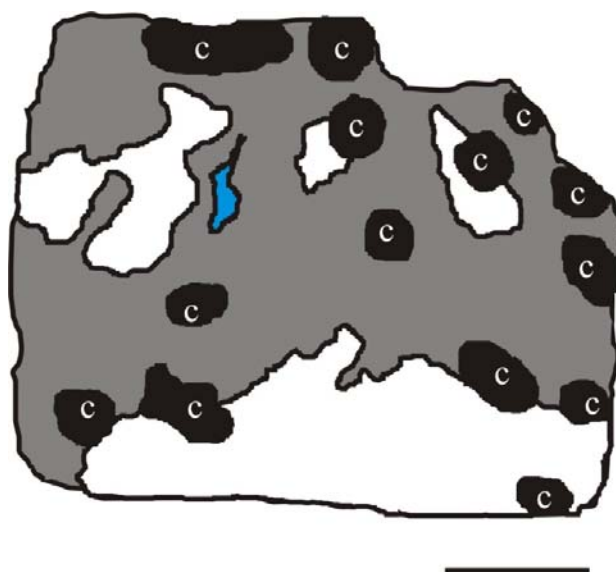
Figure 24. Microfacial map of sample FSSA XXV-7, containing part of the Chaetetid-Microencruster association. Key: c= undetermined chaetetids. Scale bar = 2 cm.

Microencrusters do not differ much from most associations, including *Koskinobulina socialis,* (**Pl. XV, Figs. 3,4)** *Girvanella,* (**Pl. XV, Fig. 5)** *Alpinophragmium perforatum, Terebella* cf. *lapilloides* **Pl. XV, Figs. 6-7)** and *Aulotortus (***Pl. XV, Fig. 8)** . Yet here a pattern of competence for substrate is somehow clear. While on the surface of some branches only a *Girvanella–K.socialis* association can be found, on others only individuals of *Aulotortus* are to be seen. In addition, microbialitic fabric surrounding these tend to have a Type 3 fabric, whereas microbialites associated to *K.socialis* and *Girvanella* are rather of Type 2.
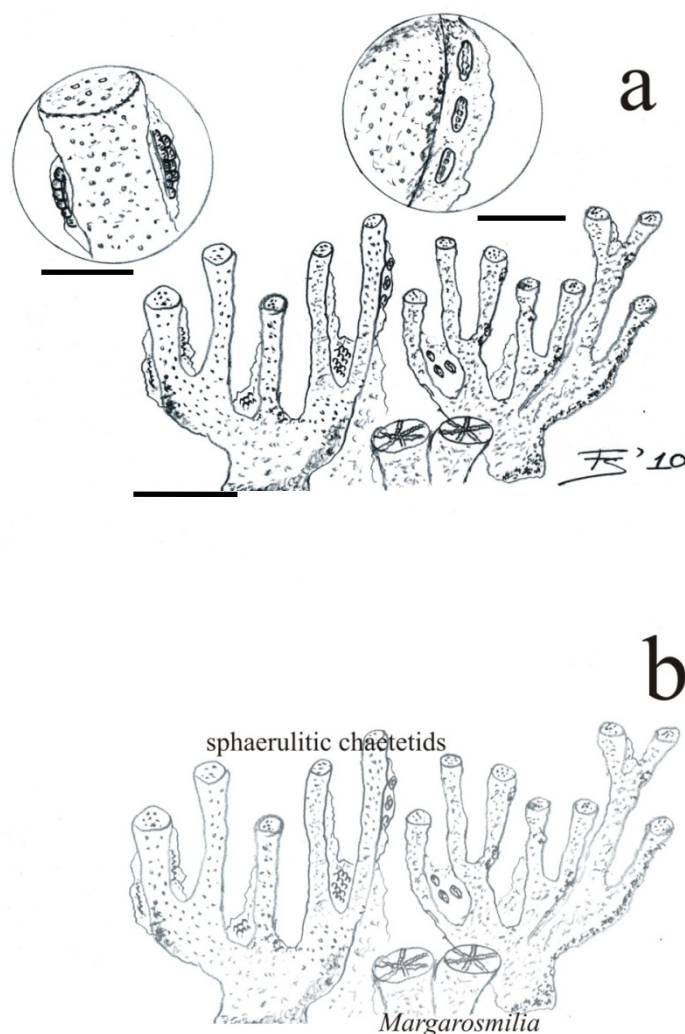
Figure 25: a) Reconstruction of a section from the chaetetid-microencruster association. Note that a microbialitic framework is almost absent. Scale bar equals approximately 2 cm. Detail in the circles: *Koskinobullina socialis* and *Girvanella* in encrusting complexes along with microbialite (left), and the same kind of encrusting complex with *Aulotortus* (right). Scale bars = 500 μm (left circle) and 2 mm (right circle). b) Taxonomic explanation for a).

Results

5.2.2.11.2. Associated facies.

Allocthtonous micrite and associated detritus can be found within primary vugs formed by microbialitic growth. They account for no more than 25% of the analyzed sections and can mainly be classified as mudstones. Detritus include gasteropod and bivalve shales, as well as echinoid spines which can even be seen from the outer surface of some boulders. Cements have barely any importance, not even reaching 1% of point counting in any analyzed thin section.

5.2.2.11.3. Discussion

The most remarkable feature of this association is its overall lack of calcareous algae, as well as its distinctive microencruster settling patterns. It cannot be assessed whether competence for substrate existed between *Aulotortus* and *Koskinobullina*. However, it is known from present studies that substrate competence can occur between different foraminifer species (Páez et al., 2001)

The association is not very diverse; nonetheless it provides sufficient criteria to make a paleoecological preassessment. It is well known that the form of branching growth generally indicates low-energy conditions (Flügel, 2004). This phenomenon has already been recorded for other Triassic localities, particularily branching corals and solenoporans at the Rötelwand and Adnet complexes (Schäfer, 1979) and sponges at Feichtenstein and the Gruber Reef (Senowbari-Daryan, 1980). This factor, the lack of high-energy microencrusters, the fabric of allochthonous components, and the lack of algae may help to infer a quiet, semi-cryptic/deep marine setting, probably below 50 m that could therefore somehow be related to the *Ceratoporella-Tubiphytes* association. Unfortunately, no further assessment is possible.

5.2.2.12. *Amblysiphonella– Megalodon* **association (A-M; Seelandalpe)**

5.2.2.12.1 Biomorpha (Fig. 26)

This association is reconstructed solely on one available thin section from Prof. Reitner's collection. However, it provides sufficient information to infer certain paleoecological features on the origin of the Cipit Boulder represented. Most of the area, around 45%, is comprised of a framework, mainly formed by coralline sponges. The most important of them is *Amblysiphonella strobiliformis* (**Pl. XVI, Figs. 1,2**), however *Taumastocoelia cassiana* and *Cassianothalamia zardini* are also present. (**Pl. XVI, Fig. 3**) Unfortunately, numerous unidentifiable fragments can however be found.

Bryozoans also play an important role. They are mainly represented by globous morphotypes. In addition, numerous specimens of *Reptonoditrypa cautica* (**Pl. XVI, Figs. 4-6**) can be seen. Although most microencrusters considered in this work do not possess the ability of building a significant

fraction of the framework, in this association *Reptonoditrypa* helps bind many skeletons together, as well as loose sponge? fragments. Belonging to the framework-building microencrusters, some serpulids can be seen.

Bivalves and brachiopods (possibly assignable to Thecideida, **Pl. XVI, Fig. 7)** also constitute an important part of this association. Particularly remarkable is the presence of a shell of *Megalodon* associated with *Tubiphytes* cf. *obscurus*, **(Pl. XVI, Fig. 8)**, which has never been reported to occur inside Cipit Boulders. Attached to the inner surface of the shell, some filamentous structures with a possible porostromate affinity can also be seen **(Pl. XVII, Figs. 1-2).**
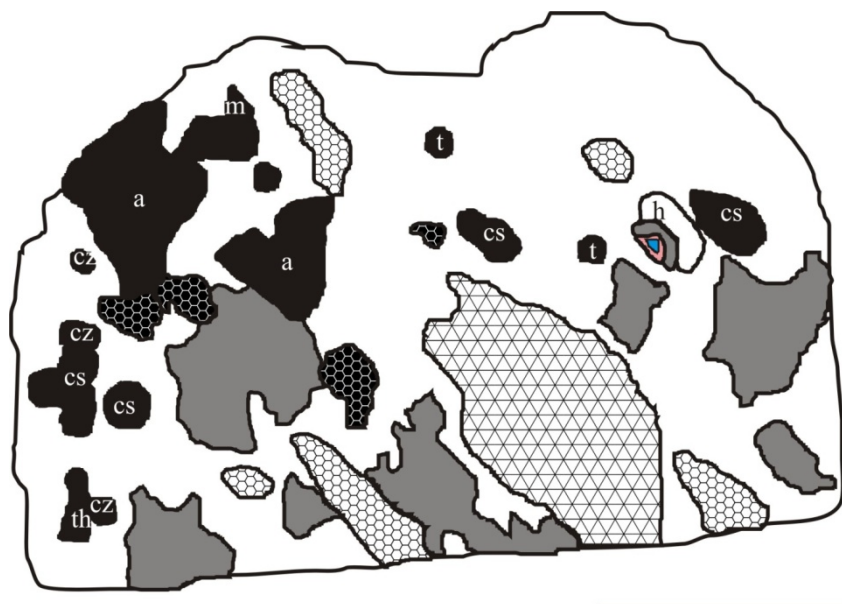
Figure 26: Microfacial map of sample JR II-65, representing the *Amblysiphonella–Megalodon* association. Key: cs= Undetermined coralline sponges; cz= *Cassianothalamia zardinii;* th= *Thaumastocoelia cassiana;* m: *Murania megaspiculata;* a= *Amblysiphonella strobiliformis;* H= Hexactinellid sponge; T=*: Terebella* cf. *lapilloides.* In hexagonal black pattern-filling: bryozoans. In hexagonal white pattern-filling: ceratoporellid chaetetids. In triangular pattern-filling: *Megalodon.* Note the diameter of *Terebella* worm tubes. Scale bar = 5 cm.

Microbialite is represented by Type 2 fabric thrombolites which grow upon the surface of the metazoan framework. Most of it is bored by *Terebella* cf. *lapilloides* tubes **(Pl. XVII, Figs. 3,4)**, as well as by occassional *Baccanella floriformis.* **(Pl. XVII, Fig. 4)** and *Microtubus communis* **(Pl. XVII, Fig. 5).** In total, it does not exceed more than 20% and thus it doesn´t represent an important fraction of the association. *Aka cassianensis* can be seen **(Pl. XVII, Fig. 6)** associated to this microbialitic fabric within pores of *A.strobiliformis*. However, the percentage of microbialite cannot be taken as definitive, since there is only one available thin section containing it. In addition, remains of a hexactinellid sponge can be seen. **(Pl. XVII, Fig. 7)** It is remarkable the similarity that this sponge

mummy has in its mode of preservation with a stromatactis. (Delecat, 2005; Neuweiler & Bernoulli, 2005; Neuweiler & Burdige, 2005).

5.2.2.12.2. Associated facies.

Associated allochthonous material is represented by mud-wackstones and constitutes approximately 21% of the total area of the thin section. Commonly it is possible to detect gastropod clasts within it. Cements are however negligible with respect to abundance, but they can easily be recognized as part of a complex, multi generational stromatactis cavity within the remains of a hexactinosid? sponge. **(Pl. XVII, Fig. 7)**

5.2.2.12.3. Discussion

The presence of *Megalodon* is undoubtedly a diagnostic feature of very shallow settings (Michalik, 1982; Nützel et al., 2009). Furthermore, it suggests an initial setting that has soft substrate. The filamentous structure inside its valves may have had an algal nature and thus additionally corroborate an assignment to an initially shallow community. A fraction of the framework, composed by *Amblysiphonella strobiliformis*, branched ceratoporellid chaetetids, indeterminable stromatoporoids and bryozoans may be related to this environment, as determined by the growth direction of some of its elements. However, some other elements are present, suggesting a deeper setting. These include the presence of *Cassianothalamia zardinii*, which has been assessed as having preferred deeper environments (Reitner, 1987a; Keupp et al., 1989, Sánchez-Beristain et al., 2008). In addition, this sponge can be seen growing on the surface of a *Thaumastocoelia cassiana*, of which the main feature is its growth direction, totally opposed to that of *Amblysiphonella* individuals.

Furthermore, most of the non-abundant microbialite is abundantly inhabited by *Terebella* cf. *lapillloides* tubes. Yet the most remarkable feature is the presence of a hexactinosid? mummy, which leaves behind a stromatactis fabric A possible explanation would be that the initially shallow-deep *Amblysiphonella*-based framework associated to *Megalodon* fell basinward into a deeper setting, where it was further covered by a microbialite layer, which in turn was colonized by *Terebella* cf.*lapilloides*. Parallelly to *Terebella*, hexactinellid sponges settled.

Considering that hexactinellids prefer deep settings since they do not have means of chemical defenses against predators (Krautter, 1998), another possibility would be to assess this setting as a part of a low depth reef cave system, where predators would practically have no access, thus representing a safe setting for the hexactinellid sponge. Finally, after the death of these sponges stromatactis fabrics would have developed.

5.2.2.13. *Cassianothalamia* **Gemeinsschaft –I (C-G I; Seelandalpe)**

5.2.2.13.1. Biomorpha (Figs. 27, 28a-b)

This association is by far the one that displays the highest diversity among the analyzed material. Furthermore, it exhibits a diverse and complete guild structure, although the most distinctive feature is the thalamid *Cassianothalamia zardinii* (**Pl. XVII, Fig. 8**), which occupies at most 31% of the analyzed thin sections. It may also act as builder, since it can help to bind other framework-building organisms, such as Disjectoporids, *Precorynella* (**Pl. XVIII, Figs. 1-3**), branched undetermined bryozoans (**Pl. XVIII, Fig. 4-5**)*, Atrochaetetes medius,* (**Pl XVIII, Fig. 6**) as well as by *Zardinia* and *Sestrostomella* ? *robusta* (**Pl. XVIII, Fig. 7**) in minor proportions. *Precorynella* has been frequently cited as important builder in Triassic systems, such as the Leckkogel Beds (Dullo & Lein, 1982), and the Bosruck Peak (Dullo et al., 1987), both of them in Austria. Fürsich and Wendt (1977) name it as one of the frame builders at the Cassian patch reefs. Regarding *Atrochaetetes*, Bernecker (2005) assesses it as a builder for the Jabal Kawr Reef from the Norian and Rhaetian from Oman. Thus, the presence of both taxa here and their assessment as part of the constructor guild is significant. All these builders form a massive framework, which in some thin sections can occupy up to 74% of area counting, and never reaching less than 50%.

Further notable features of this association include several lithistid and hexactinellid mummies (**Pl. XVIII, Figs. 6-7**), varying in proportions from one thin section to the other, as well as common *Aka-*borings. However, it is more common that lithistids surpass hexactinellids in abundance.
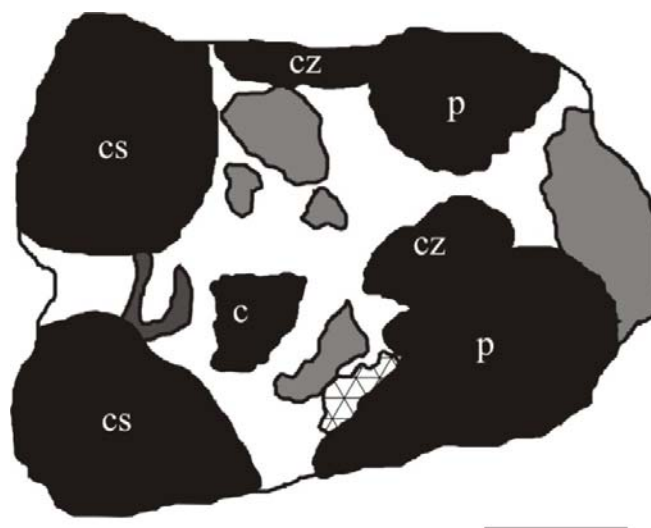
Figure 27: Microfacial map of sample CG I-23 representing the *Cassianothalamia* Gemeinschaft. Key: p= *Precorynella*; cs= undetermined coralline sponges; cz= *Cassianothalamia zardinii*; c= branched ceratoporellid chaetetids. In triangular pattern-filling: Lithistid sponges. Scale bar = 1.5 cm.

Results

Microbialite occupies at most 46% of the analyzed area, thus representing an important part of this association. It is often inhabited by a diverse encruster association, which includes abundant *Baccanella floriformis* **(Pl. XVIII, Figs. 3-4),** *Terebella* cf. *lapilloides* **(Pl XVIII, Fig. 7-8**), *Koskinobullina.socialis, Girvanella, Aulotortus* **(Pl. XIX, Fig. 1-2)** and *Tubiphytes obscurus* **(Pl. XIX, Fig. 3**). However, *K.socialis, Girvanella* and *Aulotortus* are not only strictly associated with microbialite, since they can also be found in encrusting complexes on the surface of some builders.

In some instance, preserved microbialite allows some hexactinellid spicule pseudomorphs to be recognized **(Pl. XVIII, Fig. 8; Pl. XIX, Fig. 4).**

Frequent dwellers of the association are thecideid brachiopods **(Pl. XIX, Fig. 5**), which are present in more than a half of the thin sections analyzed.
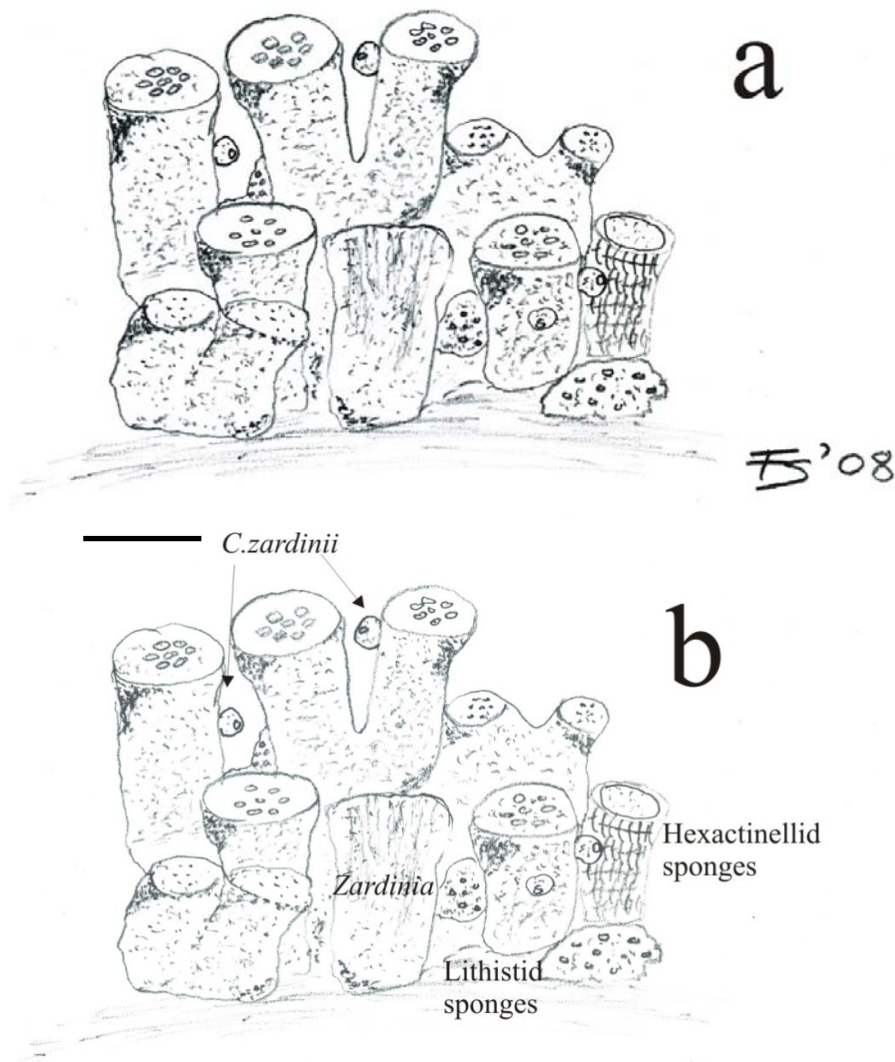
Figure 28: a) Reconstruction of a section from the *Cassianothalamia* Gemeinschaft I. Note the reduced presence of a microbialitic framework. Scale bar equals approximately 3 cm. b) Taxonomic explanation to a)

5.2.2.13.2. Associated facies.

Mud and mud-wackestones are to be found as associated allochthonous material in all thin sections containing this association within primary vugs formed by microbialite growth. However, their occurence rarely exceeds 10% thus being of little importance. Cements neither play an important role, being found in at most 7% of the samples.

5.2.2.13.3 Discussion

This is the hitherto most described association from the St. Cassian Cipit Boulders. (Keupp et al., 1989; Sánchez-Beristain & Reitner, 2008). It can be interpreted as a less depth-gradient owed variation of the CG II, since it contains a more abundant framework and more lithistids in comparison to hexactinellid sponges. Furthermore, microencrusters are more abundant and diverse, containing apparently high-energy adapted *R.cautica* and a considerable amount of *B.floriformis.*

In addition, due to the diversity it displays, an oxygen-rich environment can also be suggested, at least containing more available O_2 than the CG II.

5.2.2.14.   Mud Mound Association II (M-M II; Seelandalpe, Misurina)

5.2.2.14.1. Biomorpha (Fig. 29)

The main feature of this association is its complete lack of a metazoan fossil framework. No single metazoan could be found in seven thin sections obtained from two boulders. The only non-microbialitic organisms which can be identified are coralline algae patches, possibly belonging to *Mesophyllum.* Otherwise all thin sections in average contain more than 85% of microbialite, which is abundantly inhabited by *Terebella* cf. *lapilloides.* **(Pl. XIX, Fig. 6).**
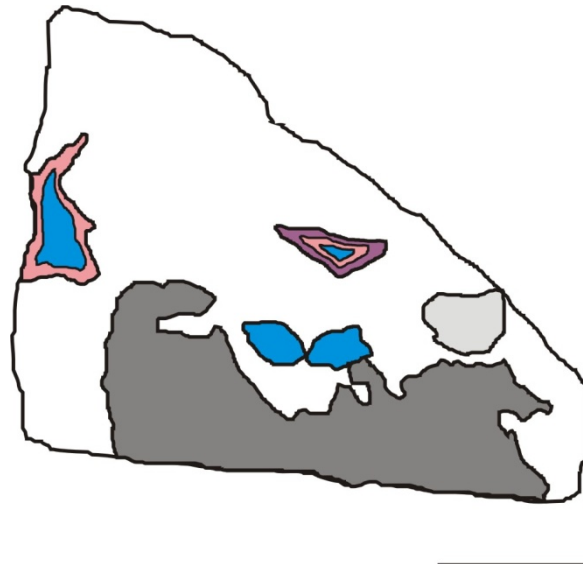
Figure 29. Microfacial map of sample M XXI -1, ,representing the Mud Mound association II.. Key: In white: microbialite framework. Light grey symbolizes *Mesophyllum* patches. In blue: secondary cements. In diverse pink tones, primary cements. Note the absolute absence of metazoans. Scale bar = 2 cm.

5.2.2.14.2. Associated facies.

Although allochthonous micrite is rather scarce (no more than 1% in average), cements constitute more than 10%. They tend to form stromatactis and stromatactoid cavities within microbialites.

5.2.2.14.3. Discussion

Since microbialite is the dominant facies in all samples and metazoans are completely absent, a deep framework setting sustained only by microbialites is the most probable interpretation. Corallinaceae are not sufficient to give evidence of a low depth (Riding, 1975, Round, 1981). Nevertheless, abundant terebellids would support such an assumption. (Wendt et al., 1989). It is noteworthy that no stromatolite is present (compare M-M I). Nevertheless no further paleoenvironmental assessment can be made.

5.3. Numerical analyses of microencruster associations

5.3.1. Microencruster ecology

Valuable information can be obtained from microencrusters present in sponge associations from the St. Cassian Formation. Since microencrusters are considered to be diagnostic for selected environmental criteria (see above), it becomes therefore important to try to infer more of their particular ecological features. Ways to achieve this goal include efforts to obtain this information with the aid of quantitative numerical methods. Unfortunately, their low diversity does not for a large array

of analyses. However, some analyses can be done in order to assess the way microencrusters are correlated, if at all.

UPGMA, WPGMA and Single Linkage (Nearest neighbour) algorithms in R-mode were performed on the datasets of Table 1a (Figs. 30 to 32) using Jaccard coefficient. In addition, WPGMA algorithm combined with Bray-Curtis coefficient was performed using abundance data from Table 1b (Fig. 33).The correlation between microencrusters obtained by means of WPGMA-Bray Curtis reveals phenograms that are very similar to those obtained by UPGMA, and WPGMA in combination with Jaccard coefficient, and furthermore these two analyses are almost identical to each other with regard to encruster pairs of *Baccanella – Reptonoditrypa, Terebella – Tubiphytes* and *Girvanella – Koskinobullina* remaining constant with high index values, proving to be consistent (Figs. 30-31).
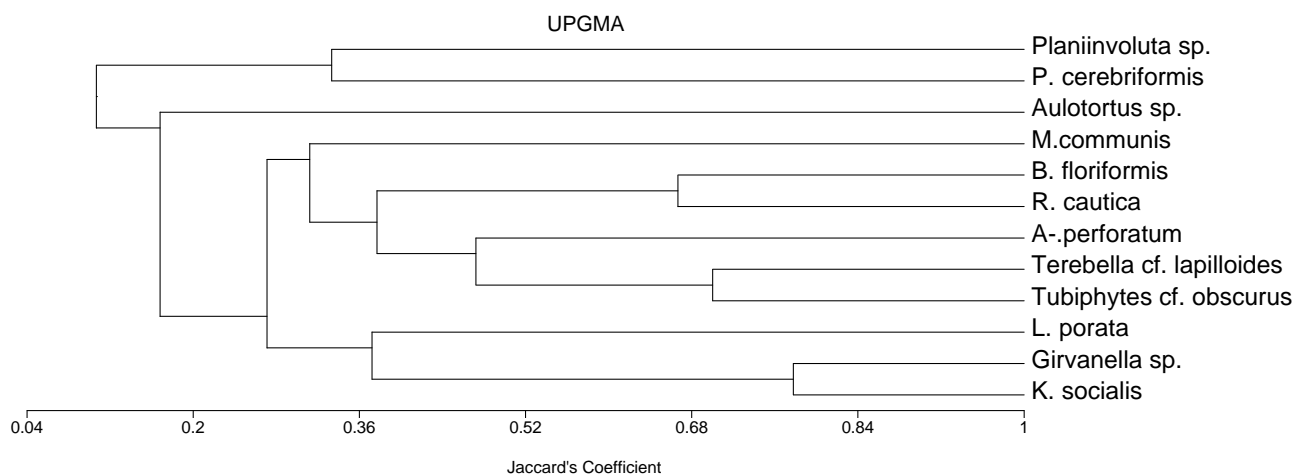
Figure 30: UPGMA–Jaccard phenogram of cluster analysis of occurrences of microencruster species contained in each association. Three encruster pairs with a J-value higher than 0.60 appear: *B.floriformis-R.cautica, Terebella* cf.*lapilloides–Tubiphytes.obscurus* and *Girvanella* sp.*-K.socialis.*

Results
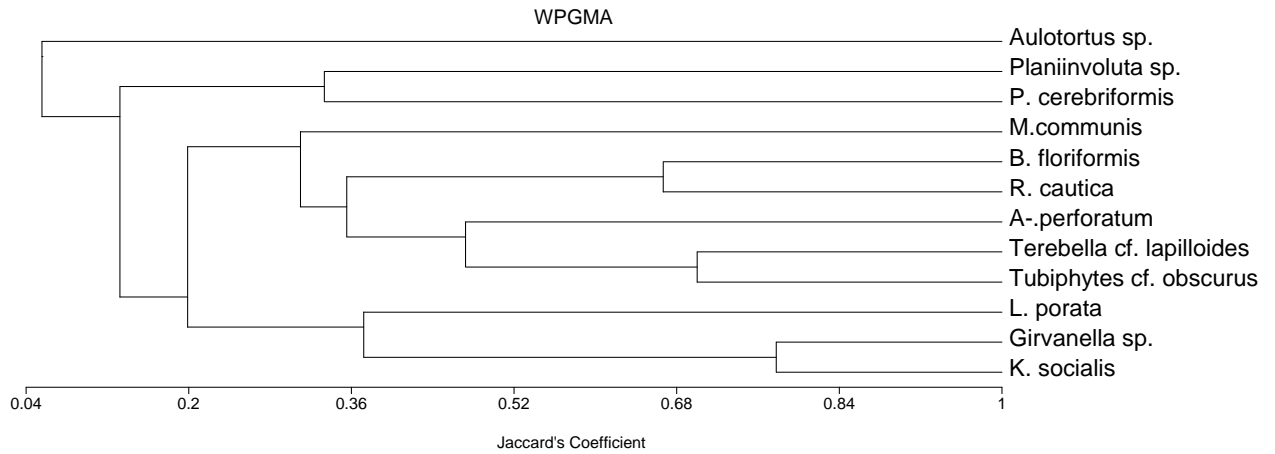
Figure 31: WPGMA–Jaccard phenogram of cluster analysis based on microencrusters contained in each association. Note the similarity with phenogram from Figure 30.
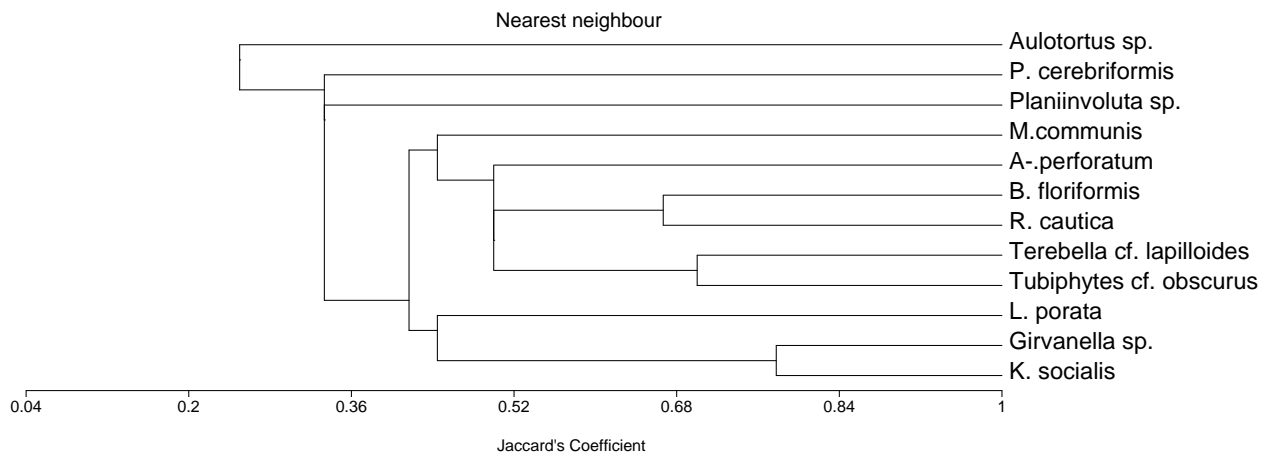
Figure 32: Nearest neighbour-Jaccard phenogram. Same microencruster pairs remain constant.
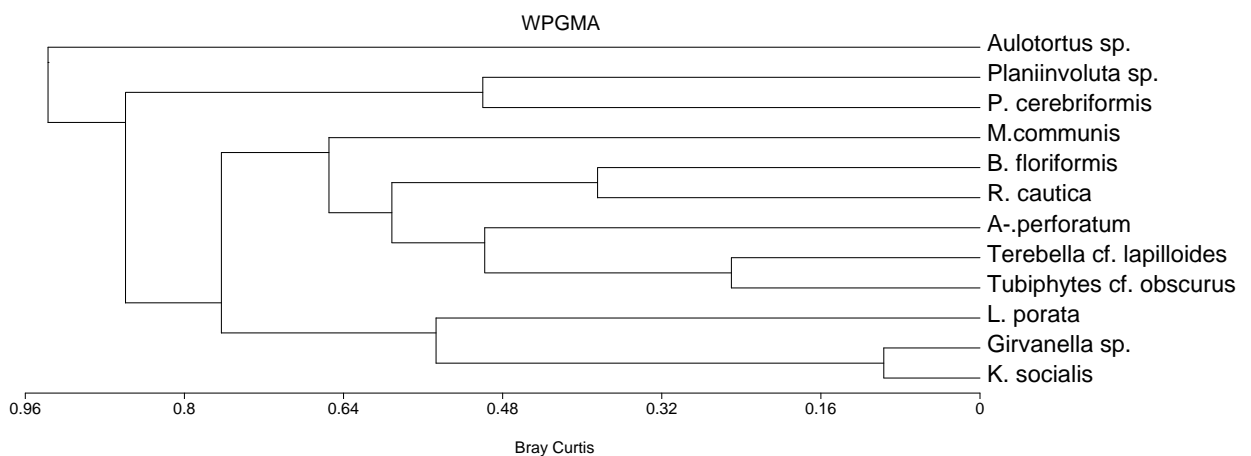
Figure 33: WPGMA-Bray Curtis abundance data phenogram. Note the low dissimilarity values for the *Girvanella* sp-*K. socialis* and *T. lapilloides–T. obscurus* pairs.

Although most cluster analyses in Paleontology are performed based on the Jaccard coefficient, values of this can be complemented with values obtained from the Simpson coefficient, which is interpreted as the value for the diversity of taxa or features within two compared samples. (Simpson, 1949; Cheetham & Hazel, 1969; Schäfer, 1979). Solid evidence of correlation is assumed in case of similar Jaccard and Simpson coefficient values for the same pair of compared taxa (Schäfer, 1979). Therefore, the existence of similar Jaccard and Simpson coefficient values for a pair of organisms (miceoencrusters), means that they display a similar distribution in the analalyzed associations and therefore they could more or less have the same ecological constraints (Table 1c).

Schäfer (1979) used both Jaccard and Simpson coefficients successfully to categorize the relations between epibionts/endobionts and their substrate in Triassic reefs. However, she included some non-biological "epibionts" in her study, such as "unbestimmte Mikritkrusten" (non-determined micrite crusts), which might have altered her final interpretation of this associations. It is thus of crucial importance to continue a selection of the microencrusters that will undergo such an examination, thus excluding such forms *a priori*. Therefore, all organisms subjected to this analyses were carefully selected considering those with potential ecological constraints described in several publications (e.g. Leinfelder et al., 1993; Schmid, 1996; Shiraishi & Kano, 2004; Schlagintweit & Gawlick, 2008; Reolid et al., 2009) as well as some which have never been studied in this regard: *Plexoramea cerebriformis* being regarded as a fungus (Flügel et al., 1988) *Ladinella porata* as an alga (Flügel et al., 1991; Nittel, 2006), the bryozoan *Reptonoditrypa cautica,* the "worm tube" *Microtubus communis* (Flügel, 1964; Bernecker, 1996), and the foraminifers *Alpinophragmium perforatum*, *Planiinvoluta sp* and *Aulotortus sp*.

In this study no phylogenetic relationship is pursued. Results point thus only to pure similarity, which is interpreted as a measure of the ecological implications in terms of microencruster interactions, as well as in the determination of fossil communities.

Results

	D-H	C-T	C-M	C-S	T-M	C-G II	P-R I	M-M I	P-R II	P-R III	C-m	A-M	C-G I	M-M II
K. socialis	0	1	0	0	1	0	1	0	1	1	1	1	1	0
Girvanella sp.	0	1	0	0	0	1	1	0	1	1	1	1	1	0
Tubiphytes cf. *obscurus*	1	1	1	1	1	1	0	0	0	0	1	1	1	0
Terebella cf. *lapilloides*	1	0	0	1	1	1	0	0	0	0	1	1	1	1
P. cerebriformis	1	0	0	0	0	0	0	0	0	0	0	0	0	0
L. porata	1	0	0	0	0	1	1	0	1	1	0	0	0	0
R. cautica	1	0	1	0	0	1	0	0	0	1	0	1	1	0
M.communis	0	1	1	0	1	0	0	0	0	0	0	1	0	0
A-.perforatum	0	0	0	0	1	1	0	0	0	0	1	1	0	0
B. floriformis	0	0	1	0	0	1	0	0	0	0	0	1	1	0
Aulotortus sp.	0	0	0	0	0	0	0	0	0	0	1	0	1	0
Planiinvoluta sp.	1	0	0	0	1	0	1	0	0	0	0	0	0	0
HEX	1	0	1	0	0	1	0	0	0	0	0	1	1	0

Table 1a showing only presence/absence of each microencruster in each association in order to perform the remaining analyses, which focus on grouping microencrusters in order to find potential ecological data. Hexactinellid sponges are included in this table, because they can be used as diagnostic organisms for considerable depths (see above); however, information provided by them was only used at the transposition of the matrix and not in normal UPGMA- Jaccard microencruster analysis (see text for details).

	D-H	C-T	C-M	C-S	T-M	C-G II	P-R I	M-M I	P-R II	P-R III	C-m	A-M	C-G I	M-M II
K. socialis	0	3	0	0	1	0	3	0	2	2	2	1	2	0
Girvanella sp.	0	3	0	0	0	1	3	0	2	1	2	1	2	0
Tubiphytes cf. *obscurus*	2	1	1	1	1	2	0	0	0	0	1	1	1	0
Terebella cf. *lapilloides*	2	0	0	1	1	2	0	0	0	0	1	2	1	3
P. cerebriformis	1	0	0	0	0	0	0	0	0	0	0	0	0	0
L. porata	2	0	0	0	0	1	2	0	3	3	0	0	0	0
R. cautica	1	0	2	0	0	1	0	0	0	1	0	1	1	0
M.communis	0	3	1	0	1	0	0	0	0	0	0	1	0	0
A-.perforatum	0	0	0	0	1	1	0	0	0	0	1	1	0	0
B. floriformis	0	0	1	0	0	1	0	0	0	0	0	1	3	0
Aulotortus sp.	0	0	0	0	0	0	0	0	0	0	1	0	1	0
Planiinvoluta sp.	1	0	0	0	1	0	1	0	0	0	0	0	0	0

Table 1b displaying the relative abundance of each microencruster species in each one of the analyzed associations, and its data were only used for a WPGMA cluster analysis with a Bray-Curtis index.

	Ks	G	To	Tl	Pc	Lp	Rc	Mc	Ap	Bf	A	P
Ks	X	**0.88**	0.63	0.50	0.00	0.60	0.50	0.75	0.75	0.50	1.00	0.67
G	**0.78**	X	0.63	0.50	0.00	0.80	0.67	0.50	0.75	0.75	1.00	0.33
To	0.42	0.42	X	**1.00**	1.00	0.40	0.83	1.00	1.00	1.00	1.00	0.67
Tl	0.33	0.33	**0.70**	X	1.00	0.40	0.67	0.50	1.00	0.75	1.00	0.67
Pc	0.00	0.00	0.11	0.13	X	1.00	1.00	0.00	0.00	0.00	0.00	1.00
Lp	0.30	0.44	0.17	0.18	0.20	X	0.60	0.00	0.25	0.25	0.00	0.67
Rc	0.27	0.40	0.50	0.40	0.17	0.38	X	0.50	0.50	**1.00**	0.50	0.33
Mc	0.33	0.20	0.44	0.20	0.00	0.00	0.25	X	0.50	0.50	0.00	0.33
Ap	0.33	0.33	0.44	0.50	0.00	0.13	0.25	0.33	X	0.50	0.50	0.33
Bf	0.20	0.33	0.44	0.33	0.00	0.13	**0.67**	0.33	0.33	X	0.50	0.00
A	0.25	0.22	0.22	0.25	0.00	0.00	0.14	0.00	0.20	0.20	X	0.00
P	0.22	0.10	0.20	0.22	0.33	0.33	0.13	0.17	0.17	0.00	0.00	X

Table 1c containing the composite matrix for Jaccard /Simpson index values of each microencruster. X axis contains Simpson Matrix Values, while Y axis shows Jaccard Values. Key: Ks= *Koskinobullina socialis;* G= *Girvanella* sp., To= *Tubiphytes* cf. *obscurus*, Tl = *Terebella* cf. *lapilloides*, Pc = *Plexoramea cerebriformis*, Lp = *Ladinella porata*, Rc= *Reptonoditrypa cautica*, Mc = *Microtubus communis*, Ap = *Alpinophragmium perforatum*, Bf = *Baccanella floriformis*, A = *Aulotortus* sp, P = *Planiinvoluta* sp.

Results show the highest Jaccard (J) value for the microencruster pair *Koskinobullina socialis – Girvanella*, with J= 0.7784 and a high Simpson (S) value of 0.875, as well as a low WPGMA Bray-Curtis (BC) value of 0.097. This further corroborates the apparent correlation between both forms. Considering this premise for these particular organisms, the following must be stated:

- Although *K. socialis* can mostly be found on skeletal substrates, *Girvanella* dwell on them as well as in microbialite substrates;

- *K.socialis* can also be found in microbialitic substrates (Thrombolite-microencruster community, Olivier et al., 2008). Nonetheless, this occurs rather rarely and neither *Girvanella* nor any other porostromate filament is associated with it;

- Not all incidences of *Girvanella* are strictly related to an incidence of *K. socialis* *(Cassianothalamia* Gemeinschaft II);

- *Girvanella* is generally found more frequently than *K. socialis.*

K.socialis grows under light and under mid-to low-energy conditions. In medium deep and semi-cryptic associations, respectively, both *K. socialis* and *Girvanella* are commonly found simultaneously. In addition, disregarding their inferred depth, colonies of both organisms appear to be broader whenever they are found directly associated, whereas in absence of *Girvanella* colonies of *K.*

Results

socialis are reduced or even absent. Furthermore, in Patch Reef communities (see above), especially where algae content is high, encrustation of both organisms is not always interlinked; and in associations where medium- to high-energy conditions prevail or where a deep setting is inferred, none is to be found. Moreover, in one encruster –rich association (Thrombolite-microencruster), no *Girvanella* could be found, which could be attributable to sampling-error (five thin sections analyzed).

All these observations provide evidence to interprete this symbiosis as a facultative mutualism, which means that both organisms can be associated and can obtain a mutual benefit from each other, yet they do not need to form any association or consortium (Townsend et al., 2008).

Table 1c also shows more or less a correlation for *Tubiphytes* cf. *obscurus* /*Terebella* cf. *lapilloides*. (J= 0.70; S= 1; BC=0.250). However the value is not as high as the case of the pair *K.socialis – Girvanella* . The following must be pointed out concerning this microencruster pair before proceeding with a discussion:

- While *Tubiphytes* can be found in both microbialites and skeletons, *Terebella* only encrusts microbialitic substrates;

- Under medium- to high-energy conditions (*Cryptocoelia–Mesophyllum* community), *Tubiphytes* can only be seen encrusting skeletal substrates.

These observations may help to explain the fact that *Tubiphytes* is far more resistant to high-energy conditions or events than *Terebella*, since it can also be found in environments of medium energy.

In this regard, it is important to assess that "*Tubiphytes* cf *obscurus*" may not have anything to do with Jurassic forms attributed to *Tubiphytes* (Riding & Guo, 1992); however, the *Tubiphytes* morph observed in this work behaves in the same way as *Tubiphytes crescenti*, the one described by Schmid (1996), Shiraishi & Kano (2004), Helm (2005), Olivier et al., (2008) and Senowbari Daryan et al.,(2008).

Actually, few Triassic publications deal with *Terebella lapilloides* (Kuss 1988; Wendt et al., 1989; Calvet & Tucker, 1995). Records from *Tubiphytes* are on the other hand very extensive (a.v.o. Schäfer, 1979; Senowbari-Daryan, 1980; Schäfer & Senowbari-Daryan ,1982; Wurm, 1982; Flügel, 1986; Dullo et al., 1987; Wood, 1999; Flügel, 2002; Payne et al., 2006), yet most of them under a systematic point of view. Only Müller-Wille & Reitner (1993) make a mention of some of its paleoautoecological features.

It would be expected that *Terebella* cf. *lapilloides* could also be found in the *Ceratoporella – Tubiphytes* association. Yet there is an important factor which may prevent its settling. Abundant *Microtubus communis* can be found in microbialites (leiolites). *Microtubus communis* has been classified as a polychaete worm (Flügel, 1964) as well as a "cyanophycean alga" (Senowbari-Daryan,

1980). Since this worm only dwells in this kind of microbialite fabric of St. Cassian samples, which is relatively widespread in the crusts surrounding metazoan frameworks in this association, this may restrict the settling of *Terebella.* Furthermore, the fact that no *Tubiphytes* can be found at some inferred deep settings (Wendt et al., 1989) may corroborate its absence in some associations contained in the St. Cassian Cipit Boulders (Chaetetid –microencruster, Mud Mound Type – II), thus suggesting that *Terebella* can withstand deeper settings than *Tubiphytes.*

The last analyzed microencruster pair corresponds to *Reptonoditrypa cautica– Baccanella floriformis.*As discussed before, *Baccanella* can been assigned to high energy environments, yet only by few publications (Martini et al., 2004). In this study, such assessments have been taken into account, yet results have not been constant, since *Baccanella* is abundant at some associations where even Hexactinellida appear (Cassianothalamia Gemeinschaft I and II) as well as where medium- to high-energy events take place (Cryptocoelia-*Mesophyllum* community). However, although it appears only in few associations, it coexists with *Reptonoditrypa cautica*, which has been interpreted as a bryozoan adapted to medium- to high-energy environments due to its unilaminar encrusting form, which is typical for such bryozoans (Smith, 1995). This bryozoan nevertheless appears also in associations related to low-energy environments (*Dendronella*-Hexactinellida and *Cassianothalamia* Gemeinschaft II), where its occurence is nonetheless low. It dwells at most in the *Cryptocoelia – Mesophyllum* community, where it shares a common niche with numerous *Uvanella* -type thalamids and numerous packstone – grainstone fillings in primary and secondary vugs can be seen.

Table 1c shows the Jaccard and Simpson coefficient values for these microencrusters, which are the lowest of the discussed pairs. (J= 0.67; S= 1 with a BC value of 0.385). The following should be also considered in evaluating coexistance:

- *Baccanella* encrusts exclusivelly on microbialitic substrates, normally in numerous and conspicuous collonies, though sometimes it can be found as isolated patches of individuals (individual = each "flower- like"structure)

- *Reptonoditrypa cautica* encrusts preferently on skeletical substrates. Yet it can occasionally be found encrusted in microbialitic fabrics (*Dendronella*- Hexactinellida association)

- In some communities, *R.cautica* constitutes an important fraction of the constructor guild (*Cassianothalamia* Gemeinschaft I)

These statements may explain the fact that Jaccard and Simpson values are the lowest of all inferred inter-depending encruster pairs. *R.cautica* may not dwell exclusively in medium to high energies (though preferentially), which can explain its presence where *Baccanella* is absent. However, *Baccanella* is present in large quantities in association with *Cassianothalamia zardinii,* which is

73

significant, because it is not present in any other association adapted to low energy. Thus, dwelling in low energy environments can also be assumed for *Baccanella*, but only in coexistence with *C.zardinii.*

Since both encrusters have such a different set of adaptive traits, numerical coefficients are thus the lowest of the interrelated organisms.

Jaccard and Simpson values for all remaining microencrusters are regarded insignificant (Table 1c; Figs. 30- 33).

5.4. Discussion

A series of interpretations has been established individually for each of the 14 examined associations/biofacies contained in the Cipit boulders. However, elaboration of an integral model will be discussed in this section. It must be pointed out again that all associations are remnants of more massive communities in any given biotope. Based on this single fact, considering individual interpretations may appear unhelpful, as any of the described associations could be literally alongside each other and thus each representing ecologically heterogeneous fragments of a single biotope. Nevertheless, each one of them permits to contribute to the elaboration of a global perspective.

By no means a model or proposal supporting one single origin of these boulders should be accepted. (Keupp et al., 1989; Russo et al., 2000; Sánchez Beristáin & Reitner, 2008) For instance, results from this study show that there are communities which originate from environments which are as different from one another as the famous Patch Reefs (Wendt, 1982) and microbialite-based buildups/"mud mounds" (e.g. Keupp et al., 1989; Reitner & Engeser, 1989a; Neuweiler & Reitner, 1995). It is due to this fact that the origin for these masses should be detailed and explained as widely as possible.

5.4.1. Community ecology

Q-mode cluster analysis was performed in order to obtain communities from groups of associations assorted according its microencruster diversity (plus hexactinellid content) using data from Table 1a, the dataset of which was transposed. The goal of this clustering is to assess if the analyzed microencrusters can serve as a diagnostic environmental tool and thus to support the interpretation individually made for each association.

UPGMA algorithm was used with Jaccard coefficient. Hexactinellid sponges were added as variable due to their environmentally diagnostical properties and their overall scarceness in the whole array of investigated samples (Fig. 34). Five communities can be seen in the phenogram displayed in Figure

34. Community I consists of only of the Mud Mound association I. Community II consists of Mud Mound Association II plus the *Cladogirvanella-* Stromatolite Association; Community III includes all "Patch Reef" Associations; Community IV comprises the chaetetid - microencruster Association, the *Ceratoporell –Tubiphytes* Association and the Thrombolite–microencruster Association. All Hexactinellida-bearing Associations are encompassed in Community V.
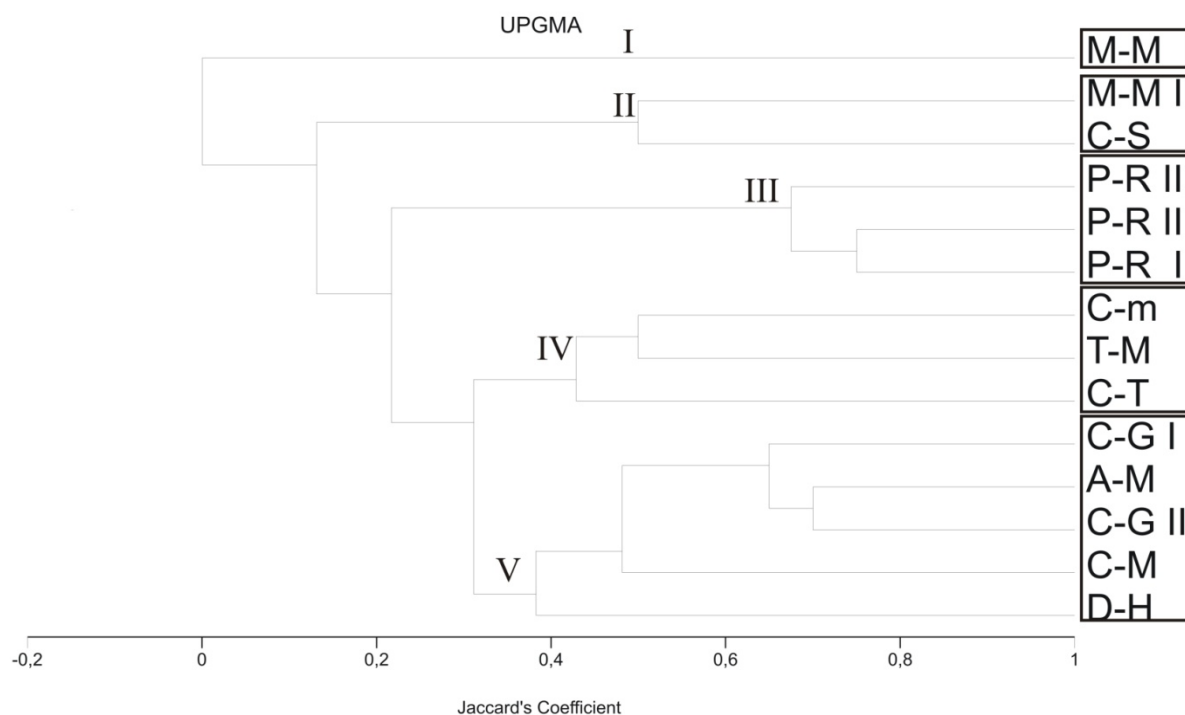
Figure 34. Phenogram of the cluster analysis in Q-mode using the data from table 1a in a transposed matrix and including Hexactinellida data, displaying the five different groups of communities obtained. See Appendix IV- for further information.

Community I consists of only one association and is the most dissimilar, not possessing associated diagnostic microencrusters. Deep environments, partially deprived of oxygen environments can be inferred, because *Terebella* alone cannot be considered as a diagnostic organism. In addition, modern Terebellids and can withstand anaerobic conditions (Robbins, 1987).

Community II includes two associations grouped in one node: The remanining mud mound Association (M-M II) and the C-S Association. Although they have a medium Jaccard-value of 0.5, inferred environments of both were relatively different, since for the C-S Association, temporary emmersion or constant shallowness with low energy conditions were presumed as the most probable paleoenvironmental constraints; whereas for the M-M II Association, sedimentary and paleontological features indicate a rather deep setting. The sole presence of a *Tubiphytes – Terebella* association in the C-S association is not sufficient to serve as criterion for unshallow depths, especially due to the

presence of a porostromate filament orientation apparently influenced by light . The only feature both associations have in common is the semi-quantitative microbialite percentage, which by no means can be considered as a grouping character due to its sensitiveness to cutting effects and sample size (Flügel, 2004; Senowbari-Daryan, pers.comm.) In this case, clustering with the help of microencruster arrays does not seem to be useful.

Community III: Associations representing Patch Reef biotopes

Another subgroup of associations encompasses those originating from the so-called "Patch Reef", altogether displaying the highest diversity of all associations. They can be found in a conspicuous part of the analyzed boulders. They were assigned to such biotopes mainly with the aid of previous descriptions (Fürsich & Wendt, 1977; Wendt, 1982) Similar "communities" have been reported extensively for the late Carnian at many locations [(e.g. the Bosruck Peak in Austria (Dullo et al., 1987) the Pantokrator Limestone of Hydra in Greece (Schäfer & Senowbari-Daryan, 1982; Turnsek & Senowbari-Daryan, 1994); the Bükk Mountains in Hungary (Flügel et al., 1991); and extensive carbonate platforms in Tyrol and Bavaria in the Northern Calcareous Alps (Rüffer & Zamparelli, 1997)] Most of these studies focus either on taxonomic or on paleobiogeographical questions and consequently detailed paleosynecological information does not exist for them.

In the attempt to delimit some paleoecological constraints of the individually analyzed associations, it should be emphasized that the three associations named here as belonging to "Patch Reefs" correspond to different degrees of light-dependant biotopes; one of them, with the least algal content, having stromatoporoids as main builders and the other two, an algal and a *Spongiomorpha ramosa*- based framework respectively. However, they can be grouped together on the basis of possessing the overall same diagnostic microencruster array, with respect to diversity as well as to abundance (Tables 1a, 1b, Fig. 34). A further criterion of its grouping, however a qualitative one, would be the metazoan/microbialite ratio (explained individually, not shown).

In comparison to builder diversity, the low diversity of microencrusters may be due to niche competition through abundant encrusting sponges.

The absence of some distinctive elements of low depth such as Dasycladaceans (Piros & Preto, 2008), or microencrusters like *Thaumatoporella* (Shiraishi & Kano, 2004 ; Schlagintweit & Gawlick, 2008) can be used as criteria for depth assessment. The absence of a *Bacinella- Lithocodium* association shall not be used as a criterion, since this association appears to have dwelled on a wide range of depth settings. (Neuweiler & Reitner, 1992; Leinfelder et al., 1993; Leinfelder et al., 1996; Rameil et al., 2010). Taking this into account, information from microencrusters suggests that either this community dwelled in a depth of 10 to 50 m, or in the subphotic zone respectively, under normally low-energy

conditions (due to their overall sedimentological .features) and in an oxygen-rich environment (high diversity).

Community IV includes three associations: microbialite-dominated T-M, and sponge –microbialite dominated C- m and C-T. Their similarity is however based on a lower Jaccard value of 0.429 for the C-T association with the Node 6 composed by C-m and T-M associations, which has a value of 0.5. Nevertheless they share the feature of practically not having algae as important component of their framework. Furthermore they do not contain any indication for evidently high-energy conditions within their allochthonous components, which also applies for *Reptonoditrypa* as well as for *Baccanella.* Although the T-M community does not have a metazoan framework at all, all three associations comprised in this community possess either *Koskinobullina* or *Girvanella*, which distinguishes them from the associations grouped in communities I and II. In addition, these associations possess either *Tubiphytes* or *Terebella*, yet in a minor proportion as in associations from deeper communities, thus resembling the *Tubiphytes – Koskinobullina* association from Schmid (1996) and Fischer et al. (2007). However, they all lack Lithistids or Hexactinellid sponges. Based on the diversity of their associations, this community can be considered as originating from either low energy, medium-deep (50-100 m) or semi-cryptic biotopes, very similar to those described by Goreau (1959), Riedl (1966), Hartman (1969), Jackson et al.(1971), and Reitner (1989, 1993).

Community V: Associations containing hexactinellid sponges

This community is the most heterogeneous, taking into account that no other hexactinellid- bearing association belongs to any other community. Discussion focuses mainly on hexactinellid content in all associations.

Most associations do not show any evidence of belonging to a reworked boulder; therefore, in case of "non-consistent" associations, any inference performed solely on fossils remains merely speculative. An example hereof would be such associations containing both hexactinellids in a low abundance and a microbialite-dominated facies. (*Cassianothalamia* Gemeinschaft-II). Hexactinellids have mostly been regarded as deep dwelling organisms (e.g. Krautter, 1997, 1998) and consequently in abundance they would indicate a deep biotope, yet they have been able to settle in shallow depths (Mehl, 1996). Nonetheless, as the abundance of hexactinellids in all thin sections analyzed remains relatively constant and coincides with the presence of a copious *Tubiphytes-Terebella* association, the proposed deep, low energy biotope can be accepted, especially if compared to the more diverse *Cassianothalamia* Gemeinschaft I, which has been described as belonging to a medium deep biotope with low influence by light (Keupp et al., 1989; Sánchez Beristain & Reitner, 2008). A further

Results

indication for a low energy environment is the scarcity of *Baccanella floriformis* in comparison to the *Cassianothalamia* Gemeinschaft I, where this microencruster thrives more profusely.

Reitner et al. (1995) gave evidence of the gradual faunal changes of a framework community for the Cenomanian-Turonian of Liencres, Spain. This could be identified due to the proportional abundances of two species. *Acanthochaetetes sp.* and *Vaceletia sp.* For shallow and medium depths, the abundance of *Acanthochaetes* surpasses that of *Vaceletia*, whereas in deeper environments, *Vaceletia* is clearly more abundant than *Acanthochaetetes.* If a biological affinity between the thalamides *Cassianothalamia* and *Vaceletia* is to be assumed, such alternation between thalamide and chaetetid sponges would also have been expected also for the Triassic. However, while comparing the two *Cassianothalamia* associations, which are interpreted as being biotopical variations, alternating relative abundances between the thalamide and any chaetetid could not be detected, possibly due to the number of thin sections compared (ca. 25 for the C-G I vs 7 for C–G II). Nonetheless, this is not as diagnostic as it is the overall diversity of both biotopes, the abundance of lithistids (almost absent in C-G II), the presence of assiduous stromatactis and stromatactoid cavities in C-G II, and the variations in the microencruster assemblage, reasons for which a biotope variability regarding to the depth can be accepted.

Considering hexactinellids as diagnostic tools for deep –and hence under generally low-light – settings, the inferred conditions for the biotope inhabited by the *Dendronella-* Hexactinellida association pose a problematic scenario for its interpretation. The magnitude of an algal framework may thus be secondary in importance to the presence of hexactinellids and a conspicuous *Tubiphytes – Terebella* association dwelling in microbialite, both of which are typical of deep mud mound settings (Wendt et al., 1989; Calvet et al., 1990; Calvet& Tucker, 1995). Drosdov et al. (2008) found evidence of cyanobacterial symbionts in the recent hexactinellid species *Pheronema raphanus* from a deep marine setting (ca. 150 m) in eastern China, implying that influence by light does not necessarily mean a shallow setting.

Chafiki et al. (2004) found a deep-water mound in the Lias of Morocco where the core of the buildup was formed by sponges (hexactinellid and lithistids) and structures (stromatolites and thrombolites) of "algal origin". However, they did not perform any sedimentological or geochemical study in order to discern the taxonomical identity of these microbialites. Nonetheless, as discussed before, red algae can live in depths up to 350 m. (Riding, 1975). In addition, modern representatives of the Florideae, to which *Dendronella articulata* has been assigned, can efficiently dwell in waters deeper than 50 m (Vergés et al., 2004; Lee, 2008).

An explanation regarding this association as originating from shallow settings based on the presence of shallow water, terrigenously influenced, algae-dominated mud mounds (Christopher, 1990) must be rejected. The St. Cassian platforms have been identified as being relatively free of terrigenes (Bosellini & Rossi, 1974; Bosellini, 1984; Wendt & Fürsich, 1980; Sánchez Beristain et al., accepted). Furthermore, the presence of determined chemical elements in Cipit Boulders is non significant and mostly attributable to their deposition in the basin (Russo, F. pers.comm; Sánchez-Beristain et al., accepted).

The possibility could exist that part of a biotope containing the algae -with its associated diverse microencruster guild- and coralline sponges fell from a shallower setting and then were recolonized by the microbialite/hexactinellid with stromatactis cavities and its associated microencrusters. But due to the lack of sufficient sedimentological evidence for reworking, the previously discussed interpretation remains most plausible, taking into account that hexactinellids are rare in the whole array of analyzed thin sections. Assigning this association as a whole to a shallow setting on the basis of algae is also to be rejected, since on one hand *Tubiphytes* is more abundant at depths from 100 to 150 m (Schmid, 1996; Olivier et al., 2008) and on the other hand, only few *Terebella* cf. *lapilloides* tubes can be found. Moreover, middle-depth light-depending *Koskinobullina socialis* could not be found at all. This fact is also remarkable, as the appearance of this encruster is abundant under its optimal living conditions of light, energy and depth (Leinfelder et al.,1996; Schmid, 1996; Aurell & Bádenas, 2004; Olivier et al., 2008; Reolid et al., 2009). Hence, this association can as a whole be assigned to a depth of 100-150 m.

In some associations studied, (*Cryptocoelia – Mesophylum*), paleoenvironmental evidence provided by hexactinellid sponges are of less importance than that provided by other features, such as the microencruster association. This association possesses an abundant encrusting bryozoans component, which is not visible in others. Furthermore, microbialite fraction is insignificant and is almost totally represented by hexactine pseudomorph bearing fabrics, which makes the reconstruction of skeletal even morphotypes (Delecat, 2005; Delecat & Reitner, 2005) impossible. Several features appear (abundance of microencrusters setting on metazoans, the presence of oncoids, overall poor sortment in grainstones), thus supporting a predominantly high-energy environment which would hinder settling of these hexactinellid sponges, and therefore justifying the hypothesis of a re-collonization after falling downslope. However, the settling of hexactinellids can also be due to changing energy conditions, as low energy is a prerequisite for hexactinellid setting (Krautter, 1997; Brückner et al., 2003).

Hexactinellid-containing associations are thus relatively heterogeneous, but can be grouped within a single community with the aid of their microencruster assemblages.

Results

Cluster analysis by means of microencruster organisms as variables can thus be used as a promising tool for the study of fossil framework building communities.

5.5. Geochemistry of selected facies from St. Cassian Cipit Boulders

Due to the remarkable state of preservation of many Cipit Boulders (see above: Introduction, Aims of this work), a number of geochemical analyses can be performed on them. Of particular interest in this work are the major and trace element geochemistry of selected microbialites and associated facies, as well as geochemical profiles (carbon and oxygen isotopes and selected element analysis) in coralline sponge skeletons and stromatolites. In order to assess a sizeably good state of preservation, qualitative, semi-quantitative and quantitative methods must be performed with different Cipit Boulder samples.

5.5.1 Criteria for sample selection

Optical microscopy with the aid of staining methods was used as first criterium for the selection of samples for geochemical analyses. At least one thin section of each analyzed boulder was stained, in order to qualitatively assess its state of preservation. Samples exhibiting a visually obvious and extended diagenetic imprint (mainly through re-crystallization) were discarded from the beginning, even without staining. However, in some of them diagenetical imprint was not detectable until stained with Alizarin/$K_3[Fe(CN)_6]$. When this method was applied, fossils with an original aragonitic composition, which otherwise should only yield pink or pale red colors, yielded a diffuse or vivid Turnbull blue.

Concomitantly, cathodoluminiscence microscopy and Raman spectroscopy were conducted to confirm preservation quality. Samples analyzed with cold cathodoluminiscence microscopy yielded an array of different colors and intensities, corresponding to the different carbonate facies that they contained. Although scarce in all samples, cements are the feature that displays the greatest variety in intensity. Secondary cements, which can be mainly found as veins within fractures, or as stromatactis/stromatactoid infillings show generally a highly luminescent orange pattern. However, they commonly show a gradational pattern from high to totally dark luminescence. (Pl. XIX, Figs. 7-8)This phenomenon was discovered by Müller–Wille and Reitner (1993). They attributed it to the content of Fe^{2+} in sediments. This was further reviewed by Flügel (2004) and Hühne (2005).

In micritic carbonates, whether of microbial or allochthonous origin, the distribution of luminescence is rather irregular and practically indistinguishable. However, allomicrites altogether display a more intense luminescence than microbialites. The only areas in microbialites that generally luminesce are

those corresponding to interstitial cements. Elseways, microbial as well as allomicrite peloids (Pl. XIX, Figs 7-8; Pl. XX, Figs 1-2) show a brownish-dark orange luminescence pattern.

A good state of preservation could be completely assessed by means of cold cathodoluminiscence. Aragonitic fossils, including calcareous algae, corals, and especially sponges, in the majority of cases, do not show luminescence at all. This is almost a constant in all analyzed samples containing either corals or sponges. Occasionally, even minimal impact of diagenesis can be recorded in the microstructure of some of them. This can be observed in the analysis of some chaetetids with sphaerulitic microstructure that show a bright orange luminescence at their centers, whereas the most distal parts are completely dark (Pl. XX, Figs 3-4). This is in agreement with the observations of Laghi et al. (1983), who found that diagenesis in aragonitic fossils with a sphaerulitic microstructure starts from the center of the sphaerulites towards their rims (medium to high Sr^{2+} concentrations). Aragonite in numerous sponge fossil skeletons could be confirmed by means of Raman spectroscopy. This method also proved useful in determining that the original mineralogy for most microbialites was High-Mg calcite (Appendix AVII), a fact that was confirmed by subsequent LA-ICP-MS and microprobe examination.

After these analyses designated to assess preservation state were performed, eight polished slabs containing microbialites and associated facies (Samples Cas 12, FSSA001, FSSA 58, MXXXII, MXXI, MI-6, MV-3 and MX-2) corresponding to the selected samples were analyzed using LA-ICP-MS in order to determine major and trace element concentrations. The focus of this study was microbialite. Appendix AVIII contains a list and a brief description of selected samples.

In addition, three polished slabs containing coralline sponges, including one containing a stromatolite were selected for geochemical profiles (stable isotope analysis, LA–ICP-MS, EDS-Microscopy).

5.5.2. Element analysis of microbialites.

In the following section, the analysis of the geochemical composition of selected microbialites with the aid of LA-ICP-MS will be detailed.

5.5.2.1. Major elements

5.5.2.1.1. *Calcium*

Calcium content was not measured directly by LA-ICP-MS, due to its use as the standard used to order to normalize the values of other elements. However, in order to obtain reliable normalization, it is necessary to obtain quantitative calcium values from another source. Microprobe results (Appendix

Results

AIX), with Ca values from 45.64% to 54.05% Mol (324,021 to 380,833 ppm) indicate a relatively high purity of carbonate in microbialites; however, the traditional value of 400,000 ppm cannot be used for this or any other facies. The average value of 360,000 ppm (obtained through the sum of all elements except for calcium in LA-ICP-MS substracted from 400,000) is used instead for normalization of LA-ICP-MS values in microbialites. In aragonitic facies (*Margarosmilia* and the chaetetid sponge), calcium reached a microprobe value of 56.05% Mol or ca. 390,000 ppm, a value that was used for normalization. This value resembles those of secondary cement facies (Appendix AIX). Allomicrite facies are the most depleted in calcium reaching at most 49.54% Mol (ca 350,000 ppm).

It must be pointed out, however, that at all kinds of facies normalization to 400,000 ppm would have only "noticeable" effects in major elements, since their concentrations are much higher than those of trace elements.

Discussion: All results point to an original calcitic mineralogy for all facies except fossils, which still retain their original aragonitic mineralogy. This is in agreement with the findings of Russo et al. (1997) and Rech (1998).

5.5.2.1.2. *Magnesium*

Magnesium content in all the microbialites ranges from 12,620 ppm (Cas12-M2) to 22,473 ppm (MV-3; Appendix AVIII) in principle indicating an original high-Mg calcite composition (Prasada Rao, 1996). This result corresponds with microprobe values ranging from ca. 4.00% to 6.76% Mol Mg (Appendix AIX) thus being beyond the accepted minimum value of 4 % Mol Mg (Dickson, 1990; Flügel, 2004). Microbialites having a high Mg calcite mineralogy have been reported widely in the literature (e.g. Reitner, 1993; Zankl, 1993; Schäfer, 2006). Raman spectra further support these findings, apart from showing relicts of organic matter (Appendix AVII).

In aragonitic fossils Magnesium concentration is at most 592 ppm (Appendix AVIII) which is also in agreement with microprobe results (Appendix AIX) and thus corresponds to normal values of this element for aragonite (Morse & McKenzie 1991). In the case of the secondary cements, the values reach at most 4,817 ppm (Appendix AVIII) corresponding to 1.67% Mol and thus having an original mineralogy of Low-Mg calcite (Veizer, 1983; Morse & McKenzie, 1991; Russo et al., 1997; Flügel, 2004).

The content of Mg in *Celyphia submarginata* is 3,668 ppm, which would correspond to a Low-Mg calcite (1.27%Mol). Mg concentration in the allochthonous micrites is considerably higher than in the microbialites (Appendix AVIII).

Discussion: LA-ICP-MS analysis of the Mg-content in microbialites showed a high Mg-calcite mineralogy that could be confirmed by Raman spectroscopy. High Mg calcite as well as aragonite agree with the proposed oceanic chemistry for the Triassic (Sandberg , 1983; Lowenstein et al., 2001; Hühne, 2005). The interpretation of the microbialitic spectra is in accordance with the good preservation state confirmed by cold cathodoluminiscene. Furthermore, Raman Spectroscopy revealed a good differentiation between the Mg-calcite mineralogy of the microbialites and the aragonitic mineralogy of the skeletal components. In addition, Raman spectra revealed organic relicts inside the microbialites as well as the skeletal components. The content of Mg for allomicritic facies might be due to the presence of small quantities of dolomitic cement within them, which was recorded by petrographical examination (Sánchez-Beristain et al., accepted). High Mg concentrations in allochthonous components were also determined by Rech (1998) by means of ADS spectroscopy.

5.5.2.1.3. *Strontium*

Sr concentrations in microbialites range from 603 ppm (Cas 12-M1) to 1,649 ppm (FSSA 58-M2). On the contrary, sparry cement values show a depleted concentration of < 239 ppm, while well-preserved aragonitic skeletons of the chaetetid and *Margarosmilia* reach values of ca. 8,700 ppm, which corroborates the interpretation of good original aragonitic preservation. It is nonetheless important to emphasize that microprobe values are slightly lower with 7800 ppm, especially in the center of some sphaerulites ((Appendix AVIII)). As mentioned above, this matches the results of Laghi et al. (1984). For *Celyphia submarginata*, Sr value reaches 4,063 ppm. Allochthonous detritus cannot be distinguished in this regard from the microbialitic facies (Appendix AVIII), because Sr values range from 817 to 1,125 ppm. There is no correlation between Si or Al and Sr (r^2 Si-Sr= 0.02; r^2 Al-Sr = 0).

Discussion: Sr concentrations correspond with mineralogical values from other fossil high–Mg calcite microbial carbonates (Jasionowski, 2004; Wang et al., 2005). The nonexistent correlation between Silicon or Aluminium and Strontium (Figs. 35-36) preclude a crustal origin of the latter element, thus reflecting the original mineralogy of microbialites.

Results
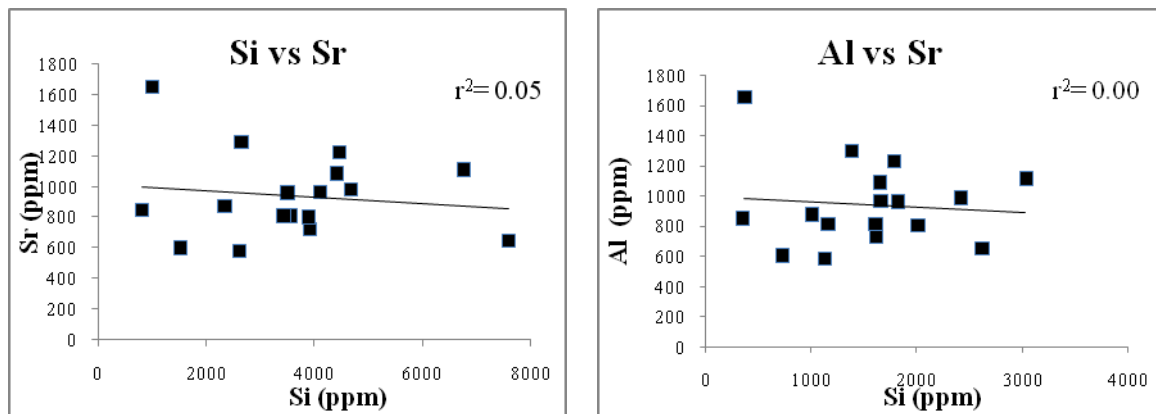
Figures 35 (left) and 36 (right): Correlation between Silicium and Aluminium to Strontium in microbialites. Note the low value of r^2. See text for further details.

High Sr values in aragonitic fossils are in agreement with microprobe results (Appendix AVII) and support the assumption of an overall good preservation of most St. Cassian aragonitic fossils (Scherer, 1977; Laghi et al., 1983; Russo et al., 1991, 1997; Sanchez Beristáin et al., accepted). In the case of *Celyphia submarginata*, however, the relatively low value can be explained by a high Fe value of 6,348 ppm., thus suggesting a medium preservation state.

It can therefore be concluded that Sr concentrations reflect the original microbialite mineralogy and thus diagenetical imprint or a crustal origin of these concentrations can be excluded. Sparry cement concentrations point to a late diagenetic origin (Russo et al., 1991, 1997).

5.5.2.1.4. *Iron*

Fe concentrations in microbialite facies range from 2,986 (MV3-M1) to 15,529 ppm (MXXI-M1; Appendix AVIII). The highest value can be compared with that of allomicrites, which ranges from 7,903 to 15,784 ppm. On the contrary, fossils (except *Celyphia submarginata* with 6,348 ppm) have concentrations as low as 68.26 ppm (thecideid brachiopod) and not higher than 356.44 ppm (*Thecosmilia* corallite). All these values are in agreement with microprobe results (Appendix AIX). Values from sparry cements range between 6,061 and 7,011 ppm.

Discussion: Russo et al. (1997) found Fe concentrations below detection limit for Cassian microbialites from Punta Grohmann using EDX microscopy. Hence, Fe values of microbialites from this work would in the first instance indicate a diagenetic imprint. However, they also cited undetectable values for Sr. Rech (1998) found values for Fe concentrations of up to 9,220 ppm in High Mg-calcite Cassian microbialites from Pralongia. Schäfer (2006) also found recent microbialites with [Fe] up to 5,435 ppm. The concentrations of Fe in skeletal material, with values comparable to values between brachiopods and aragonitic samples, indicate an extraordinary preservation state for St. Cassian fossils. Hence, high iron concentrations may not be due to meteoric influence, but be a

consequence of a reducing environment (Berner, 1980; Schäfer, 2006; Jørgensen & Kasten, 2007). Unfortunately, correlation between Fe and S is weak ($r^2= 0.19$; Fig. 37), which would enormously support this assumption.
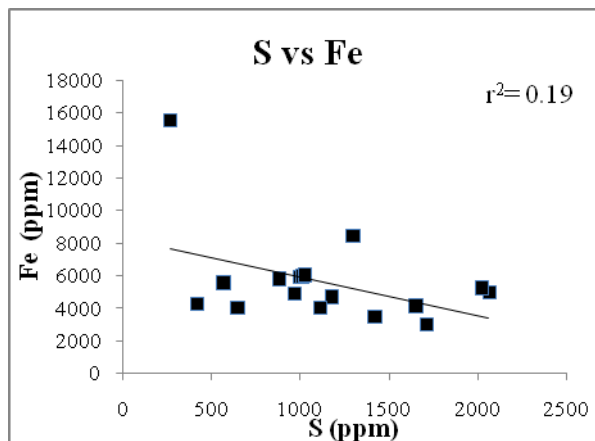
Figure 37: Correlation between Sulfur and Iron in microbialites. Only a minimal correlation can be seen, which indicates a lack of dependence of Iron concentrations on Sulfur. See text for further details.

5.5.2.1.5. *Manganese*

Manganese concentrations range from 202 ppm (MV3-M2) to 1,744 ppm (MXXI-M1) in microbialitic samples (Appendix AVIII). These values are on average slightly lower than that of allomicrites (984 to 1,248 ppm). Fossils (except *Celyphia submarginata* with 841 ppm) exhibit overall low concentrations, from 10 ppm (brachiopod) to 96 ppm (*Margarosmilia* corallite). Values from sparry cements (915 and 1,077 ppm) are comparable with those from the highest microbialite and all allomicrite Mn concentrations (Appendix AVIII) Results correspond with microprobe examinations (Appendix AIX).

Discussion: Schäfer (2006) found Mn concentrations for recent microbialites with values of up to 661 ppm. Rech (1998) obtained values of up to 853 ppm. In principle, these values would support a meteoric diagenetic origin for these concentrations (Schulz & Zabel, 2007). However, such values can also be obtained in reducing environments (Pingitore 1978; Berner, 1980; Haese, 2007). Unfortunately, correlation existing between S and Mn is also weak ($r^2=0.24$), as in the case of S-Fe (Fig. 38).

Results
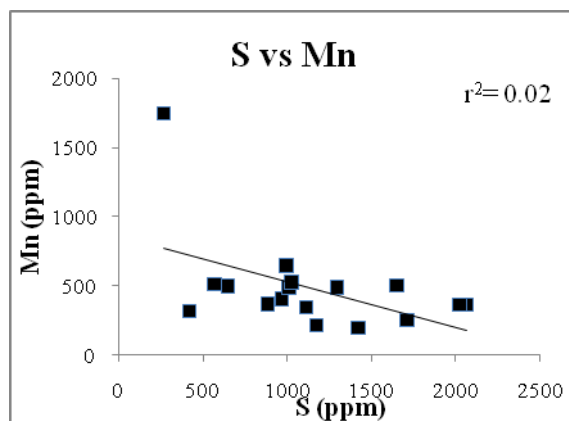
Figure 38: Correlation plot between Sulfur and Manganese in microbialites. No correlation can be seen. See text for further details.

Since a diagenetic study is not the subject of this work, this topic will not be pursued further. However, in order to determine if such high Mn concentrations could be related to meteoric diagenesis at all, plotting the relationship Mn/Sr against $\delta^{18}O$ values can be insightful. These plots may help assess an early diagenetic origin of high values of Mn concentrations. A given reference value for $\delta^{18}O$ must however be known (Halverson et al., 2002). Results from Figure 39 show that all samples are allotted to the quadrant at the lowerr left corner, (compare Halverson et al., 2002; Yoshioka et al., 2003). Therefore, it is assumed that these high Mn concentrations, despite the lack of correlation to S, reflect an early diagenetic origin related to reductive conditions. However, further assessments of diagenesis remain beyond the scope of this study.
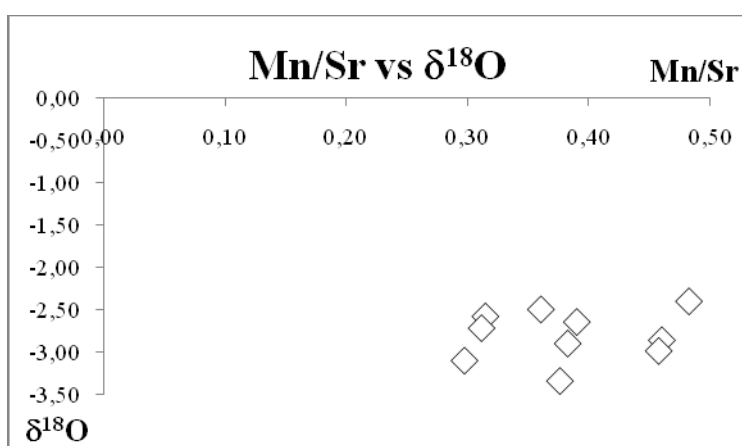
Figure 39: Correlation plot between $\delta^{18}O$ and Sr/Mn in microbialites. Note the allotment at the upper left quadrant. See text for further details.

5.5.2.1.6 *Sulfur*

Sulfur concentrations have values from 268 ppm (MXXI – M1) to 2,062 ppm (MI6-M1) in microbialites. All of them except M1 (268 ppm) have higher values than allomicrites which range from 575 to 962 ppm. In sparry cements, values range from 227 to 680 ppm, whereas in skeletal remains some variation exists. The chaetetid sponge has a value of 288 ppm. The corals have 834 ppm (*Thecosmilia*) and 854 ppm (*Margarosmilia*). Brachiopods have 452 and 502 ppm.

Discussion: Sulfur is an element with a widely known biological importance (Fraústro da Silva & Williams, 2000; Nelson & Cox, 2000) This may be the cause of sulfur enrichment in microbialites relative to allomcrites. Furthermore no correlation can be seen between this element and Si or Al (0.04 and 0.09 respectively), which rejects the possibility of a crustal origin.

No correlation exists between sulfur and nickel ($r^2 = 0.04$; Fig 40), which would support a metabolical origin for determined enzimatical activity (Schäfer, 2006). Furthermore, correlations between sulfur and iron or manganese are low, which excludes the possibility of solely supporting an early diagenetical origin for this element (e.g. Haese, 2007; Jørgensen & Kasten, 2007). Sulfur concentrations in these samples may thus be a mixture of early diagenetical activity and relicts of biological activity.
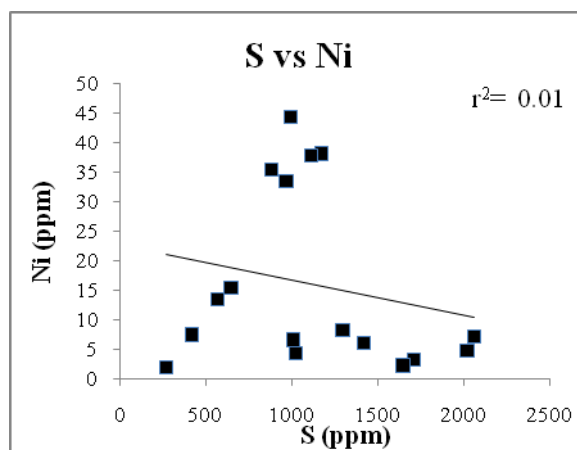
Figure 40: Correlation plot between Sulfur and Nickel in microbialites. No correlation can be seen, which precludes assigning a metabolical role to the latter. See text for further details.

The presence of high S concentrations in St Cassian sponges are in agreement with Laghi et al (1983) which supposed this element to be the relict of bacterial metabolism.

5.5.2.1.7. *Phosphorus*

Phosphorus concentrations have values from 101 ppm (Mi6-M1) to 2,710 ppm (FSSA58- M1) in microbialites (Appendix AVIII). Every sample except FSSA 58 M1 has lower concentrations than the allomicrites, which range from 789 to 1,538 ppm.

Sponges are slightly more enriched in this element than corals, with 35 ppm (chaetetid sponge) and 78 ppm (*Celyphia submarginata*) vs. 8 ppm (*Thecosmilia*) and 24 ppm (*Margarosmilia*). Thecideid brachiopods display a gross difference between each other with 5 and 116 ppm. The value in sparry cements is between 45 and 180 ppm, being more reduced than allomicrites or microbialites regarding to sulfur.

Discussion: Since P concentrations are higher in allomicrites than in any other facies, a biological influence cannot be inferred for their origin. Correlation between P and Si/Al are medium to low (0.19 – 0.25, respectively), which supports only slight crustal contamination. In the case of microbialites, phosphorus concentrations are interpreted as high, which excludes the possibility of obtaining a reliable REE + Y pattern (Nothdurft et al., 2004; Byrne et al., 1996).

5.5.2.1.8. *Silicon*

Silicon concentrations in microbialites range from 823ppm (FSSA001-M2) to 7,591 ppm (MV3-M2; Appendix AVIII). A substantial difference cannot be seen with respect to the content of this element in allomicrites, which ranges from 4,178 to 6,878 ppm. On the contrary, this value is considerably decreased in other facies. In sparry cements its value reaches from 156 to 446 ppm, whereas in skeletal components it is slightly lower, from 72 ppm (thecideid brachiopod) to 474 ppm (chaetetid sponge).

Discussion: The content of silicon in St. Cassian microbialites is higher than other known fossil and recent samples of this nature (Webb & Kamber, 2000; Nothdurft et al., 2004; Olivier & Boyet, 2006), which further excludes the possibility of analyzing REE patterns (e.g. Bau & Dulski, 1996; Webb & Kamber, 2000; Nothdurft et al., 2004). Concentrations of this element are lower in skeletal components, as no biological effect is known for this element (Fraustro da Silva & Williams, 2000). Silicate weathering has proven to be an important factor for microbialite formation in some modern cryptic environments at continental islands and it may be related to high carbonate alkalinity (Reitner, 1993). However the main cause of the high siliciclastic content in St: Cassian samples may be related to the marly nature of the St. Cassian Formation, extensively reported in the literature (e.g. Wendt & Fürsich, 1980; Russo et al., 1991; Sánchez-Beristain et al., accepted).

5.5.2.1.9 *Aluminium*

Aluminium concentrations ranges from 369 ppm (FSSA 58-M2) to 3,030 ppm (FSSA 58-M1) in microbialites (Appendix AVIII). Most values are very similar to those of allomicrites, which attain from 1,800 to 2,828 ppm. Notably, the concentrations of this element are very much lower in skeletal remains with 0 and 10.50 ppm for thecideid brachiopods, 6 ppm for chaetetid sponges, 10 and 23 ppm for corals, and 37 ppm for *Celyphia submarginata*.

Discussion: Al content in St. Cassian microbialites behaves in a way very similar to that of Si. Since biological importance is not known for this element (Fraústro da Silva & Williams, 2000), a crustal origin must be assumed.

5.5.2.2. Trace elements

5.5.2.2.1. *Crustal-related elements without a known biological effect*

In the case of zirconium and rubidium, significant enrichment can be seen with the allomicrite samples (Zr> 4.50 ppm and Rb >3.94) with respect to that of microbialites (except FSSA 58 M1, Zr <3.91 ppm, and Rb < 2.86 ppm). Whereas Zr is depleted in both the cement and in the aragonitic and alsobrachiopod skeletons, the Rb values are high in the cement, comparable to those of the microbialites with lower concentrations of this element. In the aragonitic facies this element is negligible. Titanium shows features of both Zr and Rb insofar as their concentration within the skeletons is low and in the sparry cement Ti concentrations are more similar to the lowest values of microbialites, whereas the allomicrite facies are close to or slightly higher than the highest microbialitic values (Appendix AVIII).

A further subgroup of these elements is constituted by thorium, niobium, and hafnium. Their behavior is important, since they appear enriched at most within the sparry cements, whereas their concentration in allomicritic facies is just slightly higher than in microbialites. At the aragonitic skeletons they display concentrations similar to those of the microbialites. Hf is the only element with near-background concentrations, which was taken into account for this study and therefore it has the highest uncertainties along the time series within microbialite and allomicrite samples (see Methods section).

Tantalum was measured only in 4 microbialite samples and was below the detection limit in all of them.

Discussion: Very strong correlations (r^2 coefficient) can be seen between Si and the following elements for all the microbialite data set: Rb = (0.85); Ti = (0.90); Zr = (0.78); Nb = (0.58) and Th =

Results

(0.73) (Figs. 41-45), most probably a result of their high siliciclastic content. Some of the studied samples have Zr concentrations as high as 2% relative to the Earth's crust (Wedepohl, 1995) indicating a high degree of crustal input into the material. This input can be confirmed by means of a high Th/U ratio in all samples, especially allomicrites and microbialites (Appendix AVIII). Silicate weathering has proven to be an important factor for microbialite formation in some modern cryptic environments at continental islands and it may be related to high carbonate alkalinity (Reitner, 1993). However, the main cause of the high siliciclastic content in these samples may rather be related to the marly nature of the St. Cassian Formation, extensively reported in the literature (e.g. Wendt & Fürsich, 1980; Russo et al., 1991).
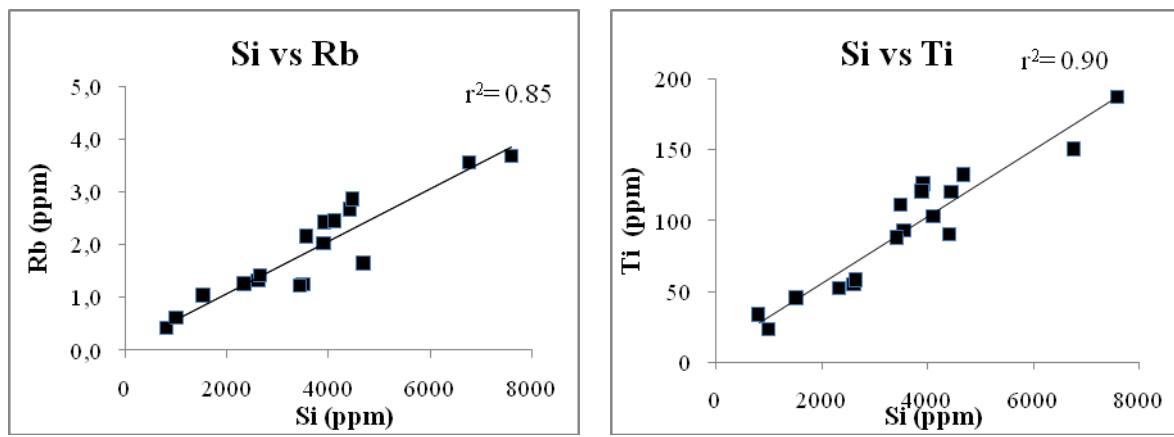
Figures 41 (left) and 42 (right): Correlation plot between Silicon and Rubidium/Titanium in microbialites. A crustal origin is evidenced for both Rb and Ti due to the high r^2 values. See text for further details. Modified from Sánchez-Beristain et al. (accepted).
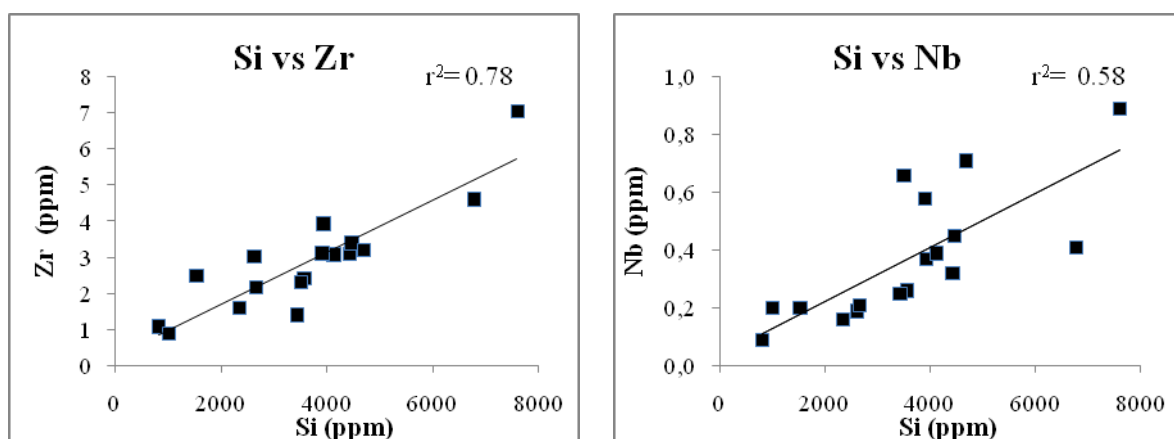
Figures 43 (left) and 44 (right): Correlation plot between Silicon and Zirconium/Niobium in microbialites. A crustal origin is evidenced for both Zr and Nb due to the high r^2 values. See text for further details. Modified from Sánchez-Beristain et al. (accepted).
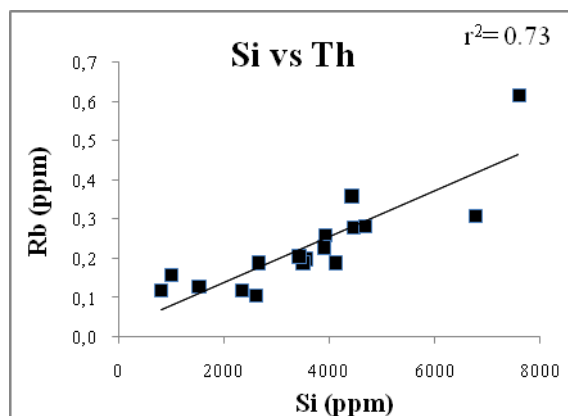
Figure 45 Correlation plot between Silicon and Thorium in microbialites. A crustal origin is evidenced for Th due to the high r^2 value. See text for further details. Modified from Sánchez-Beristain et al. (accepted).

5.5.2.2.2. *Rare Earth Elements + Yttrium*

The Rare Earth Elements (REE) include all elements from the Lanthanum (Z= 57) to Lutetium (Z=71). Their chemistry makes them particularly useful in studies of marine geochemistry such as the determination of the oxidation state and temperature of an aqueous environment, because they have a similar ionic radius and most of them a trivalent oxidation state (Elderfield & Greaves, 1982; Elderfield, 1988). Only Cerium and Europium possess different redox states (Ce IV and Eu II, respectively), which allows particular environmental determinations with their aid. Although REE are soluble, they are relatively resistant against low grade metamorphism and hydrothermal alteration (Hühne, 2005).

The natural abundances of elements resulting from nucleosynthesis show a rhythmic variation with atomic number. However, this variation can be corrected by normalization to a standard. These normalizations produce "REE patterns". Elderfield (1988) proposed the first REE pattern based on the normalization of the concentrations of REE in shale to chondrite values. Yttrium, although not an REE, behaves in a way chemically similar to most REEs and can be inserted between Dy and Ho according to its ionic radius (Byrne & Lee, 1993; Bau et al., 1997). Thus, an REE + Y pattern (REY) is to be obtained.

Apart from seawater (e.g. Elderfield & Greaves, 1982; German et al., 1991; Piepgras & Jacobsen, 1992; Bau et al., 1995; Bau et al., 1997), REE/REY patterns have been obtained from different kinds of reservoirs, such as rivers (Goldstein & Jacobsen, 1988; Elderfield et al., 1990), magmatic systems (Bau, 1996), iron formations (Bau & Dulski, 1996, Bolhar et al., 2004), hydrothermal fluids (Michard & Albarède, 1986; Bau & Dulski, 1999), ferromanganese crusts (Bau et al., 1996; Delecat, 2005), biogenic apatites (Grandjean-Lecuyer et al., 1993), and most recently, microbialites (e.g. Webb &

Results

Kamber, 2000; Kamber & Webb, 2001; Bolhar et al., 2004; Van Kranendonk et al., 2003; Delecat, 2005; Olivier & Boyet, 2006; Kamber & Webb, 2007).

REE and REY patterns, respectively, in microbialites are usually normalized to PAAS standard (McLennan, 1989). When obtaining a PAAS-normalized REY pattern, it is important to take into account the concept of "anomaly". An anomaly can be understood as any deviation from a straight line after a normalizing process, resulting from either higher (positive anomaly, value > 1) or lower concentrations (negative anomaly, value < 1) than expected.

Despite the usefulness of REE patterns, REE are very susceptible to different agents in seawater, thus altering their original pattern. Among such agents, siliciclastic/crustal input and phosphate contamination can be named. Crustal input can totally flatten an REY pattern (Nothdurft et al., 2004), while phosphates enhance the enrichment of heavy REEs (HREE) through co-precipitation (Byrne et al., 1993).

Thus, in order to find a reliable REY pattern capable to provide valuable information of important marine settings, relatively free of crustal input and phosphates are needed. Webb & Kamber (2000) successfully pioneered in determining the genuine systematics of the distribution of rare earth elements + yttrium (REY patterns) in a set of siliciclastic-free Australian Holocene microbialites from the Great Barrier Reef. However, in all studied microbialite samples, values of Si, Al, and all crustal associated trace elements discussed up to now are much more higher in comparison to other microbialites described in the literature (e.g. Webb & Kamber, 2000; Van Kranendonk et al., 2003; Nothdurft et al., 2004; Olivier & Boyet, 2006).

It was intended to obtain REE patterns for all datasets of microbialites. However, all samples have a considerable amount of crustal input (Sánchez Beristain et al., accepted). Therefore, only La, Ce, and Y were measured for control purposes in most samples. However, several differences can be observed among them (Appendix AVII) and a conclusion should not be drawn.

At high zirconium concentrations, original REY signals may be lost (Bau & Dulski, 1996). Some of the samples reach Zr concentrations as high as 2% relative to the Earth's crust (Appendix AVIII, compare Wedepohl, 1995) indicating a high degree of crustal input into the material. Furthermore, the concentration of Y in two allomicrite samples (Cas 12-A1 and Cas 12-A2) is even higher than in the continental crust (Wedepohl, 1995). Although a correlation between Si and Y, La or Ce does not exist, the increased concentrations of the latter three and their high concentrations in allomicrites and microbialites can also be interpreted as indicators for crustal contamination in St. Cassian samples. This contamination can be confirmed by means of a high Th/U ratio in all samples, especially allomicrites and microbialites (Appendix AVIII). In case there is considerable siliciclastic pollution,

REY patterns are useless, because they would not reflect the partition coefficient of seawater (e.g. Webb & Kamber, 2000; Van Kranendonk et al., 2003; Nothdurft et al., 2004). Thus it seems unlikely to find reliable REY patterns in St. Cassian microbialites, since an amount as little as 1% of siliciclastic contamination effectively masks original signals (Van Kranendonk et al., 2003). Furthermore, phosphorus reaches relatively high concentrations in microbialites (up to 568 ppm). P-free microbialites are necessary for the determination of reliable REY patterns, since it is widely known that P considerably affects their systematics due to processes like phosphate co-precipitation (Lee & Byrne et al., 1996; Nothdurft et al., 2004).

Complete REY concentrations were thus measured only in the most Si-Al depleted microbialite, sample FSSA001 M2. The obtained pattern does not resemble any known microbialitic PAAS-normalized REY patterns (Appendix AX, Fig. 46; see above for references). A typical, though exaggerated seawater positive La-anomaly (Bolhar et al., 2004, La/La* = 1282 after their calculation) can nevertheless be seen. For the calculation of Ce/Ce* which can provide information on the oxidation and alkalinity state of the water (Bau & Dulski, 1996; Webb & Kamber, 2000; Hühne, 2005), the method of Bolhar et al. (2004) was again used, since the proved better method of Olivier & Boyet (2006) takes into account the concentration of La. In this regard, the obtained value of Ce/Ce* = 3.89 would be considered as a highly positive Ce anomaly, much higher than recorded seawater-positive Ce anomalies (Bolhar et al., 2004) and thus it should not be considered as an original signature of a high pH value and reducing environment for the Carnian seawater. In order to prove at least that there would be a positive Ce anomaly, the value of Pr/Pr* is needed, assumed that Pr/Pr* cannot be found (Bau, 1996). The value of Pr/Pr* = 0.58 would support positive La/La* as well as Ce/Ce* anomalies (Bau & Dulski, 1996; Webb & Kamber, 2000; Olivier & Boyet, 2006). However, such assumptions can be neglected if a minimal Y/Ho coefficient = 1 is found, which is even lower than chondritic ratios and much lower than seawater values of 44-74 (Bau, 1996). Similar crust-related Y/Ho values were found for Triassic Adnet sediments by Delecat (2005).

Results
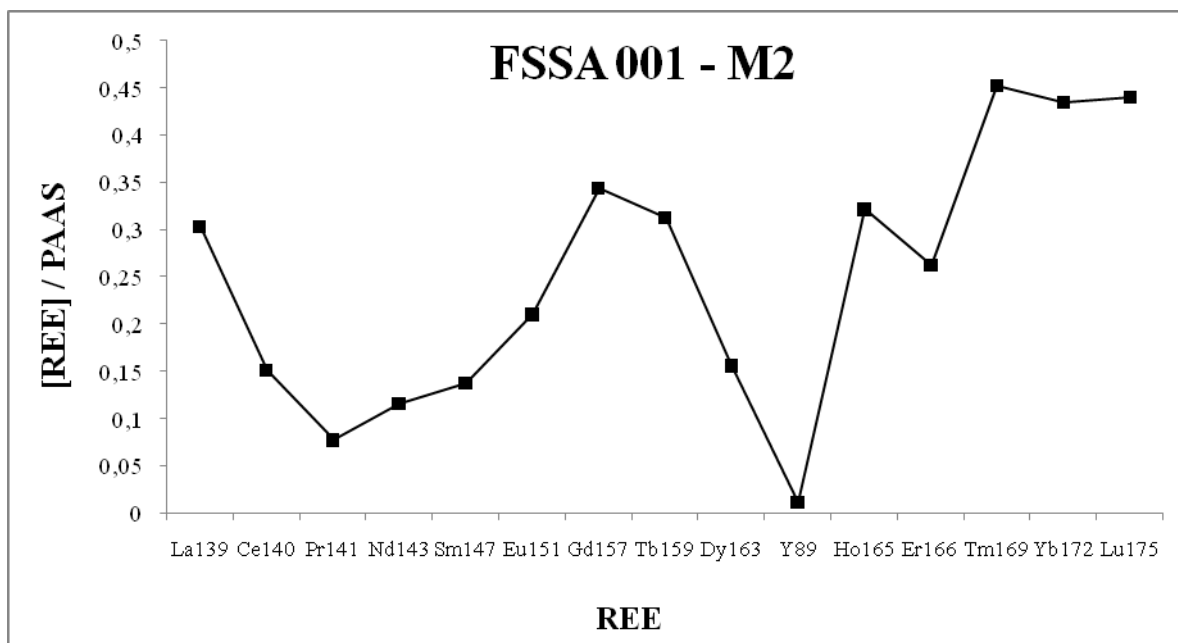
Figure 46: PAAS – Normalized plot for Rare Earth Elements + Yttrium (REY) in microbialite FSSA 001-M2. No interpretable pattern was obtained due to crustal contamination. See text for further details. See text and Appendix AX for further details.

The value of a negative Eu/Eu* = 0.87 should neither be taken as realistic. On the one hand, the peak from Eu in figure 53 in comparison to Sm could preliminarily be considered as a positive Eu anomaly, typical of the presence of hydrothermal input, as it happens in some contemporary oceans (Webb & Kamber, 2000). Yet the same plot exhibits significant enrichment in Gd which is an element used for the calculation of Europium anomalies. This Gd enrichment produces a negative value for Eu/Eu*.

An overall enrichment of HREE in comparison to LREE (Nd_{SN} / Yb_{SN} = 0.28) and MREE (Sm_{SN}/Yb_{SN} =0.31) can furthermore be seen. This enrichment is typical of modern seawater (Webb & Kamber, 2000; Nothdurft et al., 2004). Nevertheless, apart from crustal contamination, phosphates tend to enhance the concentration of HREE against MREE and LREE (Byrne et al., 1996; Nothdurft et al., 2004) and thus this signature is not reliable either.

Discussion: Despite the fact that the investigated sample has the lowest content of crustal components, the obtained REY pattern is not thought to be reliable, because there are many factors altering the plot of REE + Y in many ways. REE + Y concentrations are interpreted as strongly affected by the content of siliciclastics as well as by the amounts of phosphorus. To different extents these could be the causes of even contradictory assessments for each paleoenvironmental constraint.

5.5.2.2.3. *Elements with a known biological effect*

Elements with a possible vital effect such as vanadium, chromium, tin, antimonium, zinc, copper, molybdenum, cobalt, and nickel have significant concentrations in all the studied carbonate facies (compare Kamber & Webb, 2007). In this section, it will be discussed if they reflect vital fractionation in the microbialites.

5.5.2.2.3.1. *Vanadium and chromium*

Significant differences cannot be seen for V and Cr among corals, chaetetids, sparry cements, and some of the microbialites. Brachiopods have very low concentrations (Appendix AVIII). Sample Cas 12-M2 has a relatively high concentration of V (10.53 ppm), but due to its high Si and Al concentrations, a biological effect for this element cannot be confirmed in this sample. Allomicrites have the highest V and Cr concentrations in all the dataset.

Discussion: All microbialites show a weak to medium correlation between Si and these elements, ($r^2 =$ 0.11 for Si- V and 0.07 for Al-V; 0.37 for Si-Cr and 0.30 for Al-Cr; (Figs.47-48; 49-50; Appendix AVIII), which could explain their higher concentrations as a consequence of siliciclastic input. Furthermore, all allomicrite samples show higher concentrations of V than microbialites and than 10 of the microbialites for Cr. Therefore, no biological effect for these elements can be concluded from these samples.
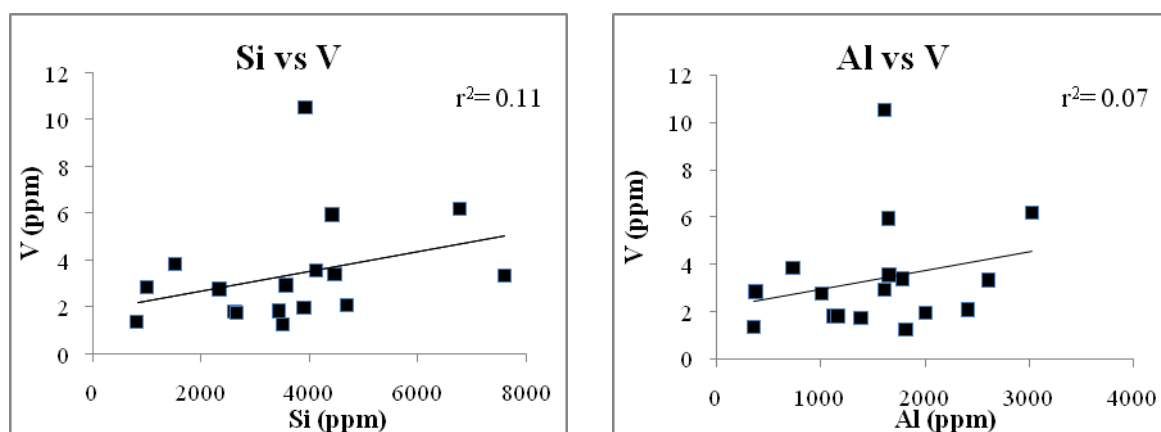
Figures 47 (left) and 48 (right): Correlation plot between Silicon /Aluminium and Vanadium in microbialites. Despite the low existing correlation, no biological effect can be concluded for V especially due to its high values in allomicrites. Modified from Sánchez-Beristain et al. (accepted). See text for further details.
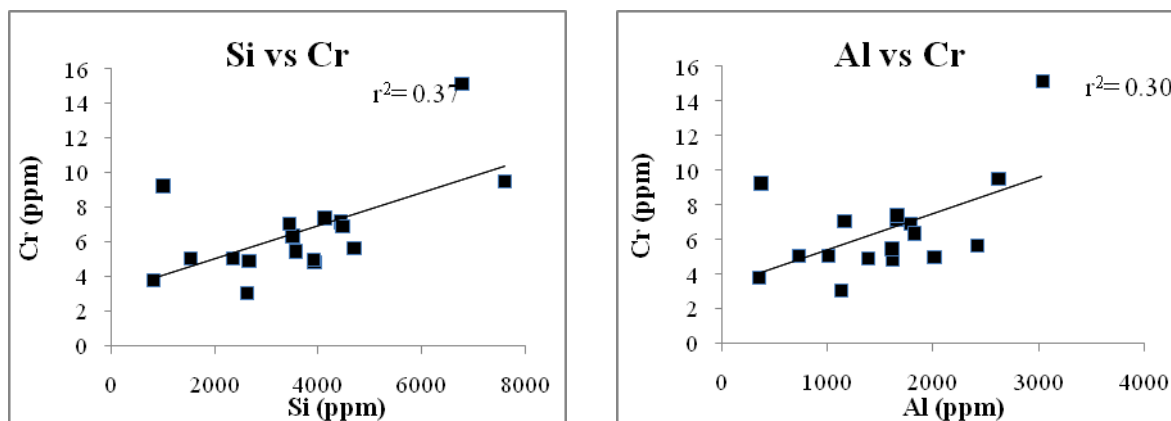
Figures 49 (left) and 50 (right): Correlation plot between Silicon /Aluminium and Chromium in microbialites. Despite the same existing correlation, no biological effect can be concluded for Cr especially due to its high values in allomicrites. Modified from Sánchez-Beristain et al. (accepted). See text for further details.

5.5.2.2.3.2. *Tin, antimony, and zinc*

The patterns of tin, antimony, and zinc are not clear. The cements are more enriched in Sn and Sb than coral skeletons, while little difference is recordable among the sponges or brachiopods. Unfortunately, concentrations of these elements exhibit large variations in microbialite samples (Appendix AVIII) and allomicrite is slightly enriched, even more than in all other samples, except Cas 12-M3 with 2.12 ppm for Sn and Cas 12-M1 and FS-SA58 M2 for Sb (6.85 and 3.19 ppm, respectively). Zinc concentrations are similar among samples except for allomicrite in which the concentration is relatively high.

Discussion: Although a significant correlation does not exist between Si or Al and these elements (r^2 for Si-Sn = 0.01, Al-Sn = 0; Si-Sb and Al-Sb = 0.16 both; Si-Zn = 0.01, Al-Zn = 0; Figs. 51-52; 53-54; 55-56), evidence of vital effect for them cannot be concluded in the microbialites, since only few of them show enrichment relative to other samples.
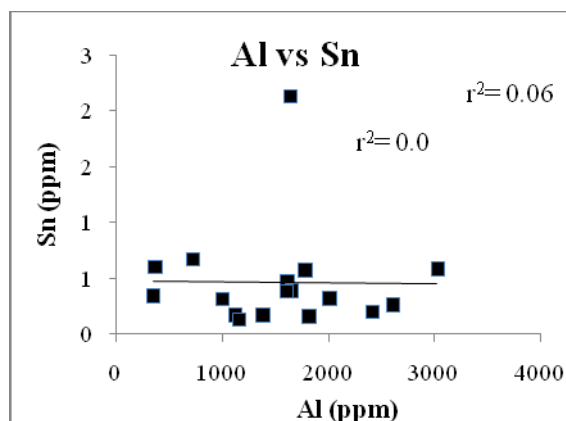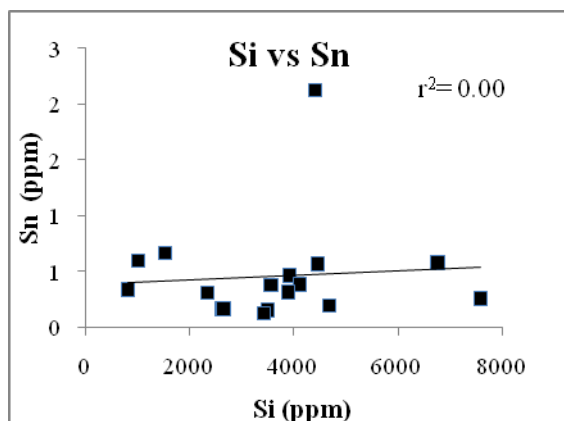
Figures 51 (left) and 52 (right): Correlation plot between Silicon /Aluminium and Tin in microbialites. Despite the same existing correlation, no biological effect can be concluded for Sn, since a considerable enrichment of this element is only present in few microbialitic samples Modified from Sánchez-Beristain et al. (accepted). See text for further details.
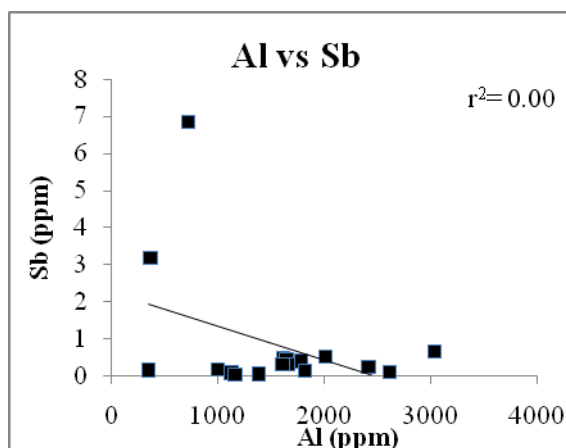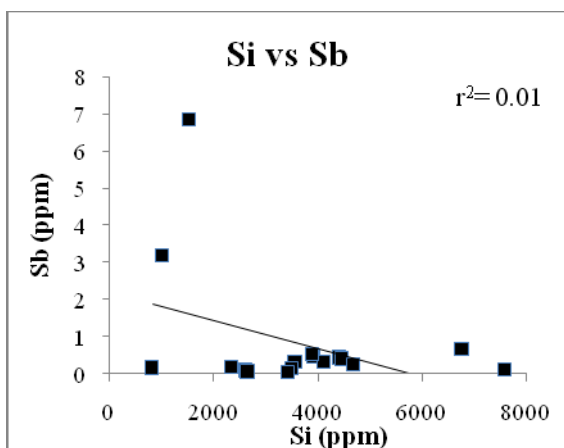
Figures 53 (left) and 54 (right): Correlation plot between Silicon /Aluminium and Antimony in microbialites. The same trend as for Sn can be noticed. Modified from Sánchez-Beristain et al. (accepted). See text for further details.
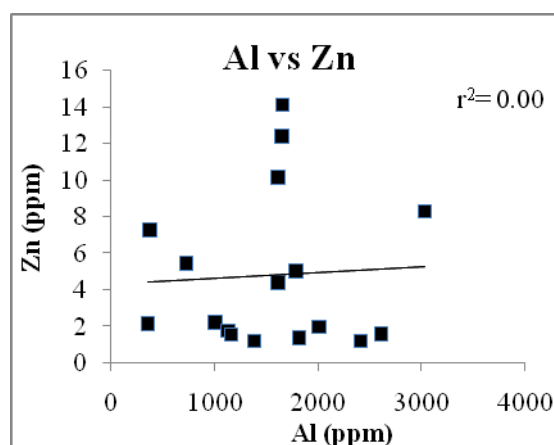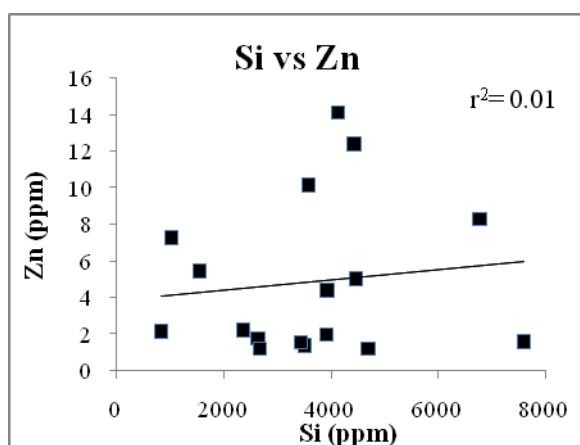
Figures 55 (left) and 56 (right): Correlation plot between Silicon /Aluminium and Zinc in microbialites. The same trend as for Sn and Sb can be assessed. Modified from Sánchez-Beristain et al. (accepted). See text for further details.

Results

5.5.2.2.3.3. *Copper and Molybdenum*

Copper and molybdenum are generally more enriched in the microbialites than in cements, sponges, brachiopods, corals, and even allomicrites. It is unclear if these elements play a biological role in the skeletal organisms, since sponges, brachiopods and corals normally have lower concentrations of all these elements than the sparry cements. Despite the moderate to high siliciclastic content in the microbialites, a correlation cannot be seen between Si and any of them (r^2 for Si-Cu= 0.02, Al-Cu =0; Si-Mo= 0.02, Al-Mo = 0; Appendix AVIII, Figs. 57-58; 59-60). Samples Cas 12-M1 (Mo) and Cas 12-M4 (Cu) have moderately high error means along the time series–ablation (not shown), but that does not seem to affect the distribution plots displayed in figures 58-61.
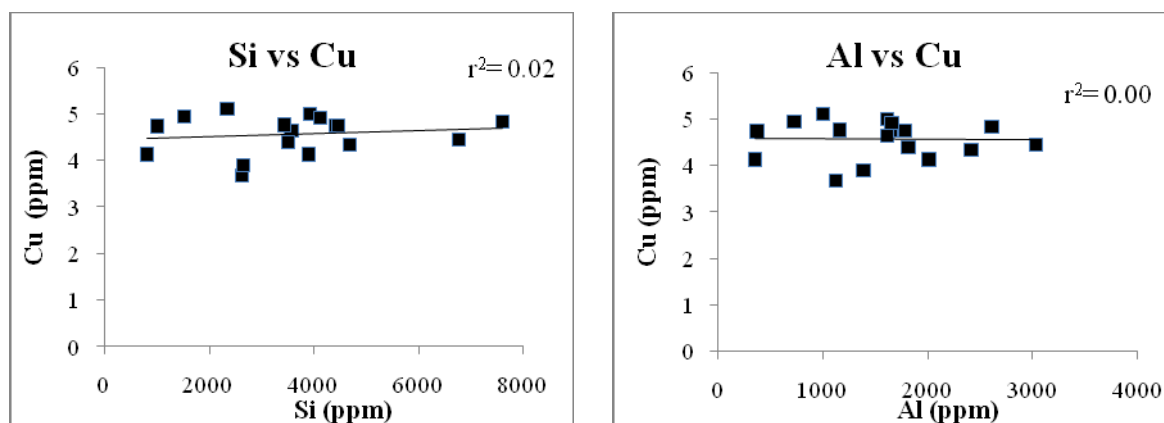
Figures 57 (left) and 58 (right): Correlation plot between silicon /aluminium and copper in microbialites. No correlation can be seen, which could mean that the concentration of this element in microbislites is a genuine remnant of microbial activity. Modified from Sánchez-Beristain et al.(accepted). See text for further details.
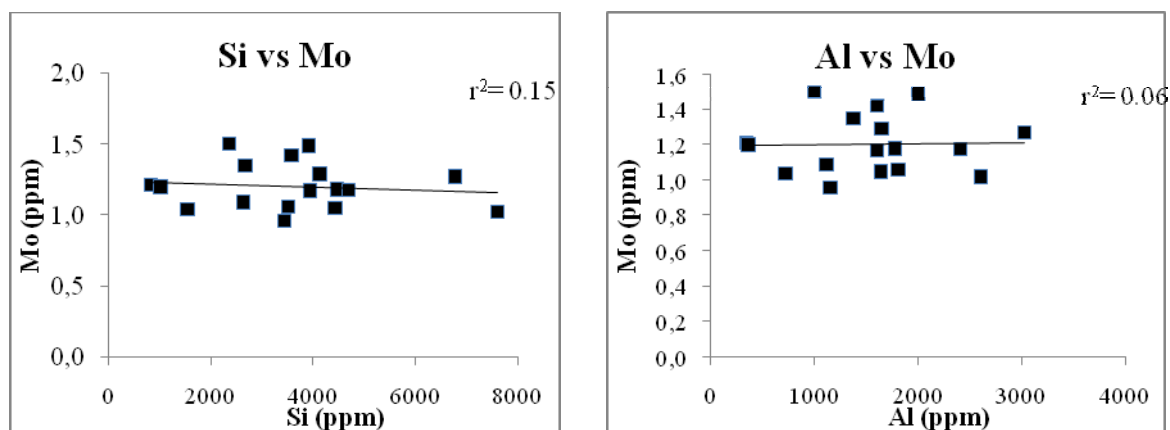
Figures 59 (left) and 60 (right): Correlation plot between silicon /aluminium and molybdenum in microbialites. No correlation can be seen, which could mean that the concentration of this element in microbislites is, as for copper, a genuine remnant of microbial activity. Modified from Sánchez-Beristain et al.(accepted). See text for further details.

Discussion: Copper and molybdenum concentrations are not related to crustal input in any sample. It is widely known that copper plays a fundamental role in the structure of certain transmembrane enzymes,

such as cytochrome c oxidase (Mathews et al., 1999) and molybdenum has been proved to be crucial in molybdate-reducing enzymes in sulfate-reducing bacteria (Tucker et al., 1997). Although a correlation between S and Mo does not exist ($r^2 = 0.01$; Fig. 61), the concentrations of Cu and Mo in microbialitic samples are most likely relics of original microbial metabolism.
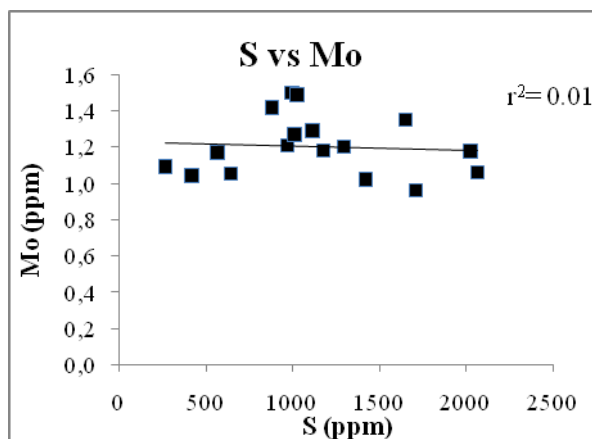
Figures 61: Correlation plot between Sulfur and Molybdenum in microbialites. No correlation can be seen. Nevertheless, this does not exclude the possibility that molybdenum concentrations may be related to the metabolism of sulphate-reducing bacteria. See text for further details.

5.5.2.2.3.4. *Cobalt and nickel*

Cobalt concentrations are only slightly higher in allomicrites than in microbialites, but on the other hand the overall trend is the same as for copper and molybdenum. Nickel concentration is significantly enriched in some of the microbialites, even more than in the allochthonous micrite. FS-SA 001-M2, the most Si-depleted microbialite sample, has a high Ni concentration of 33.57 ppm, thus being more than twice as high as in the allomicrite samples. In sparry cements and skeletons the concentrations are minimal in comparison to allomicrite and microbialite (Appendix AVIII).

Discussion: Although correlations between Si or Al to Co and Ni are negligible (Si-Co= 0.01, Al-Co = 0.02; Si-Ni = 0.03, Al-Ni= 0.05, Figs. 62-63; 64-65), there is a strong correlation ($r^2 = 0.97$) between Ni and Co in microbialite samples (Fig. 66), which would be a consequence of siliciclastic contamination, since this correlation persists ($r^2 = 0.94$) when allomicrite samples are included. Nickel and cobalt are often associated in crustal sediments as arsenides or sulfoarsenides (Ersteva & Tsymbulov, 2002). Furthermore, the Ni/Co ratio in the Earth's crust is ~2.3 (Wedepohl, 1995) and in SMOW around 400. In most of the measured microbialites, this ratio is ~8.0 as well as for the allomicrites and even sponges. Hence, high Ni and Co concentrations in microbialites rather occur due to the influence of terrigenous material than due to biological processes. Moreover, in order to support

Results

a Ni concentration in microbialites owed to metabolism, a medium to high correlation should exist between Ni and S in the samples (Schäfer, 2006) which is absent ($r^2= 0.04$) (Fig. 40).
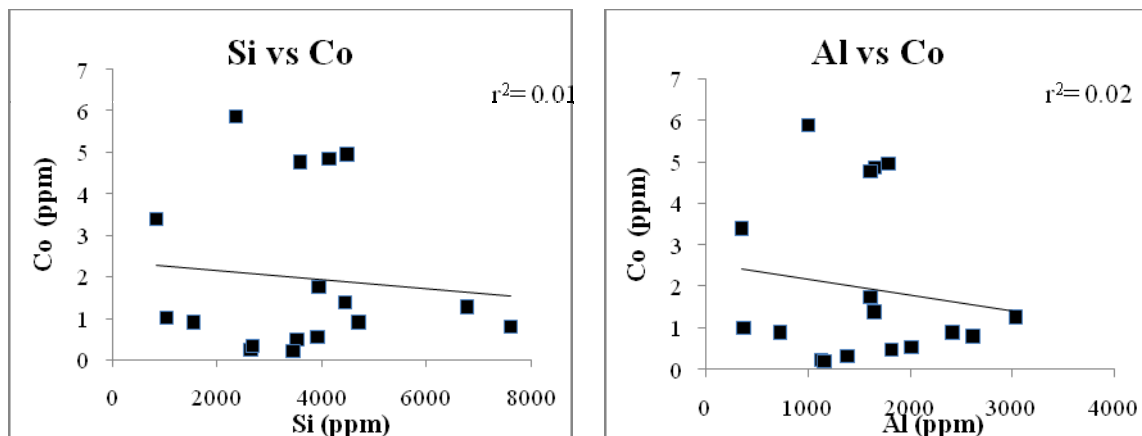

Figures 62 (left) and 63 (right): Correlation plot between Silicon /Aluminium and Cobalt in microbialites. Despite no correlation exists, no biological effect can be concluded for Co especially due to its high values in allomicrites.and to its correlation with Nickel (see Figure 66) Modified from Sánchez-Beristain et al. (accepted). See text for further details.
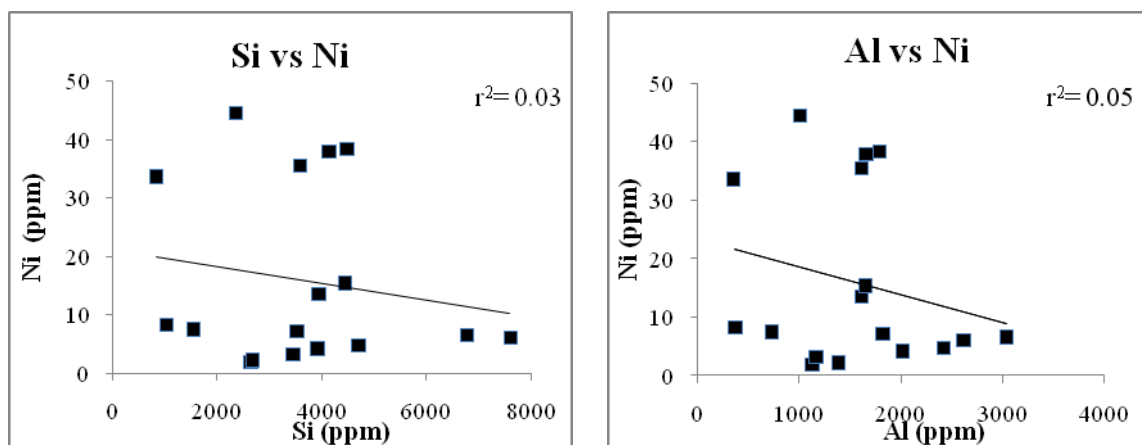
Figures 64 (left) and 65 (right): Correlation plot between Silicon /Aluminium and Nickel in microbialites. In spite of the lack of correlation and of the enrichment of Ni in microbialites, no biological effect can be concluded for this element due to its correlation with cobalt. (see Figure 66) Modified from Sánchez-Beristain et al. (accepted). See text for further details.
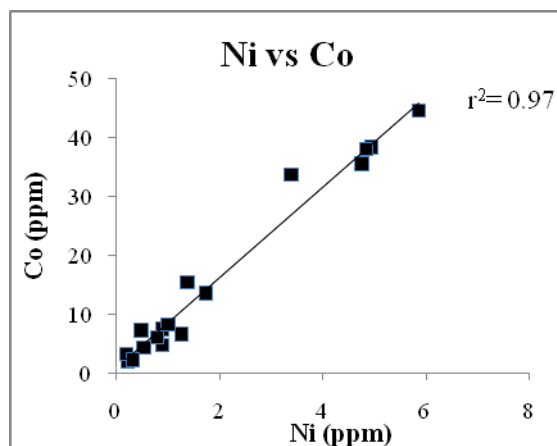
Figure 66: Correlation plot between Nickel and Cobalt in microbialites. A high r^2 value supports a probable crustal origin for both elements, since they are frequently associated with arsenides. Modified from Sánchez-Beristain et al(accepted). See text for further details.

5.5.3. Geochemical profiles on selected St. Cassian samples: Finding new suitable climate proxies for the Triassic

Despite the excellent preservation of and extensive research performed on St. Cassian fossils, few of the available works have focused on using their isotopic compositions as proxies for climate. The first works dealing with non-isolated results did not appear until the last two decades. Stanley & Swart (1995) discovered that coral-zooxanthellae symbiosis already existed in some species of Cassian corals. They compared the $\delta^{13}C$ and $\delta^{18}O$ records of five species and found that these corals possessed zooxanthellate symbioses through the absence of any correlation between the two values. In addition, they measured a temperature of 27.1°C to 33.6°C in these coral skeletons.

Nützel et al. (2009) studied three specimens of megalodontid bivalves in order to assess their $\delta^{13}C$ and $\delta^{18}O$ sclerocronological records. They concluded that a pronounced seasonality in Late Triassic tropical shallow waters took place, with inferred seasonal temperature changes from 24° to 32°C, with a possible influx of fresh water during the rainy seasons.

These results urge further investigation of this field in order to find other fossils with a potential use as paleothermometers. Sponges (in particular "sclerosponges") have proved to be useful organisms, since they are long-lived marine archives of proxy climate data which can augment, and in most instances, replace coral records. By virtue of their well-documented slow growth rate of 0.05 to 1.9 mm/year (Reitner & Gautret, 1996; Wörheide, 1997; Willenz & Hartman, 1999; Böhm et al., 2002; Haase Schramm et al., 2003; Fallon et al., 2005, Grottoli et al., 2010), they can provide information over periods of time much longer than corals (Swart et al., 1998). Furthermore, their capability of forming

their skeletons in isotopic equilibrium with the ambient environment (Böhm et al., 1996; Druffel & Benavides, 1986) means that the resulting data do not need correction for species effects (Swart et al., 1998) and therefore can provide continuous and contiguous isotopic $\delta^{18}O$ values which may be related to variations in temperature and/or environmental availability of carbon (Haase Schramm et al., 2003; Fallon et al., 2005; Rosenheim et al., 2009; Grottoli et al., 2010).

In addition to $\delta^{18}O$ values, temperature estimations in sponges can be performed by means of a Sr/Ca ratio. This proxy is directly proportional to $\delta^{18}O$ values (Haase Schramm et al., 2003; Rosenheim et al., 2004; Grottoli et al., 2010). Furthermore, it is much more exact than oxygen isotope values, since the latter proxy is prone to strong variations due to pH fluctuations (Haase-Schramm et al., 2003). In the range from pH = 6 to 9, the $\delta^{18}O$ of carbonates can decrease by about 1.5% per pH unit (Zeebe, 1999).

Carbon stable isotopes are also important paleoenvironmental proxies, since they can provide precise information on vital fractionation (e.g Reitner et al., 2001; Hedges et al., 2005; Nützel et al., 2009) and on the carbon cycle (Leng et al., 2005). In addition, their resistance against diagenesis (Veizer et al., 1999; Korte et al., 2005) predestines them as high-precision proxy.

Taking these considerations into account, both $\delta^{18}O$ and Sr content apart from $\delta^{13}C$ values of selected St. Cassian sponges and one stromatolite were analyzed and discussed in this section. Sr contents were measured with LA-ICP-MS following the line-method of Rosenheim et al. (2004). Assuming a more or less constant Ca concentration for the whole aragonitic skeleton, the Sr/Ca ratio should display a similar graphic and therefore Sr concentration is interpreted as a reflection of the Sr/Ca ratio. In addition, Fe concentrations were measured in the sponges in order to assess the nature of the state of preservation, and Mg concentration was measured additionally to Sr in the stromatolite to determine changes in carbonate primary mineralogy (Schäfer, 2006).

The mobile mean (x=5) was used to correct errors resulting from the possible remnants of ablated material (Simon, pers. comm.).

5.5.3.1. *Hispidopetra triassica* samples

Three samples of the coralline sponge *Hispidopetra triassica* Reitner were selected to perform measurements of $\delta^{18}O$ and $\delta^{13}C$ values and Sr concentrations. The preservation state of all the samples was qualitatively determined by means of optical microscopy and cathodoluminiscence. *Hispidopetra triassica* specimens can be recognized besides their spicules, through their distinctive massive basal skeleton with clinogonal to sphaerulitic microstructure and epitaxial cementation, which are in part responsible for the irregular structure of its aragonitic fascicles (Reitner, 1992). Little pyrite which is responsible for its layered coloured structure (Reitner, 1992) was detected in all specimens.

Out of nearly 40 boulders and in all thin sections, only three *H. triassica* samples could be obtained. All of them have an overall good preservation and were thus selected for geochemical analyses.

Since no data can be obtained regarding the age and growth rate of *Hispidopetra triassica* (not sufficient uranium concentrations), drillings were performed at regular distances of approximately 1 mm in each sponge skeleton. Slight variations occurred due to possible fractures. Only in sample FSSA XXX 1b the drillings were carried out following an apparent banded growth pattern. However, as the title of this section implies, this is a pilot research. A more detailed study is currently in progress with sample FSSA XXX-4b due to its higher U concentrations which may allow determining its age and possibly its growth rate (Haase-Schramm et al., 2003).

5.5.3.1.1 *Hispidopetra triassica* **sample FSSA XI (Seelandalpe, Figs. 67-69)**

This sample is the most massive of all analyzed sponge specimens. It consists of a massive secondary skeleton with a notable onset of epitaxial cements in the upper part of the secondary skeleton. Furthermore, it displays a more or less cell-like pattern in polished slab. These "cells" are composed of light-brown areas surrounded by thinner dark-brown contours. These patterns correspond with the description by Reitner (1992).

LA-ICP-MS measurements reveal a more or less constant Sr concentration of ca. 9000 ppm. Significant peaks in Sr concentrations could not be observed anywhere along the transect. Only in the sections between reading points (RP) 150-200 (t= 90-112s), 1400 and 1570 (t= 507-540s), and 2050 to 2170 (t= 905-950 s) negative peaks in Sr concentration can be seen. All these negative peaks correlate negatively with Fe peaks (Fig. 67). Altogether, Fe peaks coincide with either the section of the skeleton of the sponge where epitaxial cements are, or with weathered sections of the skeleton evidenced by a yellow-red color (Fig. 67).

Results
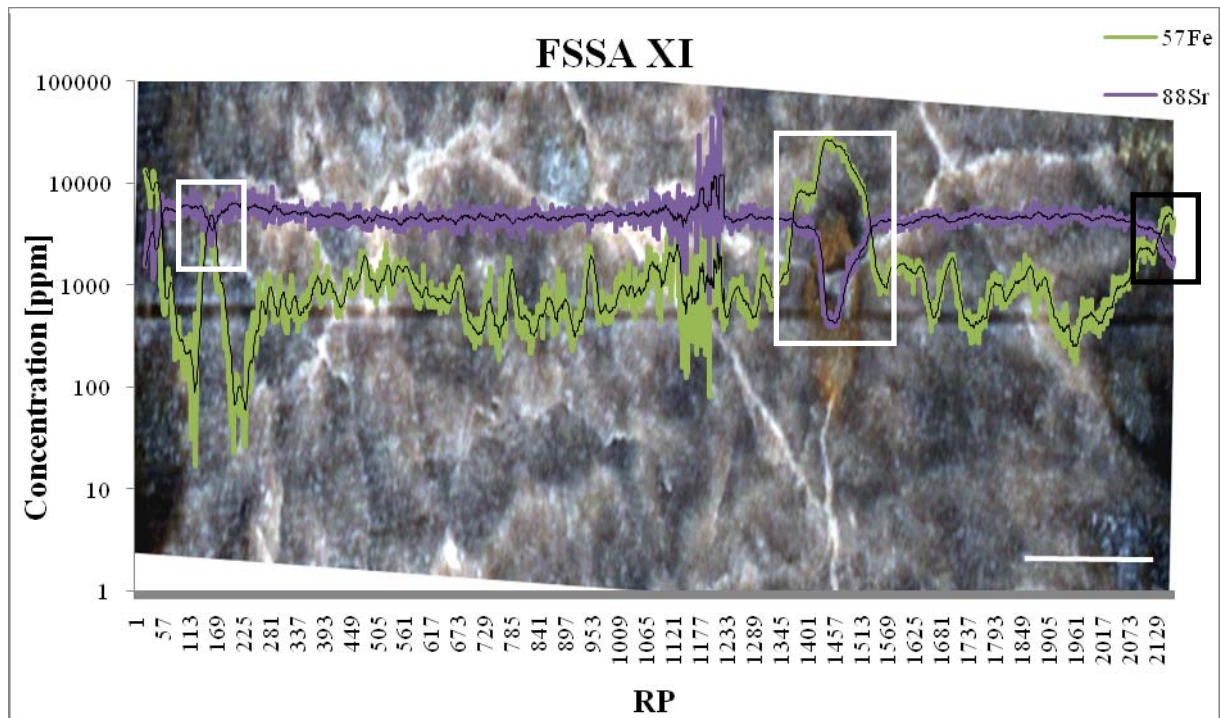
Figure 67: LA-ICP-MS Plot of *H.triassica* sample FSSA XI. Note the inverse correlation between Sr and Fe (squared areas). Scale bar = 2mm. See text for further details.

δ^{18}O values (Fig. 68, Appendix AXI) range from -4.90‰ to -2.79‰. A difference regarding the values cannot be seen between light- and dark-brown areas and the area containing epitaxial cements. In the same way, a correlation between light-/dark-brown bands and determined δ^{18}O values could not be concluded. A ciclicity pattern could not be seen.
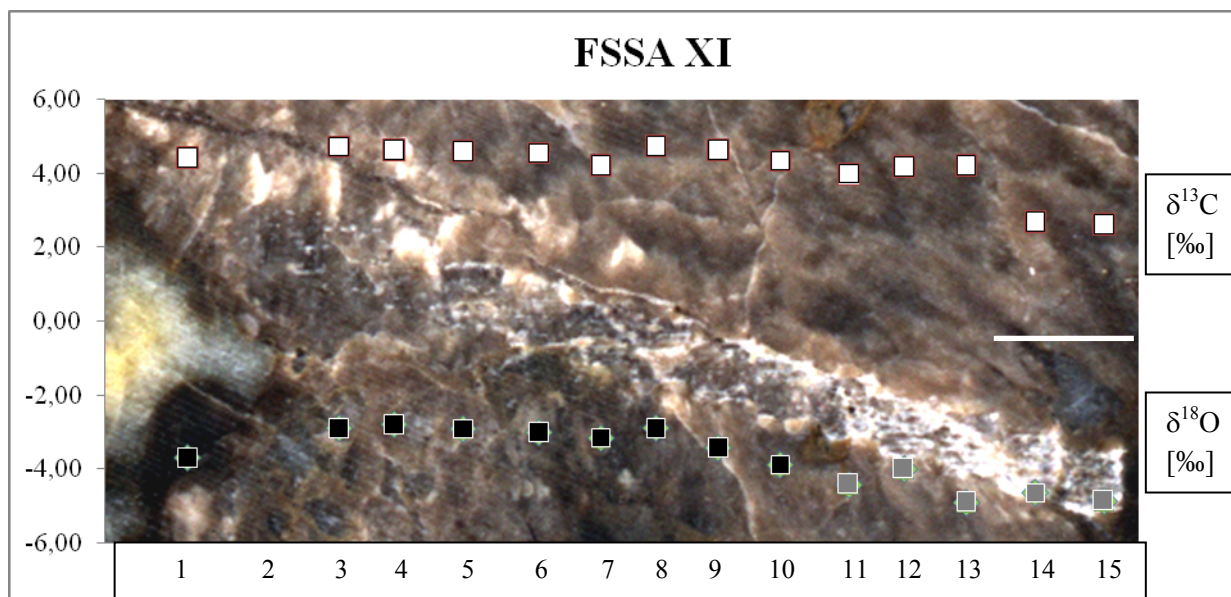
Figure 68: δ^{13}C and δ^{18}O distribution plot along *H.triassica* sample FSSA XI. X axis numeration shows successive drillings. In grey, all δ^{18}O values that were not taken into account for temperature determination. Scale bar = 2mm. See text for further details.

The values of δ^{13}C range from 2.61‰ (in the epitaxial cements) to 4.75‰ in a dark-brown band. The sponge itself has values from 3.99‰ to 4.75‰. As for the δ^{18}O values, ciclicity was not observed. Finally, a medium correlation exists ($r^2 = 0.58$) between both δ^{13}C and δ^{18}O values. This correlation decreases to 0.38 when values from FSSA XI- 11 to 15 are excluded (Fig. 69, Appendix AXI). This exclusion took place because calculated temperatures exceed 39°C, above the tolerance limit for most invertebrates (Kleypas et al., 1999). See section 5.5.3 for a further discussion.
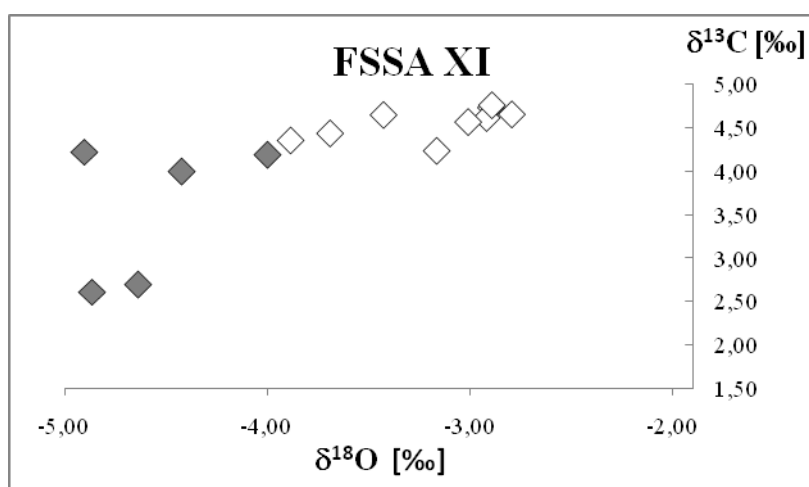
Figure 69: δ^{13}C and δ^{18}O Plot of *H.triassica* sample FSSA XI. In grey, all coupled points whose δ^{18}O values were not taken into account for temperature determination. r^2 without these values = 0.38 Scale bar = 2mm. See text for further details.

Results

5.5.3.1.2. *Hispidopetra triassica* sample FSSA XXX-1b (Seelandalpe, Figs. 70-72)

This sample corresponds to a fragmented skeleton that likewise has epitaxial cements at its uppermost part. Trace element plot (Fig. 70) of data obtained by LA-ICP-MS shows numerous peaks in Sr concentration, which is ca. 9000 ppm along the whole transect; however all these peaks are plotted in an irregular way. Sr- and Fe are negatively correlated, as in sample FSSA XI, can be seen in the boxed areas. A considerable depletion in Sr concentration is to be seen at the end of the transect. This depletion corresponds to the area of the epitaxial cements and corresponds to increased Fe content. Otherwise the distribution of Sr is relatively constant.
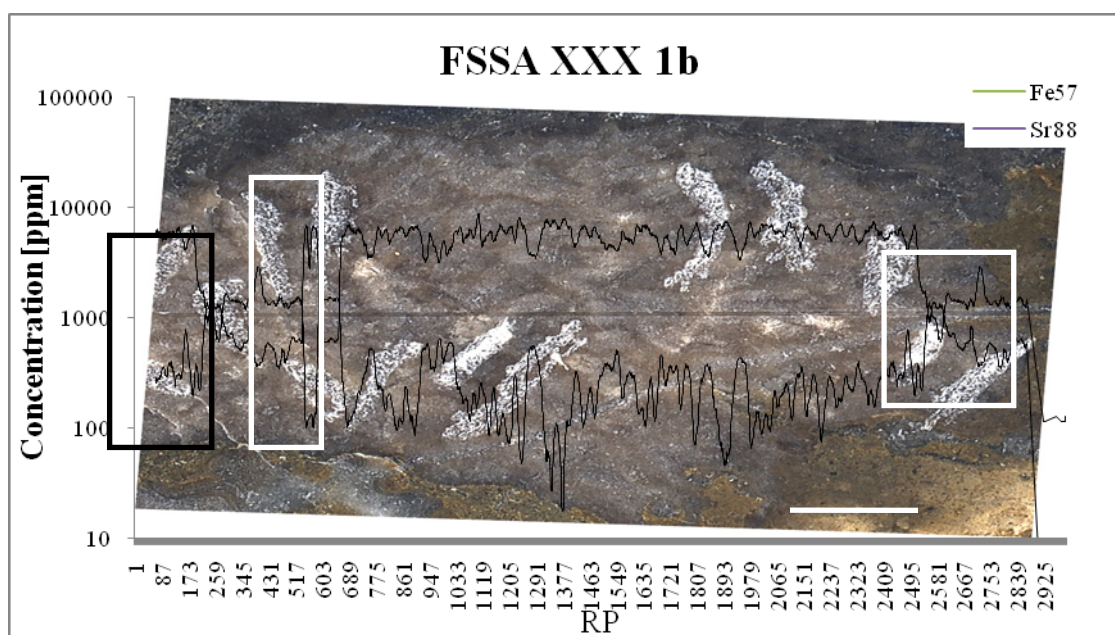
Figure 70: Plot of Fe and Sr concentrations in *H.triassica* sample FSSA XXX -1b. Note the inverse correlation between Sr and Fe (boxed areas). Scale bar = 2mm. See text for further details.

The values of $\delta^{18}O$ behave in much the same fashion of sample FSSA XI. Some values are low (FSSA XXX1b-10 = -10.3‰), yet they can be explained by means of the low pCO_2 values (see section 5.5.3). Otherwise, they range from -4.53‰ to -2.56‰ (Fig. 71, Appendix AXI). $\delta^{13}C$ values behave similarly ranging from 1.75 ‰ to 4.15 ‰, except the point FSSA XXX1b-10 ($\delta^{13}C$ = -2.17‰).
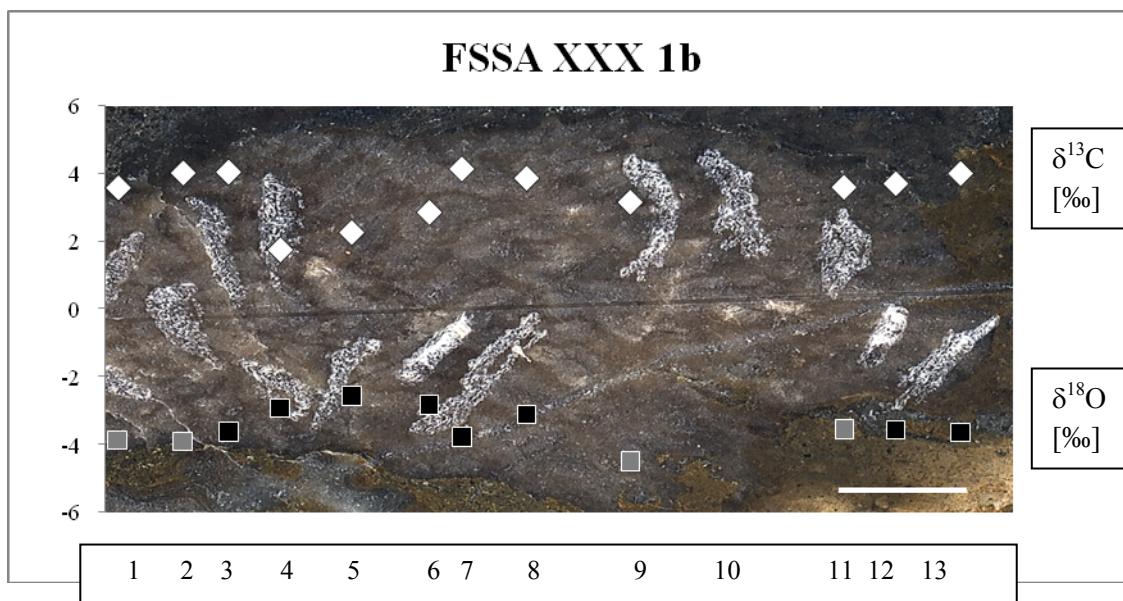
Figure 71: $\delta^{13}C$ and $\delta^{18}O$ distribution plot along *H.triassica* sample FSSA XXX 1b. X axis numeration shows successive drillings. In grey are all $\delta^{18}O$ values that were not taken into account for temperature determination. Point FSSA XXX 1b-10 is excluded to its extremely low pCO_2 value. Scale bar = 2mm. See text for further details.

In the same manner as for sample FSSA XI, cyclicity could not be observed in either of the two variables. A medium correlation (r^2= 0.67) could be observed between $\delta^{18}O$ and $\delta^{13}C$ values, even excluding points FSSA XXX1b- 1-3 and 9-11 (Fig.72).
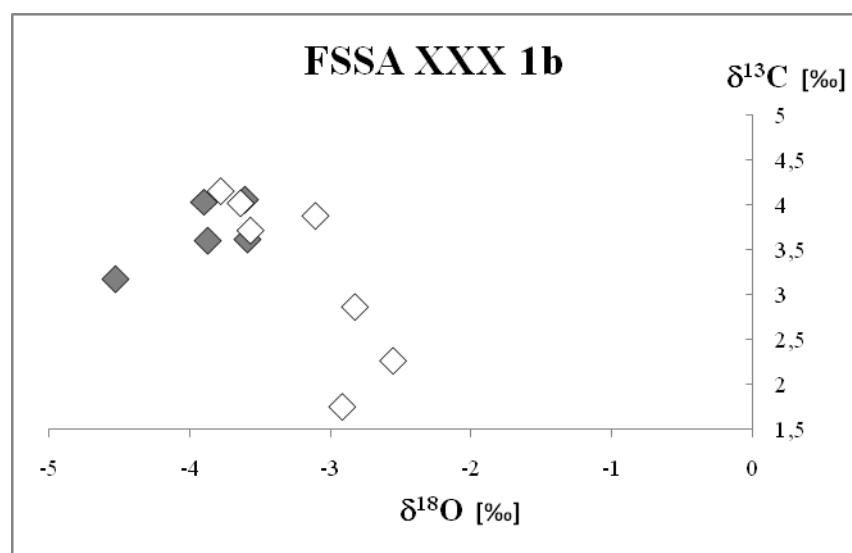
Figure 71: $\delta^{13}C$ and $\delta^{18}O$ plot of *H.triassica* sample FSSA XXX 1b. In grey are all coupled points whose $\delta^{18}O$ values were excluded from temperature determination. Point FSSA XXX 1b-10 is even excluded from the plot due to its extremely depleted values. r^2 without excluded values= 0.67. See text for further details.

Results

5.5.3.1.3. *Hispidopetra triassica* **sample FSSA XXX-4b (Seelandalpe, Figures 73-75)**

This sample is the best preserved found specimen of *Hispidopetra triassica*. It consists of a skeleton fragment with variably distinguishable dark- and light-brown bands and a conspicuous epitaxial cement area (Figs. 73-74).

LA-ICP-MS plot shows a nearly constant Sr concentration of ca. 9000 ppm, with two pronounced negative peaks, namely at RP = 1310 to 1370 (t = 593 – 628 s) and RP = 2770 – 2900 (t = 1210 – 1245s). The latter peak corresponds to the epitaxial cement zones in the same way as for other sponge samples, whereas the former corresponds to a dark-brown band. Coeval peaks in Fe concentration can also be seen (Fig. 73).
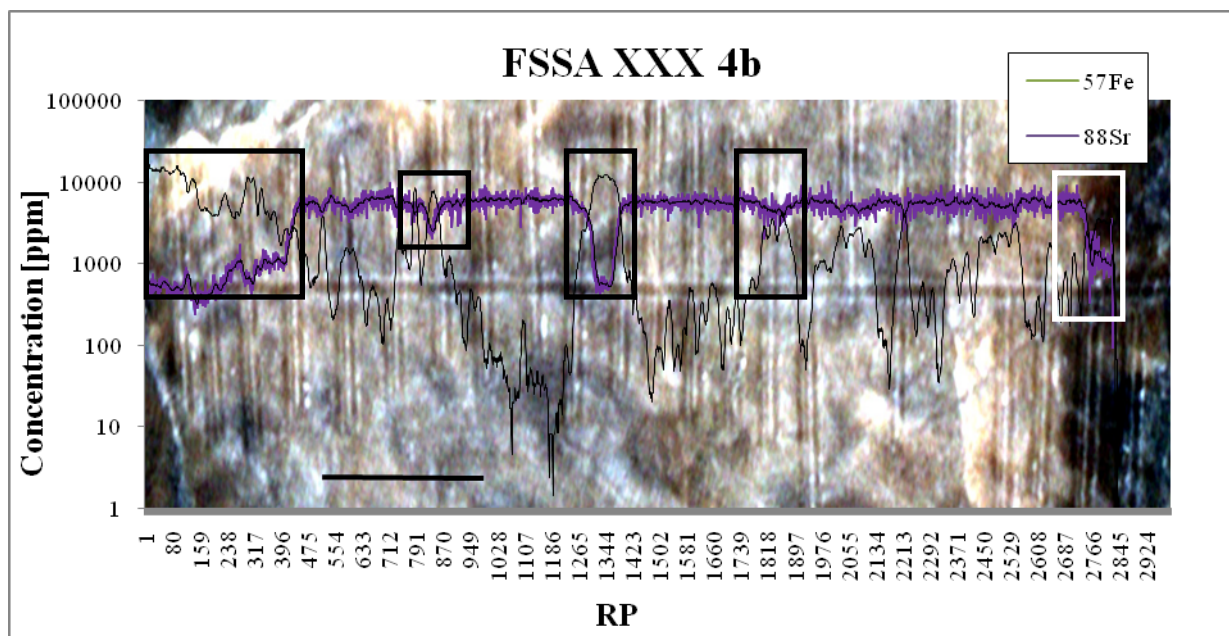
Figure 73: LA-ICP-MS Plot of *H.triassica* sample FSSA XXX 4b. Note the inverse correlation between Sr and Fe (squared areas), distributed along the whole skeleton of the sponge. Scale bar = 5 mm. See text for further details.

Values of $\delta^{18}O$ range from -4.61‰ to -2.70 ‰ (epitaxial cements + sponge, Fig. 75, Appendix AXI), thus behaving in the same manner as the values of the other samples. $\delta^{13}C$ values range from 2.94 ‰ (epitaxial cements zone) to 4.85 ‰ and cyclicity could not be determined in its plot. However, a minimum excursion can be recorded at drilling points FSSA XXX 4b - 13 and 14 (Fig. 74). Almost no correlation (r^2= 0.09) could be observed between both $\delta^{18}O$ and $\delta^{13}C$ values (Fig. 75).
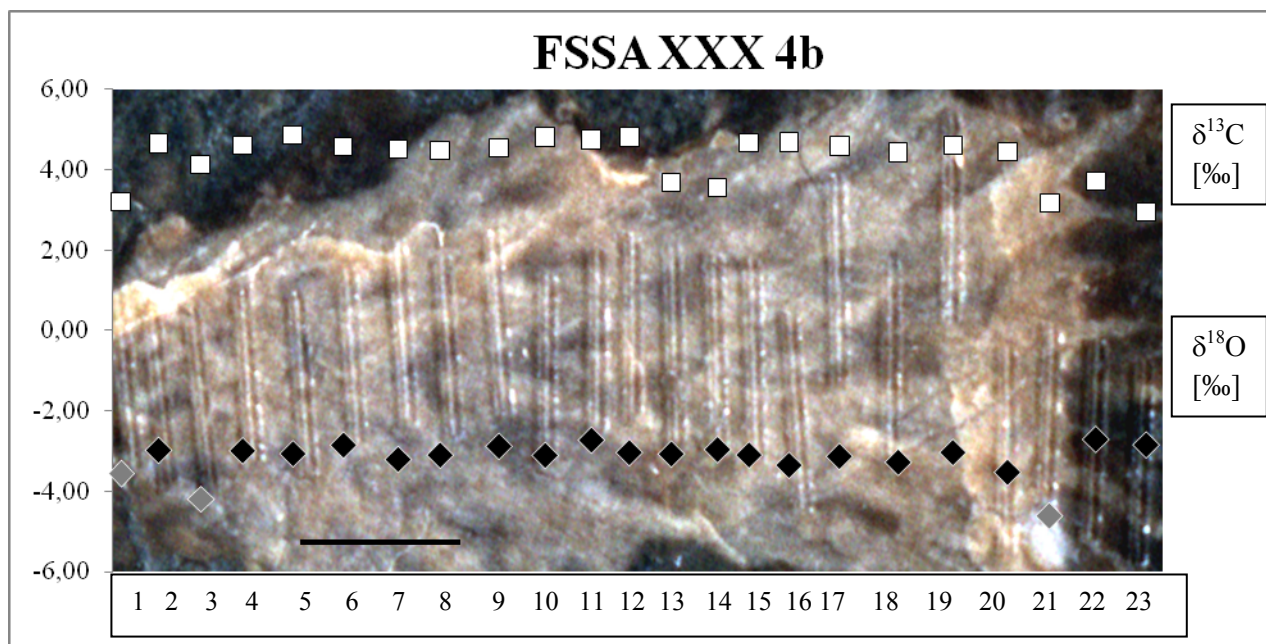
Figure 74: δ^{13}C and δ^{18}O distribution plot along *H.triassica* sample FSSA XXX 4b. X axis numeration shows successive drillings. In grey are all δ^{18}O values that were excluded from temperature determination. Scale bar = 5mm. See text for further details.
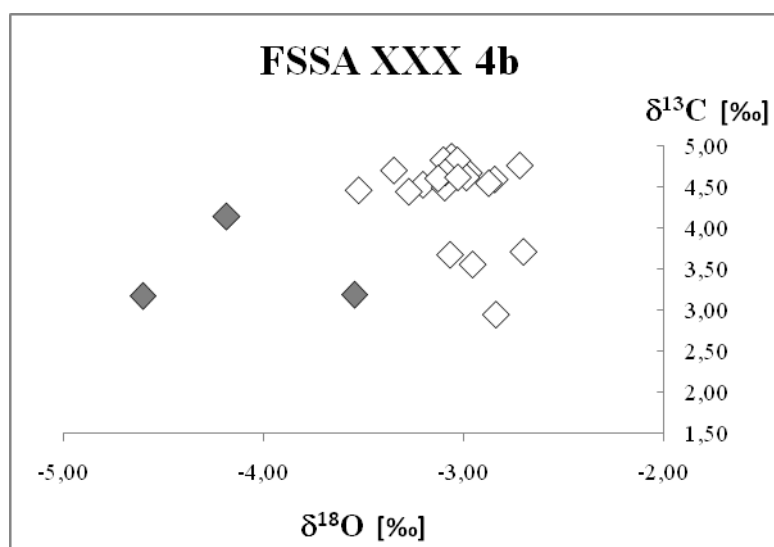
Figure 75: δ^{13}C and δ^{18}O Plot of *H.triassica* sample FSSA XXX 4b. In grey are all coupled values whose δ^{18}O were excluded from temperature determination. r[2] without excluded values= 0.09 Scale bar = 2mm. See text for further details.

Results

5.5.3.2. Stromatolitic sample M X-2 (Misurina, Figs. 76-78)

This sample consists of a peloidal stromatolite (Microbialite type 4) from the Mud Mound Association I. The size of peloids ranges from 50 to 70 μm (see section 5.2.2.8.). The sample was selected due to the good preservation state proved by optical microscopy and epifluorescence. Although some dark-grey/-black bands are to be seen at the uppermost part of the stromatolite on the slab surface (Figs. 76-77), a differential coloration could not be seen in the thin section.

Drilling to obtain stable isotope samples was performed in the stromatolite following its different-coloured banded growth.

LA-ICP-MS plot shows no representative peaks for Sr concentration (Fig. 76). Only at RP 960 - 1170 (t= 438 - 528s) a broad negative peak can to be seen. This negative peak is significant, since it corresponds to semi-quantitative values of 2400 to 3200 ppm in Sr. This is remarkable taking into account that mean concentration is 6000 ppm (σ = 1532). A narrower peak can be observed at RP 350 (t= 180s). Both peaks coincide to some extent with higher Mg concentrations. (Fig. 76)
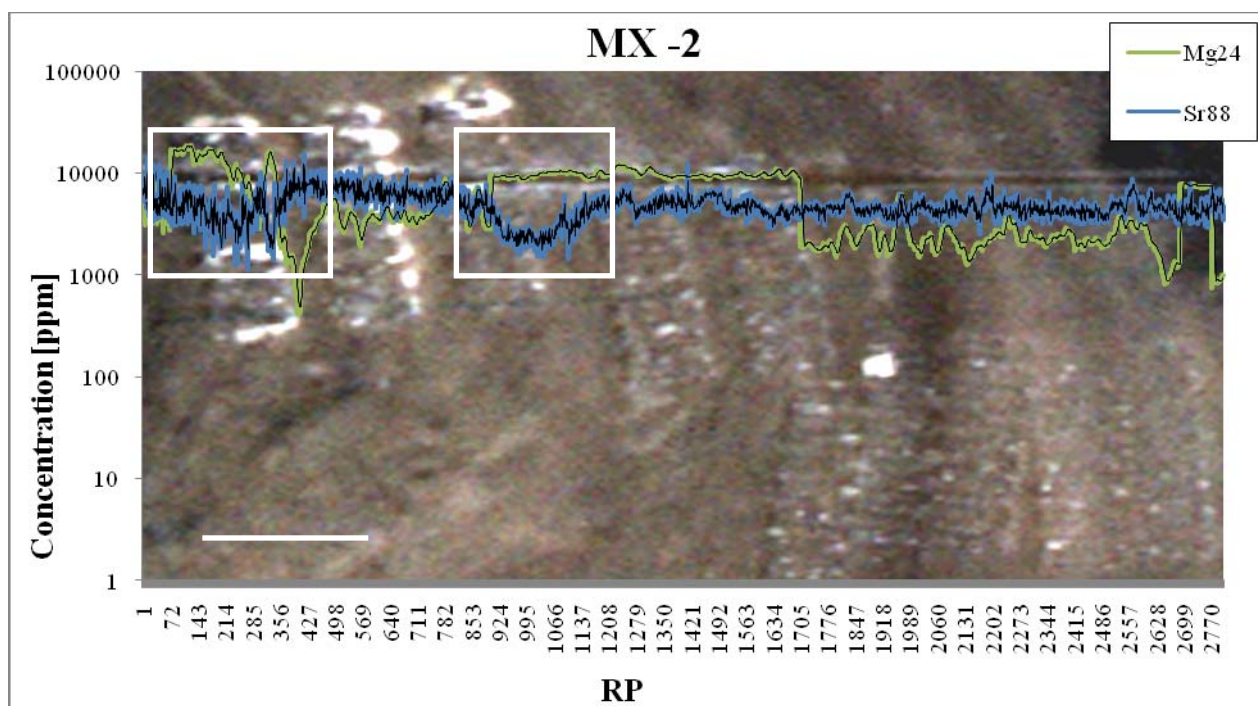
Figure 76: Plot of Mg and Sr in stromatolitic sample MX -2. Note the inverse correlation between Sr and Mg, (boxed areas). Scale bar = 2 mm. See text for further details.

Values of $\delta^{18}O$ range from -2.22‰ to -1.97‰ (Fig. 77, Appendix AXI), whereas $\delta^{13}C$ values range from 1.16‰ to 2.71‰. Correlation between both variables is medium to low with r^2 = 0.32 (Fig. 78). In the case of the carbon isotopes, they display a negative excursion towards the uppermost extreme of

the stromatolite, where the lowest value is to be seen (1.16‰). Regarding the oxygen isotopes, one of the highest values (-1.98‰) corresponds to the black layer, while the remaining similar values were obtained at the uppermost layers of the stromatolite.
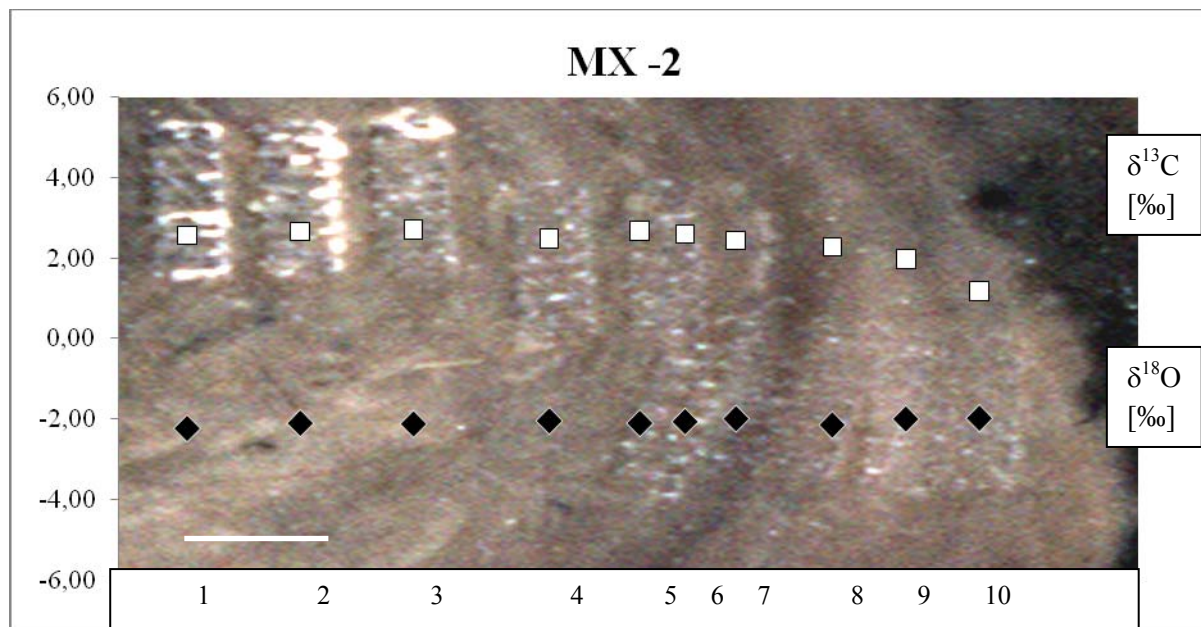
Figure 77: $\delta^{13}C$ and $\delta^{18}O$ distribution plot along stromatolitic sample MX-2. X-axis numeration shows successive drillings. All $\delta^{18}O$ values were used to determine paleotemperatures Scale bar = 2mm. See text for further details.
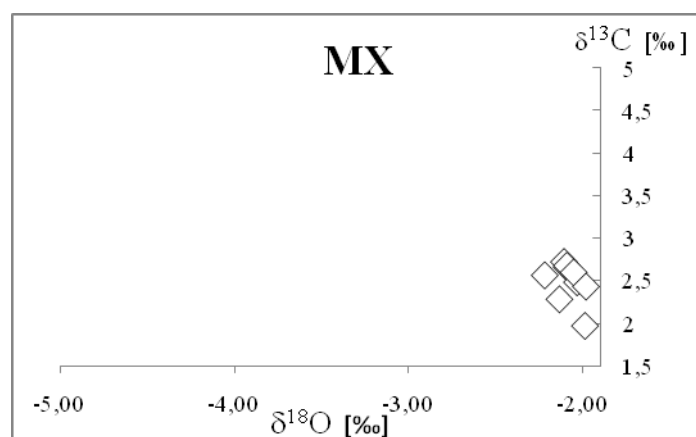
Figure 78: $\delta^{13}C$ and $\delta^{18}O$ Plot of stromatolitic sample MX-2. Note the clustering of all data. $r^2 = 0.32$. See text for further details.

5.5.3.3. Temperature determination by means of selected proxies

LA-ICP-MS did not yield Sr values that could be calibrated with those from oxygen isotopes. A cause of this phenomenon may be diagenetical imprint. Despite the extraordinary preservation of Cassian samples, evidenced in sponges by Sr concentrations of ca. 9000 ppm, they are more exposed to

Results

diagenesis than recent samples. This can be assessed by comparing Sr variations in transects of recent sponges (regarded free from diagenesis) which are on the order of mmol (Haase-Schramm et al., 2003; Rosenheim et al., 2004; Grottoli et al., 2010). Nevertheless, oxygen isotopes appear to be useful indicators of paleotemperatures. Despite being prone to the effects of diagenetical imprint (Hühne, 2005; Hoefs, 2009), most values could be plotted within "reasonable" limits for the Triassic seawater in equilibrium conditions, that is, without fractionation (compare Veizer et al., 1999; Korte et al., 2005; Nützel et al., 2009). Even six of the nine values out of a total of 68 with a pCO_2 less than 600 ppmv could be plotted within the reference temperature limits as defined in the literature. However, such oxygen isotope values from samples with low pCO_2 amounts (FSSA XXX 4b-1, 3 and 21; FSSA XXX 1b- 1-3; Appendix AXI) cannot be considered as reliable for the assessment of temperature.

Temperature was obtained from original V_{SMOW} values using the method of Kim and O'Neil (1997) and considering a value of V_{SMOW} of -1 ‰ for the Triassic seawater (Stanley & Swart, 1995; Hornung et al., 2007a; Nützel et al., 2009). Corrections of -0.6 ‰ for aragonitic samples and -0.06 ‰ for each mole Mg in magnesium calcite must be performed in $\ln\alpha$ (Tarutani et al., 1969). The determination of paleotemperatures yielded from 30.76°C (FSSA XI-4) to 36.46°C (FSSA XI-13) in sample FSSA XI, from 30.38°C (FSSAXXX 4b-11) to 34.56 °C (FSSAXXX 4b-20) in sample FSSA XXX 4b, from 29.58°C (FSSA XXX1b-5) to 35.9°C (FSSA XXX1b-7) in sample FSSA XXX 1b, and from 26.96 °C (MX- 2-10) to 28.21°C (MX-2-1) in sample MX-2. Ciclicity related to light and dark bands in the skeleton was not observed in any of the sponge samples. However, in the stromatolite from MX-2, the dark band has a very low value in comparison to most of the dark bands from the same sample, although the sample as a whole does not display ciclicity at all.

5.5.3.4. Discussion

A primary aragonitic signal ([Sr] ca. 9000 ppm) can be seen in all sponge skeletons. This can be confirmed by a negative correlation of Sr with Fe. Moreover, this negative correlation reflects a weak diagenetic effect.

The stromatolite displays a High-Mg calcite mineralogy. It must be considered, however, that Sr and Mg values may vary considerably in the different layers of stromatolites (Schäfer, 2006). In addition, mineralogy of some microbial carbonates may display tight relationships between aragonite and High Mg-calcite. No significant element concentration pattern related with the color of the bands of the stromatolite could be observed.

Original aragonitic and High-Mg calcitic mineralogies from this study agree with the model of Sandberg (1983), who divided the Phanerozoic in five cycles based on the mineralogy of non-skeletal carbonates The second "aragonitic cycle" in the history of Earth comprises from the beginning of the

Upper Carboniferous to the end of the Upper Triassic. The main cause for this cyclicity would be plate-tectonically influenced oscillations in the vapor pressure of CO_2. Lowenstein et al. (2001) provided with similar conclusions based on the study of fluid inclusions.

Although determination of age and growth rate of the sponges and microbialites was not possible, remarkable changes in the carbon and oxygen composition of the sponge skeletons and the stromatolite are observed.

Carbon isotope values from sample FSSA XI and for FSSA XXX 4b are generally in agreement with modern coralline sponges (Böhm et al., 1996, 2002; Wörheide, 1998; Reitner et al., 2001), in that $\delta^{13}C$ decreases progressively from the oldest part of the skeleton (4.43‰ and 4.66‰) towards the uppermost growing zone of the sponge, where it reaches 2.61‰ and 2.94‰. This means a difference of 1.82‰ and 1.72‰ (Figures 68, 74; Appendix AXI). This trend could also be detected in the stromatolitic sample with an overall decrease of 1.55 ‰ from point MX-2-3 to MX-2-10 (Fig. 77, Appendix AXI). However, the decreasing $\delta^{13}C$ trend mentioned before could not be seen in specimen FSSA XXX 1b, where values from the oldest to the youngest part of the sponge are reduced by only 0.04‰ (Fig. 71).

In addition, all sponge specimens show a medium negative excursion approximately at the middle section of the skeleton of up to 2.3 ‰ in comparison to their maxima (Appendix AXI, Figs. 68, 71, 74). This excursion can also be seen in the stromatolite, but in a considerably smaller way (0.24 ‰ from MX-2-3 to MX-2-4). Altogether, lighter values in the stromatolite with respect to the sponges can be explained by the enrichment of 1.7 ‰ for aragonite in comparison to calcite (Romanek et al., 1992; Nützel et al., 2009) and, thus, very similar values can be seen.

In modern sponges and microbialites, the decreasing $\delta^{13}C$-value trends towards the uppermost growing zone can be explained as a consequence of the global increase of CO_2 due to deforestation and the burning of fossil carbon during the period of industrialization after 1850 (Reitner, 1993; Böhm et al., 1996; Wörheide, 1997). Disregarding the latter cause for obvious reasons relating to Carnian times and not having enough evidence regarding the former, there must be other reasons to explain negative excursions in sponge skeletons and in the stromatolite, which will be discussed in the following paragraph.

Korte et al. (2005) obtained $\delta^{13}C$ values of 3.5 ‰ from Carnian whole rocks and brachiopods. They attributed these high values to the re-emergence of coal swamps and peatlands. In addition, they documented a negative excursion of 1.5 ‰ during the Late Cordevolian-Early Julian, which they attributed to strong volcanic activity across large portions of the Tethys. Hornung et al. (2007a,b) and Tanner (2010) associated this excursion to the onset of the "Carnian Pluvial Event/Reingraben Event

Results

(Simms & Ruffell 1989; Kozur & Bachmann, 2010). This event is characterized by an intensified siliciclastic input into wide parts of the epicontinental basins and marginal Tethyan environments due to enhanced weathering (Tanner, 2010). The isotopic decline should be due to the dissolved inorganic carbon carried into the ocean by the increased runoff. The consequences were overall more humid and warmer conditions. Simms & Ruffel (1989) suggested the presence of volcanic activity associated with the initial stages of the rifting of the North Atlantic during the Carnian. This hypothesis was supported by Veevers (1989). According to him, the final coalescence of Pangaea and the almost immediate onset of continental rifting would have had a greater input of volcanic CO_2. This event would have taken place during the Ladinian-Early Carnian, at about 230 ± 5 Ma. Richoz et al. (2007) also found a pronounced negative excursion of 0.7‰ associated to the Ladinian-Carnian boundary at the Weissenbach-Maserling section in Austria.

This Carnian/Reingraben Pluvial Event hypothesis would appear reasonable in order to explain the negative excursions at the middle section of all three sponge specimens and at the end section of the stromatolite. Nevertheless, it holds a major problem, since the thickest analyzed sponge specimen has a measure of ca 3 cm. This would mean an age of at most ca. 300 years at the lowest growing rates recorded for any coralline *Ceratoporella nicholsoni*, a modern relative of *H. triassica* (0.1 - 0.4 mm/year; Grottoli et al., 2010), and its lifespan would thus not be comparable at all with the length of the duration of the Carnian Pluvial Event which took place over the whole time span of the *austriacum* biozone of the Julian (ca. 3.2 Ma, Gradstein et al., 2004; Hornung et al., 2007b). Furthermore, all $\delta^{13}C$ values should remain considerably depleted along the whole skeleton (Korte et al., 2005), which does not happen.

A further cause of depletion/negative excursions in $\delta^{13}C$ values can be the decreasing burial rate of organic carbon in the Lower Carnian (Korte et al., 2005). Yet it seems as speculative in this work as the Carnian Pluvial Event hypothesis is, especially because an accurate dating is lacking.

The span of the negative excursions is rather short. It comprises at most 4 mm of a single skeleton (FSSA XXX 1b). This would mean 10 to 40 years considering the growth rate of modern *Ceratoporella nicholsoni*. Böhm et al. (2002) found a negative correlation between $\delta^{13}C$ values of a *C. nicholsoni* specimen from Jamaica and atmospheric pCO_2. According to them, the concentrations of atmospheric CO_2 went down to less than 280 ppmv in the period from ca. 1600 to 1800, while the $\delta^{13}C$ values from the sponge coevally reached a maximum. This cooling period corresponds to the "Little Ice Age" and is well documented in the literature (Eddy, 1976; Luterbacher et al., 2001). It would have occurred as a consequence of a solar spot minimum. Positive excursions in $\delta^{13}C$ values would thus reflect lower values of atmospheric CO_2. If the negative correlation from Böhm et al. (2002) is applied to data from Triassic sponge samples, depleted $\delta^{13}C$ values would correspond to higher atmospheric pCO_2 values and therefore, to warmer conditions. This remains a plausible cause for depleted $\delta^{13}C$

values in the sponges and eventually in the stromatolite. However, no correlation with depleted coeval $\delta^{18}O$ values exists. In addition, Wörheide (1997) attributed large decreases in $\delta^{13}C$ values of certain coralline sponges to a low degree of mixing of surface and deep waters in the Caribbean due to a high equilibraton with atmospheric CO_2. These factors combined may help to explain the intensity of the negative $\delta^{13}C$ excursions in all samples.

Vital fractionation leading to depleted $\delta^{13}C$ values through bacterial action is a further possible cause for these negative excursions and can occur either by anaerobic methane oxidation (AOM) or sulphate reduction (Hühne, 2005). The former cannot be confirmed, since AOM is associated with $\delta^{13}C$ values of ca -40‰ (Hühne, 2005). However, the possibility for the latter is larger, since associated sulphate-reduction values are not so low (Joachimski, 1991; Hühne, 2005) In addition, considerable amounts of sulphate-reducing bacteria belonging to the delta-Proteobacteria can be found in the intercellular mesohyl of modern demosponges *Petrosia ficiformis* , *Chondrosia reniformis* (Schumann-Kindel et al., 1997), and *Geodia barretti* (Hoffmann, 2003). Bacteria are highly diverse in coralline sponges and reach up to 50% and more of the total biomass of a coralline sponge (Reitner et al., 2001) and most of these bacteria are sometimes symbiotic and sponge-specific (Wilkinson, 1984).

The formation of pyrite crystals may be a product of anaerobic sulphate-reducing bacteria (Reitner & Schumman-Kindel, 1997). Reitner (1992) found abundant pyrite crystals in *Hispidopetra triassica.* Unfortunately, none of the analyzed specimens contain abundant pyrite crystals.

A general assessment supporting either uniquely a continuous warming or cooling climates due to volcanic events cannot be made on the basis of the correlation with oxygen isotope values. In some cases however, (FSSA XXX 4b – 14 and 22-23; FSSA XXX1b-4 and -6) depleted $\delta^{13}C$ values coincide with enriched $\delta^{18}O$ values, which would indicate cooling due to volcanic events, but is not conclusive (Wörheide, 1997).

Taking into account all these considerations, carbon isotopes in sponge and microbialitic samples reflect negative excursions that can be due to a variety of factors. Among these, warming climate due to a short-duration increase of atmospheric pCO_2 seems the most probable. This could have been due to a solar maximum. However, volcanic activity and the association with sulphate-reducing bacteria may also account for the depleted $\delta^{13}C$ values.

Since negative excursions are short and no vital fractionation could be assessed, carbonate precipitation in both the microbialite and the sponge skeletons should have occurred under isotopic equilibrium conditions.

Oxygen isotope values in diagenesis-free carbonates may be influenced by four factors: pH, the $\delta^{18}O$, salinity, and temperature of the water (Fabricius et al., 1970; Korte et al., 2005; Hornung et al.,

Results

2007c). Most $\delta^{18}O$ values obtained from the sponges as well as the temperature calculations obtained from them corroborate previous reports on aragonitic sponges (Scherer, 1977), brachiopods (Veizer et al., 1999; Korte et al., 2005), corals (Stanley & Swart, 1995), and bivalves (Nützel et al., 2009).

Values in sample FSSA XI from drillings 11 to 15 were excluded for temperature calculation due to depleted values of $\delta^{18}O$ = -4.42 to -4.90‰, similar to sparry cements (-5.12‰). Temperatures inferred from these values would range from 37.07 to 41.99°C (Appendix AXI). Most of these temperatures would be in excess of the 38°C tolerance limit for coeval corals and "higher" organisms (Brock, 1985; Kleypas et al., 1999; Korte et al., 2005) and are considerably higher than reported St. Cassian values (e.g. Scherer, 1977; Swart & Stanley, 1995; Nützel et al., 2009). High apparent temperatures can be attributed to $\delta^{18}O$ depletion as a consequence of diagenesis, locally detectable in thin section and by means of LA-ICP-MS.

In sample FSSA XXX 4b, drillings 1, 3, and 21 were discarded for interpretation, since apparent temperatures ranged from 34.69, 38.07, and 40.36°C, respectively. Although one of these values is below the mentioned tolerance limit, all three were disregarded due to their low pCO_2 values and were therefore not taken into consideration.

In sample FSSA XXX 1b, drillings 1, 2, and 9-11 were discarded from further interpretation also due to their low pCO_2 values. Obtained temperature values would have been 36.39, 36.54, 39.95, 75.01, and 34.88°C. Despite the consistency of some of them with permissible values (Kleypas et al., 1999), variations between these temperatures and those obtained from the remaining drillings are in average at least higher than 4°C. Any such temperature variation has never been recorded for a coralline sponge (Wörheide, 1997).

In the following paragraph, possible causes for variations between successive drillings in sponge samples and in the stromatolite will be discussed.

Since the growth rate of *Hispidopetra triassica* is not known and cannot be determined to date, sclerocronological inferences cannot be performed. Changes in oxygen isotopic values can thus be interpreted in the scope of modern coralline sponges and only as mere isolated information. Wörheide (1997) detected temperatures of 24 to 26°C for the stromatoporoid *Astrosclera willeyana* and 25 to 26°C for *Spirastrella* (*Acanthochaetetes*) *wellsi* from the Great Barrier Reef. He found a coincidence between the highest decreasing and increasing variations for $\delta^{18}O$ in skeletons with the El Niño phenomena and cooling periods due to large volcanic eruptions, respectively. In all *Hispidopetra triassica* skeletons, both increasing and decreasing trends can be seen (Figs. 68, 71, 74). However, the stromatolite of MX-2 shows an overall temperature-decreasing trend (Fig. 77). Variations between the lowest and highest inferred temperature values are 1.25°C (Appendix AXI). This difference is in complete agreement with temperature fluctuations in tropical sea surface temperature (SST) and

116

deeper oceans. Walker (1981) reported annual SST variations of up to 10°C at the Great Barrier Reef. Furthermore, Nützel et al. (2009) calculated variations of the same magnitude for St. Cassian megalodontids. Herbert et al. (2010) found variations of up to 2°C in "deep" oceans.

In the modern tropics, temperature can even decrease by 2°C from the SST values and in depths of ca. 100 m (Solomon & Wainer, 2006). Therefore, the altogether lower stromatolitic values would support the paleontological depth inference (see section 5.2.2.8.3.). Nevertheless, as all values are in full agreement with reported St. Cassian values for SST (Nützel et al., 2009), it could also contradict paleontological data.

Nützel et al. (2009) suggested the possibility that variations in $\delta^{18}O$ might not only be due to temperature, but also to salinity changes as a consequence of an increased influx of freshwater. Thus, proposed monsoonal circulation in parts of the Upper Triassic Tethys (Parrish, 1999; Hornung et al., 2007a,b) would be supported. Fresh and brackish water tend to reduce the salinity and $\delta^{18}O$ of seawater when admixed to it (Fabricius et al., 1970). However, monsoonal climate in the Cassian area can be satisfactorily assessed neither by modeling (Sellwood & Valdes, 2006) nor by paleoecological methods (Nützel et al., 2009). The onset of the Carnian Pluvial Event can thus be definitively rejected at the time of the deposition of the Cipit Boulders.

Thus, oxygen isotope variations are most probably due to "normal" temperature fluctuations, since no change in salinity has been reported and the obtained data do not provide evidence for the Carnian Pluvial Event. In this way, in can be concluded that carbonate precipitation in *Hispidopetra triassica* and in the stromatolitic sample occurred both in carbon and oxygen isotopic equilibrium.

5.6. Biomarker analyses

Biomarker analyses were carried out on five selected samples in order to identify particular microbial or sponge-specific biomarkers such as steroids, mid-chain branched fatty acids or -alkanes, derivatives of demospongic acids, which could corroborate biofacies results. Samples FSSA VIII-2, FSSAV and MXXXV belong to the Patch Reef Association I (P-R I), whereas sample M-X 2 belongs to Mud Mound I (M-M I) and sample MV to *Cassianothalamia*-Gemeinschaft II (C-G II). Additionally, an allochthonous micrite sample (lab # 849; Germer, 2010) was analyzed.

The hydrocarbon fractions of all samples showed high relative abundances of *n*-alkanes, which made up 73.2% to 89% of the total fractions. Particularly, long-chain *n*-alkanes (> C_{20}), often showing a considerable odd-over-even predominance (OEP), were the most abundant compunds. Chain length maxima around C_{23}-C_{25} occurred in samples FSSA VIII-2, MV, FSSA V and MXXXV. Sample MX

Results

and allomicrite sample 849 showed two maxima, one in the short-chain (C_{17-} MX; C_{20} -849) and one in the long-chain range (both C_{23}).

C-2- (*iso*-) and C-3- (*anteiso*-) methylated alkanes were found mainly in the short-chain range (3.3% to 20.5% of the total hydrocarbons). *Iso*-methylated alkanes showed a preference over the *anteiso*-isomers in all samples.

Phytane and pristane could be found in all samples.

Except for the Patch Reef sample MXXXV, all samples contained traces of cholestane. In addition, traces of stigmastane were found in patch reef samples FSSA VIII-2 and FSSA V. Since these copounds had low abundances and coeluted with other peaks, quantification was not possible. Hopanes occurred with much higher signal–to-noise ratios compared to steranes, usually in the range from C_{27} to $C_{35.}$

GC/MS/MS was attempted on samples MV, FSSA V, MXXXV to yield a better resolution of the sterane isomers present and to search specifically for the putative sponge-derived biomarker 24-isopropylcholestane (24-ipc; Brocks & Summons, 2004; Kodner et al., 2008; Love et al., 2009). A 24-ipc containing hydrocarbon fraction of the Cambrian Huqf Formation (Höld et al., 1999) was used as a standard to enable a sound identification of the latter compound. Only sample MV contained sufficient amounts of steranes for a detailed evaluation. However, chromatograms of the different transitions did not provide evidence of 24-isopropylcholestane (Germer, 2010).

Mid-chain branched alkanes were present in appreciable amounts in sample MV and comprised 3.3% of the total hydrocarbon fraction. $\delta^{13}C$ analyses were intended on them, but their amount was too low.

A selected GC/MS chromatogram shows most of the compounds hitherto mentioned (Fig. 79).

Traces of halogenated compounds showing a characteristic isotope pattern for bromination were found by GC/MS in St. Cassian samples (Germer, 2010). However, quantification was not possible due to the low compound concentrations. The first compound tentatively identified by comparison with literature spectra was 1,3,5-tribromo-2-(2,3-dibromopropoxy)benzene, and it was detected in the total organic extract of samples MV, FSSA V and in the aromatic fraction of MV. In addition, an unknown compound was found in the total organic extract of samples FSSA VIII-2, MV, FSSA V, MXXXV and the allomicrite sample 849. The origin of these compounds is as yet unknown. However, the absence of these compounds in blank samples processed in the same way as the ancient materials revealed no evidence for an input of the halogenated compounds during workup in the lab.

.
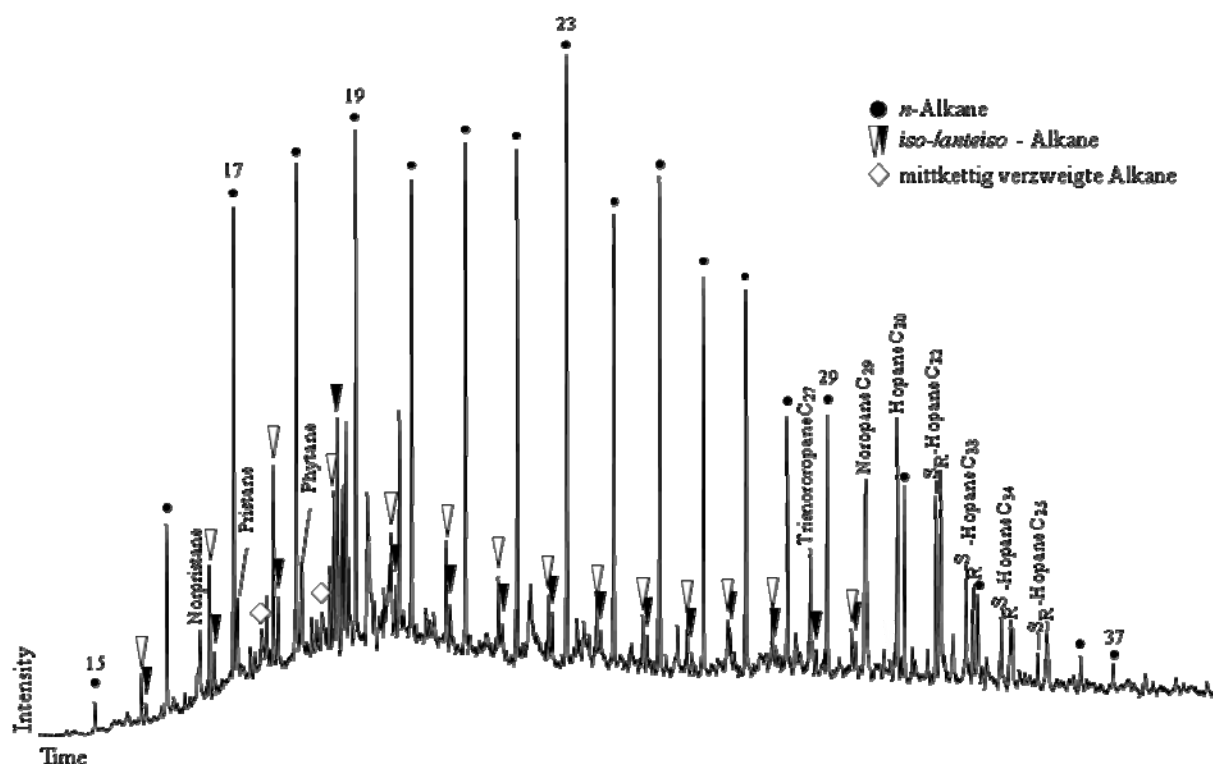
Figure 79: GC/MS chromatogram (total ion current) of the hydrocarbon fraction prepared from sample MV from the *Cassianothalamia*-Gemeinschaft, which shows the major biomarkers found. See text and Germer (2010) for further details

Discussion

No distinctive sponge-biomarkers were found in Cipit Boulder samples. However, all samples show evidence of a complex array of lipid biomarkers with different potential sources. *N*-alkanes can be derived from various membrane components such as phospholipids and sphingolipids produced by bacteria and algae. However, long chain *n*-alkanes with an OEP can be derived from plant waxes and /or terrestrial input (Brocks & Summons, 2004). The former would be in agreement with microfacies analysis results. The latter appears to be contradictory, because no plant remains have been found in the Cipit Boulders. Nevertheless, terrestrial input would, to some extent, be in agreement with LA-ICP-MS analyses, given that siliciclastic material is related to terrigenous input and not to the marly depositional environment (Sánchez-Beristain et al., accepted).

The presence of several hopanoids (Fig. 79) is a key to the identification of residues of bacterial metabolism (Roehmer et al., 1984).

Iso- anteiso alkanes are also considered important bacterial lipids, and can be in part derived from heterotrophic bacteria (Matsumoto et al., 1992). In addition, the presence of such biomarkers has already been detected in St. Cassian samples by Thiel (1997) and is in full agreement with a bacterial

origin for automicrites.

Acyclic isoprenoids such as pristane and phytane may derive from the phytyl side chain of chlorophyll a and are thus commonly related to phototrophic organisms, such as cyanobacteria. However, particularly phytane may also originate from the diagenetic alteration of archaeal membrane lipids (Peters & Moldowan, 1993). In the former case, these results agree with the presence of some cyanobacterial-related microencrusters (*Girvanella*) in microfacies analysis.

Steranes, such as cholestane and stigmastane are almost exclusively diagnostic of eukaryotic origin (Brocks & Summons, 2004), in agreement with the observed presence of metazoans in all samples.

The presence of certain halogenated compounds can be related to the metabolic processes performed by bacteria living inside sponges under reductive conditions (Ahn et al., 2003).

6.   Conclusions

- The excellent preservation state of St. Cassian samples allows a wide range of paleoecological and geochemical studies. Among them, the determination of sponge-based associations and communities by means of cluster analysis, and the determination of certain paleoecological conditions with aid of spectrometric analyses have a special significance.

- Cluster analysis proved to be an efficient method to define fossil associations from the Cipit Boulders by means of their microfacial features. Fourteen associations were defined: *Dendronella*- Hexactinellida, *Ceratoporella breviacanthostyla-Tubiphytes*, *Cryptocoelia zitteli-Mesophyllum*, *Cladogirvanella*-Stromatolite, Thrombolite-microencruster, *Cassianothalamia* Gemeinschaft II, Patch Reef I, Mud Mound I, Patch Reef II, Patch Reef III, Chaetetid-microencruster, *Amblisyphonella*, *Cassianothalamia* Gemeinschaft II and Mud Mound II.

- Certain microencrusters, due to their diagnostic paleoecological requirements, can help in providing with the determination of some paleoenvironmental constraints. In addition to recognizing some of their paleosynecological features, these microencrusters can further be helpful to define communities with the microfacial data of each one of the 14 associations by means of cluster analysis. Five communities were obtained with this method.

- Major element analysis of selected microbialites from the St. Cassian Formation supports a primary High-Mg calcite mineralogy, with minimum crustal material and an apparently early diagenetical/synsedimentary enrichment of Fe and S.

- Many trace elements do not to have any biological relevance, whereas some other reveal an apparently original biological-related signal.

- Despite minimal crustal contamination, no paleoenvironmental data can be obtained on the basis of their REE+Y (REY) pattern.

- Carbon and oxygen isotope analyses from coralline sponges and a stromatolite reflect similar trends to their modern counterparts, in that the influence of some environmental and physiological conditions can be confirmed. Different factors may have simultaneously contributed to their particular signatures. In the case of carbon isotopes, these factors may include in the first place a short- duration increasing of atmospheric pCO_2 and its associated warming. However, sulphate reduction may have also played a role in negative excursions. Most data from the oxygen isotopes allow a determination of paleotemperatures, which agree with previous results and to some extent, with paleoecological assessments from the study by means of paleoecological fossil associations. Altogether, carbonate precipitation in sponge and microbialitic samples occurred under isotopic equilibrium conditions.

Conclusions

- Results from biomarker analyses reveal only the presence of bacterially related organic matter. There is no evidence of sponge-related material.

7.   Literature

- Ahn, Y.B., Rhee, S.K., Fennell. D.E., Kerkhof, L.J., Hentschel, U. & Haeggblom, M.M. 2003. Reductive dehalogenation of brominated phenolic compounds by microorganisms associated with the marine sponge *Aplysina aerophoba.* Appl. Environ. Microbiol. 69: 4159-4166. Washington, D.C.

- Aurell, M. & Bádenas, B. 2004. Facies and depositional sequence evolution controlled by high-frequency sea-level changes in a shallow-water carbonate ramp. (late Kimmeridgian, NE Spain). Geol. Mag. 141 (6): 717-733. Cambridge.

- Austin, W.C., Conway, K.W., Barrie, J.V. & Krautter, M. 2007. Growth and morphology of a reef-   forming glass sponge, *Aphrocallistes vastus* (Hexactinellida), and implications for recovery from widespra trawl damage. *In* Custódio, M.R., Lôbo-Hajdu, G., Hajdu, E. & Muricy, G. (ed.) Porifera Research: Biodiversity, innovation and sustainability. Proceedings of the 7th International Sponge Symposium: 139 – 145. Rio de Janeiro.

- Baccelle, L. 1965. Contributo alla conoscenza petrografica e Sedimentologogica degli strati di S, Cassiano nelle Dolomiti. Studi. Trent. Sc. Nat. 42 (2): 1-19. Trento.

- Baccelle, L. & Bosellini, A. 1965. Diagrammi per la stima visiva della composizione percentuale nelle rocce sedimentarie. - Ann. Univ. Ferrara, N.S., Sez. IX, Sci. Geol. Paleont. 1/3. 59-62. Ferrara.

- Barattolo, F.; Mastandrea, A. & Russo, F. 1993 Redescription of the Carnian red alga *Dendronella articulata* Moussavian and Senowbari-Daryan 1988. *In* Barattolo, F., De Castro, P. & Parente, M. (ed.) Studies on fossil benthic algae. – Boll. Soc. Paleont. Ital. Spec. Vol., 1: 47 – 58. Modena.

- Bau, M., 1996. Controls on the fractionation of isovalent trace elements in magmatic and aqueous systems: Evidence from Y/Ho, Zr/Hf, and lanthanide tetrad effect. Contrib. Mineral. Petrol. 123: 323-333. Berlin.

- Bau, M. & Dulski, P. 1996. Distribution of yttrium and rare-earth elements in the Penge and Kuruman Iron-Formations, Transvaal Supergroup, South Africa. Precambrian Res.79: 37-55. Amsterdam.

- Bau, M. & Dulski, P. 1999. Comparing yttrium and rare earths in hydrothermal fluids from the Mid-Atlantic Ridge: implications for Y and REE behaviour during near-vent mixing and for the Y/Ho ratio of Proterozoic seawater. Chem. Geol. 155: 77-90. Amsterdam.

- Bau, M.; Dulski, P. & Möller, P. 1995. Yttrium and holmium in South Pacific seawater: Vertical distribution and possible fractionation mechanisms. Chem. d. Erde, 55: 1-15. Amsterdam.

- Bau, M.; Möller, P. & Dulski, P. 1997. Yttrium and lanthanides in eastern Mediterranean seawater and their fractionation during redox-cycling. Mar. Chem. 56: 123-131. Amsterdam.

- Bell, J.J. & Barnes, D.K.A. 2003. Effect of disturbance on assemblages: An example using Porifera. Biol. Bull. 205: 144 – 159. Woods Hole.

- Bernecker, M. 1996. Upper Triassic Reefs of the Oman Mountains: Data from the South Tethyan margin. Facies 34: 41-76. Erlangen.

Literature

- Bernecker, M. 2005. Late Triassic reefs from the Northwest and South Tethys: Distribution, setting, and biotic composition. Facies 51: 442-453. Berlin-Heidelberg.

- Berner, R.A. 1980. Early diagenesis: A theoretical approach. Princeton University Press. 245 pp. Princeton.

- Biddle, K.T. 1981. The basinal Cipit boulders: indicators of Middle to Upper Triassic buildup margins, Dolomite Alps, Italy. - Riv. Ital. Paleont. Strat. 86: 779-794. Milan.

- Biddle, K.T. 1984. Triassic sea-level change and the Ladinian-Carnian stage boundary. Nature 308: 631 – 633. London.

- Bizzarini, F. & Braga, G. 1978. Upper Triassic new genera and species of fair and questionable Bryozoa Chaetetida from the S. Cassiano Formation of the Dolomites (eastern Italy). Boll. Soc. Paleont. Ital. 17(1):28-48. Modena.

- Bolhar, R., Kamber, B.S., Moorbath, S., Fedo, C.M & Whitehouse, M.J. 2004. Characterisation of early Archaean chemical sediments by trace element signatures. Earth Planet. Sci. Lett. 222 (1): 43-60. Amsterdam.

- Bosellini, A. 1984. Progradation geometries of carbonate platforms: examples from the Triassic of the Dolomites, northern Italy. Sedimentology. 31: 1-24. Oxford.

- Bosellini, A. 1991. Geologia delle Dolomiti. Casa Editrice Ahesia. 192 pp. Bolzano.

- Bosellini, A. & Rossi, D. 1974. Triassic Carbonate Buildups of the Dolomites, Northern Italy. *In:* Laporte, L.F. (ed). Reefs in time and space: Selected examples from the recent and ancient. Soc Econ. Paleont. Miner. Spec. Publ 18: 209 – 233. Tulsa.

- Böhm, F. & Brachert T.C. 1993. Deep water Stromatolites and *Frutexites* MASLOV from the Early and Middle Jurassic of S-Germany and Austria.- Facies 28: 145-168. Erlangen.

- Böhm, F., Eisenhauer, A., Joachimski, M.M.,Lehnert, H., Dullo, W.-C. & Reitner, J. 2002. Carbon isotope history of the Caribbean surface waters revealed by coralline sponges. 14th Australian Geological Convention. Poster Presentation. Townsville.

- Böhm, F., Joachismki, M.M., Lehnert, H., Morgenroth, G., Kretschmer, W., Vacelet, J & Dullo, W.-C. 1996. Carbon isotope records from the extant Caribbean and South Pacific sponges: Evolution of $\delta^{13}C$ in surface water DIC. Earth Planet. Sci. Lett. 139: 291-303. Amsterdam.

- Böhm, F., Joachismki, M.M., Dullo, W.C., Eisenhauer, A., Lehnert, H., Reitner, J. & Wörheide, G.2000. Oxygen isotope fractionation in marine aragonite of coralline sponges. Geochim. Cosmochim Acta 64 (10): 1695-1703. New York.

- Brachert, T.C. 1999. Non-skeletal carbonate production and stromatolite growth within a deep ocean basin (Last Glacial Maximum, Red Sea).- Facies 40: 211-228. Erlangen.

- Brachert, T.C. & Dullo, W.C. 1991. Laminar micrite crusts and associated foreslope processes (Red Sea). J.Sediment Petrol. 61: 354-363. Tulsa.

- Brachert, T.C. & Dullo, W.C. 1994. Micrite crusts on Ladinian foreslopes of the Dolomites seen in the light of a modern scenario from the Red Sea. Jahrb. Geol. BA**.** 50: 57–68. Vienna.

- Braga, J.C., Martin, J.M. & Riding, R. 1995. Controls on microbial dome fabric development along a carbonate-siliciclastic shel-basin transect, Miocene, SE Spain. Palaios 10: 347-361.Tulsa.

- Brandner, R., Flügel, E. & Senowbari-Daryan, B., 1991. Microfacies of carbonate slope boulders: Indicator of the source area (Middle Triassic: Mahlknecht Cliff, Western Dolomites). Facies, 25: 279-296. Erlangen.

- Bray, J.R. & Curtis, J.T.1957. An ordination of the upland forest communities of Southern Wisconsin. Ecol. Monogr. 27: 325 – 349. Ithaca.

- Brenchley, P.J. & Harper, D.A.T. 1998. Palaeoecology: Ecosystems, environments and evolution. Chapman & Hall. 402 pp. London.

- Brocks, J.J. & Summons, R.E. 2003. Sedimentary hydrocarbons: Biomarkers for Early life. *In* Holland, E.D. (ed). Treatise on Geochemistry 8: 63-115. Amsterdam.

- Brückner, A., Janussen, D. & Schneider, S. 2003. Eine neue Poriferen-Fauna aus dem Septarienton (Oligozän, Rupelium) von Bad Freienwalde (NE-Deutschland) und der erste fossil erhaltene Vertreter der nicht-rigiden Hexactinelliden- Gattung *Asconema.* Paläont Z. 77 (2): 263-280. Stuttgart.

- Burne, R.V. & Moore, L.S. 1987. Microbialites; organosedimentary deposits of benthic microbial communities. Palaios 2(3): 241-254. Tulsa.

- Byrne, R.H. & Lee, J.H. 1993. Comparative yttrium and rare earth element chemistries in seawater. Mar. Chem. 44: 121-130. Amsterdam.

- Byrne, R.H., Liu, X. & Schijf, J. 1996. The influence of phosphate coprecipitation on rare earth distributions in natural waters. Geochim. Cosmochim. Acta 60 (17): 3341 – 3346. Amsterdam.

- Calvet, E., Tucker, M. & Henton, J. 1990. Middle Triassic carbonate ramp systems in the Catalan basin, northeastern Spain: facies, system tracts, sequences and controls. *In* Tucker, M., Wilson, J.L., Crevello, P.D., Sarg, R. & Read, J.F. (eds). Carbonate platforms – facies, sequences and evolution: International Association of Sedimentologists Spec. Pub 9: 79-108. Blackwell, Oxford.

- Calvet, E. & Tucker, M.E. 1995: Mud-Mounds with reefal caps in the upper Muschelkalk (Triassic), eastern Spain. *In:* Monty, C.L.V., Bosence, D. W. J. & Bridges, P. H (eds.). Carbonate Mud Mounds: their Origin and Evolution International Association of Sedimentologists, Spec. Pub. 23: 311- 333. Blackwell, Oxford.

- Caruthers, A.H. & Stanley, G.D. Jr. Systematic Analysis of Upper Triassic Silicified. J. Paleont. 82(3): 470 – 491. Tulsa.

- Chablais, J., Martini, R.; Samankassou, E., Onoue, T. & Sano, H. 2010. Microfacies and depositional setting of the Upper Triassic mid-oceanic atoll-type carbonates of the Sambosan Accetionary Complex (Southern Kyushu, Japan). Facies 56 (2): 249-278. Berlin-Heidelberg.

- Chafiki, D., Canérot, J., Souhel, A., El Hariri, K. & Taj Eddine, K. 2004. The Sinemurian carbonate mud-mounds from central High Atlas (Morocco): stratigraphy, geometry, sedimentology and geodynamic patterns. J. Afr. Earth. Sci. 39: 337-346. Amsterdam.

Literature

- Cheetham, A.H. & Hazel, J.E. 1969. Binary (Presence Absence) similarity coefficients. J. Paleont 43 (5): 1130-1136. Tulsa.

- Christopher, C. C. 1990. Late Mississippian Girvanella-bryozoan mud mounds in southern West Virginia. Palaios 5(5): 460-471. Tulsa.

- Conrad, M.A. & Clavel, B. 2008. A *Lithocodium* and *Bacinella* signature of a late Hauterivian, local microbial event: the Urgonian limestone in South-East France. Geologia Croatica, Vol. 61 (2/3): 239 – 250. Zagreb.

- Craig, G.Y. 1953. Fossil communities and assemblages. Am. J. Sci. 251: 547-548. New Haven.

- Cros, P. 1967. A propos de l`origine récifale de deux massifs ladino-carniens dans les Dolomites. C.R. Somm. Soc. Géol. France 6: 233. Paris.

- Cros, P. & Lagny, P. 1972. Die paleogeographische Bedeutung des pelagischen Ablagerungen im Anis und Ladin der Westlichen Karnischen Alpen und der Dolomiten (Norditalien). Mitt. Ges. Geol. Bergbaustud. 21: 169 – 192. Vienna.

- Cros, P. 1974. Un modéle de sédimentation carbonatée marine: Les plateformes dites récifales du Trias des Dolomitees et leur environment. Thése Doct. Etat Sc. Nat. Univ. Paris. 888 pp. Paris.

- Cuif, J.P. 1973. Histologie de quelques sphinctozoaires (Poriferes) Triasiques Geobios 6(2): 115 – 125. Lyon.

- Cuif, J.P. 1974. - Role des sclerosponges dans la faune recifale du Trias des Dolomites (Italie du nord). Geobios 7 (2): 139-153. Lyon.

- Cuif, J.P., Gautret P., Laghi G.F., Mastandrea, A., Pradier, B. & Russo, F.,1990 - Recherche sur la fluorescence UV du squelette aspiculaire chez les Demosponges calcitiques triasiques. Geobios 23 (1): 21-31. Lyon.

- Défarge, C., Gautret, P., Reitner, J & Trichet, J. 2009. Defining organominerals. Comment on „Defining biominerals and organominerals: Direct and indirect indicators of life" by Perry et al. (2007, Sedimentary Geology, 201, 157-179). Sediment. Geol. 213 (3/4): 152-155. Amsterdam.

- Delecat, S. 2005. Porifera-microbialites of the Lower Liassic (Northern Calcareous Alps)- Re-settlement strategies on submarine mounds of dead Rhaetian reefs by ancestral benthic communities. Ph.D. Thesis. University of Göttingen. pp 1-114. Göttingen.

- Delecat, S. & Reitner, J. 2005. Sponge communities from the Lower Liassic of Adnet (Northern Calcareous Alps, Austria). Facies 51: 385-404. Berlin-Heidelberg.

- Dickson, J. A. D. 1965. A modified staining technique for carbonates in thin section: Nature 205: 587. London.

- Dickson, J. A. D. 1966. Carbonate identification and genesis as revealed by staining: J. Sediment Petrol. 36: 491-505. Tulsa.

- Dieci, G., Antonacci, A.& Zardini, R. 1968. Le spugne cassiane (Trias medio-superiore) della regione dolomitica attorno a Cortina d´Ampezzo: Boll. Soc. Paleont. Ital. 7 (2) 94 – 155. Modena.

- Dieci, G., Russo, A. & Russo, F. 1974. Nota preliminare sulla microstruttura di spugne aragonitiche del Trias medio-superiore. Bol. Soc. Paleont. Ital 13 (2): 99-107. Modena.

- Dieci, G., Russo, A., Russo, F & Marchi, M.S. 1977. Occurence of Spicules in Triassic Chaetetids and Ceratoporellids, Boll. Soc. Paleont. Ital. 16(2) : 229–238. Modena.

- Dodd, J.R., & Stanton R. J. Jr. 1990 .Paleoecology, concepts and applications. 502 pp. John Wiley & Sons, New York.

- Dravies, J.J. & Yurewicz, D.A. 1985. Enhanced carbonate petrography using fluorescence microscopy. J. Sediment. Petrol. 55 (6): 795-804. Tulsa.

- Dronov, V., Gazdzicki, A. & Melinkova, G.K. 1982. Die triadischen Riffe im südöstlichen Pamir. Facies 6: 107-128. Erlangen.

- Drosdov, A.L., Bukin, O.A., Voznesenskii, S.S., Galkina, A.N., Golik, S.S., Zhukova, N.V., Kul'chin, Y.,N., Nagornyi, I.G. & Cherbadzhi, I.I. 2008. Symbiont cyanobacteria in the Hexactinellid sponges (Porifera:Hexactinellida)- Doklady. Biol. Sci. 420: 192-194.Berlin-Heidelberg.

- Dullo, W.C., Flügel, E., Lein, R., Riedel, P. & Senowbari-Daryan, B. 1987. Algen, Kalkschwämme und Mikroproblematika aus unterkarnischen Riffkalken des Bosruck-Gipfels (Nördliche Kalkalpen, Österreich). Jb.Geol. B.-A. 129 (3/4): 525-543. Vienna.

- Dullo, W.C. & Lein, R. 1982. Facies and Environment of the Leckkogel Beds (Carnian; Alps). Facies 6: 25-36. Erlangen.

- Dunham, R. J. 1962. Classification of carbonate rocks according to depositional texture. *In*: Ham, W. E. (ed.) Classification of carbonate rocks: Mem. Am. Assoc. Petrol. Geol: 108-121. Tulsa.

- Dupraz, C. & Strasser, A. 1999. Microbialites and micro-encrusters in shallow coral bioherms (Middle to Late Oxfordian, Swiss Jura Mountains):. Facies 40:101–130. Erlangen.

- Eddy, J.A. 1976. The Maunder Minimum. Science 192 (4245): 1189–1202. Washington.

- Elderfield, H. 1988. The oceanic chemistry of the rare-earth elements: Phil. Trans. Roy. Soc. London. ser. A 325:. 105–126. London.

- Elderfield, H & Greaves, M.J. 1982. The rare-earth elements in sea-water. Nature 296: 214-219. London.

- Emmerich, A., Zamparelli, V., Bechstädt, T; & Zühlke, R. 2005. The reefal margin and slope of a Middle Triassic carbonate platform: the Latemar (Dolomites, Italy). Facies, 50, 573-614. Erlangen.

- Engeser, T. & Appold, T. 1988: Ein neues Vorkommen des Sphinctozoen *Cassianothalamia zardinii* Reitner, 1987 (Demospongiae, Porifera) aus den oberkarnischen Leckkogelschichten von Poelling bei Launsdorf (Kärnten, Österreich). Mitt. Geol.-Palaeont. Inst. Univ.Hamb. 67: 73-87.Hamburg.

Literature

- Ersteva, L.N. & Tsymbulov, L.B. On transformations of iron, nickel and cobalt arsenides and sulfoarsenides under thermal treatment in various media. Russ. J. Appl. Chem. 75 (10): 1585-1593. New York.

- Fabricius, F., Friedrichsen, H. & Jacobshagen, V. 1970. Paläotemperaturen und Paläoklima in Obertrias und Lias der Alpen. Geol. Rundsch 59: 805-826. Berlin-Heidelberg.

- Fagerstrom, J.A. 1964. Fossil communities in Paleoecology: Their recognition and significance. Geol.Soc.Am.Bull. 75: 1197 – 1216. Boulder.

- Fagerstrom, J.A. 1987. The evolution of reef communities. John Wiley & Sons. 600 pp. New York.

- Fallon, S.J., McCulloch, M.T. & Guilderson, T.P. 2005. Interpreting environmental signals from the coralline sponge *Astrosclera willeyana.* Palaeogeogr. Palaeoclimatol. Palaeoecol. 228: 58-69. Amsterdam.

- Farris, J. S. 1969. On the cophenetic correlation coefficient. Systematic Zoology 16: 174-175. Oxford.

- Ferrari, J. R., Nakamoto, K. & Brown, C.W. 2003.Introductory RAMAN spectroscopy. Academic Press. 434 pp. Amsterdam.

- Fischer, R., Michalzik, D. & Helm, C. 2007. Microhermal nodules of *Renalcis-* like calcimicrobes from Oxfordian limestones of the Sierra Madre Oriental (Novillo Formation, Mexico). Facies 53: 239-248. Berlin-Heidelberg.

- Folk, R.L. 1958. Practical petrographic classification of limestone. Bull. Amer. Asoc. Petr. Geol. Mem. 1: 62-84. Tulsa.

- Flügel, E. 1964. Mikroproblematika aus den rhäthischen Riffkalken der Nordalpen. Paläont. Z. 38 (1/2): 74-87. Stuttgart.

- Flügel, E. 1986. Zur Mikrofazies oberanisischer Riffkalke in den östlichen Nordkarawanken, Kärnten. Carinthia II 96: 463-478. Klagenfurt.

- Flügel, E. 2002. Triassic reef patterns. In Kieslling, W., Flügel, E. & Golonka, J. (eds.): Phanerozoic reef patterns. SEPM Spec. Publ. 72: 391 – 464. Tulsa.

- Flügel, E. 2004. Microfacies of carbonate rocks. Analysis, interpretation, application. 997 pp. Springer. Berlin-Heidelberg-New York.

- Flügel, E. & Flügel-Kähler, E. 1992. Phanerozoic reef evolution: Basic questions and data base. Facies 26: 167- 278. Erlangen.

- Flügel, E. & Link, M. 1996. Upper Triassic Reefs of Southwestern Turkey: Evidence of Reef Boulders ("Cipits"). . Göttinger Arb. Geol. Paläont. Sonderband 2: 279-283. Göttingen.

- Flügel, E., Riedel, P. & Senowbari-Daryan, B. 1988. *Plexoramea cerebriformis* MELLO, ein häufiges Mikrofossil in triadischen Flachwasserkalken: Alge oder Pilz?. Mitt. Ges. Geol. Bergbaustud. 34/35: 263-277. Vienna.

- Flügel, E., Velledits, F., Senowbari-Daryan, B. & Riedel, P. 1991. Rifforganismen aus „Wettersteinkalken" (Karn?) des Bükk-Gebirges, Ungarn. Geol. Paläont. Mitt. Innsbruck 18: 35-62. Innsbruck.

- Fraústro da Silva, J.J.R. & Williams, R.J.P. 1991 The biological chemistry of the elements. Clarendon Press. 561 pp. Oxford.

- Frech, F. 1890. Die Korallenfauna der Trias (Schluß). Palaeontographica 37 (2-4): 33-116. Stuttgart.

- Frost, S.H. 1971. Cenozoic reef systems of Caribbean-prospects for paleoecological systems. Stud. Geol. 4: 93-110.Tulsa.

- Fuchs, G., Widder, R.W. & Tuladhar, R. 1988. Contributions to the Geology of the Annapurna Range (Manang Area, Nepal). Jb. Geol-B.-A. 131 (4): 593-607. Vienna.

- Fürsich, F.T. & Wendt, J. 1976. Faziesanalyse and paläogeogeographische Rekonstruktion des Ablagerungsraumes der Cassiner Schichten (Mittel- bis Oebrtrias, Langobard –Cordevol, Jul? –Südalpen) *In* Seilacher,A. (ed.) Palökologie: Lagerstätten, Diagenese, Konstruktionsmorphologie, Vergesselschaftungen. Bericht 1970 – 1975. Zentralbl. Geol Paläontol. II: 233 - 238. Stuttgart.

- Fürsich, F.T. & Wendt, J. 1977. Biostratinomy and Palaeoecology of the Cassian Formation (Triassic) of the Southern Alps. Paleogeogr. Palaeoclimatol. Palaeoecol 22: 257 – 323. Amsterdam.

- Fürsich, F.T. 2000. Die Cassianer Schichten. In Meischner, D., & Pinna, G (eds.) Europäische Fossillagerstätte: 79-82. Springer. Berlin Heidelberg.

- Garaffoni, A.R.S., & Lana, P.C. Species of *Terebellides* (Polychaeta, Terebellidae, Trichobranchinae) from the Brazilian coast. Iheringia Sér Zool. 93 (4): 355-363. Porto Alegre.

- German, C.R.; Holliday, B.P. & Elderfield, H. 1991. Redox cycling of rare earth elements in the suboxic zone of the Black Sea . Geochim. Cosmochim. Acta. 55(12): 3553-3558. Amsterdam.

- Germer, J. 2010. Sedimentary preservation of sponge-derived lipid biomarkers. Unpublished Diploma Thesis. University of Göttingen. 68 pp. Göttingen.

- Gilbert, J. & Churchill, G.C. 1864. The Dolomite Mountains. Excursions through Tyrol, Carinthia, Carniola & Friuli in 1861, 1862 & 1863. 576 pp. Longman, Roberts & Green. London.

- Goreau, T.F. 1959.The ecology of Jamaican coral reefs. I. Species composition and zonation. Ecology 40 (1): 67-90. Washington.

- Goreau, T.F., Lang, J.C., Graham, E.A., & Goreau, P.D. 1972. Structure and ecology of the Saipan reefs in relation to predation by *Acanthaster planci* (Linnaeus). Bull. Mar. Sci. 22: 114-152. Miami.

- Götz , S., Löser, H. & Schmid, D.U. 2005. Reef development on a deepening platform: two Early Cretaceous coralgal patch reefs (Catí, Llàcova Formation, eastern Spain) compared.Cretaceous Res. 26: 864-881. Amsterdam.

Literature

- Gradstein, F., Ogg, J. & Smith, A. 2004. A Geologic Time Scale 2004. Cambridge University Press. 589 pp. Cambridge.

- Grandjean-Lecuyer, P., Feist, R & Albàrede, F. 1993. Rare earth elements in old biogenic apatites. Geochim. Cosmochim. Acta 57: 2507-2514. Amsterdam.

- Grottoli, A.G., Adkins, J.F., Panero, W.R., Reaman, D.M & Moots, K. 2010. Growth rates, stable isotopes ($\delta^{18}O$) and strontium (Sr/Ca) composition in two species of Pacific sclerosponges (Acanthochaetetes wellsi and Astrosclera willeyana) with $\delta^{18}O$ calibration and application to paleooceanography. J. Geophys. Res. 115: doi: 10.1029/2009JC005586.

- Haese, R.R. The reactivity of iron. *In* Schulz, H.D. & Zabel, M. (eds). Marine geochemistry: 241-270. Springer. Berlin-Heidelberg.

- Halverson, G.P., Hoffman, P.F., Schrag, D.P. & Kaufman, A.J. 2002. A major perturbation of the carbon cycle before the Ghaub glaciation (Neoproterozoic) in Namibia: Prelude to snowball Earth? Geochem. Geophys. Geosys**.** 3(6), 10.1029/ 2001GC000244. St. Louis.

- Hartman, W.D. 1969. New genera and species of coralline sponges (Porifera) from Jamaica. Postilla 137: 1-39. New Haven.

- Hartman, W.D. & Goreau, T.F. 1970. Jamaican coralline sponges: their morphology, ecology and fossil relatives. Symp. Zool. Soc. London. 25: 205-243. London.

- Hasse-Schramm, A., Böhm, F., Eisenhauer, A., Dullo, W.C., Joachimski, M., Hansen, B., & Reitner, J. 2003. Sr/Ca ratios and oxygen isotopes from sclerosponges: Temperature history of the caribbean mixed layer and thermocline during the Little Ice Age. Paleoceanography 18 (3): 1073. 15 pp.

- Hedges, R.E.M., Stevens, R.E & Koch, P.L. 2005. Isotopes in bones and teeth. *In* Leng, M.E. Isotopes in paleoenvironmental research:117-146. Springer. Dordrecht.

- Helm, C. 2005. Riffe und fazielle Entwicklung der *florigemma*-Bank (Korallenoolith, Oxfordium) im Süntel und östlichen Wesergebirge (NW-Deutschland). Geol. Beitr. Hannover 7: 3-339. Hannover.

- Hennig, W. 1966. Phylogenetic Systematics. 263 pp. University of Illinois Press. Urbana.

- Hoefs, J. 2009. Stable isotope geochemistry. 285 pp. 6th ed. Springer. Berlin-Heidelberg.

- Hoffmann, F. 2003. Microbial sulfate reduction in the tissue of the cold-water sponge *Geodia-barretti* (Tetractinellida, Demospongiae). Ph.D. Thesis. 48 pp. University of Göttingen.

- Höld, I.M., Schouten, S., Jellema, J. & Damsté, J.S. 1999. Origin of free and bound mid.chained methyl alkanes in oil, bitumens and kerogens of the marine, Infracambrian Huqf Formation (Oman). Org Geochem. 30: 1411-1428. Amsterdam.

- Hornung, T., Spatzenegger, A. & Joachismki, M.M. 2007a. Multistratigraphy of condensed ammonoid beds of the Rappolstein (Berchtesgaden, southern Germany): unravelling palaeoenvironmental conditions on "Hallstatt deep swells" during the Reingraben Event (Late Lower Carnian). Facies 53: 267-292. Berlin-Heidelberg.

- Hornung, T., Krystyn, L. & Brandner, R. 2007b. A Tethys-wide mid-Carnian (Upepr Triassic) carbonate productivity crisis: Evidence for the Alpine Reingraben from Spiti (Indian Himalaya): J. Asian Earth Sci. 30: 285-302. Amsterdam.

- Hornung, T., Brandner, R., Krystyn, L., Joachimski, M.M & Keim, L. 2007c. Multistratigraphic constraints on the NW Tethyan 'Carnin Crisis' - *In*: Lucas, S.G., Spielmann, J.A. (eds.): The Global Triassic. New Mexico Museum of Natural History Bulletin, 41: 59-67. Albuquerque.

- Hudson, R.G.S. 1959. A revision of Jurassic stromatoporoids *Actinostromina*, *Astrostylopsis*, and *Trupetostromaria* . Palaeont. 1: 87-98. London.

- Hühne, C. 2005. Geochemie Porifera Reicher Mud-Mounds und Mikrobialithe des Mittel- und Oberdevons (Westaustralien, Nordfrankreich). University of Göttingen. Ph.D. Thesis. pp 1-133. Göttingen .

- Jaap, W.C. 1984. The ecology of the south Florida coral reefs: a community profile. U.S. Fish Wild. Serv. FWS/OBS 82.08. 138 pp. Florida.

- Jackson, J.B.C. 1991. Adaptation and diversity of reef corals. BioScience 41 (7): 475-482. Reston.

- Jackson, J.B.C., Goreau, T.F. & Hartman, W.D. 1971. Recent Brachiopod-Coralline Sponge Communities and Their Paleoecological Significance. Science13 (173): 623-625. Washington, D.C.

- James, N.P., & Bourque, P.-A. 1992. Reefs and mounds. *In:* Walker, R.G. and James, N.P. (eds.): Facies models. Response to sea level change. Geological Association of Canada. 323-347. St. John's.

- Jasionowski, M. 2004. Geochemistry of the Sarmatian (Middle Miocene) reefal carbonates of the medobory region (Paratethys, western Ukraine): paleoenvironmental implications. 23rd IAS Meeting of Sedimentology, Abstracts Book: 152. Coimbra.

- Joachismki, M.M. 1991. Stabile Isotope (C,O) und Geochemie der Purbeck-Mikrite in Abhängigkeit von Fazies und Diagenese (Berriasian/Schweizer und Französischer Jura, Südengland). Erlanger. Geol. Abh. 119: 1-114. Erlangen.

- Jørgensen, B.B. & Kasten, S. 2007. Sulfur cycling and methane oxidation. *In* Schulz, H.D. & Zabel, M. (eds). Marine geochemistry: 271-310. Springer. Berlin-Heidelberg.

- Kamber, B.S. & Webb, G.E. 2001. The geochemistry of late Archaean microbial carbonate: Implications for ocean chemistry and continental erosion history. Geochim. Cosmochim. Acta 65 (15): 2509-2525. Amsterdam.

- Kamber, B.S. & Webb, G.E. 2007. Transition metal abundances in microbial carbonate: A pilot study based on in situ LA-ICP-MS analysis. Geobiology 5: 375-389. New York.

- Keim, L. & Schlager, W. 1998. Automicrite Facies on steep slopes. (Triassic, Dolomites, Italy). Facies 41: 15-26. Erlangen.

- Keim, L. & Schlager, W. 2001. Quantitative compositional analyses of a Triassic carbonate platform (Southern Alps, Italy). Sediment. Geol. 139:261-283. Amsterdam.

Literature

- Kennard, J.M. & James, N.P. 1986. Thrombolites and stromatolites: Two distinct types of microbial structures. Palaios 1: 492-503. Tulsa.

- Keupp, H., Jenisch, A., Herrmann, R., Neuweiler, F. & Reitner, J.1993. Microbial carbonate crusts: a key to the environmental analysis of fossil spongiolites? Facies 29: 41-54. Erlangen.

- Keupp, H., Reitner, J. & Salomon, D. 1989. Kieselschwämme (Hexactinellida und "Lithistida") aus den Cipit-Kalken der Cassianer Schichten (Karn, Südtirol).- Berliner geowiss.Abh., A 106: 221-241. Berlin.

- Keupp, H., & Arp,G. 1990. Aphotische Stromatolithe aus dem süddeutschen Jura (Lias, Dogger). Berliner geowiss. Abh. A. 124: 3-33. Berlin.

- Kiessling, W., Flügel, E. 2002. Paleoreefs - a database on Phanerozoic reefs. *In* Kieslling, W., Flügel, E. & Golonka, J. (eds.): Phanerozoic reef patterns. SEPM Spec. Publ. 72: 77-92 Tulsa.

- Kim, S.T. & O'Neil, J.R. 1997. Equilibrium and non-equilibrium oxygen isotope effects in synthetic carbonates. Geochim. Cosmochim. Acta 61 (16): 3461-3475. New York.

- Klipstein, A. 1843. Beiträge zur Geologischen Kenntnis der Östlichen Alpen. 311 p. Gießen.

- Koch, R., Moussavian, E., Ogolerec, B, Skaberne, D. & Bucur, I.I. 2002. Development of a *Lithocodium* (syn. *Bacinella irregularis*) –reef-mound- A patch within Middle Aptian lagoonal limestone sequence near Nova Gorica (Sabotin Mountain, W-Slovenia). Geologija 45 (1): 71-90. Ljubljana.

- Kodner, R.B., Summons, R.E., Pearson, A., King, N. & Knoll, A.H. 2008. Sterols in a unicellular relative of the metazoans. Proc. Nat.Acad.Sci. 105 (29): 9897-9902. Washington, D.C.

- Korte, C., Kozur, H. & Veizer, J. 2005. δ^{13}C and δ^{18}O values of Triassic brachiopods and carbonate rocks as proxies for coeval seawater and palaeotemperature. Palaeogeogr. Palaeoclimatol. Palaeoecol. 226: 287-306. Amsterdam.

- Kozur, H.W. & Bachmann, G.H. 2010. The Middle Carnian wet intermezzo of the Stuttgart Formation (Schlifsandstein) Germanic Basin. Palaeogeogr. Palaeoclimatol. Palaeoecol. 290: 107-119. Amsterdam.

- Krautter, M. 1997. Aspekte zur Paläökologie postpaläozoischer Kieselschwämme. Profil 11: 199-324. Stuttgart.

- Krautter, M. 1998. Ecology of siliceous sponges- Application to the environmental interpretation of the Upper Jurassic sponge facies (oxfordian) from Spain. Cuad. Geol Ibérica 24: 223-239. Madrid.

- Kuss, J. 1988. Mikrofacies and Foraminifera of Middle Triassic Limestones (Anisian-Carnian?) from Gebel Araif el Naqa (Sinai, Egypt). Facies 19: 61-76. Erlangen.

- Laghi G., Martinelli, G., & Russo, F. 1983. Localization of minor elements by EDS microanalysis in aragonitic sponges from the St. Cassian beds, Italian Dolomites. Lethaia 17: 133 – 138.Oslo.

- Laube, G. 1864. Bemerkungen über die Münster'schen Arten von St. Cassian in der Münchener paläontologischen Sammlung. Jb.K.K.geol. Reichanstalt 14: 402 – 412. Vienna.

- Lee, R.E. 2008. Phycology. Cambridge University Press. 624 pp. Cambridge.

- Leinfelder, R.R., Nose, M., Schmid, D.U. & Werner, W. 1993. Microbial crusts of the late Jurassic: Composition, palaeoecological significance and importance in reef construction. Facies 29: 195- 230. Erlangen.

- Leinfelder, R.R., Krautter, M., Laternser, R. , Nose, M., Schmid, D.U., Schweigert, G., Werner, W., Keupp, H., Brugger, H., Herrmann, R., Rehfeld-Kiefer, U., Schroeder, J. H., Reinhold, C., Koch, R., Zeiss, A., Schweizer, V., Christmann, H., Menges, G. & Luterbacher, H.-P. 1994. The origin of Jurassic reefs: Current research developments and results. Facies 31: 1-56.Erlangen.

- Leinfelder, R.R., Werner, W., Nose, M. Scdmid, D.U., Krautter, M., Laternser, R., Takacs, M & Hartmann, D. 1996. Paleoecology, growth parameters and dynamics of coral, sponge and microbialite reefs from the Late Jurassic. *In* Reitner, J., Neuweiler, F. & Gunkel, F. Glolal and regional controls on biogenic sedimentation I: Reef Evolution. Research Reports. Göttinger Arb. Geol. Paläont Sb2: 227-248. Göttingen.

- Leng, M.J. Lamb, A.L., Heaton,T.H.E., Marshall, J.D., Wolfe, B.B., Jones, M.D., Holmes, J.A. & Arrowsmith, C. 2005. Isotopes in lake sediments. *In* Leng, M.E. Isotopes in paleoenvironmental research: 147-184. Springer. Dordrecht.

- Leonardi, P. 1961. Triassic coralligenous reefs in the Dolomites. Ann. Univ. Ferrara 8: 127 – 157. Ferrara.

- Leonardi, P. 1967. Le Dolomiti. Geologia dei Monti tra Isarco e Piave, Vol 1 & 2. Manfrini. 1019 pp. Rovereto.

- Leonardi, P. 1979. Sedimentologyogical-stratigraphic considerations regarding the Triassic. 'reefs' of the Dolomites (Italy).- Geol. Mijnbouw, 58, 139-144. The Hague.

- Logan, A. 2008. Holocene thecideide brachiopods from the north-western Pacific ocean: systematic, life habitats and ontogeny. Syst Biodiv 6(3): 405-413. Cambridge.

- Loretz, H. 1875. Einige Petrefakten der alpinen Trias aus den Südalpen. Z. Dtsch. Geol. Ges. 27: 784 – 842. Stuttgart.

- Love, G.D., Grosjean, E., Stalvies,C., Fike, D.A., Grotzinger, J.P., Bradley, A.S., Kelly, A.E., Meredith, W., Snape, C.E., Bowring, S.A., Condon, D.J. & Summons, R.E. 2009. Fossil steroids record the appearance of Demospongiae during the Cryogenian period. Nature 457: 718-721. London.

- Lowenstein, T.K., Timofeef, M.N., Brennan, S.T., Hardie, L.A & Demicco, R.V. 2001. Oscillations in Phanerozoic Seawater Chemistry: Evidence from fluid inclusions. Science 294: 1086-1088. Washington, D.C.

- Luterbacher, J., Rickli, R., Xoplaki, E., Tinguely, C., Beck, C.,Pfister, C. & Wanner, H. 2001. The Late Maunder Minimum (1675-1715)-A key period for studying decadal scale. Climatic Change 49 (4): 441-462. Berlin-Heidelberg.

Literature

- Lüter, C., Wörheide, G & Reitner, J. 2003. A new thecideid genus and species (Brachiopoda, Recent) from submarine caves of Osprey Reef (Queensland Plateau, Coral Sea, Australia). J. Nat. Hist. 37: 1423-1432. London.

- Maliva, R.G., Missimer, T.M., Leo, K.C., Statom, R.A., Dupraz, C., Lynn, M. & Dickson, J.A.D. 2000: Unusual calcite stromatolites and pisoids from a landfill leachate collection system. Geology 28: 931-834. Boulder.

- Martínez- Hernández, E. & Ramírez-Arriaga, E. 2006. Tertiary palinofloristic correlations between Mexican Formations with emphasis in dating the Balsas Group. *In* Vega,F.J., Nyborg, T.G., Perrilliat, M.C., Montellano-Ballesteros, M., Cevalloz Ferriz, S.R.S. & Quiroz-Barroso, S.A. Studies on Mexican Paleontology: 19-45. Springer. Berlin-Heidelberg.

- Martínez- Rodríguez, M., Reitner, J. & Más, R. 2010. Micro-framework reconstruction from peloidal-dominated mud mounds (Viséan, SW Spain)-. Facies 56: 139-156. Springer. Berlin-Heidelberg.

- Martini, R., Zaninetti, L., Lathullière, B., Cirilli, S., Cornée, J.-J. & Villeneuve, M. 2004. Upper Triassic carbonate deposits of Seram (Indonesia): palaeogeographic and geodynamic implications. Palaeogeogr. Palaeoclimatol. Palaeoecol. 206: 75-102. Amsterdam.

- Mathews CK, Van Holde KE, Ahern KG (1999) Biochemistry. Addison Wesley. 1190 pp. San Francisco.

- Matsumoto, G.I., Friedman, E.I., Watanuki, K. & Ocampo-Friedmann, R. 1992. Novel long-chain *anteiso*-alkanes and *anteiso*-alkanoic acids in Antarctic rocks colonized by living and fossil cryptoendolithic microorganisms. J.Cromatog. 598: 267-276. Amsterdam.

- McLennan, S. 1989. Rare earth elements in sedimentary rocks: Influence of provenance and sedimentary processes. *In*: Lipin, B.R. & McKay, G.A. (eds). Geochemistry and Mineralogy of Rare Earth Elements: Rev. Mineral. 21: 169–200. Washington, D.C.

- Mehl, D. 1996. Phylogenie und Evolutionsökologie der Hexactinellida (Porifera) im Paläozoikum. Geol. Paläont. Mitt. Insbruck S4: 1-55. Innsbruck.

- Michalik, J. 1982. Uppermost Triassic short-lived bioherm complexes in the Fatric, Western Carpathians. Facies 6: 129-146. Erlangen.

- Michard, A. & Albarede, F. 1986. The REE content of some hydrothermal fluids. Chem. Geol. 55 : 51–60. Amsterdam.

- Michie, M.G. 1982. Use of the Bray-Curtis similarity measure in Cluster Analysis of foraminiferal data. Math. Geol. 14 (6): 661-667. New York.

- Montanaro Galitelli, E., Morandi, N. & Pirani, R. 1973. Corallofauna triassica aragonitica ad alto contenuto in stronzio: studio analitico e considerazioni. Bol. Soc. Paleont. Italiana. 12: 130 – 144. Modena.

- Morse, J.W & McKenzie, F.T. 1990. Geochemistry of sedimentary carbonates. Developments in Sedimentology 48: pp 1- 690. Amsterdam.

- Moussavian, E. & Senowbari-Daryan, B. 1988. *Dendronella articulata.* n. gen., n. sp.: Eine neue Kalkalge aus den Cassianer Schichten (Obertrias/Karn; Südalpen). Facies 19 (1): 251-257. Erlangen.

- Mutschlechner, G. 1933. Geologie des Gebietes zwischen St. Cassian und Buchenstein (Südtiroler Dolomiten) Jahrb. Geol. B.-A, 83: 199 – 232. Vienna.

- Müller-Wille, S. & Reitner, J. 1993. Palaeobiological Recontructions of selected sphinctozoan sponges from the Cassian Beds (Lower Carnian) of the Dolomites (Northern Italy), Berliner geowiss Abh. E 9: 253-281. Berlin.

- Münster, G. 1834. Über das Kalkmergel –Lager von St. Cassian in Tyrol und die darin vorkommenden Ceratiten. Neues Jahrbuch für Mineralogie, Geognosie, Geologie und Petrefaktenkunde, 1834: 1-15. Stuttgart.

- Münster, G. 1841: Beschreibung und Abbildung der in den Kalkmergelschichten von St. Cassian gefundenen Versteinerungen. *In* Wissmann, H.L. & Münster, G.G.. Beiträge zur Geognosie und Petrefakten-Kunde des Südöstlichen Tirols vorzüglich der Schichten von St. Cassian: 25 – 152. 4.Buchner. Bayreuth.

- Neuweiler, F. 1993. Development of Albian microbialites and microbialite reefs at marginal platform areas of the Vasco-Cantabrian Basin (Soba Reef Area, Cantabria, N.Spain). Facies 29: 231-250. Erlangen.

- Neuweiler, F. & Bernoulli, D. 2005. Mesozoic (Lower Jurassic) red stromatactis limestones from the Southern Alps (Arzo, Switzerland): calcite mineral authigenesis and syneresis-type deformation. Int. J. Earth. Sci. 94(1): 130-146. Berlin-Heidelberg.

- Neuweiler, F., Bourque, P.A. & Boulvain, F. 2001. Why is stromatactis so rare in Mesozoic carbonate mud mounds ? . Terra Nova 13 : 338- 346. Oxford.

- Neuweiler, F. & Burdige D.J. 2005. The modern calcifying sponge *Spheciospongia vesparium* (Lamarck, 1815), Great Bahama Bank: Implications for ancient sponge mud-mounds: Sediment. Geol.. 175:89– 98. Amsterdam.

- Neuweiler, F. & Reitner, J. 1992. Karbonatbänke mit *Lithocodium aggregatum* ELLIOT/ *Baccinella irregularis* RADOICIC. Palöobathymetrie, Palöoökologie und stratigraphisches Äquivalent zu thrombolithischen Mud Mounds. Berliner geowiss. Abh. E (3) : 273-293. Berlin.

- Neuweiler, F. & Reitner, J. 1995. Epifluorescence-microscopy of selected automicrites from lower Carnian Cipit-boulders of the Cassian Formation (Seeland Alpe, Dolomites). Facies 32: 26-28. Erlangen.

- Nicol, S. A. 1987. A down-slope Upper Triassic Reef Mound : Aflenz Limestone, Hochschwab Mountains, Northern Calcareous Alps. Facies 16 : 23-36. Erlangen.

- Nittel, P. 2006. Beiträge zur Stratographie und Mikropaläontologie der Mitteltrias der Innsbrucker Nordkette (Nördliche Kalkalpen, Austria). Geo. Alp. 3 : 93-145. Innsbruck.

- Nothdurft L.D.; Webb, G.E. & Kamber, B.S. 2004. Rare earth element geochemistry of Late Devonian reefal carbonates, Canning Basin, Western Australia: Confirmation of a seawater REE proxy in ancient limestones. Geochim Cosmochim Acta 68 (2): 263 – 283. Amsterdam.

- Nöth, L. 1929. Geologie des mittleren Cordevolgebietes zwischen Vallazza und Cencenighe (Dolomiten). Jg. Geol. Bundesanstalt 79: 129 – 202. Vienna.

Literature

- Nützel, A., Joachimski, M. & López Correa, M. 2009. Pronounced seasonal climatic fluctuations in the Late Triassic tropics - high-resolution oxygen isotope records from aragonitic bivalve shells (Cassian Formation, Northern Italy).- Palaeogeogr. Palaeoclimatol. Palaeoecol. 285, 194-204. Amsterdam.

- Ogilvie, M.M. 1893. Contributions to the Geology of Wengen and St. Cassian Strata in Southern Tyrol. Quart. J. Geol. Soc. London 49: 1-78. London.

- Ogilvie-Gordon, M.M. 1900 . On the fauna of the Upper Cassian Zone in Falzarego Valley. South Tyrol. Geol. Mag. N.S. (4) 7 : 337- 348. Cambridge.

- Ogilvie-Gordon, M.M. 1929. Geologie des Gebietes Von Piave (Buchenstein), St. Cassian und Cortina d´Ámpezzo . Jahrb. Geol. B-A. 79: 357 – 424. Vienna.

- Olivier, N. & Boyet, M. 2006. Rare earth and trace elements of microbialites in Upper Jurassic coral- and sponge-microbialite reefs. Chem. Geol. 230: 105 – 123. Amsterdam,

- Olivier, N., Pittet, B., Werner, W., Hantzpergue, P. & Gaillard, C. 2008. Facies distribution and coral-microbialite reef development on a low Energy carbonate ramp (Chay Peninsula, Kimmeridgian, western France). Sediment. Geol. 205: 14-33. Amsterdam.

- Olóriz, F., Reolid, M. & Rodríguez-Tovar, F.J. 2003. A Late Jurassic Carbonate ramp colonized by sponges and benthic microbial communities (External Prebetic, southern Spain). Palaios 18 : 528-545. Tulsa.

- Olóriz, F., Reolid, M., & Rodríguez-Tovar, F.J. 2006. Approaching trophic structure in Late Jurassic neritic shelves : A western Tethys example from Southern Iberia. Earth Sci. Rev. 79 : 101-139. Amsterdam.

- Páez, M., Zuniga, O., Valdés, J & Ortlieb, J. 2001. Foraminíferos bentónicos recientes en sedimentos micróxicos de la bahía Mejillones del Sur (23°S), Chile. Rev. Biol Mar. Oceanogr. 36(2) : 129-139. Valparaíso.

- Parrish, J.T. 1999. Pangaea und das Klima der Trias. *In* Hauschke, N. & Wilde, V. (eds). Die Trias : Eine ganz andere Welt. : 37-42. München.

- Payne, J.L., Lehrmann, D.J., Christensen, S., Wei, J & Knoll, A.H. 2006. Environmental and biological controls on the initiation and growth of a Middle Triassic (Anisian) reef complex on the great bank of Guizhou, Guizhou Province, China. Palaios 21 : 325-343. Tulsa.

- Peters, J.K. & Moldowan, J.M. The Biomarker Guide. Prentice Hall. 490 pp. Englewood Cliffs.

- Pia, J. 1937. Stratigraphie und Tektonik der Pragser Dolomiten in Südtirol. Self publishing. 248 pp. Vienna.

- Piepgras, D.J. & Jacobsen, S.B. 1992. The behavior of rare earth in seawater: precise determination of variations in the North Pacific water column. Geochim. Cosmochim. Acta. 56: 1851-1862. Amsterdam

- Pingitore, N.E. 1978. The behavior of Zn^{2+} and Mn^{2+} during carbonate diagenesis: theory and applications. J. Sediment. Petrol. 48: 799–814. Tulsa.

- Piros, O. & Preto, N. 2008. Dasycladacean algae distribution in ammonoid-bearing Middle Triassic platforms (Dolomites, Italy). Facies 54: 581-595. Berlin-Heidelberg.

- Prasada Rao, C. 1996. Modern Carbonates tropical temperate polar. Introduction to sedimentology and geochemistry. University of Tasmania Press. 206 pp. Howrah.

- Pratt, B.R. 1995. The origin, biota and evolution of deep-water mud mounds. *In* Monty, C.L.V., Bosence, D.W.J. , Bridges, P.D. & Pratt , B.R. (eds). Carbonate mud-mounds: their origin and evolution.. Int Assoc. Sedimentol. Spec. Publ 23: 49-123. Oxford.

- Rameil, N., Immenhauser, A., Warrlich, G., Hillgärtner, H. & Droste, H.J. 2010. Morphological patterns of Aptian *Lithocodium–Bacinella* geobodies: relation to environment and scale. Sedimentol. 57(3): 883-911. Oxford.

- Rech, H. 1998. Geobiologie der sogenannten „Cipit-Kalke" der Beckenfazies der Cassianer-Schcihten, S`St. Kassian, Dolomiten. Diplomarbeit am Institut für Geologie und Paläontologie der Georg-August Universität Göttingen. 136 pp. Göttingen.

- Reed, S.J.B. 1996. Electron Microprobe Analysis and Scanning Electron Microscopy in Geology. Cambridge University Press, 201 pp. Cambridge.

- Reif, W.-E. & Robinson, J.A. 1976. On functional morphology og the skeleton in lychnisc sponges (Porifera, Hexactinellida). Paläont. Z. 50 (1/2): 57-69. Stuttgart.

- Reitner, J. 1987a. A new calcitic sphinctozoan sponge belonging to the Demospongiae from the Cassian Formation (Lower Carnian; Dolomites, Northern Italy) and its phylogenetic relationship. Geobios, 20: 571-589. Lyon.

- Reitner, J. 1987b. Phylogenie und Konvergenzen bei rezenten und fossilen Calcarea (Porifera) mit einem kalkigen Basalskelett ("Inozoa", "Pharetronida"). Berliner geowiss Abh. A. 1987 (86): 87-125. Berlin.

- Reitner, J. 1987c. *Euzkadiella erenoenis* n.gen. n. sp. Ein Stromatopore mit spikulärem Skelett aus dem Oberapt von Ereno (Prov. Guipuzcoa, Nordspanien) und die systematische Stellung der Stromatoporen. Paläont. Z. 61 (3/4): 203-222. Stuttgart.

- Reitner, J. 1987d. Mikrofazielle, palöökologische und paläogeographische Analyse ausgewählter Vorkommen flachmariner Karbonate im Basko-kantabrischen Strike Slip Fault-Becken-System (Nordspanien) an der Wende von der Unterkreide zur Oberkreide. Documenta naturae 40: 1-239. München

- Reitner, J. 1989. Lower and Mid-Cretaceous coralline sponge communities of the Boreal and Tethyan realms in comparison with the modern ones- Palaeoecological and palaeogeographic implications. In Wiedmann, J. (ed). Cretaceous of the Western Tethys. Proceedings of the 3rd International Cretaceous Symposium, Tübingen 1987: 851 – 858. Stuttgart

- Reitner, J. 1990. Polyphyletic origin of the Sphinctozoans. *In:* Rützler, K. New perspectives in sponge biology 33-42. Smithsonian Institute Press. Washington.

- Reitner, J. 1992. "Coralline Spongien". Der Versuch einer phylogenetisch-taxonomischen Analyse. Berliner geowiss Abh. E (1): 1-352. Berlin.

- Reitner, J. 1993. Modern cryptic mivrobialite/metazoan facies from lizard Island (Great Barrier Reef, Australia). Formation and concepts. Facies 29: 3-40. Erlangen.

Literature

- Reitner, J. & Engeser, T. 1983. Contributions to the systematics and the paleoecology of the Family Acanthochaetetidae FISCHER, 1970 (Order Tabulospongida, class Sclerospongiae, Geobios 16 : 773–779. Lyon.

- Reitner, J. & Engeser, T. 1985. Revision der Demospongien mit einem thalamiden, aragonitischen Basalskelett. Berliner geowiss. Abh. A 60: 151 – 193. Berlin

- Reitner, J. & Engeser, T. 1989a: *Chaetosclera klipsteini* n. gen. n. sp. (Halichondria, Demospongiae) aus dem Unterkarn der Cassianer-Schichten (Dolomiten, Italien). Mitt Geol. Palaeont. Inst. Univ. Hamburg 68: 159-165. Hamburg., Nordspanien). Mitt. Geol.-Paläont. Inst. Univ. Hamburg. 167-177. Hamburg.

- Reitner, J. & Engeser, T. 1989b. Coralline Demospongiae (Porifera) aus dem Campan von Pobla de Segur (Pyrenäen). Mitt. Geol.-Paläont. Inst. Univ. Hamburg. 68: 167-177. Hamburg.

- Reitner, J. & Gautret, P. 1996. Skeletal formation in the modern but ultraconservative chaetetid sponge *Spirastrella* (*Acanthochaetetes*) *wellsi* (Demospongiae, Porifera). Facies 34: 193-208. Erlangen.

- Reitner, J. & Schlagintweit, F. 1990. *Calcicuberites stromatoporoides* n. gen. n. sp., ein neues Taxon der Hadromerida (Demospongiae, Porifera) mit einem kalkigen Basalskelett aus der tethyalen Unterkreide. Berliner. geowiss. Abh A 124: 247 – 257. Berlin.

- Reitner, J. & Schumann.Kindel, G. 1997. Pyrite in mineralized sponge tissue- Product of sulphate reducing related bacteria?. *In* Neuweiler, F., Reitner, J & Monty, C. (eds): Biosedimentology of microbial build-ups. IGCP Project. No. 380. Proceedings of 2nd Meeting, Göttingen/Germany 1996. Facies 36: 272 - 276. Erlangen.

- Reitner, J. & Keupp, H. 1989. Basalskelette bei Schwämmen - Beispiel einer polyphyletischen Entwicklung. Die Geowissenschaften, 7 (3): 71-78. Weinheim.

- Reitner, J. & Keupp, H. 1991. The fossil record of the haplosclerid excavating sponge *Aka* de Laubenfels. In Reitner,J. & Keupp, H.(eds.) Fossil and Recent Sponges: 102-120. Springer. Berlin-New York-Heidelberg .

- Reitner, J. & Neuweiler, F.1995. Mud Mounds: A polygenetic spectrum of fine-grained carbonate buildups. Facies 32: 1-70. Erlangen.

- Reitner, J., Wilmsen, M., & Neuweiler, F. 1995. Cenomanian/Turonian sponge microbialite deep-water hardground community (Liencres, Northern Spain). Facies 32: 203-212. Erlangen.

- Reitner, J., Wörheide, G., Lange, R & Schumann-Kindel, G. 2001. Coralline demosponges: a geobiological portrait. Bull. Ohoku Univ. Museum 1: 219-235. Sendai.

- Reolid, M., Molina, J.M., Löser, H., Navarro, V. & Ruiz-Ortiz, P.A. 2009. Coral biostromes of the Middle Jurassic from the Subbetic (Betic Cordillera, southern Spain): facies, coral taxonomy, taphonomy and palaeoecology. Facies 55: 575 – 593. Berlin-Heidelberg.

- Richoz, S., Krystyn, L. & Spötl, C. 2007. First detailed carbon isotope through the Ladinian-Carnian boundary: The Weissenabch section (Austria). Albertiana 36: 98-101. Utrecht.

- Riding, R. 1975. *Girvanella* and other algae as depth indicators. Lethaia 8: 173-179. Oslo.

- Riding, R. 2000. Microbial carbonates: the geological record of calcified bacterial-algal mats and biofilms. Sedimentology 47: 179-214. Oxford.

- Riding, R. 2002. Structure and composition of organic reefs and carbonate mud mounds: concepts and categories. Earth Sci Rev 58: 163–231. Amsterdam.

- Riding, R. & Guo, L. 1992. Affinity of *Tubiphytes*. Palaeontology 35. 37–49. London.

- Riedel, P. 1988. Facies and development of the "Wilde Kirche" reef complex (Rhaetian, Upper Triassic, Karwendelgebirge, Austria). Facies 18: 205-218. Erlangen.

- Riedl, R., 1966. Biologie der Meereshöhlen. Paul Parey 636 pp. Hamburg & Berlin

- Robbins, I.J., Warren, L.M., Bestwick, B.W. & Rusin, J. 1987. Functional anaerobiosis in the polychaete *Terebella lapidaria* L. Comp. Biochem. Physiol 87A (1): 171-174. Oxford.

- Roehmer, M., Bouvier-Nave, P., & Ourisson, G. 1984. Distrubution of hopanoid triterpenes in Procaryotes. J. Gen. Microbiol 1: 255-271. Reading.

- Romanek, C.S., Grossman, E.L. & Morse, J.W. 1992. Carbon isotope fractionation in synthetic aragonite and calcite: Effects of temperature and precipitation rate. Geochim. Cosmochim. Acta 56: 4319-4325. Amsterdam.

- Rosenheim, B.E., Swart, P.K., Thorrold, S.R., Willenz, P., Berry, L. & Latkoczy, C. 2004. High-resolution Sr/Ca records in sclerosponges calibrated to temperature in situ. Geology 32 (2): 145-148. Boulder.

- Rosenheim, B.E., Swart, P.K., & Willenz, P. 2009. Calibration of sclerosponge oxygen isotope records using high-resolution $\delta^{18}O$ data. Geochim. Cosmochim. Acta 73: 5308-5319. Amsterdam.

- Round, F. E. 1981. The Ecology of Algae. Cambridge University Press. 653 pp. Cambridge.

- Russo, F. 1981. Nuove spugne calcaree triassiche di Campo. (Cortina dÁmpezzo, Belluno). Boll. Soc. Paleont. Ital. 20 (1/3): 3-17. Modena.

- Russo, F. 2005. Biofacies evolution in the Triassic platforms of the Dolomites, Italy. Ann. Univ. Stud. Ferrara. Mus. Sci. Nat. vol. Spec. 2005: 33 – 45. Ferrara.

- Russo, F., Mastandrea, A., Stefani, M. & Neri, C. 2000 Carbonate facies dominated by syndepositional cements: a key component of Middle Triassic platforms. The Marmolada case history (Dolomites, Italy). Facies 42: 211- 226. Erlangen.

- Russo, F., Neri, C., Mastandrea, A. & Baracca, A. 1997. The Mud Mound Nature of the Cassian Platform Margins of the Dolomites. A Case History: the Cipit Boulders from Punta Grohmann (Sasso Piatto Massif, Northern Italy). Facies 36: 25 -36. Erlangen.

- Russo, F., Neri, C., Mastandrea, A. & Laghi, G. 1991. Depositional and diagenetic history of the Alpe di Specie (Seelandalpe) fauna (Carnian, Northeastern Dolomites) Facies 25: 187 – 210. Erlangen.

- Rüffer, T. & Zamparelli, V. 1997. Facies and biota of Anisian to Carnian carbonate platforms in the Northern Calcareous Alps (Tyrol and Bavaria). Facies 37: 115-136. Erlangen.

Literature

- Saitou,N., & Nei, M. 1987. The neighbor-joining method: a new method for reconstructing phylogenetic trees. Mol Biol Evol. 4: 406-425. Oxford.

- Salomon, W. 1895. Geologische und palaeontlogische Studien über die Marmolata. Palaeontographica 42: 1-210. Stuttgart.

- Sánchez Beristain, J.F. & Reitner, J. 2008. Association diversity among sponge boundstones from the Lower Carnian Cassian Formation (Dolomites, Northern Italy). Erlanger Geologische Abhandlungen. Sonderband 6- Jahrestagung der Paläontologischen Gesellschaft: 54. Erlangen.

- Sánchez Beristain, J.F. , Schäfer, N., Simon, K. & Reitner, J. (accepted in Lecture Notes for Earth Sciences). New methods to characterize the microbialites from the St. Cassian Formation, Dolomites, Northeastern Italy. 18 pp.

- Sandberg, P.A. 1983. An oscillating trend in Phanerozoic non-skeletal carbonate mineralogy. Nature 305 : 19-22. London.

- Schäfer, P. 1979. Fazielle Entwicklung und palökologische Zonierung zweier obertriadischer Riffstrukturen in den Nördlichen Kalkalpen („Oberrhät"-Riff-Kalke, Salzburg). Facies 1: 3-245. Erlangen.

- Schäfer, P. & Senowbari-Daryan, B. 1982. The Upper Triassic Pantokrator Limestone of Hydra (Greece): An example of a prograding reef complex. Facies 6: 147-164: Erlangen.

- Schäfer, N. 2006. Ni-Anomalien in Cold-Seep Karbonaten aus dem nordwestlichen Schwarzen Meer. Ist Ni ein kritisches Element bei der anaeroben Oxidation von Methan? University of Göttingen. Diploma Thesis. 81 pp. Göttingen.

- Schäfer, P. & Fois, E. 1987. Systematics and evolution of Triassic Bryozoa. Geol. Palaeont. 21: 173-225. Marburg.

- Scherer, M. 1976. Diagenese aragonitischer Fossilien (Hexakorallen und Kalkschwämme) der Cassianer Schichten, Karn. Zentralbl. Geol Paläontol. II: 365-368. Stuttgart

- Scherer, M. 1977. Preservation, alteration and multiple cementation of aragonitic skeletons from the Cassian Beds (U.Triassic, Southern Alps): Petrographic and geochemical evidence. N.Jb.Geol. Paläont. Abh. 154 (2): 213-262. Stuttgart.

- Schlagintweit, F. & Gawlick, H.-J. 2008. The occurerence and role of the microencrusterframeworks in Late Jurassic to Early Cretaceous platform margin deposits of the Northern Calcareous Alps (Austria). Facies 54: 207-231. Berlin-Heidelberg.

- Schlagintweit, F. & Gawlick, H.-J. 2009. Enigmatic tubes associated with microbial crusts from the Late Jurassic of the Northern Calcareous Alps (Austria): a mutualistic sponge-epibiont consortium?.Lethaia: 42: 452–461. Oslo.

- Schmid, D.U. 1996. Marine mikrobolithe und mikroinkrustierer aus dem Oberjura. Profil 9: 101-251. Stuttgart.

- Schumacher, H. & Plewka, M. 1981. Mechanical resistance of reefbuilders through time. Oecologia 49: 279-282. Berlin-Heidelberg.

- Schumann-Kindel, G., Bergbauer, M., Manz, W., Szewzyk, U & Reitner, J. 1997. Aerobic and anaerobic microorganisms in modern sponges: A possible relationship to fossilization

processes. *In* Neuweiler, F., Reitner, J & Monty, C. (eds): Biosedimentology of microbial build-ups. IGCP Project. No. 380. Proceedings of 2nd Meeting, Göttingen/Germany 1996. Facies 36: 268-272. Erlangen.

- Senowbari-Daryan, B. 1980. Fazielle und paläontologische Untersuchungen in oberrhätischen Riffen (Feichtenstein- und Gruberriff bei Hintersee, Salzburg, Nördliche Kalkalpen) Facies 3: 1-237. Erlangen.

- Senowbari-Daryan, B. 1990. Die systematische Stellung der thalamiden Schwämme und ihre Bedeutung in der Erdgeschichte. - Münchner Geowiss. Abh. 21: 1-326. München.

- Senowbari-Daryan, B., Bucur, I.I., Schlagintweit, F., Sasaran, E & Matyszkiewicz. J. 2008. *Crescentiella*, a new name for „*Tubiphytes*" *morronensis* CRESCENTI, 1969: an enigmatic Jurassic-Cretaceous microfossil. Geol. Croatica 61 (2/3): 185-214. Zagreb.

- Senowbari-Daryan, B., Caruthers, A.H. & Stanley, G.D.Jr. 2008. The first Upper Triassic silicified hypercalcified sponges from the Alexander Terrane, Gravina Island and Keku Strait, Southeast Alaska. J. Paleont. 82(2): 344-350. Tulsa.

- Senowbari-Daryan, B., Schäfer, P. & Abate, B. 1983. Obertriadische Riffe und Rifforganismen in Sizilien (Beiträge zur Paläontologie und Mikrofazies obertriadischer Riffe im alpin-mediterranen Raum, 27). Facies 6: 165-184. Erlangen.

- Sellwood, B.W. & Valdes, P.J.2006. Mesozoic climates. General circulation models and rock record. Sediment. Geol. 190: 269-287. Amsterdam.

- Shapiro, R.S. 2004. Neoproterozoic-Cambrian microbialite Record. Paleontol. Soc. Paper 10: 5-15. Tulsa.

- Shen, J.-W. & Qing, H. 2008. Calcimicrobes, microbial fabrics, and algae in Mississippian Midale Beds, Midale and Glen Ewen pools, Williston Basin, Southeastern Saskatchewan. Saskatchewan Geol. Surv. Summary of Investigations 1:10. Regina.

- Sheppard, C.R.C, Davy, S.K. Pilling, G.M. 2009. The biology of coral reefs. 352 pp. Oxford

- Shiraishi, F. & Kano, A. 2004. Composition and spatial distribution of microencrusters and microbial crusts in upper Jurassic-lowermost Cretaceous reef limestone (Torinosu Limestone, Southwest Japan). Facies 50: 217-227. Erlangen.

- Simms, M.J. & Ruffel, A.H. 1989. Sinchoreneity of climatic change and extinctions in the late Triassic. Geology 17: 265-268.. Geology 17: 784-787. Boulder.

- Simpson, E.H. 1949. Measurement of Diversity. Nature 163: 688. London.

- Smith, A. M. 1995. Palaeoenvironmental interpretation using bryozoans: A review. In Bosence, D.W.J. & Allison, P.A.(eds). Marine Palaeoenvironmental Analysis from Fossils. Geol. Soc. London Spec. Pub. 83:231–243. London.

- Sneath, P.H. 1957. Computers in taxonomy. J Gen.Microbiol 17: 201-226. Reading.

Literature

- Sokal, R. R. & Sneath P. H. A. 1963. Principles of Numerical Taxonomy. 573 pp. W. H. Freeman, San Francisco.

- Sokal, R. R., & Rohlf, F. J. 1970. The intelligent ignoramus, an experiment in numerical taxonomy. Taxon 19: 305-319. Vienna.

- Stanley, G.D. Jr. 1994. Upper Triassic spongiomorph and coral association dredged off the northwestern Australian shelf. J. Australian Geol Geophys 15 (1): 127-133. Canberra.

- Stanley, G.D. Jr. & Flügel, E. 1987. Paleoecology of Upper Triassic Reefs in the Northern Calcareous Alps: Reef communities. Facies 16: 157-186. Erlangen.

- Stanley, G.D. Jr. & Swart, P. 1995. Evolution of the coral-zooxanthellate symbiosis during the Triassic: A geochemical approach. Paleobiology 21: 179-199. Tulsa.

- Stanley, G.D. Jr. & Whalen, M-T- 1989. Triassic corals and spongiomorphs from hells Canyon, Wallowa Terrane, Oregon. J.Paleont. 63: 800-819. Tulsa.

- Steinmann, G. 1882. Pharetronen-Studien N. Jb. Geol. Paläont 2: 139 – 191. Stuttgart.

- Stokes, G.G. 1852. On the change of refrangibility of light. Phil. Trans. R. Soc. London.142: 463-562. London.

- Stur, D. 1868 Eine Exkursion in die Umgebung von St. Cassian. Jahrb. k.-k. geol. Reichanstalt 18: 529-568. Vienna.

- Swart, P.K., Rubesntone, J.L., Charles, C. & Reitner, J. 1998. Sclerosponges. A new proxy indicator of climate. Report from the workshop on the use of sclerosponges as proxy indicators of climate. March 22-24, 1998. 20 pp. Miami.

- Tanaka, K. 2002. Growth dynamics and mortality of the intertidal encrusting sponge *Halichondria okadai* (Demospongiae, Halichondrida). Mar. Biol. 140 (2): 383-389. Berlin-Heidelberg.

- Tanner, L. 2010. The Triassic isotope record. Geol. Soc. London Spec. Pub. 334: 103-118. London.

- Tarutani, T., Clayton, R.N. & Mayeda, T.K. 1969. The effect of polymorphism and magnesium substitution on oxygen isotope fractionation between calcium carbonate and water. Geochim. Cosmochim. Acta 33: 987-996. Belfast.

- Thiel, V. 1997. Organische Verbindungen in Porifera und biogenen Carbonaten- Fazies, Chemotaxonomie und molekulare Fossilien. Ph.D. Thesis, University of Hamburg. 145 pp. Hamburg.

- Townsend, C.R., Begon, M. & Harper, J.L. 2008. Essentials of ecology. 3rd edition. Wiley-Blackwell. 532 pp. New York.

- Tucker, M.D., Barton, L.L & Thomson, B.M .1997. Reduction and immobilization of molybdenum by *Desulfovibrio desulfuricans*, J. Environ. Qual. 26: 1146 – 1152. Madison.

- Tucker, M. E.1996. Sedimentary Petrology. 260 pp. Blackwell Science. Oxford.

- Turnsek, D. & Senowbari-Daryan, B. 1994. Upper Triassic (Carnian-Lowermost Norian) corals from the Pantokrator Limestone of Hydra (Greece). Abh. Geol. B.-A. 50: 477-507. Vienna.

- Turón, X., Tarjuelo, I & Uriz, M.J. 1998. Growth dynamics and mortality of the encrusting sponge *Crambe crambe* (Poecilosclerida) in contrastinmg habitats: correlation with population structure and investment in defence. Funct. Ecol 12: 631-639. Oxford.

- Tway, L. 1979. Pennsylvanian ichthyoliths from the Shawnee Group of Eastern Kansas. Univ Kansas Paleont. Contr. 96: 1-24. Lawrence.

- Ulrichs, M. 1974. Zur St ratigraphie und Ammonitenfauna der Cassianer Schichten von Cassian (Dolomiten/Italien). Österr. Akad. Wiss. Schriftenr. Erdwiss. Komm. 2: 207-222. Vienna.

- Valduga, A. 1962. Osservazioni stratigrafico-paleontologiche sui rapporti fra la seria Raibliana dello Sciliar e i „Tufi a Pachicardie" dell'Alpe di Suisi. Atti. Istit. Veneto Sci. Lett. Arti, Cl. Sci.mat.-natur. 120: 165-189. Venice.

- Van Guzel, P. 1979. Manual of the techniques and some geological applications of fluorescence microscopy. Am. Assoc. Strat. Palynologists. 55 pp. Dallas.

- Van Houten, L. 1930 . Geologie des Pelmo-Gebietes in den Dolomiten von Cadore. Jb. Geol. Bundesanstalt 80: 147 -230. Vienna.

- Van Kranendonk, M.,Webb, G. & Kamber, B.S. 2003. New geological and trace element evidence from 3.45 Ga stromatolitic carbonates in the Pilbara Craton: support of a marine, biogenic origin and for a reducing Archaean ocean. Geobiology 1: 91 – 108. New York.

- Veevers, J.J. 1989. Middle/Late Triassic (230+-5 Ma) singularity in the stratigfrahic and magmatic history of the pangean heat anomaly. Geology 17(9): 784-787. Boulder.

- Veizer, J. & Wendt, J. 1976. Mineralogy and chemical composition of Recent and fossil skeletons of calcareous sponges. N. Jb. Geol. Paläont. Mh. 1976 (9). 558 – 573. Sttutgart.

- Veizer, J. 1983. Chemical diagenesis of carbonates. Theory and application of trace element technique. *In:* Arthur, M.A., Anderson, T.F., Kaplan, I.R., Veizer, J. & Land, L.S. (eds): Stable isotopes in sedimentary geology. SEPM Short Courses 10: 1-100. Tulsa.

- Veizer, J., Ala, D., Azmy, K., Bruckschen, P., Buhl, D., Bruhn, F., Carden, G.A.F., Diener, A., Ebneth, S., Godderis, Y., Jasper, T., Korte, C., Pawellek, F., Podlaha,O.G & Strauss, H. 1999. $^{87}Sr/^{86}Sr$, $\delta^{13}C$ and $\delta^{18}O$ evolution of Phanerozoic seawater. Chem. Geol. 161: 59-88. Amsterdam.

- Vergés, A., Utgé, J.M. & Rodríguez-Prieto, C. 2004. Life histories of *Predaea ollivieri* and *P. pusilla* (Nematostomatales, Rhodophyta). Eur. J. Phycol 39: 411-421. London.

- Von Buch, L. 1822. Ueber Dolomit als Gebirgsart. Abh. Kgl. Akad. Wiss. Berlin: 83-136. Berlin

Literature

- Von Hauer, F. 1858. Erläuterungen zu einer geologischen Übersichtskarte der Schictgebirge der Lombardei, Jahrb. K.-K. Geol. Reichsanst. 9: 445–496.Vienna.

- Von Mojsisovics, E. 1874. Die Faunengebiete und Faciesgebiete der Triasperiode in den Ostalpen. Jb. k.k. geol. Reichanst. 24: 81-134. Vienna.

- Von Mojsisovics, E. 1875. Über die Ausdehnung und die Structur der südtirolischer Dolomitstöcke. Sitzungsber. k.k. Akad. Wiss. Wien,, math-naturwiss. Kl. 71: 719 – 736. Vienna.

- Von Mojsisovics, E. 1879. Die Dolomit-Riffe von Südtirol und Venetien. Beiträge zur Bildungsgeschichte der Alpen. Alfred Hölder. 552 pp. Vienna.

- Von Richthofen, F. 1860. Geognostische Beschreibung der Umgegend von Pedrazzo, St. Cassian und der Seiser Alpe in Südtirol. 327 pp. Gotha.

- Wang, Y., Tong, J., Wang, J. & Zhou, X. 2005. Calcimicrobialite after end-Permian mass extinction in South China and ist paleoenvironmental significance. Chin. Sci. Bull 50 (7): 665-671. Beijing.

- Ward, J.H. Jr. 1963. Hierarchical Grouping to optimize an objective function. J. Am. Stat. Assoc. 58 (301): 236-244. Alexandria.

- Webb, G. 1996. Was Phanerozoic reef history controlled by the distribution of non-enzymatically secreted reef carbonates (microbial carbonate and biologically induced cement)? Sedimentology. 43: 947-971. New York.

- Webb, G. & Kamber, B.S 2000. Rare earth elements in Holocene reefal microbialites: A new shallow seawater proxy. Geochim. Cosmochim. Acta 64 (9): 1557 – 1565. Amsterdam.
- Wedepohl K.H. 1995. The composition of the continental crust. Geochim. Cosmochim. Acta 59 (7): 1219 – 1232. Amsterdam.

- Weidlich, O. & Benecker, M. 2007. Differential severity of Permian-Triassic environmental changes on Tethyan shallow-water carbonate plaftorms. Glob. Planet. Ch. 55: 209-235. Amsterdam.

- Wendt, J. 1974. Der Skelettbau aragonitischer Kalkschwämme aus der alpinen Obertrias. - N. Jb. Geol. Paläont. Mh., 8: 498-511; Stuttgart

- Wendt, J. 1975. Aragonitische Stromatoporen aus der alpinen Obertrias- N. Jb. Geol. Paläont. Abh. 150 (1): 111-125. Stuttgart.

- Wendt, J. 1976. Der Skelettbau mesozoischer und rezenter Kalkswchämme. *In* Seilacher,A. (ed.) Palökologie: Lagerstätten, Diagenese, Konstruktionsmorphologie, Vergesselschaftungen. Bericht 1970 – 1975. Zentralbl. Geol Paläontol. II: 321-325. Stuttgart

- Wendt, J. 1979. Development of skeletal formation, microstructure, and mineralogy of rigid calcareous sponges from the Late Palaeozoic to Recent. Coll. Inter. CNRS. Paris 291: 449-475- Paris.

- Wendt, J. 1982. The Cassian Patch Reefs (Lower Carnian,. Southern Alps). Facies 6: 185-202. Erlangen

- Wendt, J. 1984 Skeletal and spicular mineralogy, microstructure and diagenesis of coralline calcareous sponges. Paleont. Americana 54: 326 – 336. Ithaca.

- Wendt, J. & Fürsich,F.T. 1980. Facies analysis and paleogeography of the Cassian Formation,Triassic, Southern Alps. Riv. Ital. Paleont. Strat 85 (3/4): 1003- 1028. Milan.

- Wendt, J., Xichun, W. & Reinhardt, J.W. 1989. Deep-water hexactinellid sponge mounds from the Upper Triassic of northern Sichuan (China). Paleogeogr. Paleoclimatol. Paleoecol. 76: 17-29. Amsterdam.

- Wiedner, E.A. 2004. Laborexperimente zur kinetischen Fraktionierung stabiler Isotope bei der Sinterbildung. Ph.D. Thesis. University of Heidelberg. 94. pp. Heidelberg

- Wilkinson, C.R., Garrone, R. & Vacelet, J. 1984. Marine sponges discriminate between food bacteria and bacterial symbionts: electron microscope radioautography and *in situ* evidence. Proc. Roy.Soc. London B220: 519-528. London.

- Willenz, P. & Hartman, W.D. 1999. Growth and regeneration rates of the calcareous skeleton of the Caribbean coralline sponge *Ceratoporella nicholsoni*: a long term survey. Mem. Queensl. Mus. 44: 675-685. Brisbane.

- Wissmann, H.L. & Münster, G. 1841. Beiträge zur Geognosie und Petrefacten-Kunde des südöstlichen Tirols vorzüglich der Schichten von St. Cassian. Beitr. Petrefactenk. 4: 1-152. Bayreuth.

- Wolf, K.H. 1965. Gradational sedimentary products of calcareous algae. Sedimentology. 5: 1-37. Oxford.

- Wood, R. A. 1999. Reef evolution. Oxford University Press. 414 pp. Oxford.

- Wörheide, G. 1997. The reef cave dwelling ultraconservative demosponge *Astrosclera willeyana* Lister 1900 from the Indo-Pacific. University of Göttingen Ph.D. Thesis pp 1-78. Göttingen.

- Wulff, J. 2010. Regeneration of spongs in ecological context: Is regeneration an integral part of life history and morphological strategies? Integr. Comp. Biol. Advance Access published online on August 17, 2010*: 1-12.

- Wurm, D. 1982. Mikrofazies, Paläontologie und Palökologie der Dachsteinriffkalke (Nor) des Gosaukammes, Österreich, Facies 6 : 203–296. Erlangen.

- Yancey, T.E. & Stanley, G.D. Jr. 1999. Giant alatoform Bivalves in the Upper Triassic of Western North America. Palaeont 42 (1): 1-23. London.

- Yancey, T.E., Stanley, G.D. Jr & Piller, W.E. & Woods, M.A. 2005. Biogeography of the Late Triassic wallowaconchid megalodontid bivalves. Lethaia 38: 351-365. Oslo.

- Yarnell, J.M. 2000. Paleontology of two North American Triassic reef faunas: Implications for terrane paleogeography. University of Montana, M.Sc. Thesis. 137 pp. Missoula.

- Yoshioka, H., Asahara,Y., Tojo, B. & Kamakami, S. 2003. Systematic variations in C, O and Sr isotopes and elemental concentrations in Neoproterozoic carbonates in Namibia:

implications for a glacial and interglacial transition. Precambrian Res. 124: 69-85. Amsterdam.

- Zankl, H. 1993. The origin of High-Mg-Calcite microbialites in cryptic habitats of Caribbean Coral Reefs – their dependence on light and turbulence. Facies 29: 55 – 60. Erlangen.

- Zar, J.H. 2009. Biostatistical Analysis. Prentice Hall. 960 pp. Upper Saddle River.

- Zeebe, R.E. 1999. An explanation of the effect of seawater carbonate concentration on foraminiferal oxagen isotopes. Geochim. Cosmochim. Acta 63: 2001-2007. Amsterdam.

- Zittel, K.A. 1879. Studien über fossile Spongien. Teil 3: Bayer. Akad. Wiss. Math.-naturwiss. Cl. Abh. 13: 91-138. Munich.

Plates I - XX

Appendix

Plate I

Dendronella – Hexactinellida association

1.- The alga *Dendronella articulata.* Scale bar = 2mm.

2.- Serpulid worm tubes between the branches of *D. articulata.* Scale bar = 500 μm.

3.- *Plexoramea cerebriformis* , a microproblematicum to be found within *D.articulata*. Scale bar = 500 μm.

4.- *Tubiphytes* sp. , a common microproblematicum in the Cipit Boulders. Note automicritic deposits within the branches of *Dendronella.* Scale bar = 500 μm.

5.- *Ladinella porata* (arrow), associated to *D. articulata.* Scale bar = 500 μm.

6.- The bryozoan *Reptonoditrypa cautica* in longitudinal section. Scale bar = 500 μm.

7.- *R. cautica* encrustation atop a brachiopod? Bioclast. Scale bar = 500 μm.

8.- *Atrochaetetes* cf. *medius* encrusted by an association of *Tubiphytes* (arrow) and a nubecularid foraminifer amidst automicrite. Scale bar = 5 mm.

Plate I
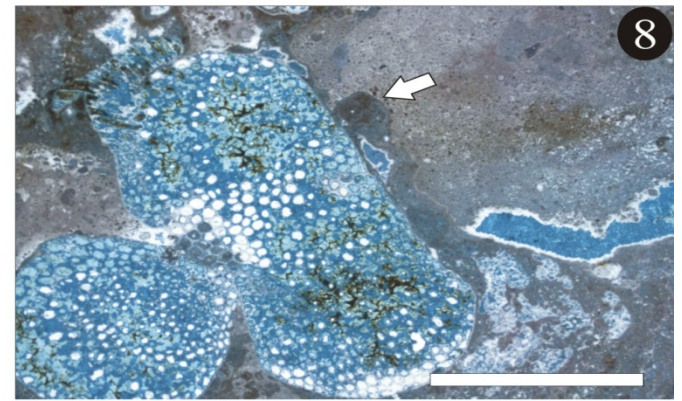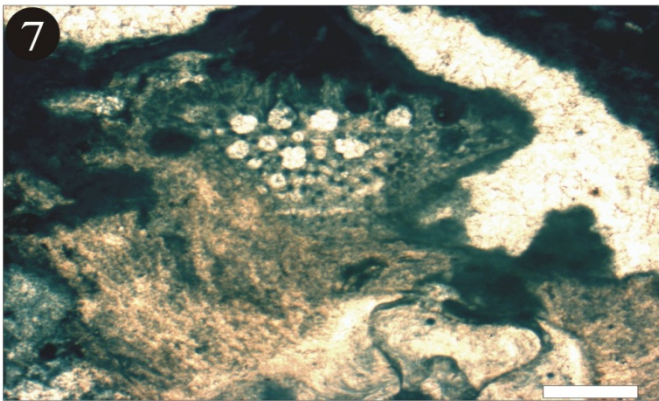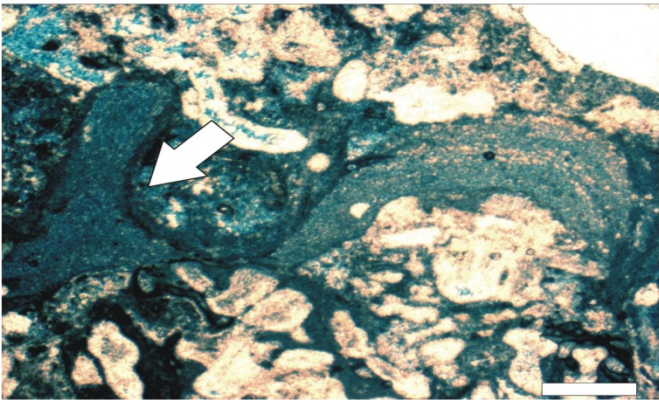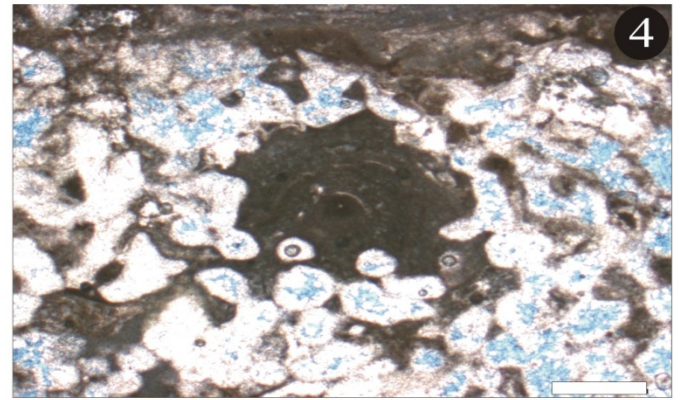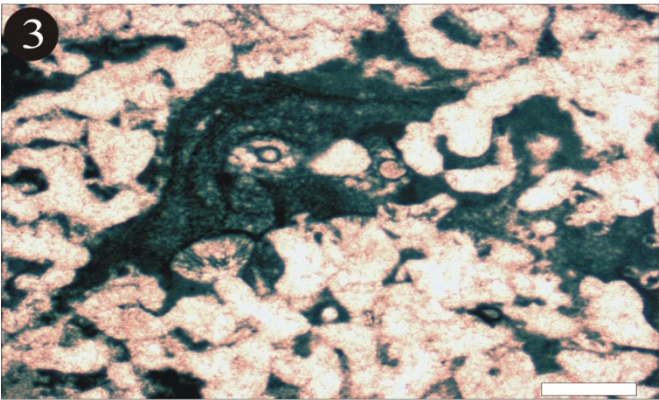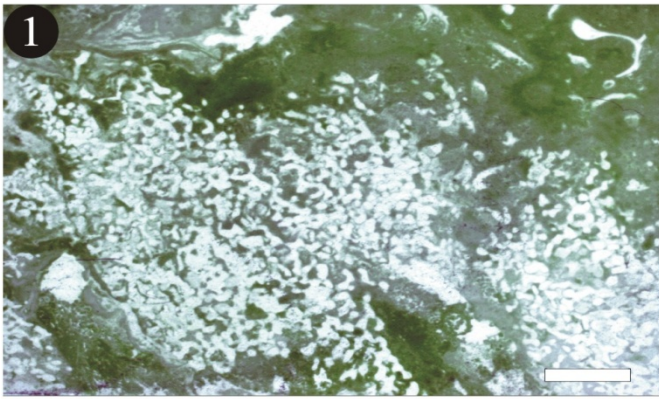
Plate II

Dendronella – Hexactinellida association

1.- *Petrosistroma stearni*. Arrow points to a boring of unknown origin, filled with auto?micritic deposits. Scale bar = 5 mm.

2.- Recrystallized bivalve shell (arrow) fallen into a sponge mummy. Scale bar = 5 mm.

3.- Detail on the hexactines from 2. Scale bar = 500 μm.

4.- Another bivalve shell associated to this hexactinellid-algal community. Scale bar = 500 μm.

5. Epifluorescence view of 2. Note the intensity of the emitted light near the bivalve. Scale bar = 500 μm.

6.- *Microtubus communis* (white arrow) and *Terebella cf. lapilloides* (black arrow) dwelling on automicrite substrate. Scale bar = 2 mm.

7.- *Tubiphytes obscurus* (arrow) encrusted in automicritic deposits. Scale bar = 2 mm.

8.- Enlargement of 7. Scale bar = 500 μm.
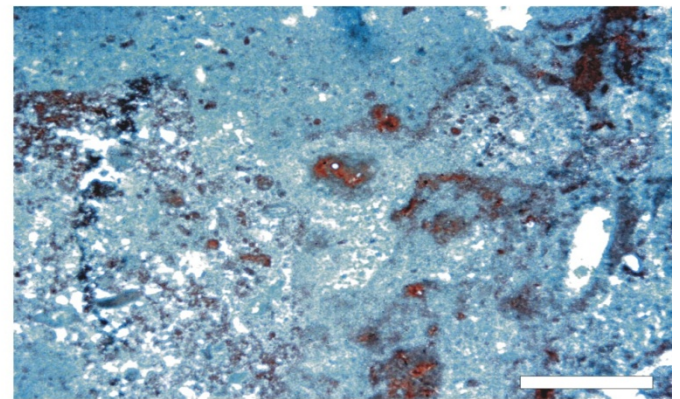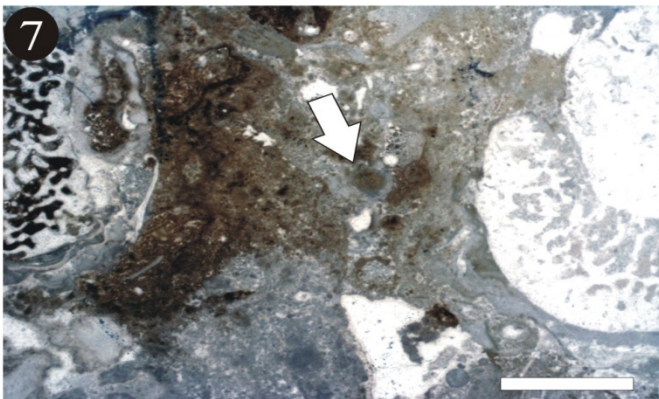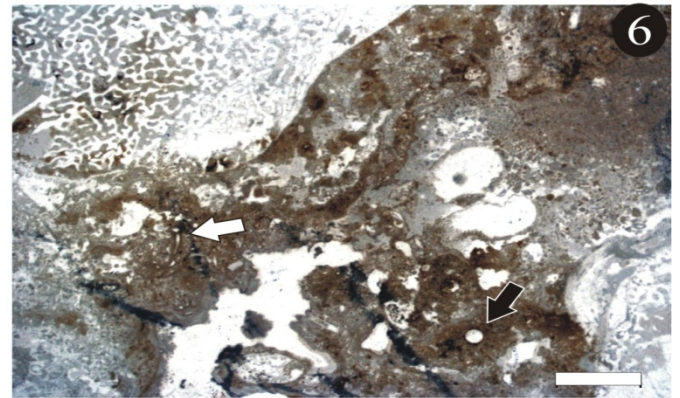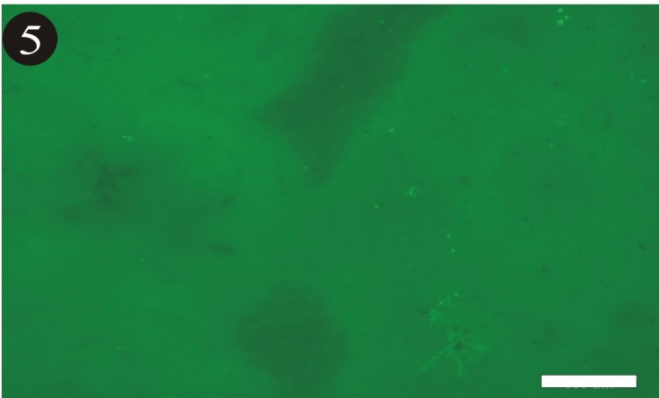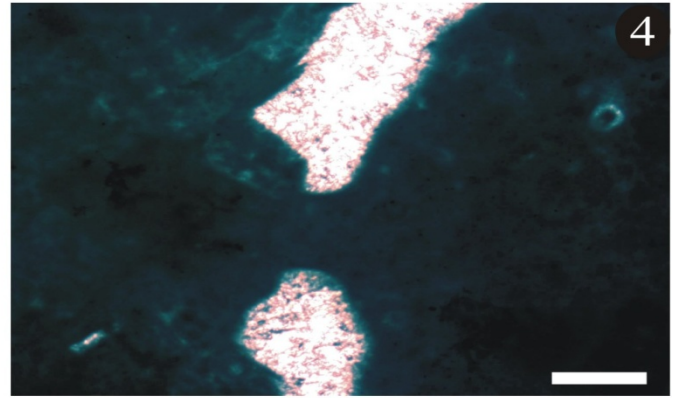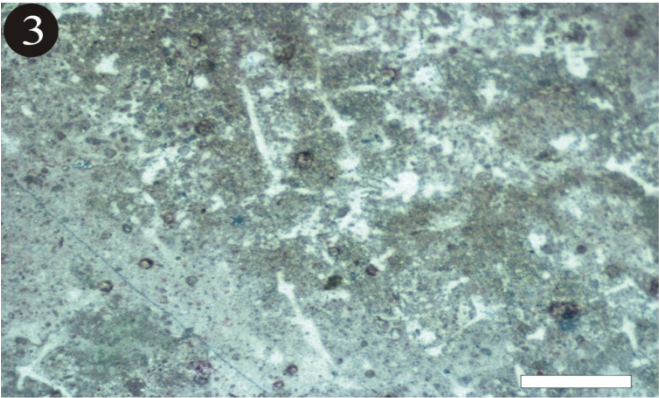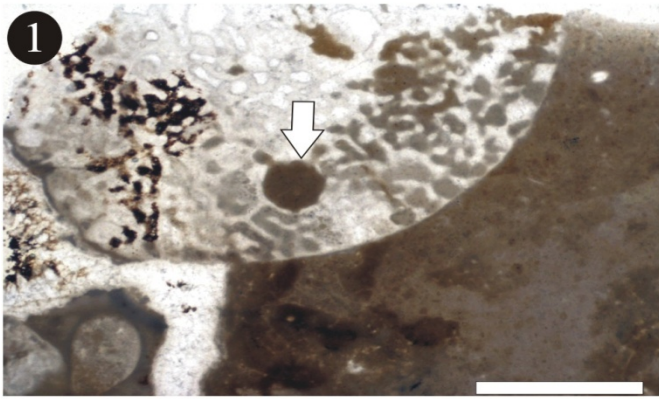
Plate II

Plate III

Dendronella – Hexactinellida association (Fig. 1-6)

Ceratoporella breviacanthostyla – Tubiphytes association (Figs. 7-8)

1.- Detail of Pl. I, Fig. 8, showing the *Tubiphytes* – nubecullarid association atop *Atrochaetetes* (white arrow) and *Terebella cf. lapilloides* (black arrow). Scale bar = 2 mm.

2.- Enlargement of 1, displaying in detail the association of *Tubiphytes* and the nubecullarid foraminifer growing on its micritic envelope (arrow). Scale bar = 500 μm.

3.- *Terebella cf. lapilloides.* Note spicule pseudomorphs (probably oxeae) being agglutinated in the wall (arrows). Scale bar = 500 μm.

4.- Thalamide encrusting sponge (arrow) conferred to *Uvanella irregularis*. Scale bar = 500 μm.

5. Uniseriate foraminifer within allochthonous detritus. Scale bar = 100 μm.

6.- Stromatactis cavity with 5 cement generations (white arrows), the last being baroque dolomite. Note *Terebella cf. lapilloides* (black arrows) dwelling on microbialitic crusts atop *Atrochaetetes* . Scale bar = 2 mm.

7.- Thecideid brachiopod (center) growing on a specimen of *Colospongia* sp (below, left). *Ceratoporella breviacanthostyla* encrusts the top of the sequence (above). Scale bar = 1.5 mm.

8.- *C. breviacanthostyla* encrustation on a stromatoporoid. Scale bar = 2 mm.

Plate III
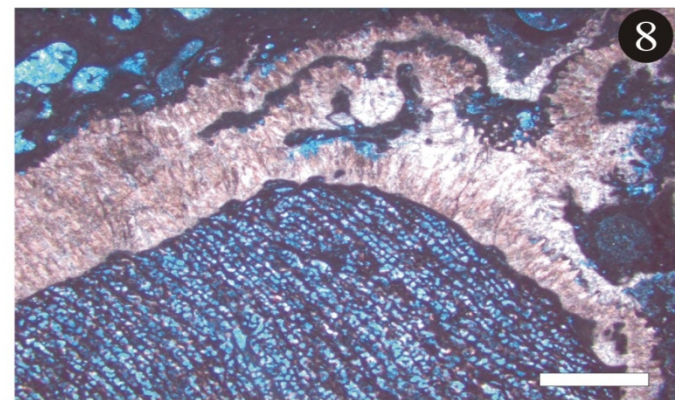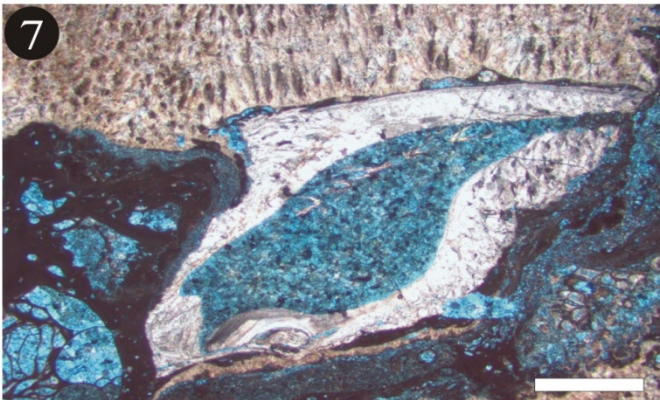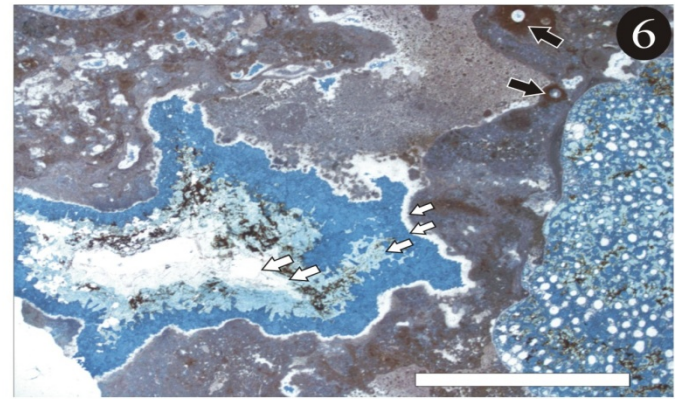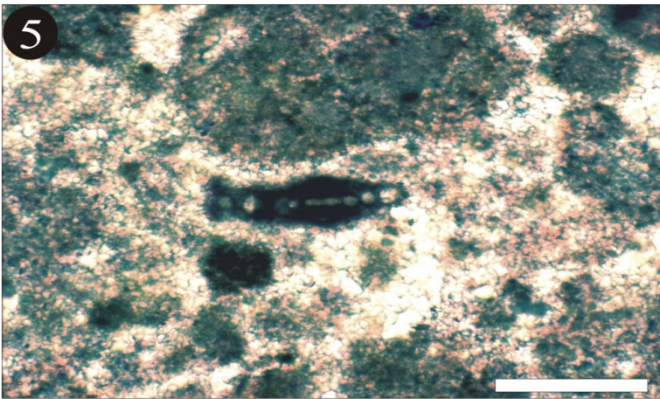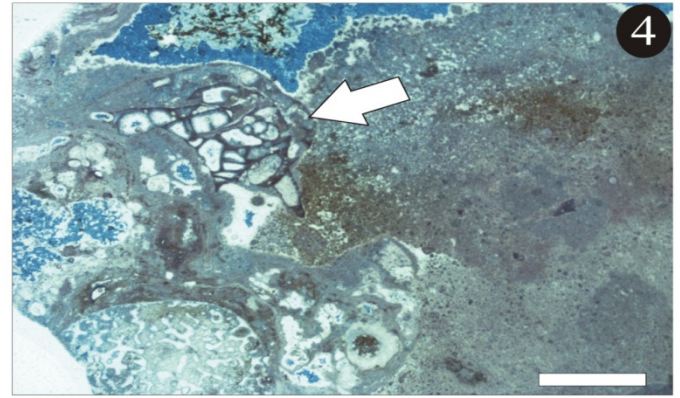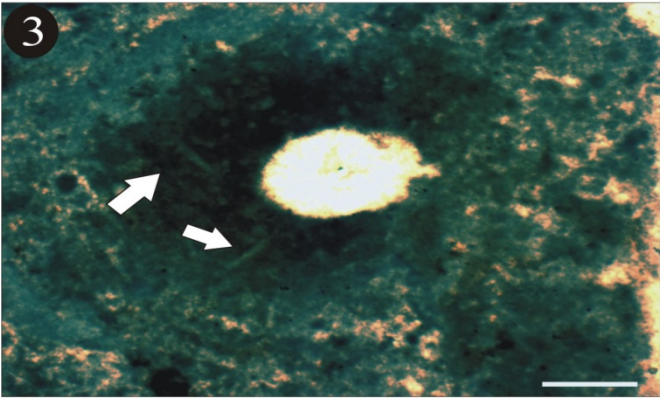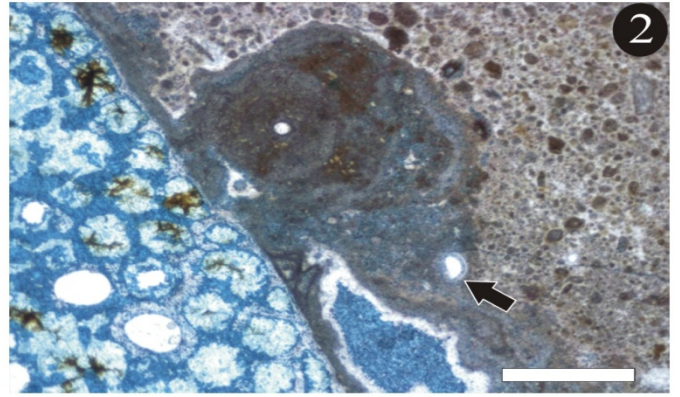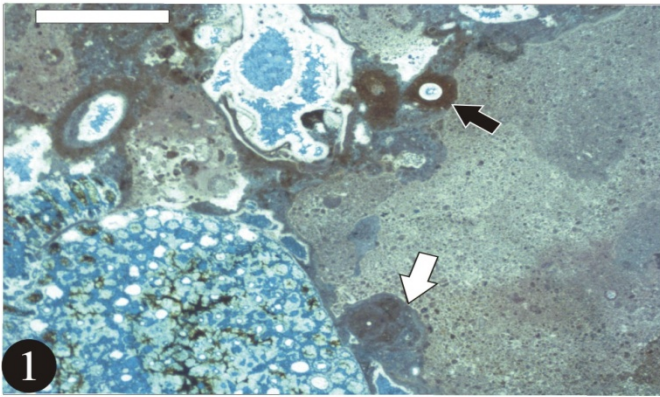
Plate IV

Ceratoporella breviacanthostyla – Tubiphytes association

1.- *Tubiphytes* (arrow) encrustation on *Ceratoporella breviacanthostyla*. Scale bar = 100 μm.

2.- Serpulid worm tubes (arrows) on the surface of *Dendronella articulata*. Scale bar = 500 μm.

3.- Encrusting sequence of an undetermined thalamide sponge (far right) on the surface of *C.breviacanthostyla* (center), which lies upon *Colospongia* (left). Scale bar = 5 mm.

4.- Thalamide sponge (arrow) encrusting and being encrusted by *C. breviacanthostyla*. Scale bar = 500 μm.

5. *Koskinobullina socialis* (arrow) encrustation on microbialite. Scale bar = 200 μm.

6.- *K. socialis* (arrow) on the surface of an undetermined chaetetid sponge. Scale bar = 100 μm

7.- Filaments of *Girvanella* (arrow) encrusting and being encrusted by *C. breviacanthostyla*. Scale bar = 500 μm.

8.- Encrusting guild composed by undetermined thalamides (square), *K. socialis* (black arrows), *Girvanella* (white arrows) and *C.breviacanthostyla*. Note furthermore *Microtubus communis* (Grey arrow) dwelling on microbialite. Scale bar = 500 μm.

Plate IV
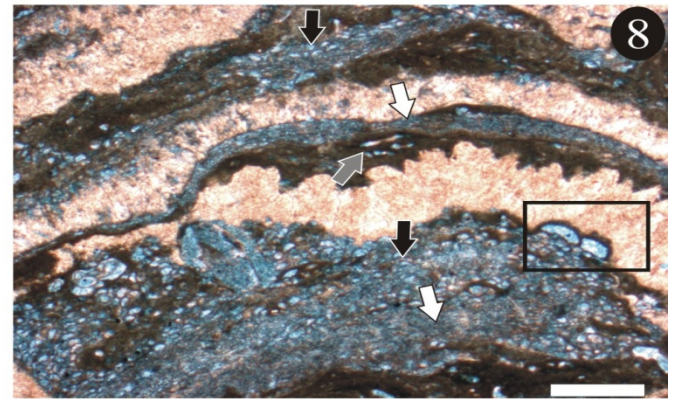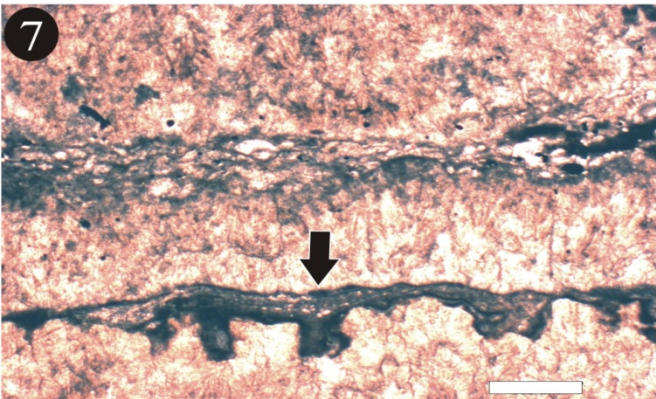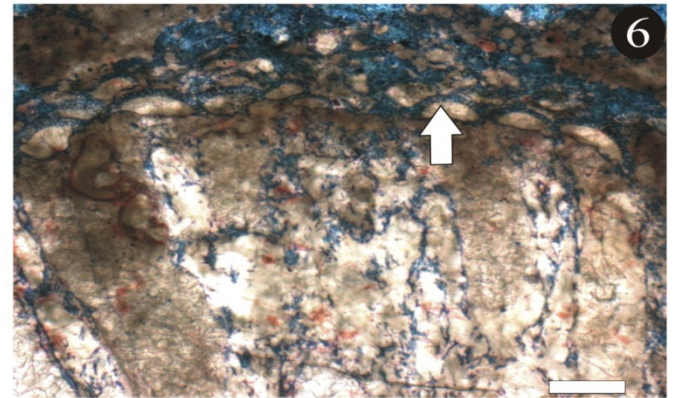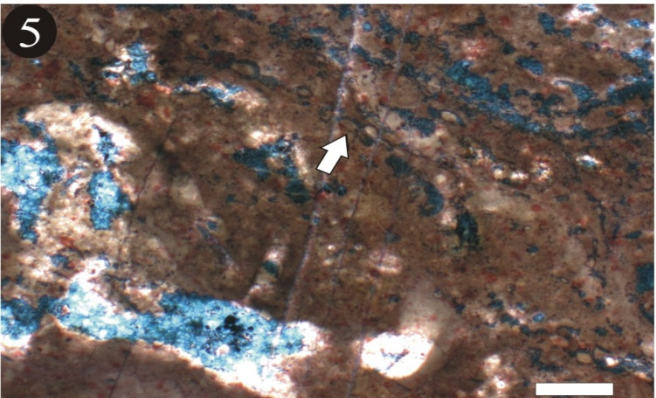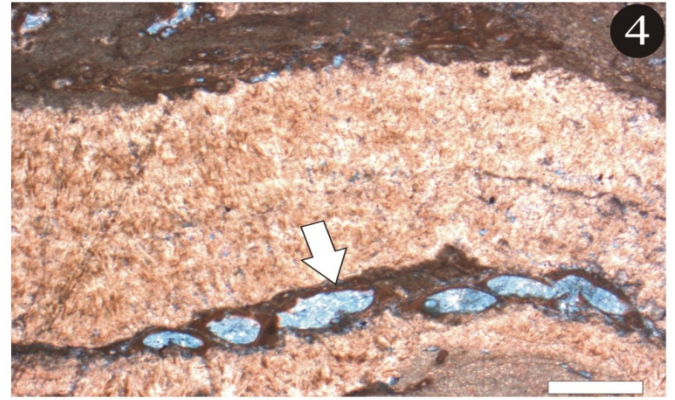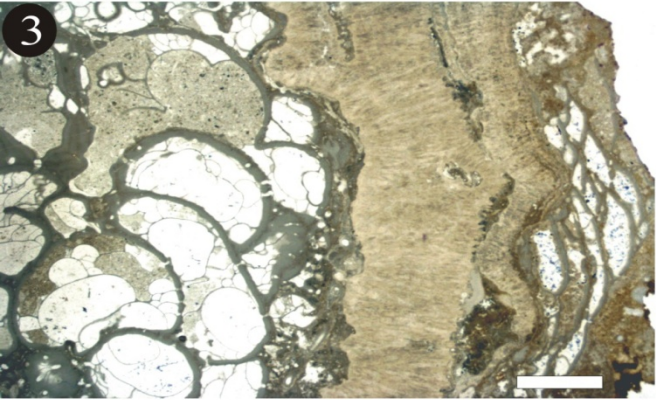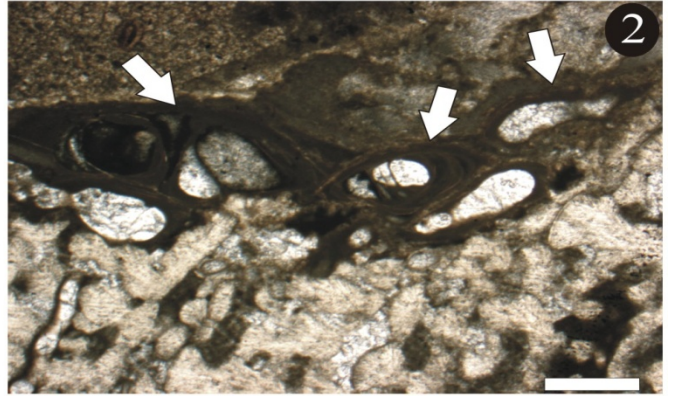
Plate V

Ceratoporella breviacanthostyla – Tubiphytes association

1.- Acanthostyle from a specimen of *Ceratoporella breviacanthostyla*. Scale bar = 50 μm.

2.- Various acanthostyles inside the secondary skeleton of *C.breviacanthostyla.* Scale bar = 100 μm.

3.- *Hispidopetra triassica* encrustation on a specimen of *Petrosistroma?*. Scale bar = 5 mm.

4.-. Type 3 Microbialite deposits (arrows) intermixed with more abundant Type 2 = 5 mm.

5.- *Microtubus communis* dwelling on leiolithic fabrics (dark grey) strongly associated with *C.breviacanthostyla* (light brown) Scale bar = 500 μm.

6.- A colony of *M. communis* in microbialitic substrate (dark brown), associated with *C.breviacanthostyla* (above). Scale bar = 100 μm

7.-. Allochthonous micrite with detritus in primary vugs, containing foraminifer oncoids, automicrite fragments and gasteropods. Scale bar = 500 μm.

8.-. Allochthonous material in direct contact with an undetermined chaetetid sponge. Note *Koskinobullina socialis* growing atop of the sponge. Scale bar = 500 μm.
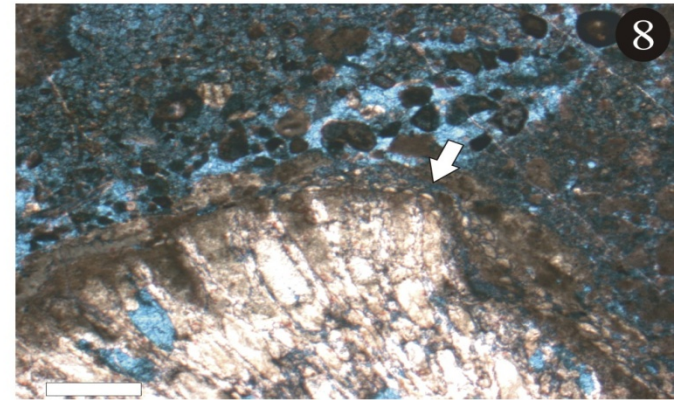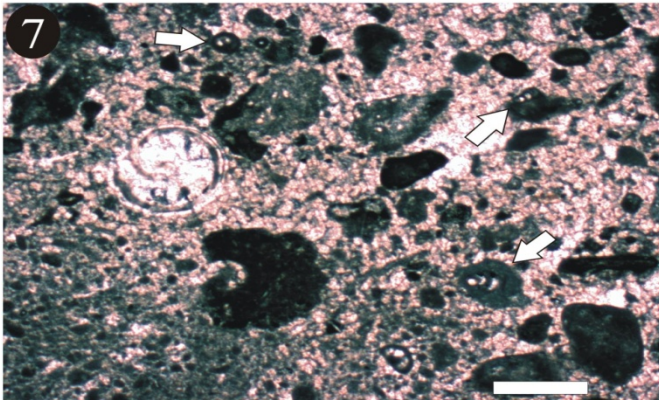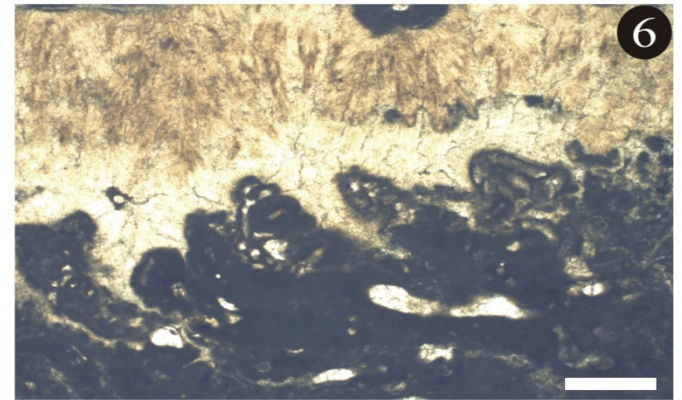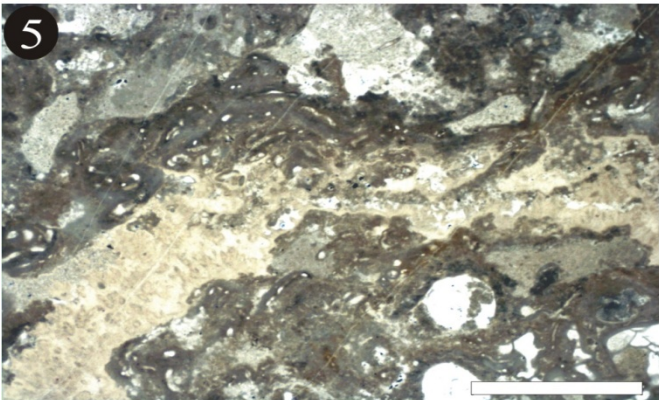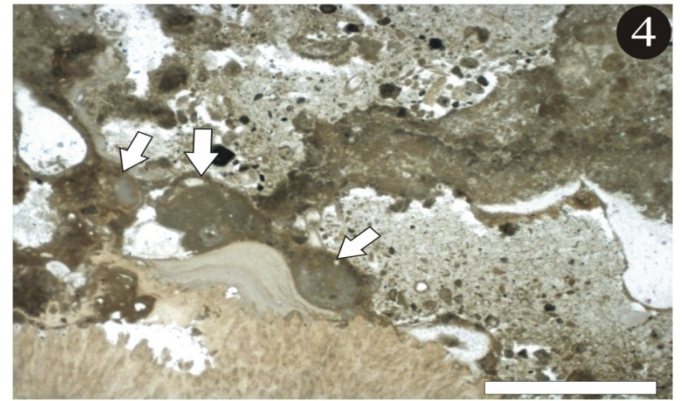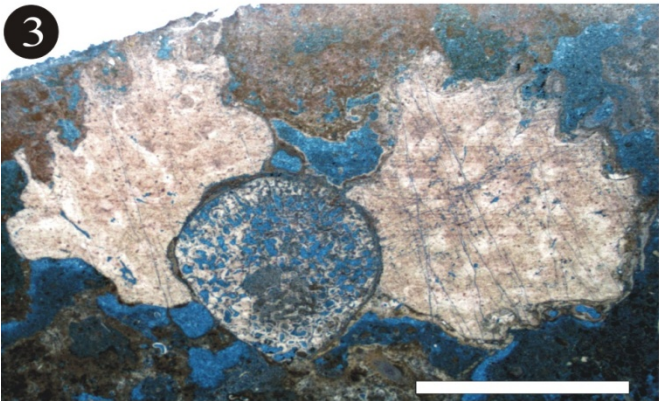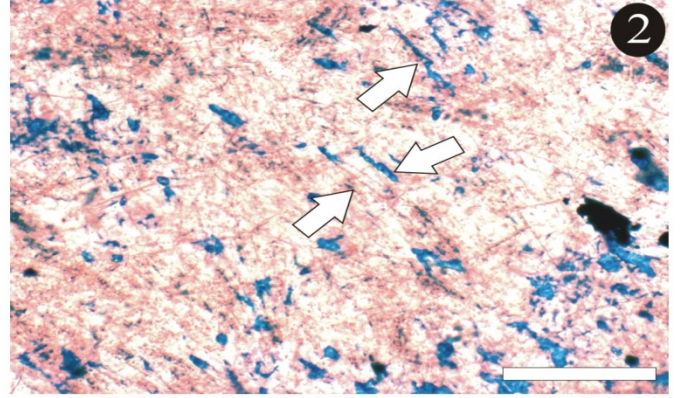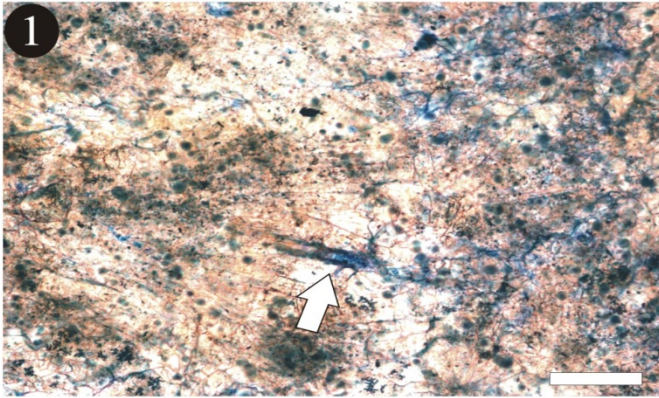
Plate V

Plate VI

Ceratoporella breviacanthostyla – Tubiphytes association (Figs. 1-2)

Cryptocoelia zitteli – Mesophyllum association (Figs. 3-8)

1.- Cross section of an ammonoid *Ceratoporella breviacanthostyla*. Scale bar = 2 mm.

2.- Sphaerulitic microestructure of the ammonite depicted in 1. Scale bar = 50 μm.

3.- *Cryptocoelia zitteli* (above, left), which is the most prominent poriferan in this community. The coralline alga *Mesophyllum* (in grey) can be recognized. The bryozoan *Reptonoditrypa cautica* can be observed in cross section (white arrow) as well in longitudinal section (black arrow). Scale bar = 5 mm.

4.-. A coralline sponge assigned to the genus *Corynella*. Note foraminifer oncoids (arrow) Scale bar = 5 mm.

5.- An undetermined ceratoporellid chaetetid sponge, with multiple epitactic cements. Scale bar = 500 μm.

6.- Encrusting thalamide on the surface of *C. zitteli*. Scale bar = 500 μm.

7.-. Encrusting thalamides with vesicles (white arrows) and *R. cautica* (black arrow) as important members of the encrusting guild of this community. Scale bar = 5 mm.

8.-. *Tubiphytes* (arrow), encrustation on the surface of *C. zitteli*. Scale bar = 500 μm.
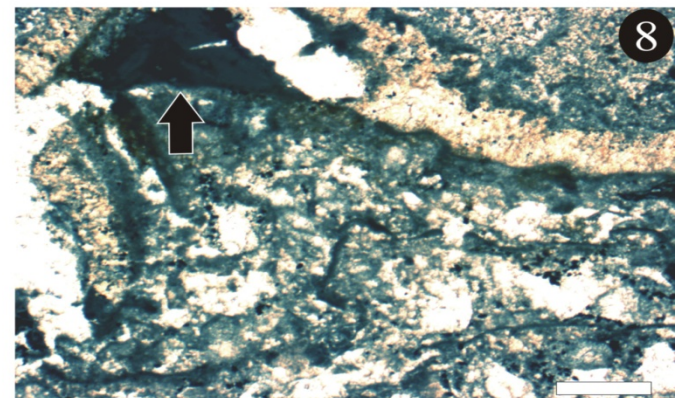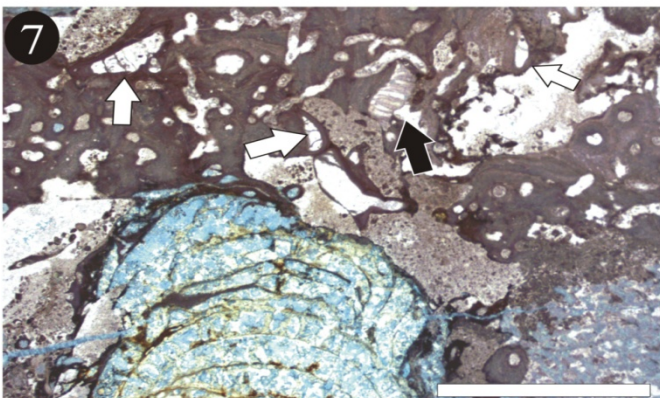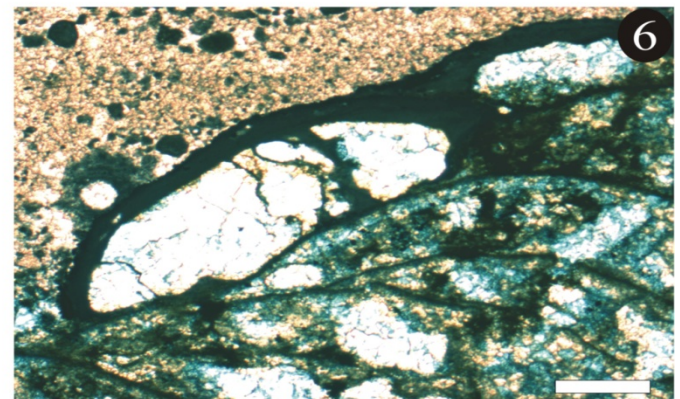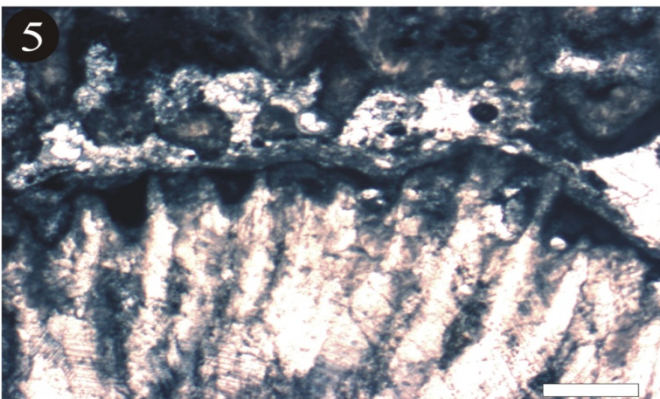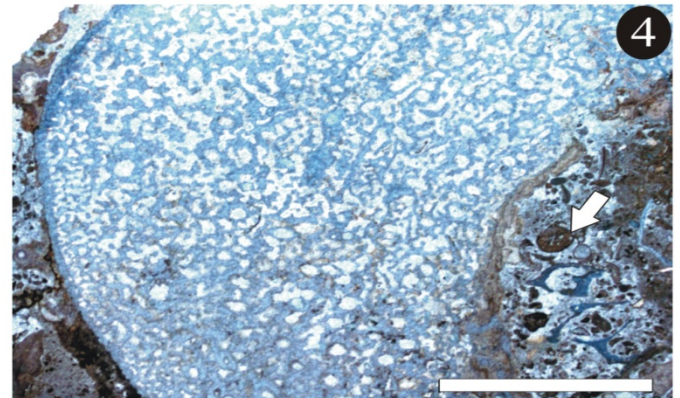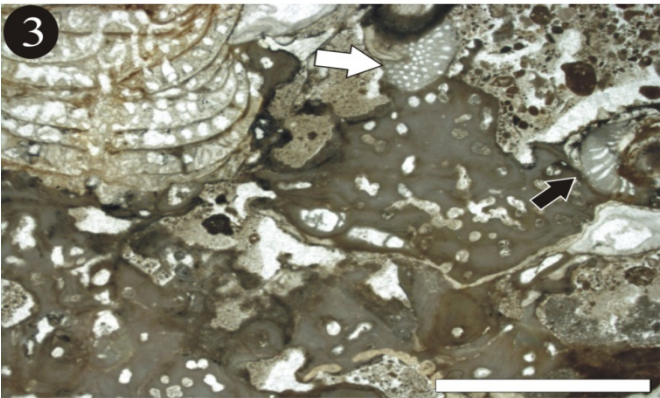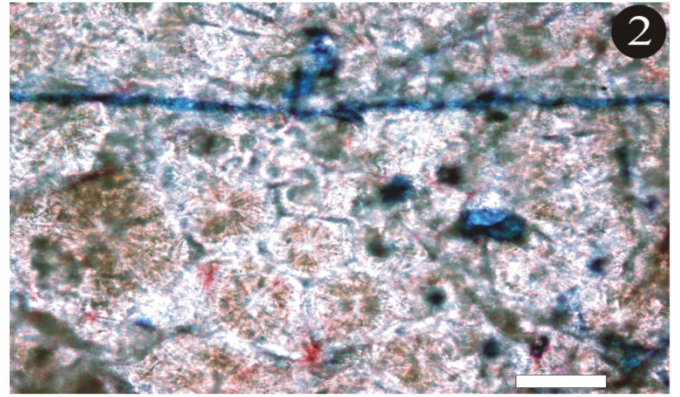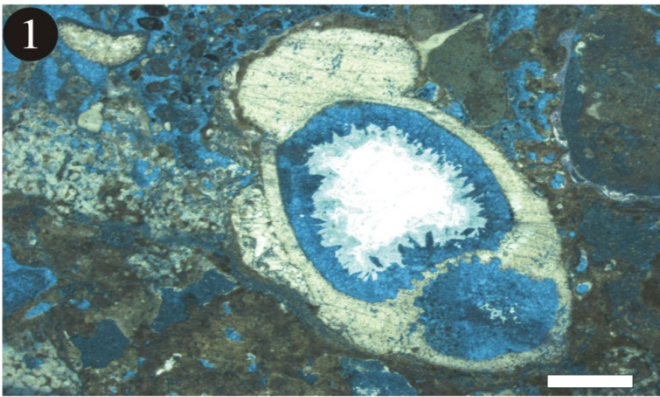
Plate VI

Plate VII

Cryptocoelia zitteli – Mesophyllum association (Figs. 1-5)

Cladogirvanella cipitensis stromatolite association (Figs. 6-8)

1.- Serpullid worm tubes found in microbialite. Scale bar = 500 μm.

2.- *Baccanella floriformis* (arrows), a microproblematicum associated to high energy conditions, which dwells exclusively on microbialitic substrates. Scale bar = 100 μm.

3.- Lychniscosid spicules in a peloidal microbialite sponge mummy. Scale bar = 500 μm.

4.- Allomicrite containing detrital material such as isolated *Lameliconus* cf.*cordevolicus* (arrow). Scale bar = 100 μm.

5.- Allochthonous material, where numerous foraminifer oncoids (arrows) can be seen. Scale bar = 500 μm.

6.- *Cladogirvanella cipitensis* branches in Type 1 microbialite fabrics. Scale bar = 100 μm.

7.- Undetermined ceratoporellid chaetetids covered by Type 4 stromatolitic fabrics. Scale bar = 500 μm.

8.- Encrusting complex on a lithistid sponge composed by serpullid worm tubes (black arrow), synsedimentary cements/*Murania* (white arrow) and microbialite (dark grey) with a Type 3 leiolitic fabric. Scale bar = 500 mm.

PlateVII
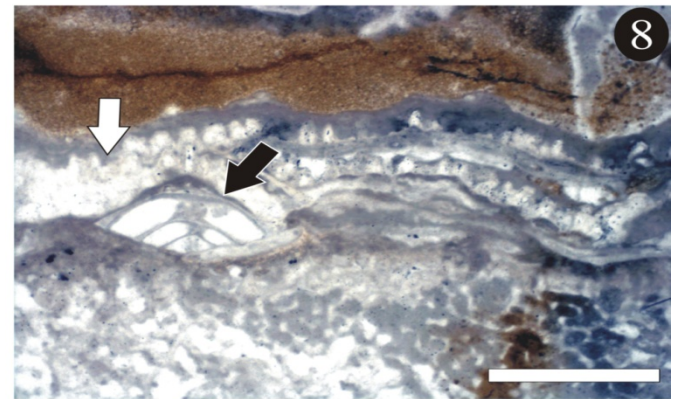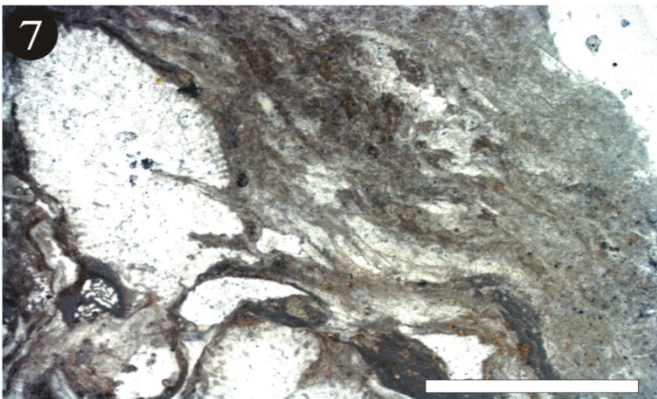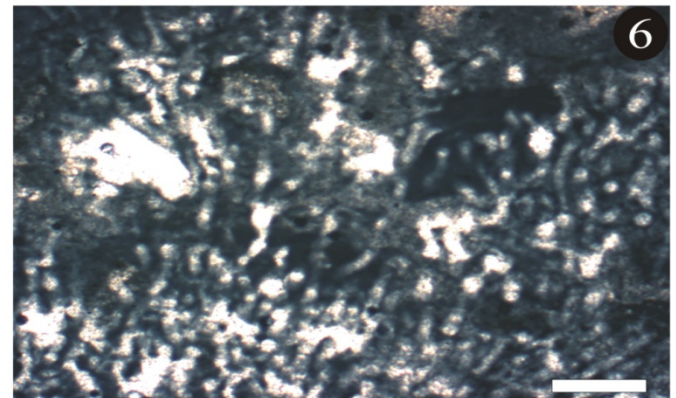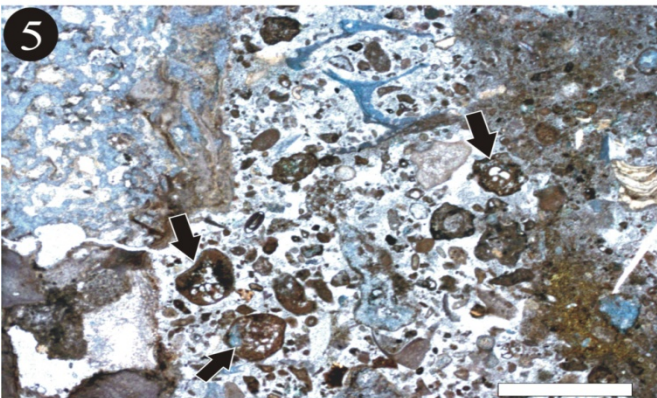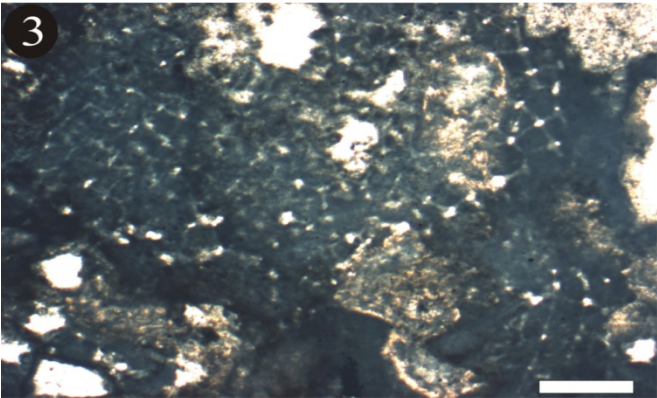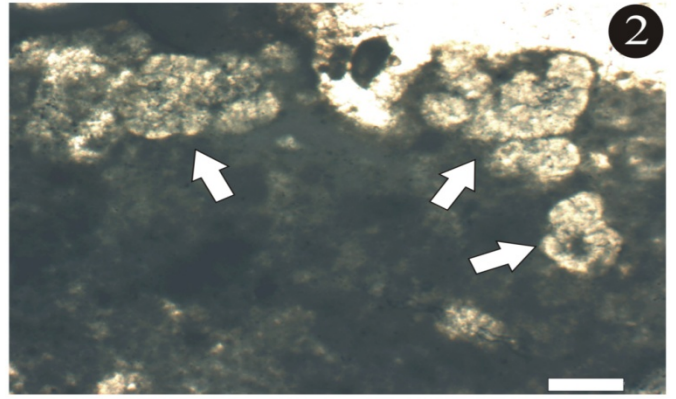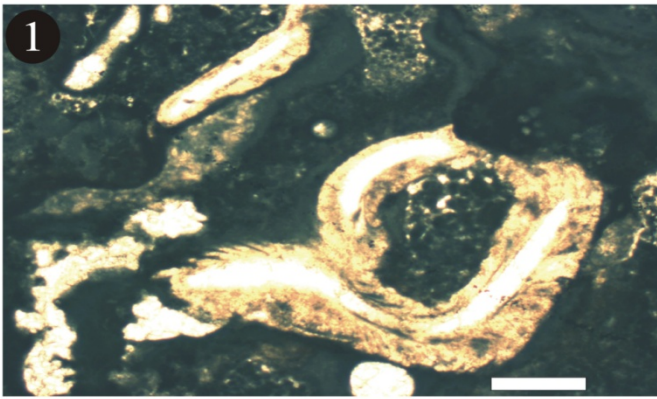
Plate VIII

Cladogirvanella cipitensis stromatolite association (Figs. 1-5)

Thrombolite - microencruster association (Figs. 6-8)

1.- *Tubiphytes* cf. *obscurus*(white arrow) and *Terebella cf. lapilloides* (black arrow). Scale bar = 500 μm.

2.- Enlargement of 1. Scale bar = 200 μm.

3.- *Terebella cf. lapilloides* (below, right) in microbialitic substrate. Note the agglutinated wall consisting exclusively of pelloids Scale bar = 200 μm.

4.- Calcified filaments, possibly of bacterial origin. Scale bar = 100 μm.

5.- *Tubiphytes* cf. *obscurus* in allochthonous micrite. Scale bar = 500 μm.

6.- Numerous "chimneys" of *Tubiphytes* cf. *obscurus*. Scale bar = 500 μm.

7.- *Planiinvoluta* sp. (arrow) in peloidal Type 2 matrix. Scale bar = 500 μm.

8.- *Alpinophragmium perforatum* encrustation on automicritic substrate. Scale bar = 500 mm.

PlateVIII
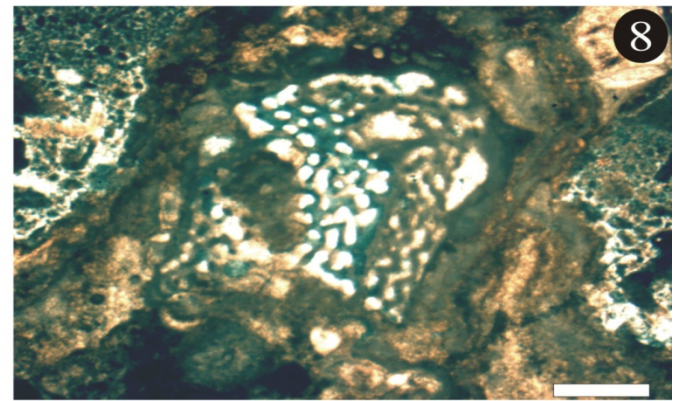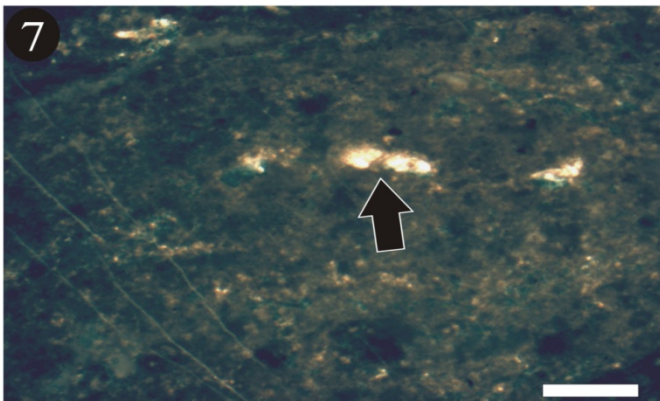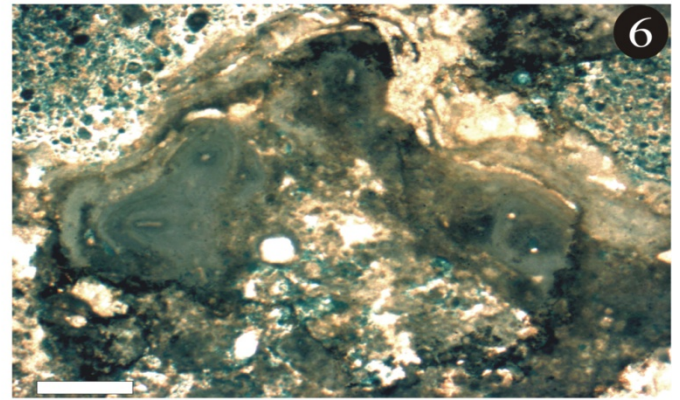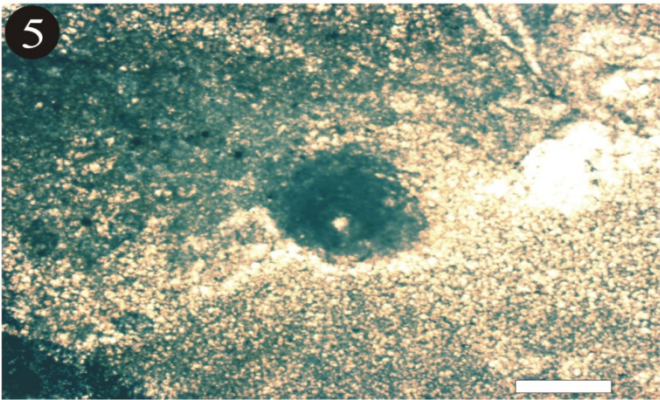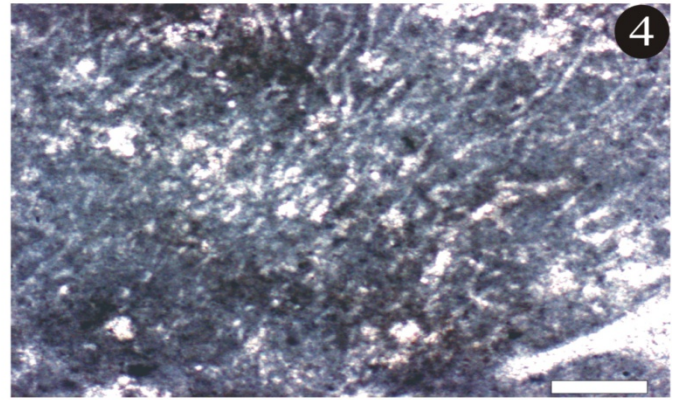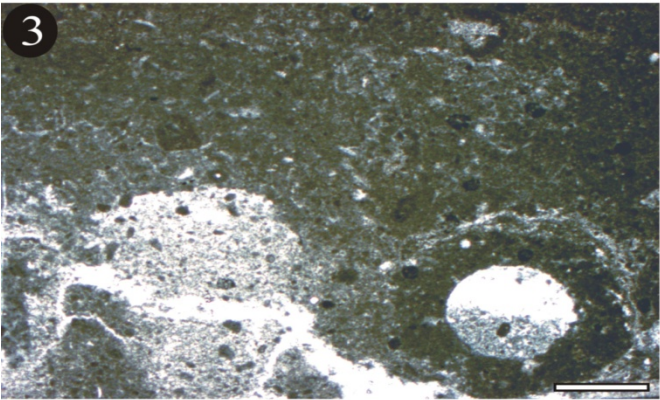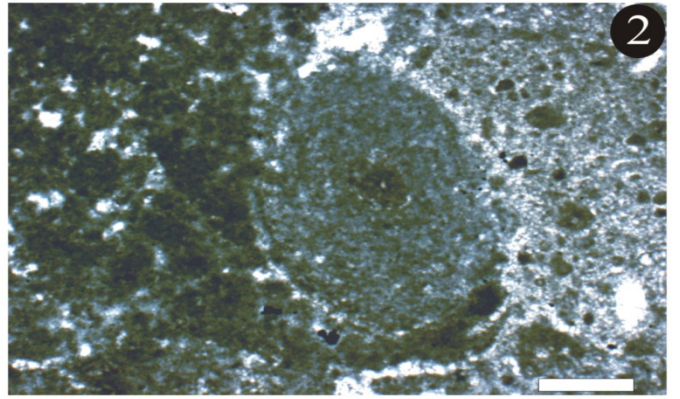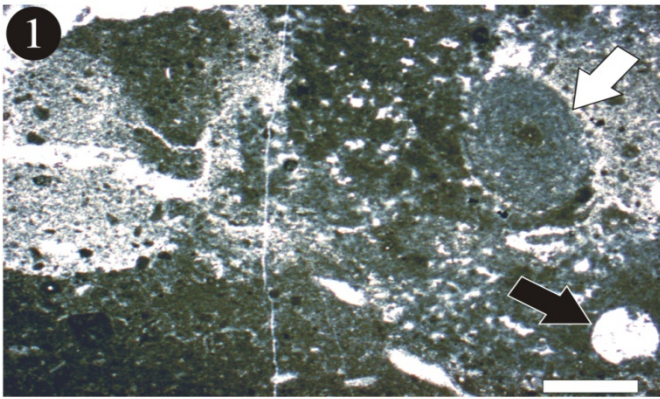
Plate IX

<u>Thrombolite - microencruster association</u> (Figs. 1-5)

<u>*Cassianothalamia* Gemeinschaft II</u> (Figs. 6-8)

1.- Colony of *Koskinobullina socialis* (arrow) in a filamentous disposition. Scale bar = 500 μm.

2.- Enlargement of 1. Scale bar = 200 μm.

3.- *Microtubus communis* (arrows) associated with Type 3 leiolites. Scale bar = 500 μm.

4.- Pyrite framboids (arrows), which can be found abundantly within microbialites. Scale bar = 100 μm.

5.- Botryoid cement (arrow), possibly of aragonitic composition. Scale bar = 500 μm.

6.- *Baccanella floriformis*(arrow) encrustation on microbialitic substrate. Scale bar = 500 μm.

7.- *B.floriformis* (white arrows) in microbialite, delimited by botryoid cements (black arrows). Scale bar = 500 μm.

8.- *Ladinella porata* (black arrow) and longitudinal section of *Tubiphytes* (white arrows), surrounded in part by microbialite. Scale bar = 500 mm.

Plate IX
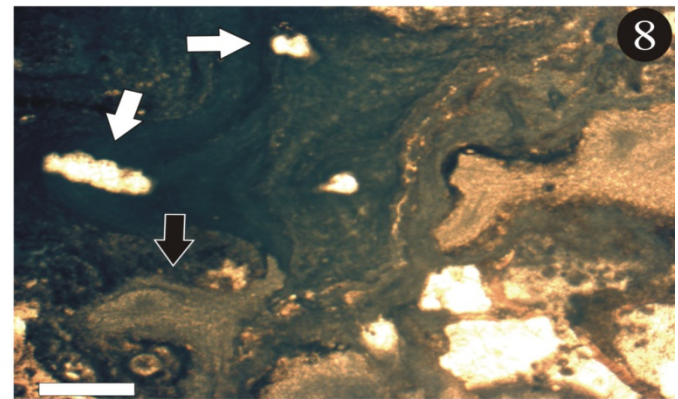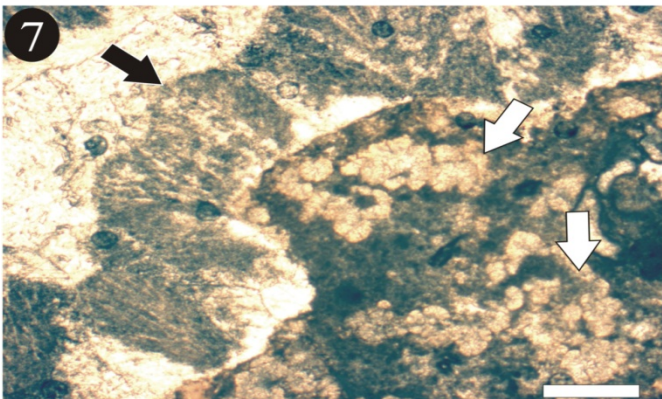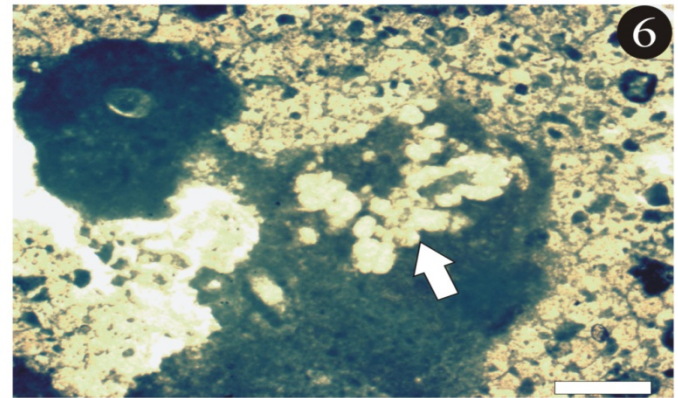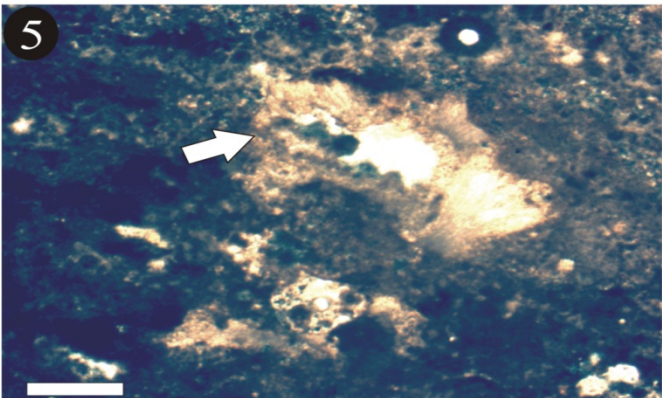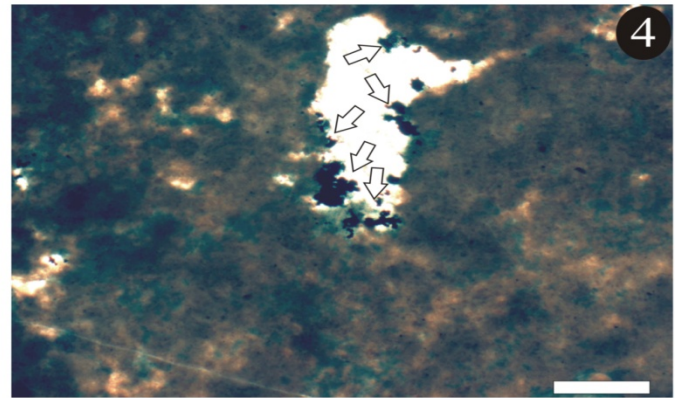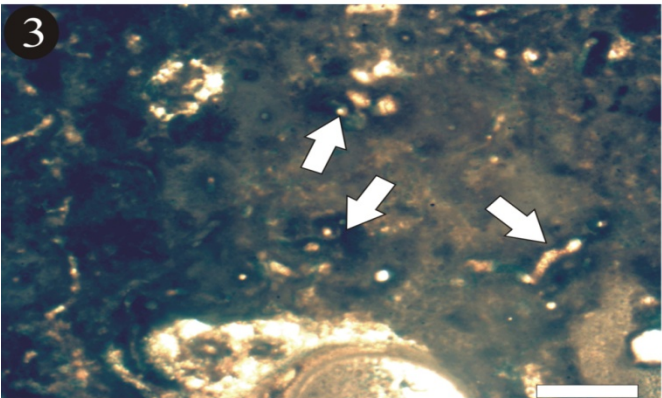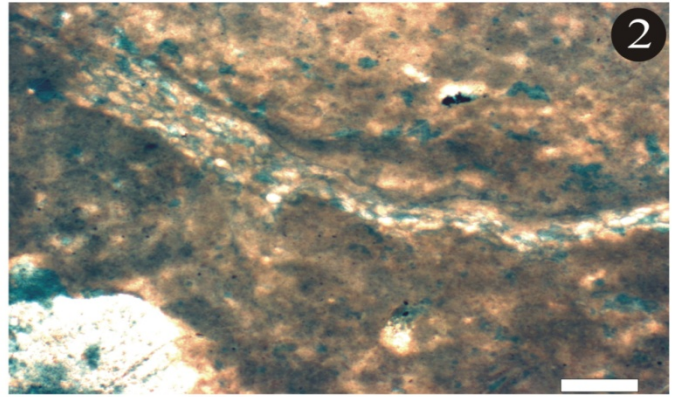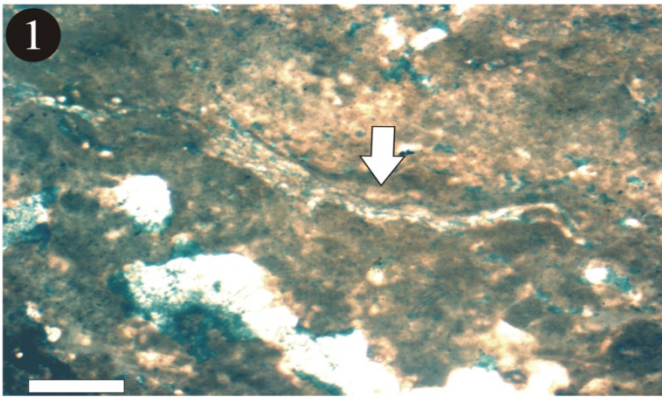
Plate X

Cassianothalamia Gemeinschaft II

1.- Tubes of *Terebella cf. lapilloides* (arrows) in Type 2 microbialitic fabrics. Scale bar = 500 μm.

2.- *Girvanella* like porostromate filaments, in microbialite. Scale bar = 200 μm.

3.- *Cassianothalamia zardinii* (right) encrustation on a *Reptonoditrypa cautica* specimen (above, left) Scale bar = 500 μm.

4.- Sponge mummy with hexactinosid calcite pseudomorphs. Scale bar = 500 μm.

5.- *C.zardinii* (below, right) encrusting a coral of the genus *Thecosmilia*. In the mid- upper section of the picture, desmae pseudomorphs can be seen immersed in a Type 1 microbialitic fabric (arrow). Scale bar = 500 μm.

6.- Vase –shaped structure conformed exclusively by peloids which has probably a Porifera origin. Unfortunately, no spicules could be assessed. Scale bar = 1 mm.

7.- Unknown borings in microbialite. Note geopetal filling.. Scale bar = 500 μm.

8.- *Aka cassianensis* spicules in automicrite. Associated is *B.floriformis* (arrow). Scale bar = 500 mm.
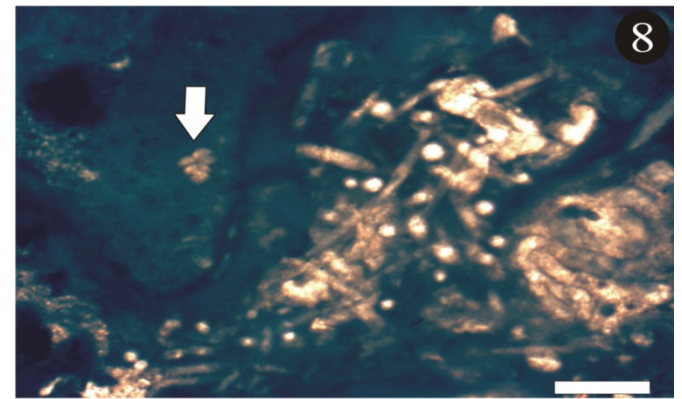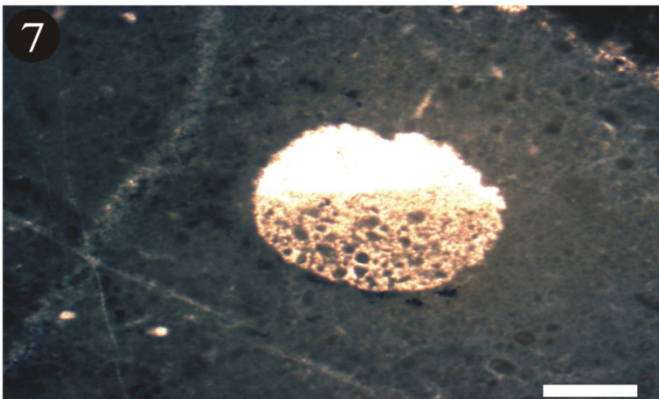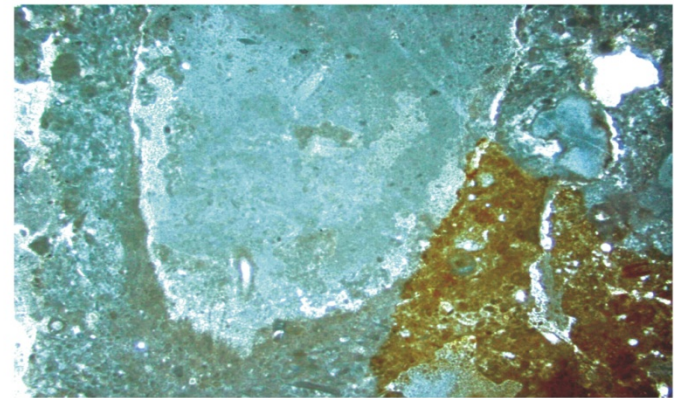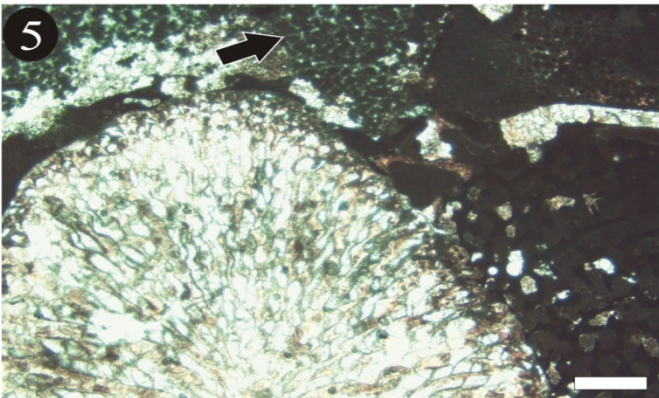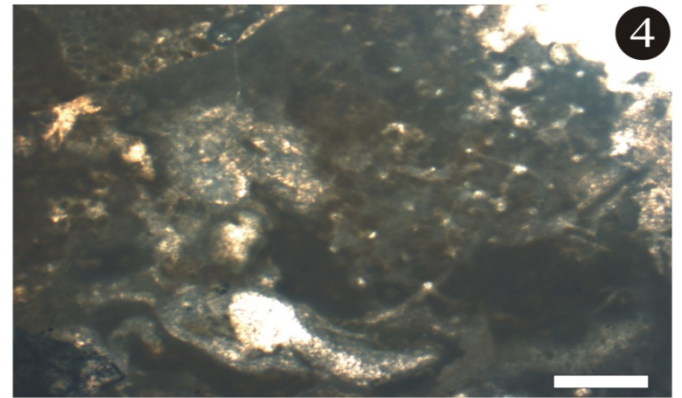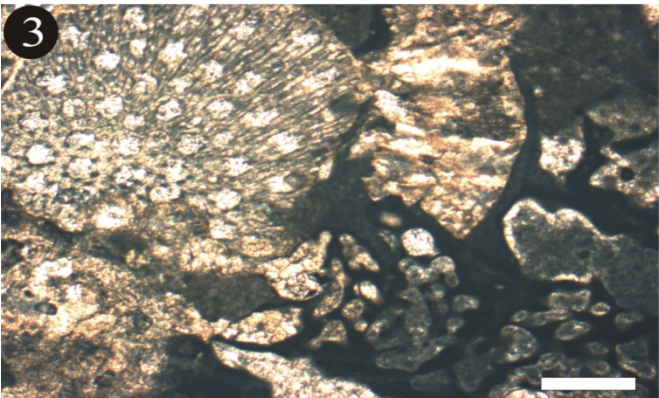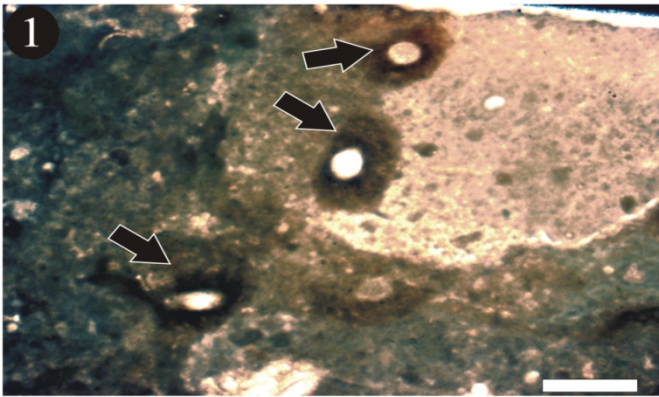
Plate X

Plate XI

Cassianothalamia Gemeinschaft II (Fig. 1)

Patch Reef association I (Figs. 2-8)

1.- Stromatactis cavity, which can be often found associated with microbialites from this community. Scale bar = 5 mm.

2.- The stromatoporoid *Balatonia*, an important builder at St. Cassian. Patch Reefs. Scale bar = 5 mm.

3.- Encrusting coralline sponge, possibly related to *Ceratoporella* encrusting a *Margarophylia* corallite Type 3 leiolites. Scale bar = 1.5 mm.

4.- *Murania kazmierczaki* encrusting a chaetetid sponge. Note associated *Planiinvoluta* (arrows). Scale bar = 5 mm.

5.- Encrusting coralline sponge with clinogonal microstructure. Scale bar = 5 mm.

6.- Encrusting coralline sponge. Note growth bands with approximately the same width, yet with an alternating color pattern Scale bar = 5 mm.

7.- Detail of 4. Above: Normal view. Below: Epifluorescence view. Note the presence of *Planiinvoluta* encrusting within microbialite. (arrows) .*Murania kazmierczaki* encrusts the top of the sequence (above). A similar quantity of organic matter for *Murania* and the microbialite can be inferred from the intensity of the empite light. Scale bar = 500 mm.

8.- Detail of 7, showing the good preservation of the wall of *Planiinvoluta*. Scale bar = 100 mm.

Plate XI
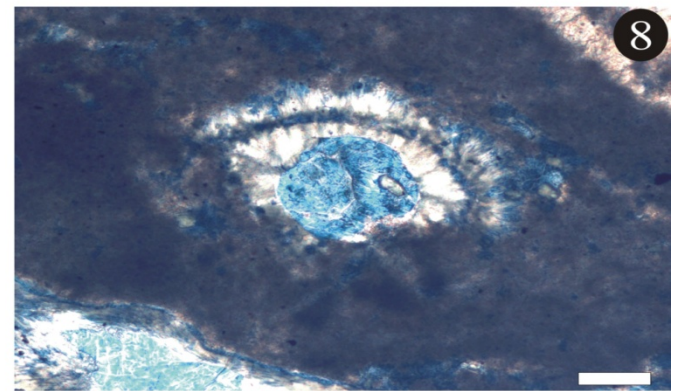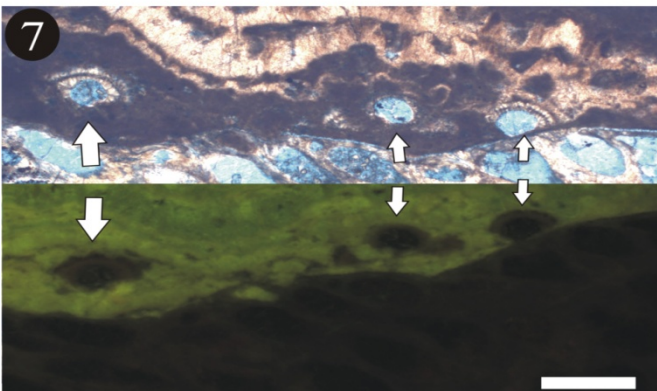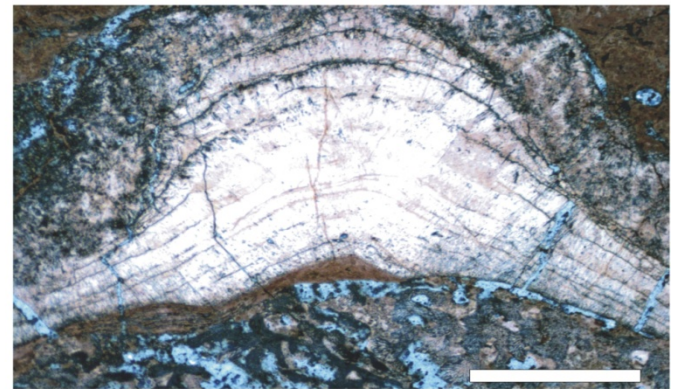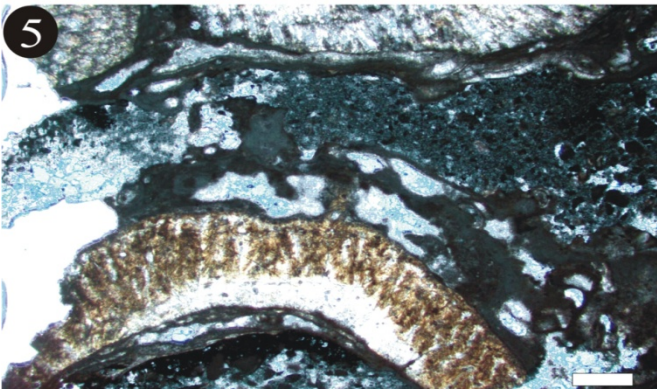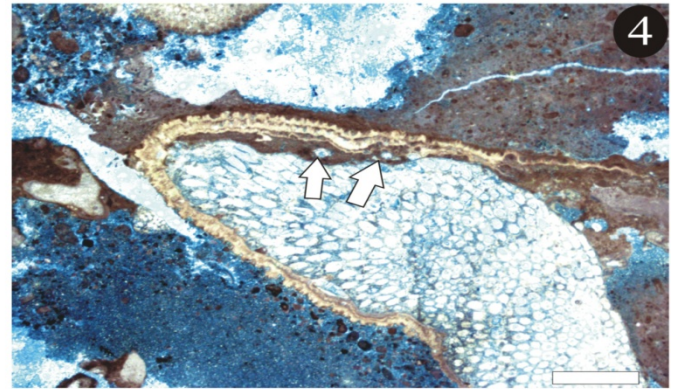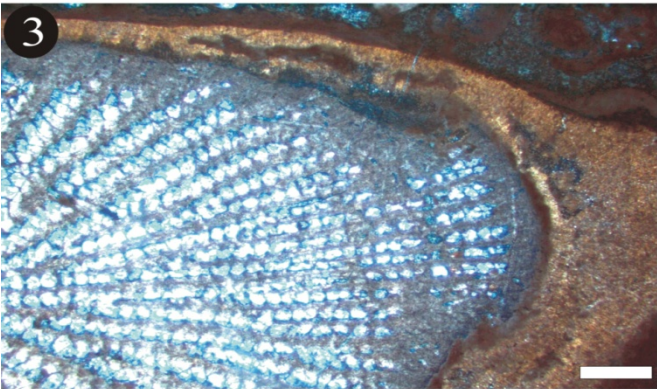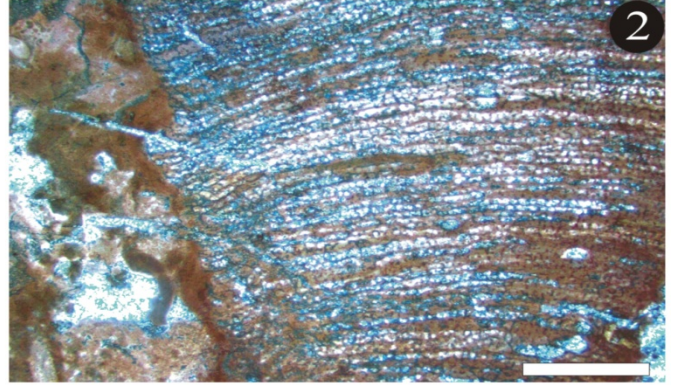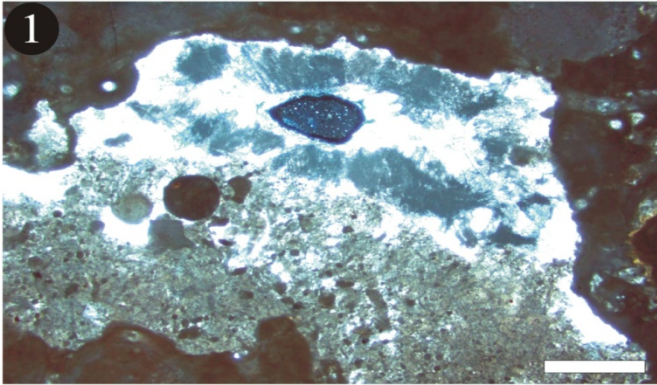
Plate XII

Patch Reef association I (Figs. 1-3)

Mud Mound association I (Figs. 4-6)

Dendronella – Solenopora association (Figs. 7-8)

1.- A colony of *Koskinobullina socialis* (arrow) encrusting the surface of a ceratoporellid chaetetid. Scale bar = 500 μm.

2.- Tubes of unknown origin (arrow), probably serpulids, encrusting a specimen of *Balatonia* sp.. Scale bar = 500 μm.

3.- Phylloid alga (center) encrusted along with microbialite on a stromatoporoid. Scale bar = 500 μm.

4.- A branching ceratoporellid chaetetid, one of the only sponges found as a part of this association. Scale bar = 5 mm.

5.- Type 4 stromatolitic facies located in a different growth direction (arrow) in comparison to the ceratoporellid chaetetid and the encrusting thrombolite upon it. Scale bar = 5 mm.

6.- Cement succession in a stromatactis. Note the four generations (arrows). Scale bar = 2 mm.

7.- *Solenopora* cf. *cassiana* (left) associated with *Dendronella articulata* . Scale bar = 500 μm.

8.- Hexactines (arrow) in Type 2 microbialitic matrix between branches of *D.articulata.* Scale bar = 500 μm.
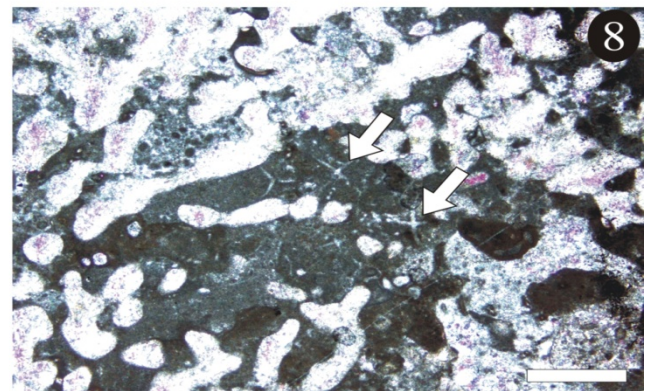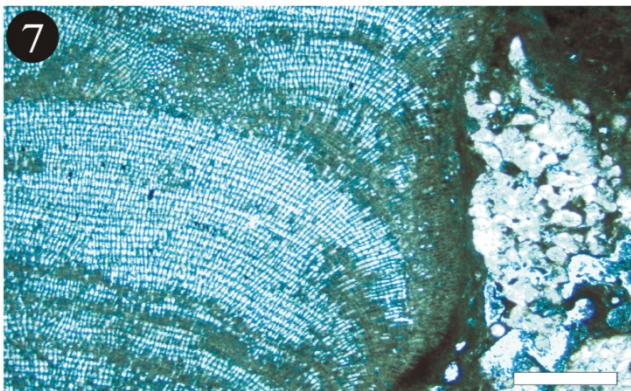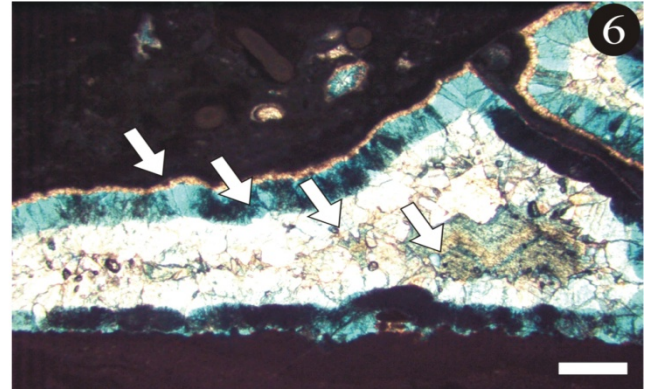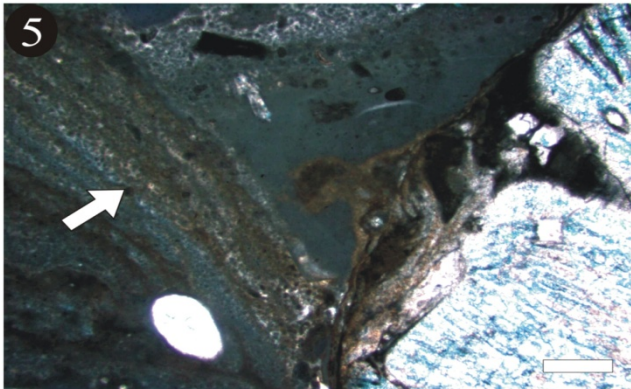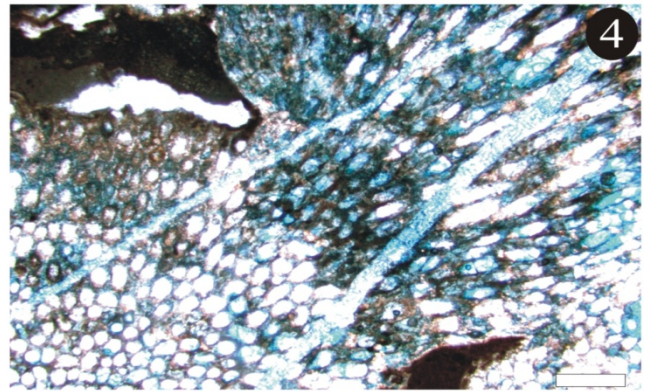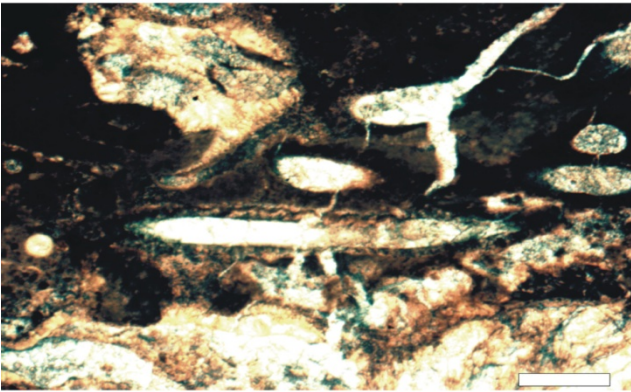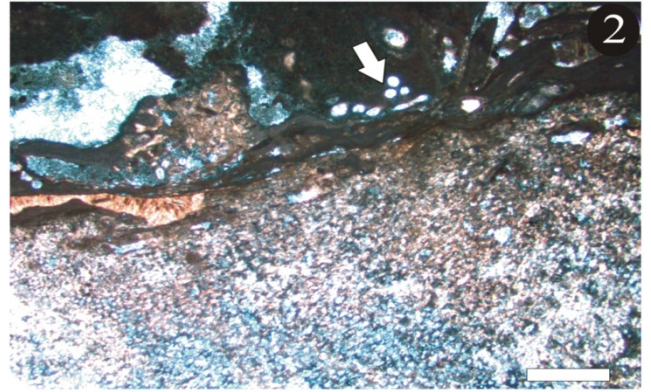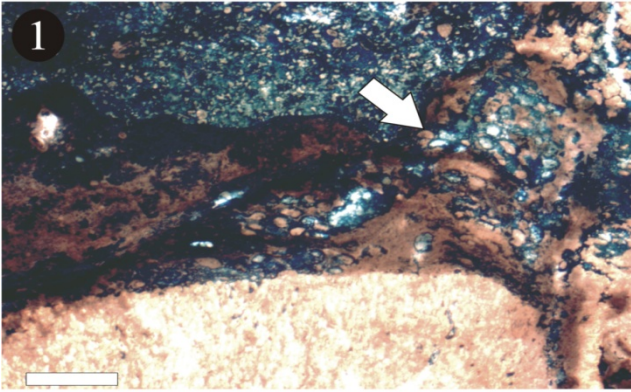
Plate XII

Plate XIII

Dendronella – Solenopora association

1.- Enlargement of Pl.XII, Fig. 8. Scale bar = 200 μm.

2.- Encrusting complex of *Uvanella* – like thalamides (white arrow) and *Koskinobullina socialis – Girvanella* (black arrow). Scale bar = 500 μm.

3.- Enlargement of 2, showing *K. socialis* (white arrow) and *Girvanella* (black arrow) Scale bar = 100 μm.

4.- *Ladinella porata* (arrows) associated to microbialites on top of *S. cassiana.* Scale bar = 200 μm.

5.- *K.socialis.* on top of a (ceratoporellid) sponge? Scale bar = 500 μm.

6.- Enlargement of 5. Scale bar = 100 μm.

7.- Allochthonous sediment in primary vugs. Scale bar = 500 μm.

8.- *Lamelliconus cordevolicus* (arrow) in allochthonous micrite/microsparite. Scale bar = 500 μm.
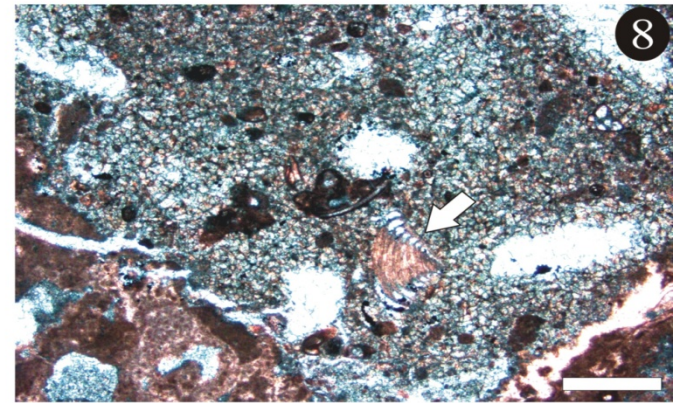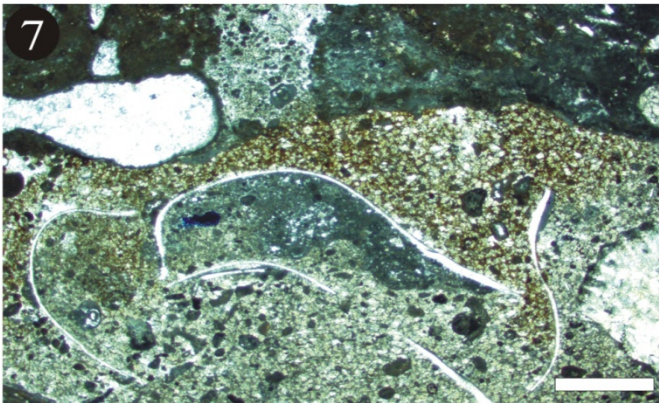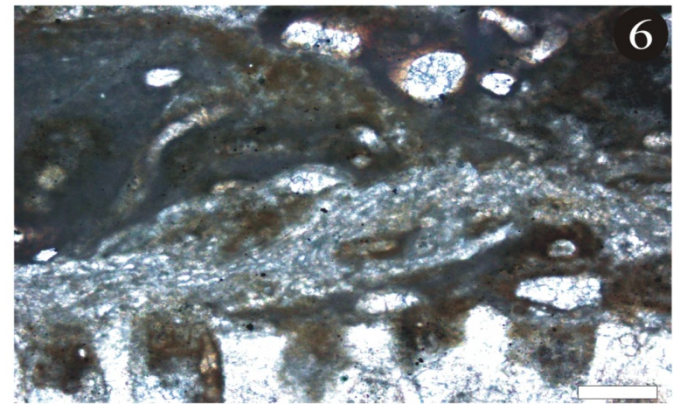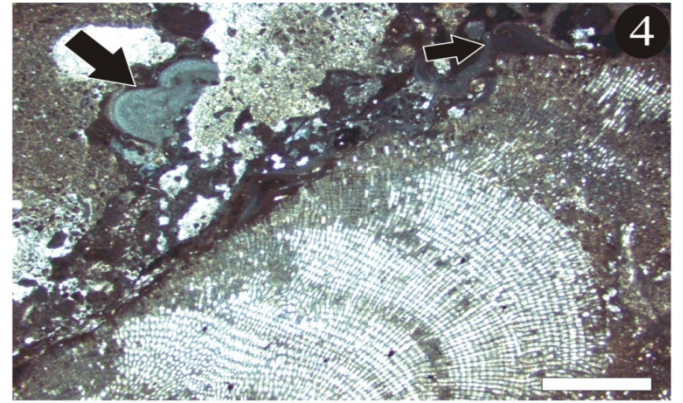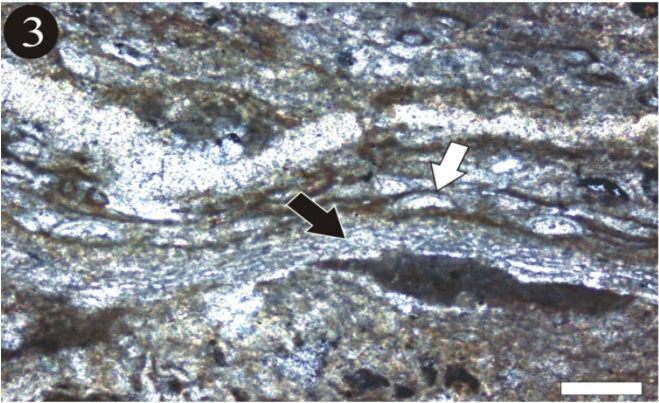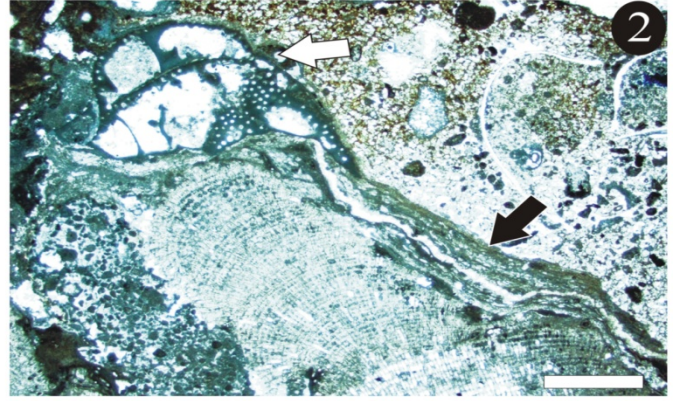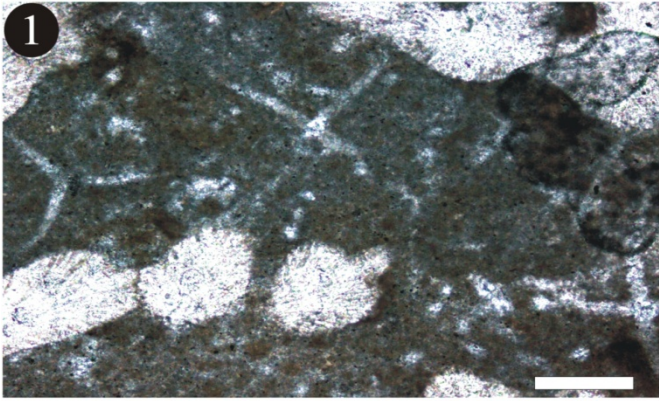
Plate XIII

Plate XIV

Spongiomorpha ramosa association (Figs. 1-7)

Chaetetid - microencruster association (Fig. 8)

1.- Cross section of *Eudea polymorpha.* Scale bar = 500 μm.

2.- *Girvanella* – like porostromate organisms (white arrow), associated with *Koskinobullina socialis.*(black arrow). Sample is partially diagenetically altered. Scale bar = 500 μm.

3.- Thalamide encrusters (white arrow) and *Reptonoditrypa cautica* (black arrow) on top of *Spongiomorpha ramosa.* Scale bar = 1 mm.

4.- Enlargement of 3. Scale bar = 500 μm.

5.- *Uvanella* – like thalamides encrusting on top of *Spongiomorpha ramosa.* Scale bar = 1 mm.

6.- Encrusting complex of microbialite and *Ladinella porata* (arrow) on the surface of *S. ramosa.* Scale bar = 500 μm.

7.- Microbialitic clot containing hexactine spicule pseudomorphs. Scale bar = 500 μm.

8.- Cross section of a branch of a chaetetid with sphaerulitic microstructure. Note encrustations containing *Aulotortus* (arrow) in Type 3 Microbialite. Scale bar = 1 mm.

Plate XIV
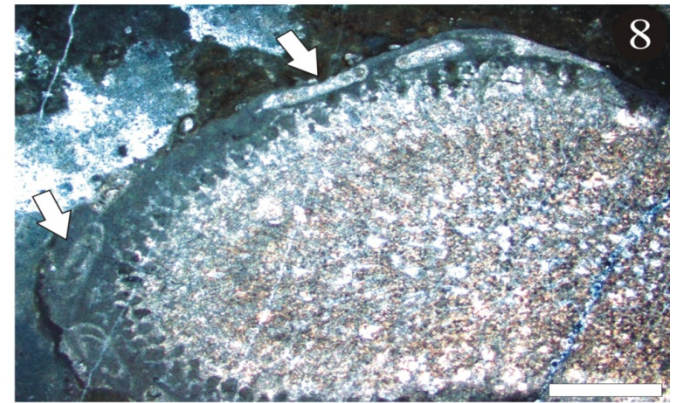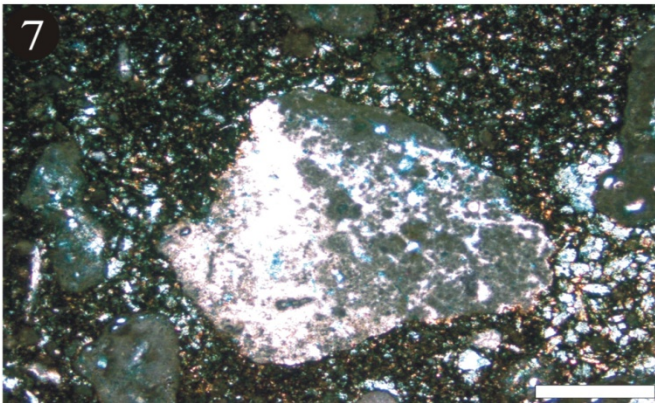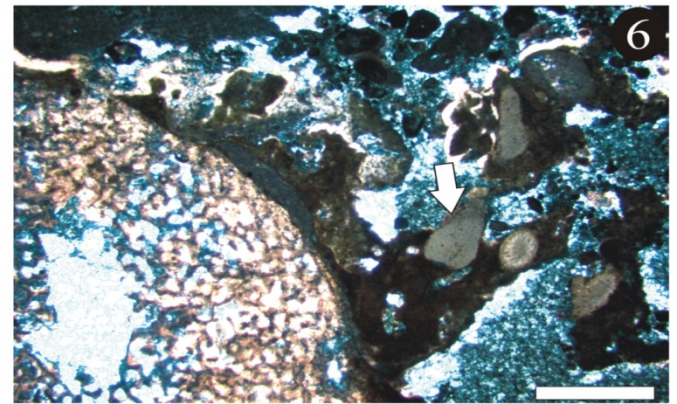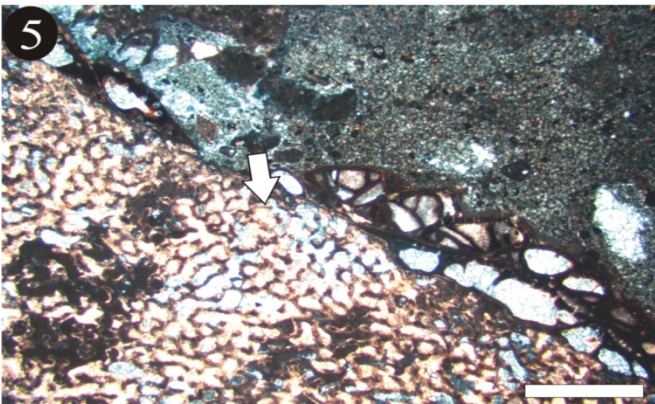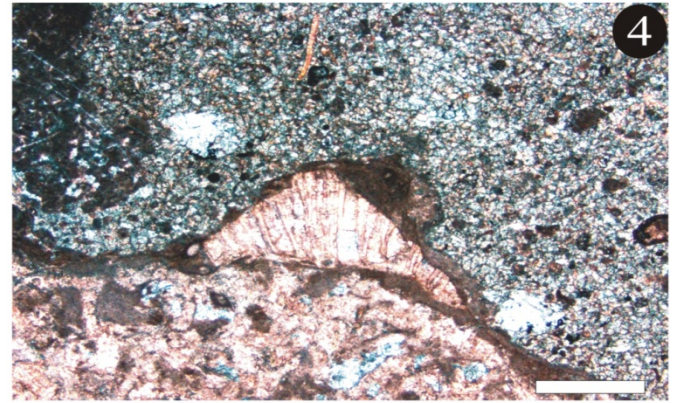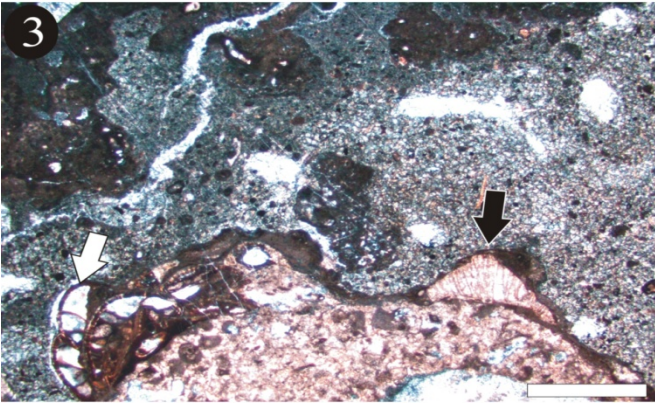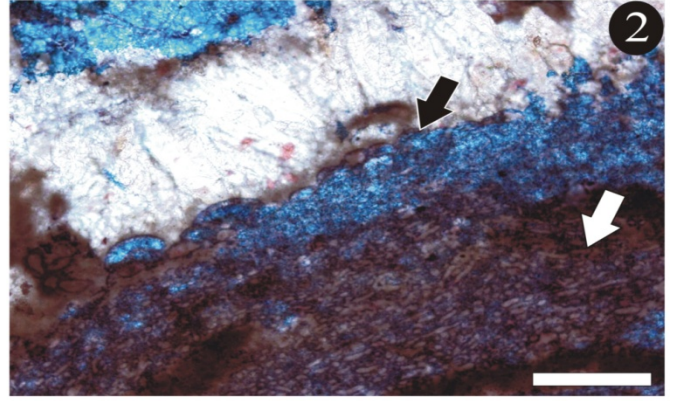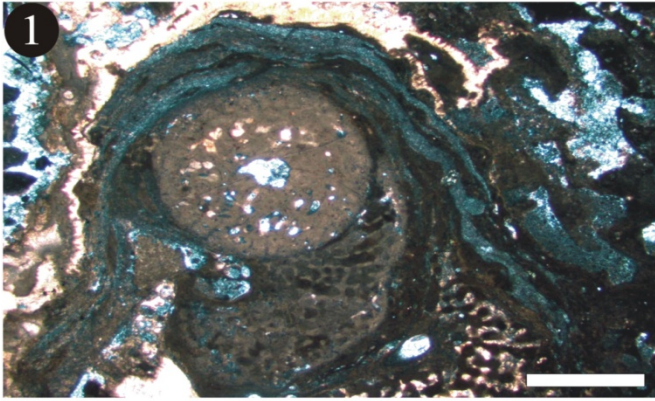
Plate XV

Chaetetid - microencruster association

1.- Sphaerulites (arrow) of a branched chaetetid sponge. Scale bar = 100 μm.

2.- Microencruster association (above, center) on the surface of a chaetetid sponge. Scale bar = 1 mm.

3.- Enlargement of 2, displaying *Koskinobullina socialis* (black arrow) and *Aulotortus* (white arrow) Scale bar = 500 μm.

4.- *Koskinobullina socialis*. Scale bar = 100 μm.

5.- *Girvanella* associated to Type 2 microbialite. Scale bar = 200 μm.

6.- *Alpinophragmium perforatum* (center) and *Terebella* cf. *lapilloides* (arrow). Scale bar = 1 mm.

7.- *Terebella* cf. *lapilloides* tubes immerse in Type 2 microbialite. Scale bar = 500 μm.

8.- *Aulotortus* sp. (arrow) encrusted in Type 3 microbialite Scale bar = 500 μm.
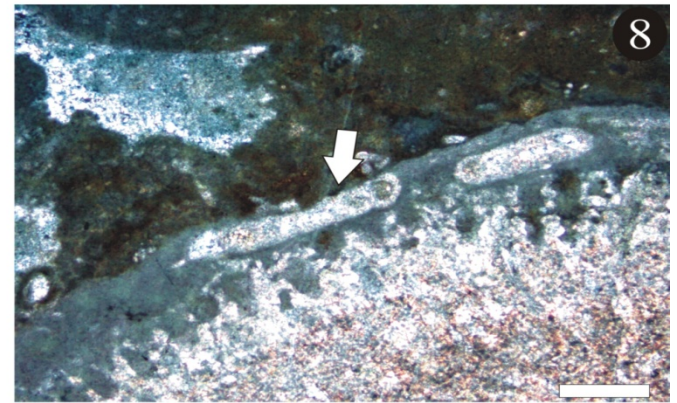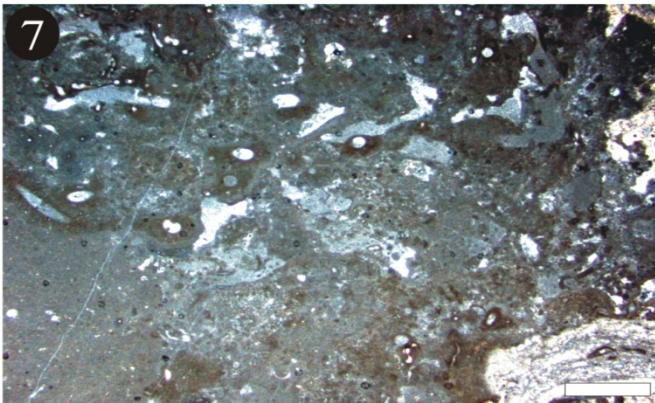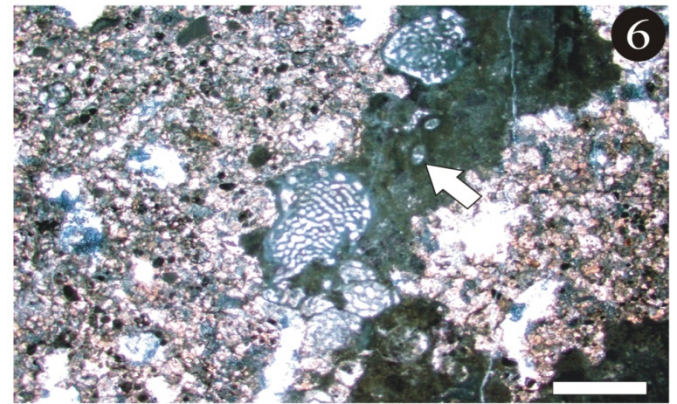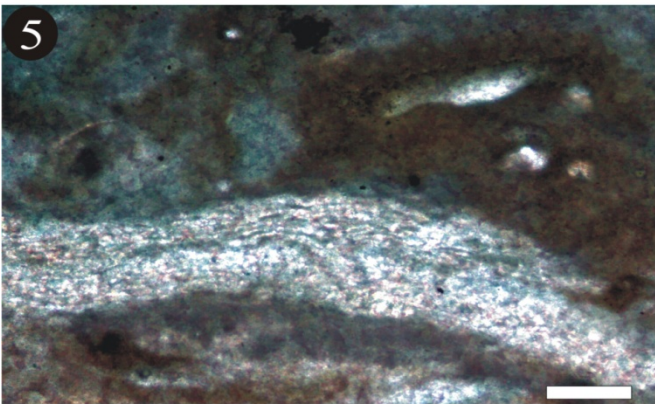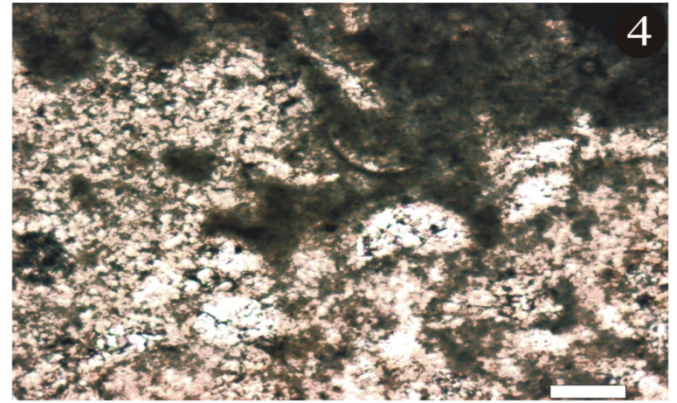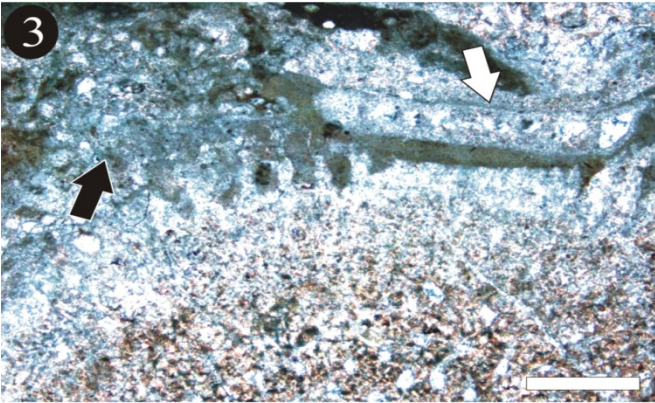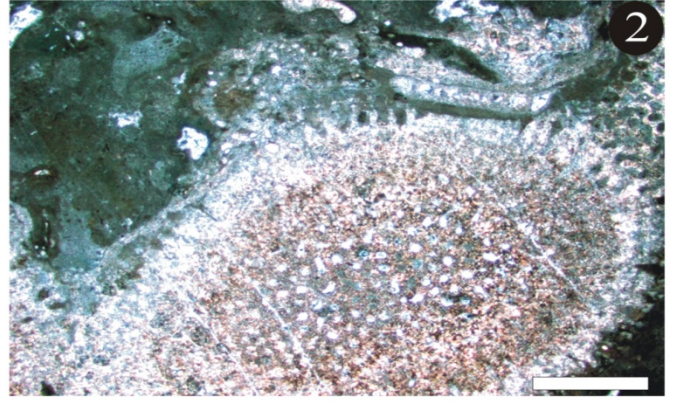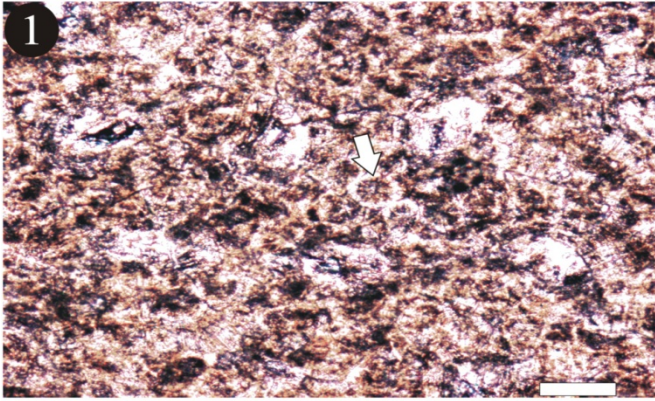
Plate XV

Plate XVI

Amblysiphonella – Megalodon association

1.- *Amblysiphonella strobiliformis*. Note primary cement (arrow) encrusting the sponge and bryozoans (upper right corner). Scale bar = 5 mm.

2.- Undetermined coralline sponge (stromatoporoid?) on the surface of *A. strobiliformis*. Scale bar = 2 mm.

3.- *Thaumastocoelia cassiana* (center) with an encrustation of *Cassianothalamia zardinii* (left). Scale bar = 2 mm.

4.- Multiple colonies of *Reptonoditrypa cautica* (arrows) dwelling in microbialitic substrate. Scale bar = 1 mm.

5.- Encrusting complex including *R.cautica* (black arrow), serpullid worm tubes (white arrow), *Terebella* cf. *lapilloides* (grey arrow) and microbialite. Scale bar = 1 mm.

6.- Numerous colonies of *R.cautica* and undetermined thalamides encrusting the top of a bryozoan. Scale bar = 1 mm.

7.- Thecideid? brachiopod (center) encrusting an undetermined coralline sponge . Scale bar = 1 mm.

8.- Numerous *Tubiphytes* individuals (dark grey- black) on the surface of a *Megalodon* shell (lower left corner). Scale bar = 1 mm.

Plate XVI
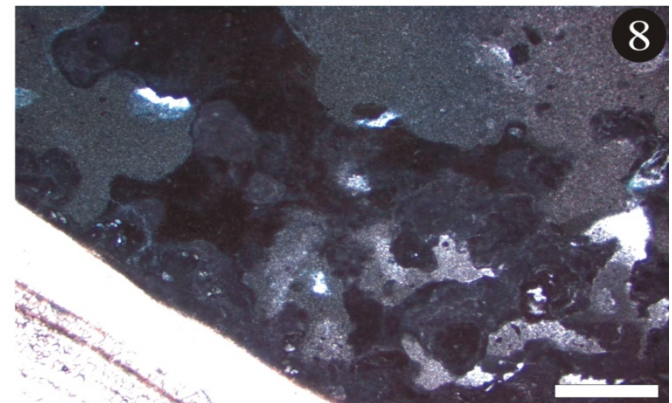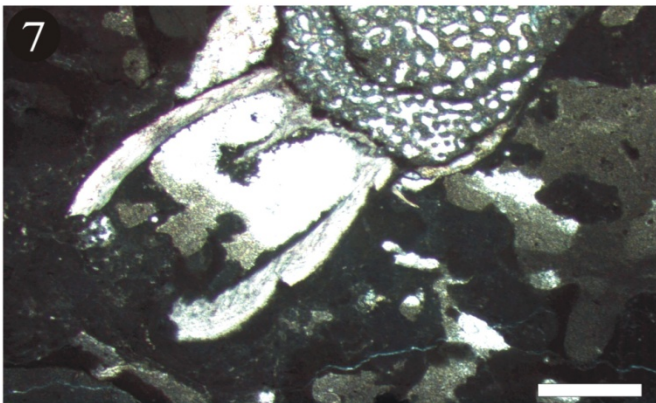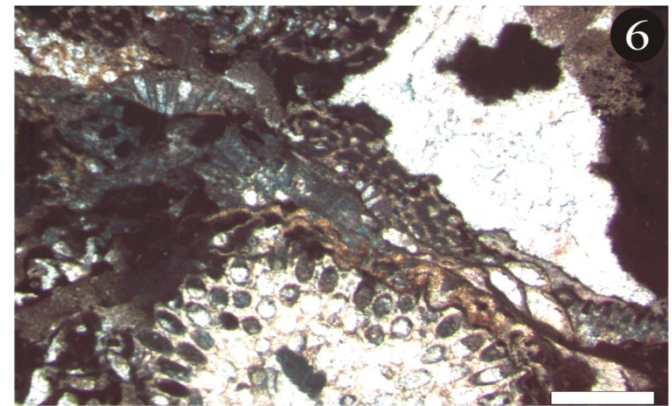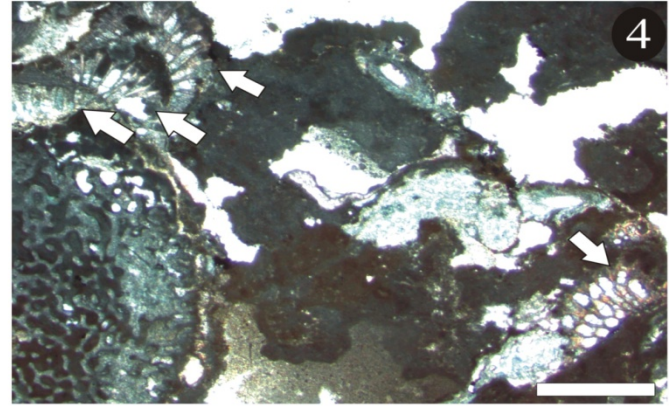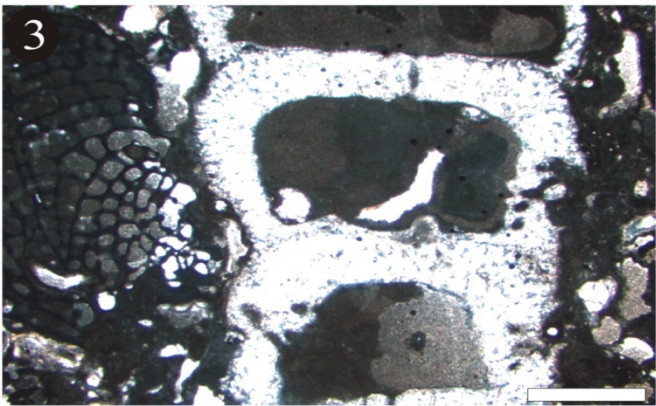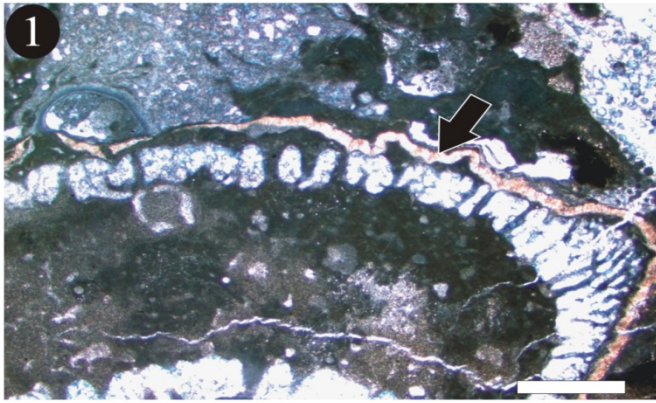
Plate XVII

<u>*Amblysiphonella – Megalodon* association</u> (Figs. 1-7)

<u>*Cassianothalamia* Gemeinschaft I</u> (Fig. 8)

1.- Filamentous porostromate-like structures (arrow) on the inner surface of *Megalodon*. Scale bar = 2 mm.

2.- Detail of 1. Scale bar = 1 mm.

3.- *Cassianothalamia zardinii* (center) associated to microbialitic crusts and *Terebella cf. lapilloides* (arrow). Scale bar = 5 mm.

4.- *Terebella* cf. *lapilloides* worm tube with geopetal infilling (above, center) and *Baccanella floriformis* dwelling in Type 2-microbialite. Scale bar = 1 mm.

5.- *Microtubus communis* (arrows) in microbialitic substrate. Scale bar = 500 μm.

6.- *Aka* ? cf. *cassianensis* spicules. Scale bar = 500 μm.

7.- Hexactinellid sponge mummy with some *Terebella cf. lapilloides* dwellings (arrow). Note stromatactoid cavity (upper right corner). Scale bar = 2 mm.

8.- *Cassianothalamia zardinii* (upper right corner) encrustation on top of a cement crust and a hexactinellid sponge. Scale bar = 5 mm.

Plate XVII
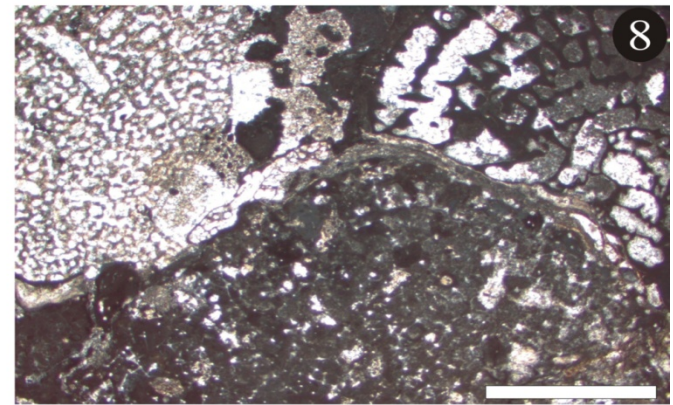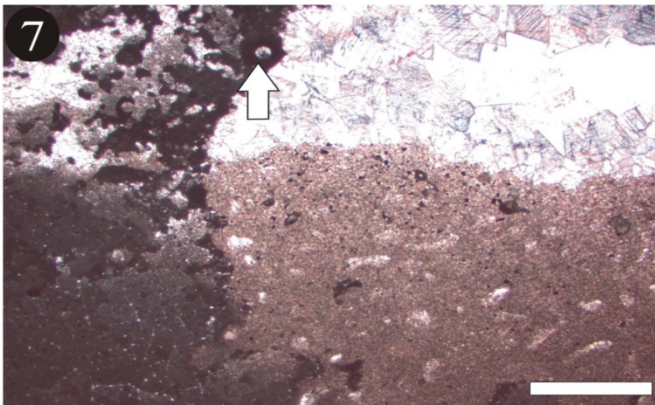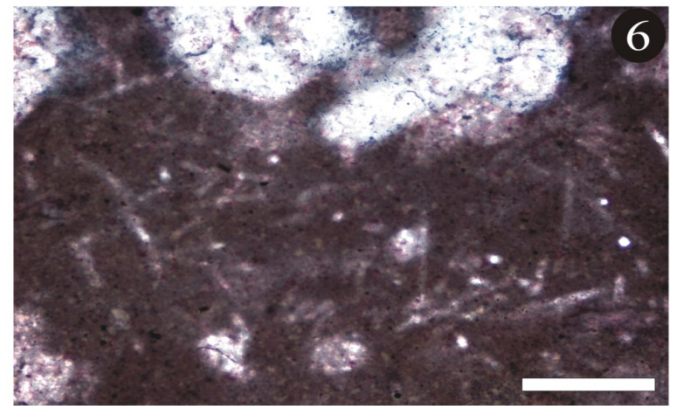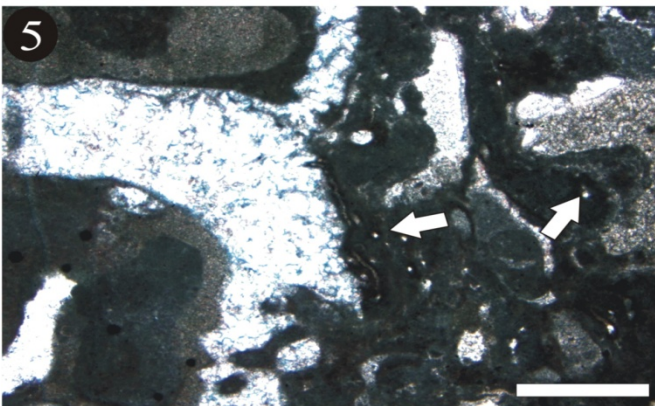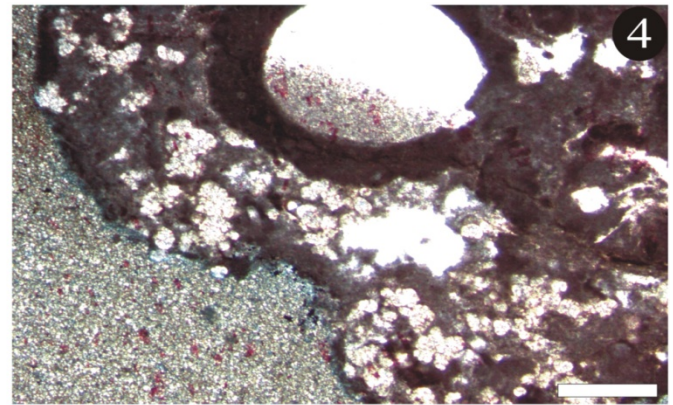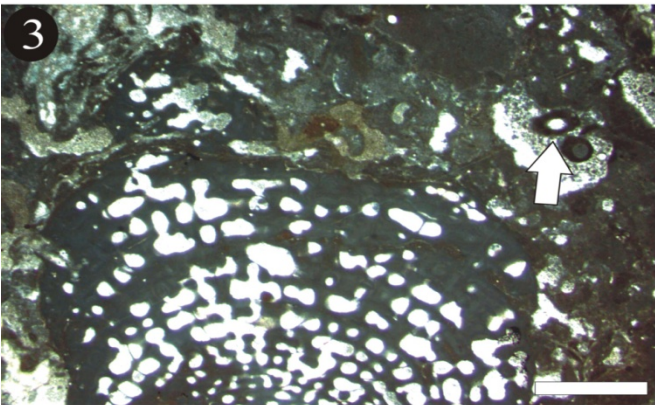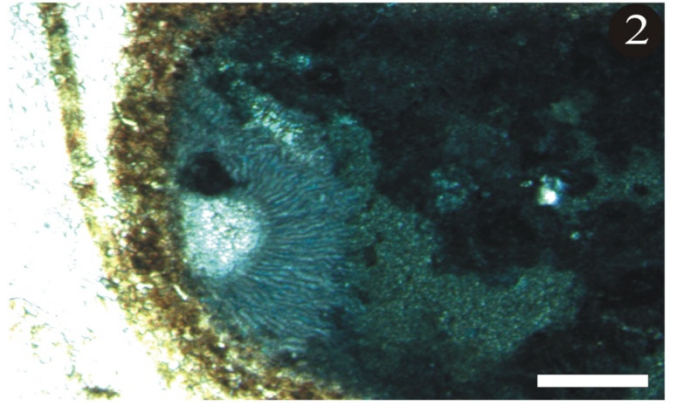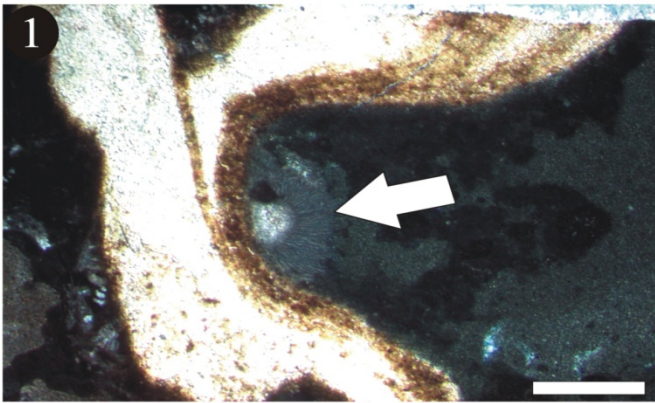
Plate XVIII

Cassianothalamia Gemeinschaft I

1.- The frame building sponge *Praecorynella.* Scale bar = 1 cm.

2.- *Aka* (arrow) boring in a microbialitic crust on top of *Praecorynella.* Scale bar = 500 μm

3.- *Baccanella floriformis* (center, right) in microbialitic crust associated to *Praecorynella.* Scale bar = 200 μm

4.- Branched undetermined bryozoans , being encrusted by *C. zardinii* (arrow) and by crust composed of microbialite and *Baccanella.* Scale bar = 5 mm

5.- *C. zardinii* encrustation atop an undetermined coralline sponge and being encrusted by a bryozoan. Scale bar = 5 mm.

6.- Lithistid sponge encrustation between *Atrochaetetes medius* (lower right corner) and an undetermined coralline sponge (*Zardinia*?) (compare Keupp et al., 1989) Scale bar = 5mm.

7.- *Sestrostomella* ? *robusta* with several *Terebella cf. lapilloides* worm tubes (arrows) Scale bar = 5 mm.

8.- Hexactine pseudomorphs associated with *Terebella cf. lapilloides* worm tubes (arrows). Scale bar = 2 mm.

Plate XVIII
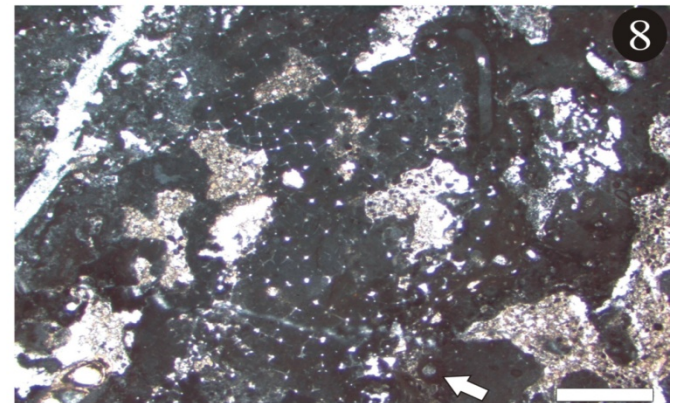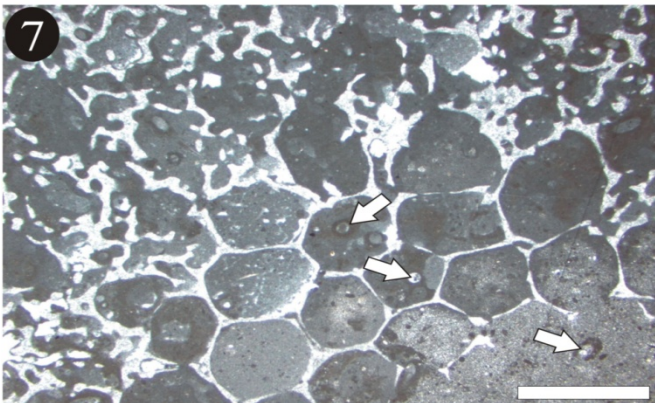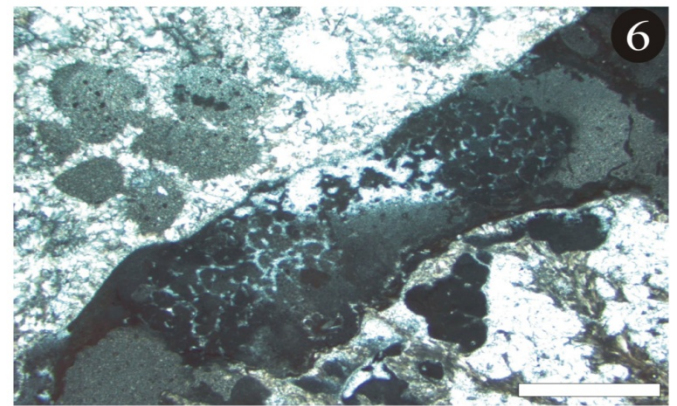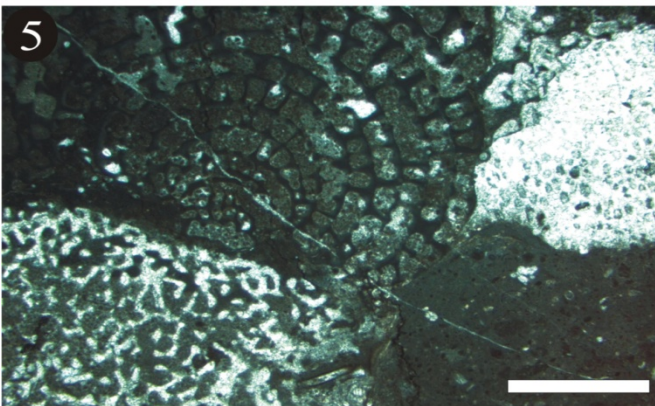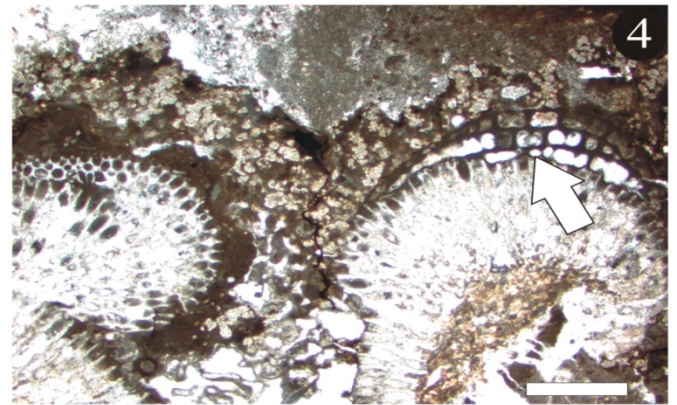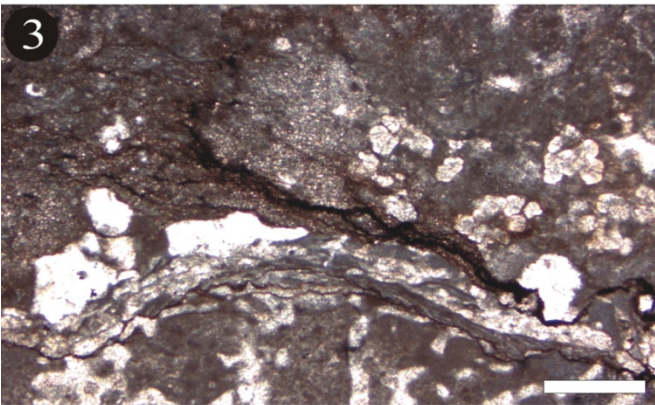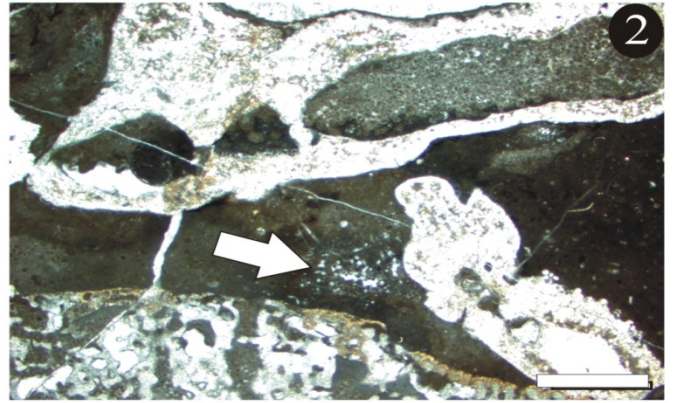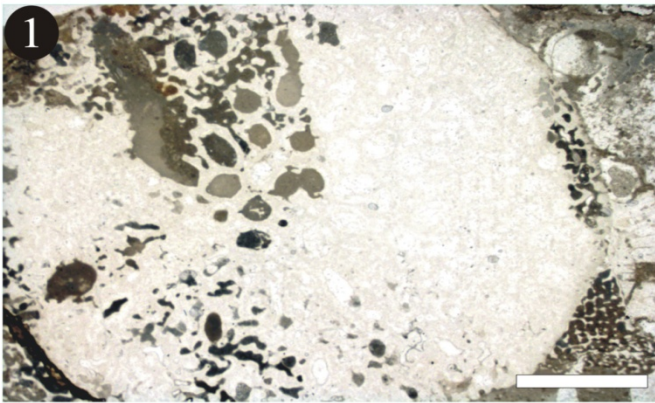
Plate XIX

<u>*Cassianothalamia* Gemeinschaft I</u> (Figs. 1-5)

<u>Mud Mound association II</u> (Fig. 6)

<u>Cathodoluminiscence of stromatactis</u> (Figs. 7-8)

1.- Encrusting complex of *Aulotortus* and *Koskinobullina socialis* (arrow). Scale bar = 1 cm.

2.- Enlargement of 1, showing *K.socialis* (white arrow) *and Aulotortus* (black arrow). Scale bar = 500 μm

3.- *Tubiphytes* cf. *obscurus* dwelling in a microbialitic crust on top of *Cassianothalamia zardinii*. Scale bar = 500 μm

4.- Hexactinellid sponge mummy, showing part of the ectosomal skeleton, constituted in part by dicho? triaenes (arrow). Scale bar = 500 μm

5.- Thecideid brachiopods, common dwellers of this community. Scale bar = 2 mm.

6.- *Terebella* cf. *lapilloides* (arrows) dwelling in microbialitic substrate. Scale bar = 500 μm

7.- Stromatactis cavity showing three generations of secondary (?) cements (White to black arrow) Normal view Scale bar = 500 μm.

8.- Same view of 7 under cathodoluminescence microscopy. Note the three generations of cements showing different luminescence. The outermost cement has a bright orange color, whereas the innermost cement displays a black color, possibly due to higher iron content (white to the black arrow). Scale bar = 500 μm.
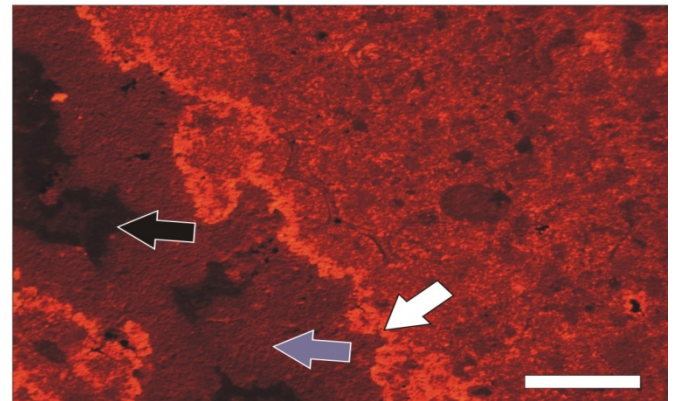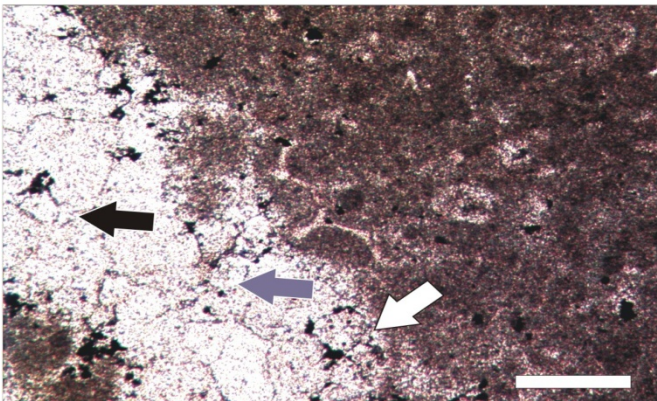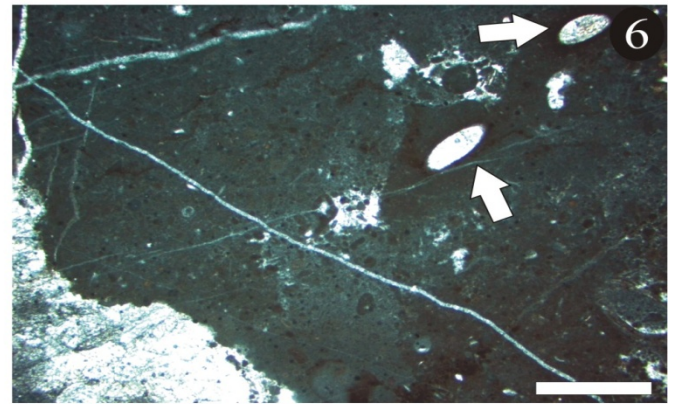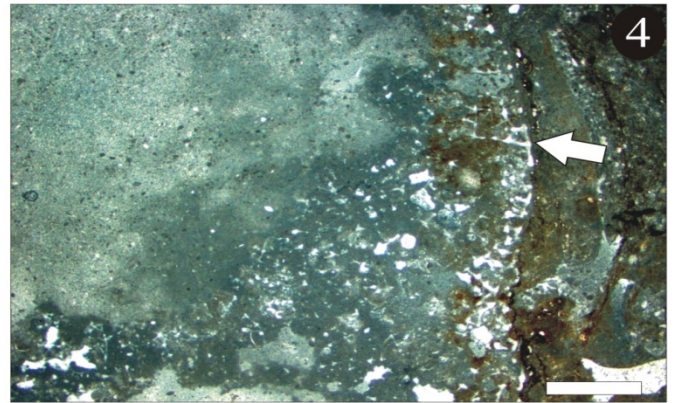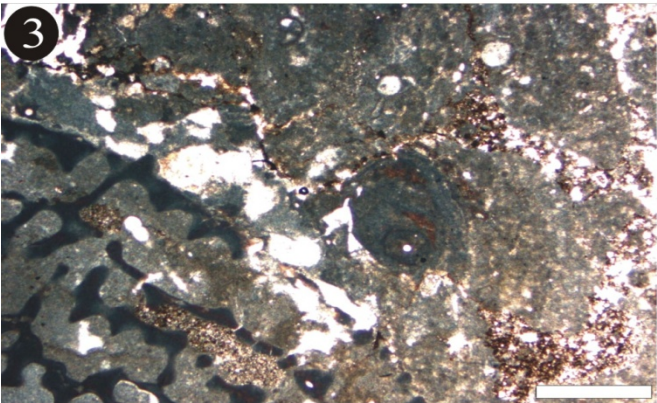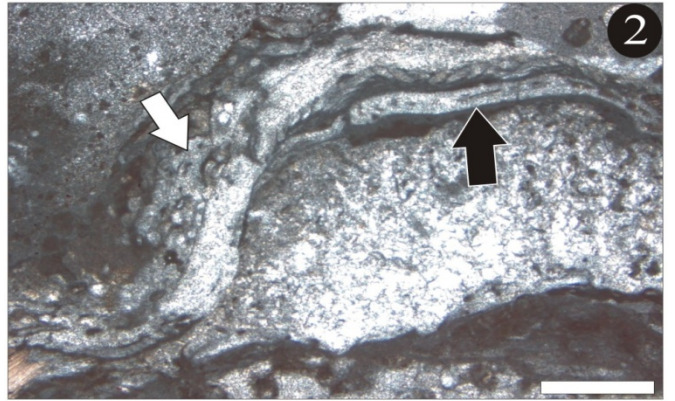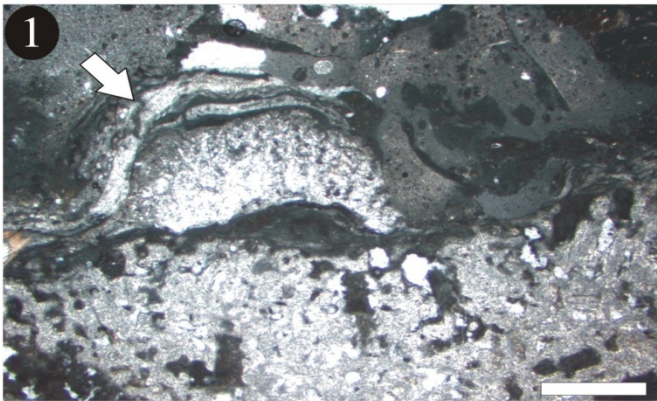
Plate XIX

Plate XX

<u>Cathodoluminiscence of selected facies</u> (Figs. 1-4)

1.- Microbialite type 1, showing a "cloudy" fabric. Normal view. Scale bar = 500 μm

2.- Same view of 1 under cathodoluminescence microscopy. Note the dark brown to orange color of peloids and the orange bright color of interstitial primary cements (arrow) Scale bar = 500 μm.

3.- Sphaerulitic microstructure of a chaetetid (white arrow). Secondary cements fill the pores (black arrow) Note the excellent preservation of the aragonite. Modified from Sánchez-Beristain et al. (accepted). Scale bar = 100 μm.

4.- Cathodoluminescence view of 3. Note the start of diagenesis from the center of the sphaerulite (white arrow), displaying a similar luminescence to the secondary cement (black arrow). Modified from Sánchez-Beristain et al. (accepted). Scale bar = 100 μm. Scale bar = 100 μm.

Plate XX
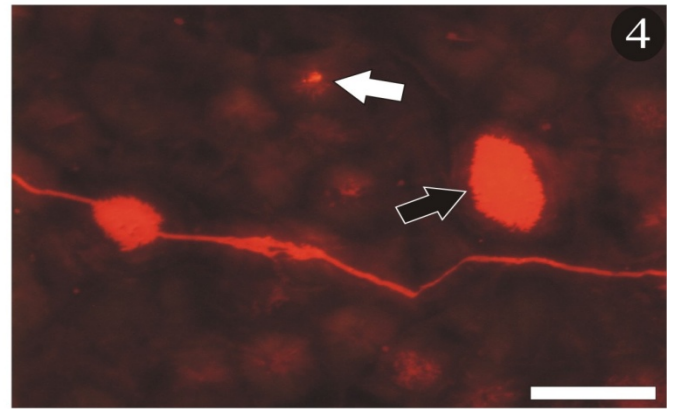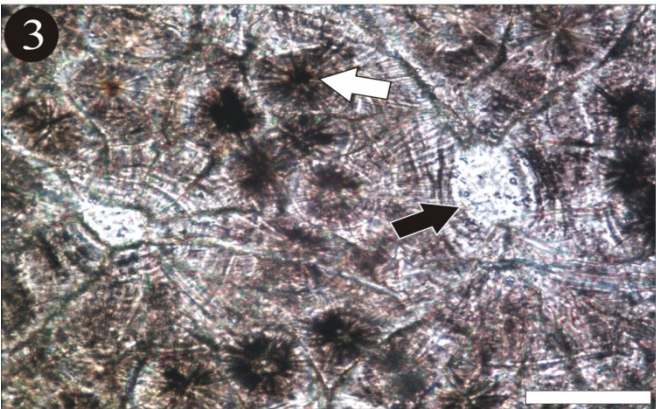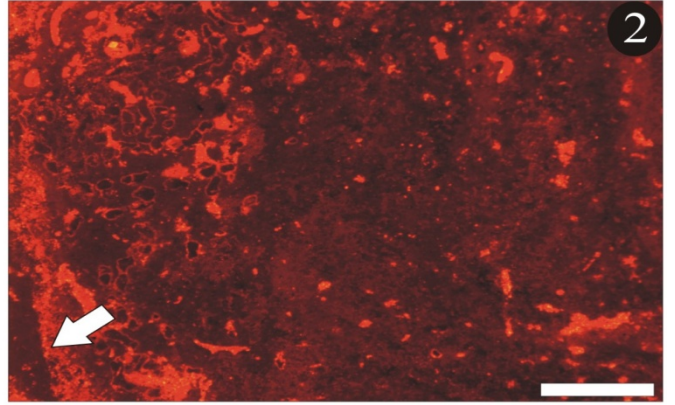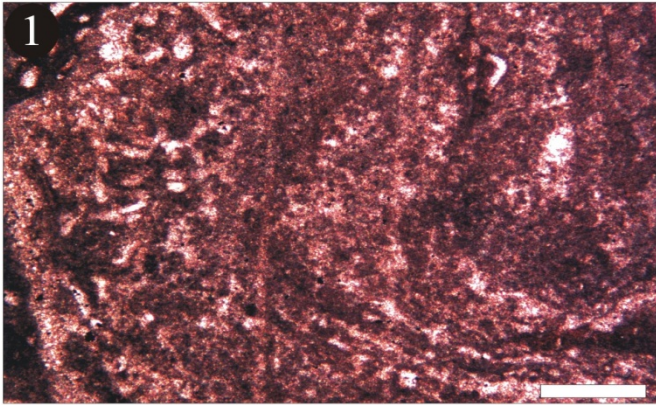
Appendix AI

Data matrix from 112 thin section samples and their corresponding microfacial percentages. Information is expressed in area percentage. See Appendix AII for key.

	Thin section	Remarks	Sample code	MIC	Dart	HEX	Cbr	Htr	St-1	St-2	C-1	Col	Pst	Srb	Prc	Mes	Ccip	P-1	Scas	S-1
1	J R III - 1		D-H 1	8	32	4	0	0	0	0	0	0	8	0	0	0	0	0	0	0
2	J R III - 10		D-H 2	10	37	5	0	0	0	0	0	0	4	0	0	0	0	0	0	0
3	J R III - 58		D-H 3	9	36	4	0	0	0	0	0	0	5	0	0	0	0	0	0	0
4	J R III - 79		D-H 4	6	39	4	0	0	0	0	0	0	15	0	0	0	0	0	0	0
5	J R III -88		D-H 5	8	34	6	0	0	0	0	0	0	13	0	0	0	0	0	0	0
6	J R III-16		D-H 6	8	40	4	0	0	0	0	0	0	5	0	0	0	0	0	0	0
7	J R III- 19		C-T 1	38	5	0	4	0	8	6	6	10	5	0	0	0	0	0	0	0
8	J R III - 33		C-T 2	50	0	0	3	5	4	3	13	6	0	0	0	0	0	0	0	0
9	J R III - 68		C-T 3	54	3	0	0	7	0	11	0	10	5	0	0	0	0	0	0	0
10	J R III - 2		C-T 4	45	9	0	0	9	0	9	0	7	7	0	0	0	0	0	0	0
11	IP FUB/ J R 1989	H.trias. Holot	C-T 5	35	0	0	0	5	0	0	15	8	0	0	0	0	0	0	0	0
12	J R II -50		C-T 6	61	0	0	0	3	0	0	3	4	0	0	0	0	0	0	0	0
13	IP FUB/ J R 1989	C.brev.holot	C-T 7	51	4	0	1	0	0	0	4	5	0	0	0	0	0	0	0	0
14	J R III - 53		C-M 1	3	0	4	0	0	0	0	0	0	0	0	0	23	0	0	0	0
15	J R III - A1		C-M 2	2	0	2	0	0	0	0	0	0	0	0	0	41	0	0	0	0
16	J R III - 46		C-M 3	5	4	0	0	0	0	0	0	0	0	0	0	28	0	0	0	0
17	J R III - 45		C-M 4	1	1	0	0	0	0	0	0	0	0	0	0	34	0	0	0	0
18	J R II - 69		C-M 5	1	0	5	0	0	0	0	0	0	0	0	0	26	0	0	0	0
19	J R III - B3 47		C-M 6	5	1	7	0	0	0	0	0	0	0	0	0	29	0	0	0	0
20	J R III - 99		C-M 7	2	0	1	0	0	0	0	0	0	0	0	0	20	0	0	0	0
21	J R III P G 1- 42		C-S 1	72	3	0	0	0	0	0	0	0	0	0	0	0	0.1	0.1	0	0
22	J R III P G 1 - 80		C-S 2	68	12	0	0	0	0	0	0	0	0	0	0	0	0.1	0.1	0	0
23	J R III P G 1- 103		C-S 3	57	11	0	0	0	0	0	0	0	0	0	0	0	0.1	0.1	0	0
24	J R III P G 1- 104		C-S 4	76	3	0	0	0	0	0	0	0	0	0	0	0	0.1	0.1	0	0
25	J R III P G 1- 74		C-S 5	68	10	0	0	0	0	0	0	0	0	0	0	0	0.1	0.1	0	0
26	J R II P G 1- 20		C-S 6	64	0	0	0	0	0	0	0	0	0	0	0	0	0.1	0.1	0	0
27	J R II P G 1- 21		C-S 7	71	5	0	0	0	0	0	0	0	0	0	0	0	0.1	0.1	0	0
28	J R II P G 1- 22		C-S 8	60	18	0	0	0	0	0	0	0	0	0	0	0	0.1	0.1	0	0
29	MI - 6		T-M 1	80	5	0	0	0	0	0	0	0	0	0	4	0	0	0	0	0
30	MI - 10/ 1		T-M 2	66	9	0	0	0	0	0	0	0	0	0	5	0	0	0	0	0
31	J R III - 106		T-M 3	70	0	0	0	0	0	0	0	0	0	0	9	0	0	0	0	0
32	J R III - 32		T-M 4	72	6	0	0	0	0	0	0	0	0	0	1	0	0	0	0	0
33	MI - 7		T-M 5	70	10	0	0	0	0	0	0	0	0	0	1	0	0	0	0	0
34	MI - 9		T-M 6	54	0	0	0	0	0	0	0	0	0	0	0	0	0	0	0	0
35	M IV -2		C-G II 1	55	0	2	0	0	0	0	0	0	0	0	0	0	0	0	0	0
36	M IV -3		C-G II 2	55	0	0	0	0	0	0	0	0	0	0	0	0	0	0	0	0
37	M VI-11		C-G II 3	31	0	10	0	0	0	0	0	0	0	0	0	0	0	0	0	0
38	M V -3		C-G II 4	56	0	2	0	0	0	0	0	0	0	0	0	0	0	0	0	0
39	M V -5		C-G II 5	52	0	5	0	0	0	0	0	0	0	0	0	0	0	0	0	0
40	M V -2		C-G II 6	62	0	2	0	0	0	0	0	0	0	0	0	0	0	0	0	0
41	M VII - 3		P-R I 1	17	4	0	0	0	0	0	0	0	0	0	0	0	0	0	0	0
42	M VIII - 2		P-R I 2	15	0	0	0	0	0	0	0	0	0	0	0	0	0	0	0	0
43	M VIII - 3		P-R I 3	17	0	0	0	0	0	0	0	0	0	0	0	0	0	0	0	0
44	M IX -3		P-R I 4	16	7	0	0	0	0	0	0	0	0	0	0	0	0	0	0	0
45	M XXXII - 2		P-R I 5	24	3	0	0	0	0	0	0	0	0	0	0	0	0	0	0	0
46	M XXXII - 5L		P-R I 6	26	4	0	0	0	0	0	0	0	0	0	0	0	0	0	4	0
47	FSSA V - 4L		P-R I 7	25	0	0	0	4	0	0	0	0	0	0	0	0	0	0	0	0
48	FSSA V - 7D		P-R I 8	21	0	4	0	0	0	0	0	0	0	0	0	0	0	0	0	0
49	FSSA V - 7U		P-R I 9	47	0	0	0	0	0	0	0	0	0	0	0	0	0	0	0	0
50	FSSA VII - 3		P-R I 10	26	5	0	0	0	0	0	0	0	0	0	27	0	0	0	0	0
51	FSSA VII - 4		P-R I 11	21	7	0	0	0	0	0	0	0	0	0	34	0	0	0	0	0
52	FSSA VII - 6		P-R I 12	15	1	0	0	0	0	0	0	0	0	0	20	0	0	0	0	0
53	IP FUB J R/ 1992	M. mega holot	P-R I 13	22	3	0	0	0	0	0	0	0	0	0	0	0	0	0	0	0
54	IP FUB J R/ 1989	M kazm holot.	P-R I 14	33	6	0	0	0	0	0	0	0	0	0	0	0	0	0	10	0
55	M X - 5		M-M 1	85	0	0	0	0	0	0	0	0	0	0	0	0	0	0	0	0
56	M X - 8		M-M 2	76	0	0	0	0	0	0	0	0	0	0	0	0	0	0	0	0
57	M X - 2L		M-M 3	74	0	0	0	0	0	0	0	0	0	0	0	0	0	0	0	0
58	M X - 2R		M-M 4	74	0	0	0	0	0	0	0	0	0	0	0	0	0	0	0	0
59	M X -6		M-M 5	69	0	0	0	0	0	0	0	0	0	0	0	0	0	0	0	0
60	J R III - 76		P-R II 1	32	13	0	0	0	0	0	0	0	0	0	0	0	0	0	30	0
61	J R III - 25		P-R II 2	31	9	0	0	0	0	0	0	0	0	0	0	0	0	0	33	4
62	J R III - 4		P-R II 3	24	9	0	0	0	0	0	0	0	0	0	0	0	0	0	43	3
63	J R III - 11		P-R II 4	15	8	0	0	0	0	0	0	0	0	0	0	0	0	0	17	0
64	J R III - 70		P-R II 5	23	12	0	0	0	0	0	0	0	0	0	0	0	0	0	49	6
65	J R III - 121		P-R III 1	13	0	0	0	0	0	0	0	0	0	0	0	0	0	0	0	0
66	J R III - 29		P-R III 2	9	0	0	0	0	0	0	0	0	0	0	0	0	0	0	0	0
67	J R III - 14		P-R III 3	15	0	0	0	0	0	0	0	0	0	0	0	0	0	0	0	0
68	J R III - 20		P-R III 4	10	0	0	0	0	0	0	0	0	0	0	0	0	0	0	0	0
69	FSSA XXV 1		C-m 1	24	0	0	0	0	0	0	0	0	0	0	0	0	0	0	0	0
70	FSSA XXV - 7		C-m 2	26	0	0	0	0	0	0	0	0	0	0	0	0	0	0	0	0
71	FSSA XXV - 3L		C-m 3	30	0	0	0	0	0	0	0	0	0	0	0	0	0	0	0	0
72	FSSA XXV - 2L		C-m 4	19	0	0	0	0	0	0	0	0	0	0	0	0	0	0	0	0
73	FSSA XXV - 6		C-m 5	35	0	0	0	0	0	0	0	0	0	0	0	0	0	0	0	0
74	FSSA XXV - 4		C-m 6	33	0	0	0	0	0	0	0	0	0	0	0	0	0	0	0	0
75	FSSA XXV - 8		C-m 7	22	0	0	0	0	0	0	0	0	0	0	0	0	0	0	0	0
76	FSSA XXV - 11		C-m 8	35	0	0	0	0	0	0	0	0	0	0	0	0	0	0	0	0
77	FSSA XXV - 9		C-m 9	37	0	0	0	0	0	0	0	0	0	0	0	0	0	0	0	0
78	J R Cas 27		C-m 10	26	0	0	0	0	0	0	0	0	0	0	0	0	0	0	0	0
79	J R II - 2		A-M 1	25	0	0	0	0	0	2	0	0	0	0	0	0	0	0	0	0
80	CG I - 1		C-G I 1	32	0	6	0	0	2	0	0	0	0	0	16	0	0	0	1	0
81	CG I - 2		C-G I 2	27	0	14	0	0	0	0	0	0	0	0	12	0	0	0	0	0
82	J R Cas 22		C-G I 3	22	0	10	0	0	0	0	0	0	0	0	21	0	0	0	0	0
83	CG I - 4		C-G I 4	41	0	10	0	0	0	0	0	0	0	0	0	0	0	0	0	0
84	CG I - 5		C-G I 5	13	0	19	0	0	0	0	0	0	0	0	35	0	0	0	0	0
85	J R Cas 14		C-G I 6	25	0	10	0	0	0	0	0	0	0	0	16	0	0	0	0	0
86	J R Cas 21		C-G I 7	23	0	14	0	0	0	0	0	0	0	0	32	0	0	0	0	0
87	CG I - 8		C-G I 8	20	0	5	0	0	0	0	0	0	0	0	27	0	0	0	0	0
88	J R Cas 13		C-G I 9	34	0	0	0	0	0	0	0	0	0	0	24	0	0	0	0	0
89	CG I - 10		C-G I 10	36	0	0	0	0	0	0	0	0	0	0	13	0	0	0	0	0
90	J R . Cas 7		C-G I 11	37	0	10	0	0	0	0	0	0	0	0	0	0	0	0	0	0
91	CG I - 12		C-G I 12	29	0	0	0	0	0	0	0	0	7	0	0	0	0	0	0	0
92	CG I - 13		C-G I 13	25	0	0	0	0	0	0	0	0	0	5	12	0	0	0	0	0
93	CG I - 14		C-G I 14	51	0	0	0	0	0	0	0	0	0	0	0	0	0	0	0	0
94	CG I - 15		C-G I 15	32	0	19	0	0	0	0	0	0	0	0	18	0	0	0	0	0
95	CG I - 16		C-G I 16	33	0	21	0	0	0	0	0	0	0	0	12	0	0	0	0	0
96	CG I - 17		C-G I 17	46	0	11	0	0	0	0	0	0	0	0	26	0	0	0	0	0
97	J R II - 5		C-G I 18	21	0	10	0	0	0	0	0	0	0	0	16	0	0	0	0	0
98	CG I - 19		C-G I 19	27	0	0	0	0	0	0	0	0	0	0	11	0	0	0	0	0
99	CG I - 20		C-G I 20	26	0	0	0	0	0	0	0	0	0	0	0	0	0	0	0	0
100	J R/ IP FUB 87-1	C.zardinii Holot.	C-G I 21	29	0	9	0	0	0	0	0	0	0	0	0	0	0	0	0	0
101	CG I - 22		C-G I 22	20	0	16	0	0	0	0	0	0	0	0	0	0	0	0	0	0
102	CG I - 23		C-G I 23	15	3	12	0	0	0	0	0	0	0	0	13	0	0	0	0	0
103	J R II - 15		C-G I 24	24	0	13	0	0	0	0	0	0	0	0	16	0	0	0	0	0
104	M XL - 1		M-M II 1	84	0	0	0	0	0	0	0	0	0	0	0	0	0	0	0	0
105	M XL - 2		M-M II 2	90	0	0	0	0	0	0	0	0	0	0	0	0	0	0	0	0
106	M XL - 3		M-M II 3	70	0	0	0	0	0	0	0	0	0	0	0	0	0	0	0	0
107	M XL - 4		M-M II 4	72	0	0	0	0	0	0	0	0	0	0	0	2	0	0	0	0
108	M XVII - 5R		M-M II 5	90	0	0	0	0	0	0	0	0	0	0	0	2	0	0	0	0
109	M XXI - 1		M-M II 6	92	0	0	0	0	0	0	0	0	0	0	0	0	0	0	0	0
110	M XXI - 2		M-M II 7	89	0	0	0	0	0	0	2	0	0	0	0	0	0	0	0	0
111	M XXI - 3		M-M II 8	80	0	0	0	0	0	0	0	0	0	0	0	0	0	0	0	0
112	M XXI - 4		M-M II 9	76	0	0	0	0	0	0	0	0	0	0	0	0	0	0	0	0

Appendix AI (continued)

Data matrix from 112 thin section samples and their corresponding microfacial percentages. Information is expressed in area percentage. See Appendix AII for key.

#	Thin section	Remarks	Sample code	Czit	Astr	Disj	Mkaz	Mmeg	LITH	Sram	Cass	Tcas	Zard	Epol	Thec	Mgp	Mgs	Ves	B-ch	Sph-C
1	JR III - 1		D-H 1	0	0	0	0	0	0	0	0	0	0	0	0	0	0	0	0	0
2	JR III - 10		D-H 2	0	0	0	0	0	0	0	0	0	0	0	0	0	0	0	0	0
3	JR III - 58		D-H 3	0	0	0	0	0	0	0	0	0	0	0	0	0	0	0	0	0
4	JR III - 79		D-H 4	0	0	0	0	0	0	0	0	0	0	0	0	0	0	0	0	0
5	JR III - 88		D-H 5	0	0	0	0	0	0	0	0	0	0	0	0	0	0	0	0	0
6	JR III - 16		D-H 6	0	0	0	0	0	0	0	0	0	0	0	0	0	0	0	0	0
7	JR III - 19		C-T 1	0	0	0	0	0	0	0	0	0	0	0	0	0	0	0	0	0
8	JR III - 33		C-T 2	0	0	0	0	0	0	0	0	0	0	0	0	0	0	0	0	0
9	JR III - 68		C-T 3	0	0	0	0	0	0	0	0	0	0	0	0	0	0	0	0	0
10	JR III - 2		C-T 4	0	0	0	0	0	0	0	0	0	0	0	0	0	0	0	0	0
11	IP FUB / JR 1989	H.trias. Holot	C-T 5	0	0	0	0	0	0	0	0	0	0	0	0	0	0	0	0	0
12	JR II - 50		C-T 6	0	0	0	0	0	0	0	0	0	0	0	0	0	0	0	0	0
13	IP FUB / JR 1989	C.brev.holot	C-T 7	0	0	0	0	0	0	0	0	0	0	0	0	0	0	0	0	0
14	JR III - 53		C-M 1	5	0	0	0	0	0	0	0	0	0	0	0	0	0	0	0	0
15	JR III - A1		C-M 2	5	0	0	0	0	0	0	0	0	0	0	0	0	0	0	0	0
16	JR III - 46		C-M 3	4	0	0	0	0	0	0	0	0	0	0	0	0	0	0	0	0
17	JR III - 45		C-M 4	0	0	0	0	0	0	0	0	0	0	0	0	0	0	0	0	0
18	JR II - 69		C-M 5	7	0	0	0	0	0	0	0	0	0	0	0	0	0	0	0	0
19	JR III - B3 47		C-M 6	10	0	0	0	0	0	0	0	0	0	0	0	0	0	0	0	0
20	JR III - 99		C-M 7	16	0	0	0	0	0	0	0	0	0	0	0	0	0	0	0	0
21	JR III PG 1- 42		C-S 1	0	0	0	0	0	5	0	0	0	0	0	0	0	0	0	4	0
22	JR III PG 1 - 80		C-S 2	0	0	0	0	0	0	0	0	0	0	0	0	0	0	0	3	0
23	JR III PG 1- 103		C-S 3	0	0	0	0	0	12	0	0	0	0	0	0	0	0	0	7	0
24	JR III PG 1- 104		C-S 4	0	0	0	0	0	3	0	0	0	0	0	0	0	0	0	5	0
25	JR III PG 1- 74		C-S 5	0	0	0	0	0	7	0	0	0	0	0	0	0	0	0	5	0
26	JR II PG 1- 20		C-S 6	0	0	0	0	0	11	0	0	0	0	0	0	0	0	0	2	0
27	JR II PG 1- 21		C-S 7	0	0	0	0	0	2	0	0	0	0	0	0	0	0	0	10	0
28	JR II PG 1- 22		C-S 8	0	0	0	0	0	0	0	0	0	0	0	0	0	0	0	2	0
29	MI - 6		T-M 1	0	0	0	0	0	0	0	0	0	0	0	0	0	0	0	4	0
30	MI - 10/ 1		T-M 2	0	0	0	0	0	0	0	0	0	0	0	0	0	0	0	2	0
31	JR III - 106		T-M 3	0	0	0	0	0	0	0	0	0	0	0	0	0	0	0	0	0
32	JR III - 32		T-M 4	0	0	0	0	0	0	0	0	0	0	0	0	0	0	0	0	0
33	MI - 7		T-M 5	0	0	0	0	0	0	0	0	0	0	0	0	0	0	0	5	0
34	MI - 9		T-M 6	0	0	0	0	0	0	0	0	0	0	0	0	0	0	0	0	0
35	M IV -2		C-G II 1	0	0	0	0	0	4	0	5	0	0	3	0	0	0	0	12	0
36	M IV -3		C-G II 2	0	0	0	0	0	6	0	6	0	0	5	0	0	0	0	8	0
37	M VI-11		C-G II 3	0	0	0	0	0	5	0	2	0	0	7	0	0	0	0	4	0
38	M V -3		C-G II 4	0	0	0	0	0	2	0	7	0	0	2	0	0	0	0	5	0
39	M V - 5		C-G II 5	0	0	0	0	0	2	0	12	0	0	1	0	0	0	0	9	0
40	M V - 2		C-G II 6	0	0	0	0	0	3	0	11	0	0	3	0	0	0	0	3	0
41	M VII - 3		P-R I 1	0	0	0	0	0	0	0	0	0	0	0	5	0	0	0	0	0
42	M VIII - 2		P-R I 2	0	0	0	1	0	0	0	0	0	0	6	0	1	0	0	0	0
43	M VIII - 3		P-R I 3	0	0	0	0	0	0	0	0	0	0	0	0	0	0	11	0	0
44	M IX -3		P-R I 4	0	0	0	0	1	0	0	2	0	0	0	0	0	0	7	0	0
45	M XXXII - 2		P-R I 5	0	0	0	0	0	0	0	0	0	0	0	5	0	0	4	0	0
46	M XXXII - 5L		P-R I 6	0	0	0	1	0	0	0	0	0	0	3	0	0	6	0	0	0
47	FSSA V - 4L		P-R I 7	2	0	0	0	0	0	0	0	0	3	3	0	0	0	0	0	0
48	FSSA V - 7D		P-R I 8	0	0	0	0	0	5	0	0	0	0	5	0	0	0	0	0	0
49	FSSA V - 7U		P-R I 9	0	0	0	0	0	0	0	0	0	14	2	0	0	0	0	0	0
50	FSSA VII - 3		P-R I 10	0	0	0	2	0	0	0	2	0	0	0	0	0	0	0	0	0
51	FSSA VII - 4		P-R I 11	0	0	0	2	0	0	0	0	0	0	1	0	8	0	0	0	0
52	FSSA VII - 6		P-R I 12	0	0	0	1	0	0	0	0	0	0	0	0	0	0	0	0	0
53	IP FUB JR/ 1992	M. mega holot	P-R I 13	5	0	0	0	3	0	0	0	0	0	0	0	0	0	0	0	0
54	IP FUB JR/ 1989	M kazm holot.	P-R I 14	0	0	0	2	0	0	0	0	0	0	0	0	0	0	0	0	0
55	M X - 5		M-M 1	0	0	0	0	0	0	0	0	0	0	0	0	0	0	0	0	0
56	M X - 8		M-M 2	0	0	0	0	0	0	0	0	0	0	0	0	0	0	0	0	0
57	M X - 2L		M-M 3	0	0	0	0	0	0	0	0	0	0	0	0	0	0	0	0	0
58	M X - 2R		M-M 4	0	0	0	0	0	0	0	0	0	0	0	0	0	0	0	0	0
59	MX - 6		M-M 5	0	0	0	0	0	0	0	0	0	0	0	0	0	0	11	0	0
60	JR III - 76		P-R II 1	0	0	0	0	0	0	0	0	0	0	0	0	0	0	0	0	0
61	JR III - 25		P-R II 2	0	0	0	0	0	0	0	0	0	0	0	0	0	0	0	0	0
62	JR III - 4		P-R II 3	0	0	0	0	0	0	0	0	0	0	0	0	0	7	0	0	0
63	JR III - 11		P-R II 4	0	0	0	0	0	0	0	0	0	0	0	0	0	5	0	0	0
64	JR III - 70		P-R II 5	0	0	0	0	0	0	0	0	0	0	0	0	0	0	0	0	0
65	JR III - 121		P-R III 1	0	0	0	0	0	36	0	0	0	0	10	0	0	0	0	9	0
66	JR III - 29		P-R III 2	0	0	0	0	0	29	0	0	0	0	3	0	0	0	0	11	0
67	JR III - 14		P-R III 3	0	0	0	0	0	20	0	0	0	0	7	0	0	0	0	7	0
68	JR III - 20		P-R III 4	0	0	0	0	0	38	0	0	0	0	4	0	0	0	0	13	0
69	FSSA XXV 1		C-m 1	0	0	0	0	0	0	0	0	0	0	0	0	0	0	0	0	42
70	FSSA XXV - 7		C-m 2	0	0	0	0	0	0	0	0	0	0	0	0	0	0	0	0	29
71	FSSA XXV - 3L		C-m 3	0	0	0	0	0	0	0	0	0	0	0	0	0	0	0	0	37
72	FSSA XXV - 2L		C-m 4	0	0	0	0	0	0	0	0	0	0	0	0	0	0	0	0	18
73	FSSA XXV - 6		C-m 5	0	0	0	0	0	0	0	0	0	0	0	0	0	0	0	0	29
74	FSSA XXV - 4		C-m 6	0	0	0	0	0	0	0	0	0	0	0	0	0	0	0	0	41
75	FSSA XXV - 8		C-m 7	0	0	0	0	0	0	0	0	0	0	0	0	0	0	0	0	36
76	FSSA XXV - 11		C-m 8	0	0	0	0	0	0	0	0	0	0	0	0	0	0	0	0	34
77	FSSA XXV - 9		C-m 9	0	0	0	0	0	0	0	0	0	0	0	0	0	0	0	0	30
78	JR Cas 27		C-m 10	0	0	0	0	0	0	0	0	0	0	0	0	0	0	0	0	35
79	JR II - 2		A-M 1	0	18	0	0	0	0	3	2	2	0	0	0	0	0	4	0	0
80	CG I - 1		C-G I 1	0	0	0	0	0	11	0	15	0	0	0	0	0	0	0	0	0
81	CG I - 2		C-G I 2	0	0	0	0	0	24	0	7	0	0	0	0	0	0	0	0	0
82	JR Cas 22		C-G I 3	0	0	0	0	0	21	0	12	0	0	0	0	0	0	0	0	0
83	CG I - 4		C-G I 4	0	0	0	0	0	9	0	2	0	0	0	0	0	0	0	0	0
84	CG I - 5		C-G I 5	0	0	0	0	0	20	0	0	0	0	0	0	0	0	0	0	0
85	JR Cas 14		C-G I 6	0	0	0	0	0	18	0	21	0	0	0	0	0	0	0	0	0
86	JR Cas 21		C-G I 7	0	0	9	0	0	0	0	12	0	0	0	0	0	0	0	0	0
87	CG I - 8		C-G I 8	0	0	0	0	0	16	0	4	0	0	0	0	0	0	0	0	0
88	JR Cas 13		C-G I 9	0	0	0	0	0	7	0	3	0	0	0	0	0	0	0	0	0
89	CG I - 10		C-G I 10	0	0	0	0	0	15	0	24	0	0	0	0	0	0	0	0	0
90	JR . Cas 7		C-G I 11	0	0	0	0	0	16	0	12	0	0	0	0	0	0	0	0	0
91	CG I - 12		C-G I 12	0	0	0	0	0	12	0	24	0	0	0	0	0	0	0	0	0
92	CG I - 13		C-G I 13	0	0	0	0	0	16	0	2	0	0	0	0	0	0	0	0	0
93	CG I - 14		C-G I 14	0	0	0	0	0	12	0	6	0	5	0	0	0	0	0	0	0
94	CG I - 15		C-G I 15	0	0	0	0	0	10	0	5	0	0	0	0	0	0	0	0	0
95	CG I - 16		C-G I 16	0	0	0	0	0	13	0	11	0	0	0	0	0	0	0	0	0
96	CG I - 17		C-G I 17	0	0	0	0	0	0	0	8	0	0	0	0	0	0	0	0	0
97	JR II - 5		C-G I 18	0	0	0	0	0	0	0	12	0	0	0	0	0	0	0	0	0
98	CG I - 19		C-G I 19	0	0	0	0	0	16	0	13	0	0	0	0	0	0	0	0	0
99	CG I - 20		C-G I 20	0	0	0	0	0	14	0	21	0	0	0	0	0	0	0	0	0
100	JR/ IPFUB 87-1	C.zardinii Holot.	C-G I 21	0	0	0	0	0	17	0	16	0	0	0	0	0	0	0	0	0
101	CG I - 22		C-G I 22	0	0	0	0	0	15	0	8	0	0	0	0	0	0	0	0	0
102	CG I - 23		C-G I 23	0	0	0	0	0	19	0	3	0	0	0	0	0	0	0	0	0
103	JR II - 15		C-G I 24	0	0	0	0	0	7	0	9	0	0	0	0	0	0	0	0	0
104	M XL - 1		M-M II 1	0	0	0	0	0	0	0	0	0	0	0	0	0	0	0	0	0
105	M XL - 2		M-M II 2	0	0	0	0	0	0	0	0	0	0	0	0	0	0	0	0	0
106	M XL - 3		M-M II 3	0	0	0	0	0	0	0	0	0	0	0	0	0	0	0	0	0
107	M XL - 4		M-M II 4	0	0	0	0	0	0	0	0	0	0	4	0	0	0	0	0	0
108	M XVII - 5R		M-M II 5	0	0	0	0	0	0	0	0	0	0	0	0	0	0	0	0	0
109	M XXI - 1		M-M II 6	0	0	0	0	0	0	0	0	0	0	0	0	0	0	0	0	0
110	M XXI - 2		M-M II 7	0	0	0	0	0	0	0	3	0	0	0	0	0	0	0	0	0
111	M XXI - 3		M-M II 8	0	0	0	0	0	0	0	0	0	0	0	0	0	0	0	0	0
112	M XXI - 4		M-M II 9	0	0	0	0	0	0	0	0	0	0	0	0	0	0	0	0	0

Appendix AI (continued)

Data matrix from 112 thin section samples and their corresponding microfacial percentages. Information is expressed in area percentage. See Appendix AII for key.

	Thin section	Remarks	Sample code	Br-1	Th-B	Meg	Amed	Ecc-1	Ecc-2	Ecc-3	Bal	Cor	Uv	Sr p1	Sr p2	Sr p3	Ch-2	Aul	Plex	Plv
1	J R III - 1		D-H 1	0	0	0	0	0	0	0	0	0	0.033	0.03	0	0	0	0	0.033	0.033
2	J R III - 10		D-H 2	0	0	0	0	0	0	0	0	0	0.033	0.03	0	0	0	0	0.033	0.033
3	J R III - 58		D-H 3	0	0	0	0	0	0	0	0	0	0.033	0.03	0	0	0	0	0	0.033
4	J R III - 79		D-H 4	0	0	0	0	0	0	0	0	0	0.066	0	0	0	0	0	0.033	0
5	J R III -88		D-H 5	0	0	0	0	0	0	0	0	0	0.033	0	0	0	0	0	0	0.033
6	J R III -16		D-H 6	0	0	0	0	0	0	0	0	0	0	0	0	0	0	0	0.033	0.033
7	J R III- 19		C-T 1	0	0	0	0	0	0	0	0	0	0	0	0.03	0	0	0	0	0
8	J R III - 33		C-T 2	0	0	0	0	0	0	0	0	0	0.03	0	0.03	0	0	0	0	0
9	J R III - 68		C-T 3	0	0	0	0	0	0	0	0	0	0	0	0.03	0	0	0	0	0
10	J R III - 2		C-T 4	0	0	0	0	0	0	0	0	0	0.03	0	0.03	0	0	0	0	0
11	IP FUB/ J R 1989	H.trias. Holot	C-T 5	0	0	0	0	0	0	0	0	0	0	0	0	0	0	0	0	0
12	J R II-50		C-T 6	0	0	0	0	0	0	0	0	0	0.03	0	0	0	0	0	0	0
13	IP FUB/ J R 1989	C.brev.holot	C-T 7	0	0	0	0	0	0	0	0	0	0	0	0	0	0	0	0	0
14	J R III - 53		C-M 1	0	0	0	0	0	0	0	0	12	0	0	0	0	0.03	0	0	0
15	J R III - A1		C-M 2	0	0	0	0	0	0	0	0	5	0	0	0	0	0.03	0	0	0
16	J R III - 46		C-M 3	0	0	0	0	0	0	0	0	3	0	0	0	0	0.03	0	0	0
17	J R III - 45		C-M 4	0	0	0	0	0	0	0	0	3	0.07	0	0	0	0.03	0	0	0
18	J R II - 69		C-M 5	0	0	0	0	0	0	0	0	6	0.07	0	0	0	0.07	0	0	0
19	J R III - B3 47		C-M 6	0	0	0	0	0	0	0	0	14	0	0	0	0	0	0	0	0
20	J R III - 99		C-M 7	0	0	0	0	0	0	0	0	0	0.03	0	0	0	0	0	0	0
21	J R III PG 1- 42		C-S 1	0	0	0	0	0	0	0	0	0	0	0	0.03	0	0	0	0	0
22	J R III PG 1 - 80		C-S 2	0	0	0	0	0	0	0	0	0	0	0	0.03	0	0	0	0	0
23	J R III PG 1- 103		C-S 3	0	0	0	0	0	0	0	0	0	0	0	0	0	0	0	0	0
24	J R III PG 1- 104		C-S 4	0	0	0	0	0	0	0	0	0	0	0	0.03	0	0	0	0	0
25	J R III PG 1- 74		C-S 5	0	0	0	0	0	0	0	0	0	0	0	0.03	0	0	0	0	0
26	J R II PG 1- 20		C-S 6	0	0	0	0	0	0	0	0	0	0	0	0	0	0	0	0	0
27	J R II PG 1- 21		C-S 7	0	0	0	0	0	0	0	0	0	0	0	0	0	0	0	0	0
28	J R II PG 1- 22		C-S 8	0	0	0	0	0	0	0	0	0	0	0	0	0	0	0	0	0
29	MI - 6		T-M 1	0	0	0	0	0	0	0	0	0	0	0	0	0	0	0	0	0.033
30	MI - 10/ 1		T-M 2	0	0	0	0	0	0	0	0	0	0	0	0	0	0	0	0	0
31	J R III - 106		T-M 3	0	0	0	0	0	0	0	0	0	0	0	0	0	0	0	0	0
32	J R III - 32		T-M 4	0	0	0	0	0	0	0	0	0	0	0	0	0	0	0	0	0.033
33	MI - 7		T-M 5	0	0	0	0	0	0	0	0	0	0	0	0	0	0	0	0	0
34	MI - 9		T-M 6	0	0	0	0	0	0	0	0	0	0.033	0	0	0	0	0	0	0.033
35	M IV -2		C-G II 1	0	0	0	0	0	0	0	0	0	0	0	0	0	0	0	0	0
36	M IV -3		C-G II 2	0	0	0	0	0	0	0	0	0	0	0	0	0	0	0	0	0
37	M VI-11		C-G II 3	0	0	0	0	0	0	0	0	0	0.03	0	0	0	0	0	0	0
38	M V -3		C-G II 4	0	0	0	0	0	0	0	0	0	0	0	0	0	0	0	0	0
39	M V -5		C-G II 5	0	0	0	0	0	0	0	0	0	0	0	0	0	0	0	0	0
40	M V -2		C-G II 6	0	0	0	0	0	0	0	0	0	0	0	0	0	0	0	0	0
41	M VII - 3		P-R I 1	0	0	0	0	1	0	0	34	0	0.03	0	0	0	0	0	0	0
42	M VIII - 2		P-R I 2	0	2	0	0	0	2	0	24	0	0	0	0	0	10	0	0	0.033
43	M VIII - 3		P-R I 3	0	0	0	0	0	1	0	41	0	0	0	0	0	13	0	0	0
44	M IX -3		P-R I 4	0	0	0	0	0	0	2	0	0	0	0	0	0.03	21	0	0	0
45	M XXXII - 2		P-R I 5	0	3	0	0	0	0	0	7	0	0	0	0	0	2	0	0	0
46	M XXXII - 5L		P-R I 6	0	0	0	0	3	0	0	15	0	0.03	0	0.03	0	0	0	0	0
47	FSSA V - 4L		P-R I 7	0	2	0	0	0	0	0	0	0	0.03	0	0.03	0	7	0	0	0
48	FSSA V - 7D		P-R I 8	0	0	0	0	0	0	0	0	0	0.03	0	0.03	0	12	0	0	0.033
49	FSSA V - 7U		P-R I 9	0	0	0	0	0	3	0	0	0	0.03	0	0	0	7	0	0	0
50	FSSA VII - 3		P-R I 10	0	4	0	0	0	0	1	0	0	0	0	0	0	0	0	0	0
51	FSSA VII - 4		P-R I 11	0	0	0	0	0	0	0	0	0	0	0	0	0	0	0	0	0
52	FSSA VII - 6		P-R I 12	0	4	0	0	0	0	0	0	0	0	0	0	0.03	15	0	0	0.033
53	IP FUB J R/ 1992	M. mega holot	P-R I 13	0	0	0	0	0	0	0	7	0	0	0	0	0	0	0	0	0
54	IP FUB J R/ 1989	M kazm holot.	P-R I 14	0	0	0	0	0	0	0	3	0	0	0	0	0	0	0	0	0
55	M X - 5		M-M 1	0	0	0	0	0	0	0	0	0	0	0	0	0	0	0	0	0
56	M X - 8		M-M 2	0	0	0	0	0	0	0	0	0	0	0	0	0	6	0	0	0
57	M X - 2L		M-M 3	0	0	0	0	0	0	0	0	0	0	0	0	0	12	0	0	0
58	M X - 2R		M-M 4	0	0	0	0	0	0	0	0	0	0	0	0	0	8	0	0	0
59	MX -6		M-M 5	0	0	0	0	0	0	0	0	0	0	0	0	0	0	0	0	0
60	J R III - 76		P-R II 1	0	0	0	0	0	0	0	0	0	0.03	0	0	0	0	0	0	0
61	J R III - 25		P-R II 2	0	0	0	0	0	0	0	0	0	0	0	0	0	0	0	0	0
62	J R III - 4		P-R II 3	0	0	0	0	0	0	0	0	0	0	0	0	0	0	0	0	0
63	J R III - 11		P-R II 4	0	0	0	0	0	0	0	0	0	0	0	0	0	0	0	0	0
64	J R III - 70		P-R II 5	0	0	0	0	0	0	0	0	0	0	0	0	0	0	0	0	0
65	J R III - 121		P-R III 1	0	0	0	0	0	0	0	0	0	0	0	0	0	0	0	0	0
66	J R III - 29		P-R III 2	0		0	0	0	0	0	0	0	0	0	0	0	0	0	0	0
67	J R III - 14		P-R III 3	0	0	0	0	0	0	0	0	0	0	0	0	0	6	0	0	0
68	J R III - 20		P-R III 4	0	0	0	0	0	0	0	0	0	0	0	0	0	0	0	0	0
69	FSSA XXV 1		C-m 1	0	0	0	0	0	0	0	0	0	0.03	0	0	0	0	0.033	0	0
70	FSSA XXV - 7		C-m 2	0	0	0	0	0	0	0	0	0	0.03	0	0	0	0	0.033	0	0
71	FSSA XXV - 3L		C-m 3	0	0	0	0	0	0	0	0	0	0.03	0	0	0	0	0.033	0	0
72	FSSA XXV - 2L		C-m 4	0	0	0	0	0	0	0	0	0	0	0	0	0	0	0.033	0	0
73	FSSA XXV - 6		C-m 5	0	0	0	0	0	0	0	0	0	0	0	0	0	0	0.033	0	0
74	FSSA XXV - 4		C-m 6	0	0	0	0	0	0	0	0	0	0	0	0	0	0	0.033	0	0
75	FSSA XXV - 8		C-m 7	0	0	0	0	0	0	0	0	0	0	0	0	0	0	0.033	0	0
76	FSSA XXV - 11		C-m 8	0	0	0	0	0	0	0	0	0	0	0	0	0	0	0.066	0	0
77	FSSA XXV - 9		C-m 9	0	0	0	0	0	0	0	0	0	0	0	0	0	0	0.066	0	0
78	J R Cas 27		C-m 10	0	0	0	0	0	0	0	0	0	0	0	0	0	0	0.066	0	0
79	J R II - 2		A-M 1	6	0	13	0	0	0	0	0	0	0	0	0	0	0	0	0	0
80	CG I - 1		C-G I 1	2	0	0	0	0	0	0	0	0	0.03	0.03	0	0	0	0	0	0
81	CG I - 2		C-G I 2	5	0	0	0	0	0	0	0	0	0	0	0.03	0	0	0	0	0
82	J R Cas 22		C-G I 3	3	1	0	1	0	0	0	0	0	0	0	0.03	0	0	0	0	0
83	CG I - 4		C-G I 4	10	0	0	11	0	0	0	0	0	0	0	0.03	0	0	0	0	0
84	CG I - 5		C-G I 5	0	0	0	0	0	0	0	0	0	0	0	0	0	0	0	0	0
85	J R Cas 14		C-G I 6	0	2	0	0	0	0	0	0	0	0.07	0	0	0	0	0	0	0
86	J R Cas 21		C-G I 7	0	0	0	0	0	0	0	0	0	0	0	0	0	0	0	0	0
87	CG I - 8		C-G I 8	8	0	0	0	0	0	0	0	0	0	0	0	0	0	0	0	0
88	J R Cas 13		C-G I 9	3	0	0	4	0	0	0	0	0	0.07	0	0	0	10	0	0	0
89	CG I - 10		C-G I 10	0	1	0	2	0	0	0	0	0	0	0	0	0	0	0	0	0
90	J R . Cas 7		C-G I 11	0	1	0	10	0	0	0	0	0	0.03	0	0	0	0	0	0	0
91	CG I - 12		C-G I 12	2	1	0	3	0	0	0	0	0	0	0	0	0	0	0	0	0
92	CG I - 13		C-G I 13	10	1	0	16	0	0	0	0	0	0	0	0.03	0	0	0	0	0
93	CG I - 14		C-G I 14	12	1	0	0	0	0	0	0	0	0	0	0	0	0	0	0	0
94	CG I - 15		C-G I 15	3	0	0	0	0	0	0	0	0	0.03	0	0.03	0	0	0	0	0
95	CG I - 16		C-G I 16	7	0	0	0	0	0	0	0	0	0.03	0	0	0	0	0	0	0
96	CG I - 17		C-G I 17	4	3	0	0	0	0	0	0	0	0	0	0	0	0	0	0	0
97	J R II - 5		C-G I 18	1	0	0	15	0	0	0	0	0	0.03	0	0	0	0	0	0	0
98	CG I - 19		C-G I 19	1	3	0	21	0	0	0	0	0	0.03	0	0	0	0	0	0	0
99	CG I - 20		C-G I 20	3	1	0	18	0	0	0	0	0	0	0	0	0	0	0	0	0
100	J R/ IP FUB 87-1	C.zardinii Holot.	C-G I 21	2	1	0	0	0	0	0	0	0	0	0	0.03	0	0	0	0	0
101	CG I - 22		C-G I 22	4	1	0	0	0	0	0	0	0	0	0	0	0	0	0	0	0
102	CG I - 23		C-G I 23	3	0	0	13	0	0	0	0	0	0	0	0	0	0	0	0	0
103	J R II - 15		C-G I 24	3	2	0	0	0	0	0	0	0	0.07	0	0.03	0	0	0	0	0
104	M XL - 1		M-M II 1	0	0	0	0	0	0	0	0	0	0	0	0	0	0	0	0	0
105	M XL - 2		M-M II 2	0	0	0	0	0	0	0	0	0	0	0	0	0	0	0	0	0
106	M XL - 3		M-M II 3	0	0	0	0	0	0	0	0	0	0	0	0	0	0	0	0	0
107	M XL - 4		M-M II 4	0	0	0	0	0	0	0	0	0	0	0	0	0	0	0	0	0
108	M XVII - 5R		M-M II 5	0	0	0	0	0	0	0	0	0	0	0	0	0	0	0	0	0
109	M XXI - 1		M-M II 6	0	0	0	0	0	0	0	0	0	0	0	0	0	0	0	0	0
110	M XXI - 2		M-M II 7	0	0	0	0	0	0	0	0	0	0	0	0	0	0	0	0	0
111	M XXI - 3		M-M II 8	0	0	0	0	0	0	0	0	0	0	0	0	0	0	0	0	0
112	M XXI - 4		M-M II 9	0	0	0	0	0	0	0	0	0	0	0	0	0	0	0	0	0

Appendix AI (continued)

Data matrix from 112 thin section samples and their corresponding microfacial percentages. Information is expressed in area percentage. See Appendix AII for key.

|	Thin section	Remarks	Sample code	Mcom	Apfr	Ter	Tub	Bacf	Rct	Lpor	Girv	Aka	Ks	*ISB*	Alloct	UDTD	MESP	CEM	total
1	JR III-1		D-H 1	0	0	0.066	0	0	0.033	0.066	0	0	0	2	30	9	0	6	99.3
2	JR III-10		D-H 2	0	0	0.066	0.066	0	0	0.033	0	0	0	1	26	11	0	5	99.3
3	JR III-58		D-H 3	0	0	0.066	0.033	0	0.033	0.066	0	0	0	1	26	11	0	5	97.3
4	JR III-79		D-H 4	0	0	0.066	0.066	0	0.033	0.066	0	0	0	2	18	9	0	6	99.3
5	JR III-88		D-H 5	0	0	0.033	0.066	0	0	0.033	0	0	0	2	23	7	0	4	97.2
6	JR III-16		D-H 6	0	0	0.066	0.066	0	0	0.033	0	0	0	1	26	9	0	6	99.2
7	JR III-19		C-T 1	1	0	0	0.03	0	0	0	0.1	0	0.1	0	13	1	2	0	99.3
8	JR III-33		C-T 2	1	0	0	0.03	0	0	0	0.1	0	0.1	0	11	2	1	0	99.3
9	JR III-68		C-T 3	1	0	0	0	0	0	0	0.1	0	0.066	0	5	1	1	0	98.2
10	JR III-2		C-T 4	0.033	0	0	0	0	0	0	0.1	0	0.1	0	10	0	0	1	97.3
11	IPFUB/JR 1989	H.trias. Holot	C-T 5	0.033	0	0	0	0	0	0	0.1	0	0.1	0	24	5	0	3	95.2
12	JR II-50		C-T 6	0.066	0	0	0	0	0	0	0.066	0	0.066	0	24	0	2	2	97.2
13	IPFUB/JR 1989	C.brev.holot	C-T 7	0.033	0	0	0	0	0	0	0.03	0	0.1	0	28	3	1	0	97.2
14	JR III-53		C-M 1	0	0	0	0.033	0.033	1	0	0	0	0	0	47	2	1	1	99.1
15	JR III-A1		C-M 2	0	0	0	0.033	0.033	0.066	0	0	0	0	0	27	11	1	4	98.2
16	JR III-46		C-M 3	0.033	0	0	0.033	0.033	0.033	0	0	0	0	0	45	5	1	3	98.2
17	JR III-45		C-M 4	0	0	0	0	0.033	0.033	0	0	0	0	0	38	10	1	7	95.2
18	JR II-69		C-M 5	0.033	0	0	0.033	0.033	0.066	0	0	0	0	0	50	4	0	0	99.3
19	JR III-B3 47		C-M 6	0.033	0	0	0.033	0.033	0.066	0	0	0	0	0	25	2	1	5	99.2
20	JR III-99		C-M 7	0.033	0	0	0.033	0	0.066	0	0	0	0	0	41	18	1	1	100.2
21	JR III PG1-42		C-S 1	0	0	0.033	0.033	0	0	0	0	0	0	0	6	2	0	2	94.3
22	JR III PG1-80		C-S 2	0	0	0.033	0.033	0	0	0	0	0	0	0	6	3	0	3	95.3
23	JR III PG1-103		C-S 3	0	0	0.033	0	0	0	0	0	0	0	0	4	0	2	1	94.2
24	JR III PG1-104		C-S 4	0	0	0.033	0.033	0	0	0	0	0	0	0	1	6	3	5	97.3
25	JR III PG1-74		C-S 5	0	0	0.033	0.033	0	0	0	0	0	0	0	7	0	0	1	98.3
26	JR II PG1-20		C-S 6	0	0	0.033	0.033	0	0	0	0	0	0	0	5	11	1	4	98.3
27	JR II PG1-21		C-S 7	0	0	0	0.033	0	0	0	0	0	0	0	4	4	2	1	99.2
28	JR II PG1-22		C-S 8	0	0	0.033	1	0	0	0	0	0	0	0	5	7	1	3	96.3
29	MI-6		T-M 1	0.033	0.033	0.033	0.033	0	0	0	0	0	0.033	0	6	0	0	1	100.2
30	MI-10/1		T-M 2	0.033	0.033	0	0.033	0	0	0	0	0	0.033	0	14	1	0	1	98.1
31	JR III-106		T-M 3	0.033	0.033	0.033	0.033	0	0	0	0	0	0	0	11	4	0	0	94.1
32	JR III-32		T-M 4	0.033	0	0.033	0.033	0	0	0	0	0	0.033	0	13	3	0	0	95.2
33	MI-7		T-M 5	0.033	0	0.033	0.033	0	0	0	0	0	0	0	5	5	0	1	97.1
34	MI-9		T-M 6	0	0	0.033	0.033	0	0	0	0	0	0.033	0	12	29	0	3	98.2
35	M IV-2		C-GII 1	0	0.033	0.066	0.033	0.033	0	0	0.033	0	0	0	0	16	1	1	99.2
36	M IV-3		C-GII 2	0	0.033	0.066	0.066	0.033	0	0	0	0.033	0	0	0	19	1	0	100.2
37	M VI-11		C-GII 3	0	0.033	0.066	0.066	0.033	0	0	0.033	0.033	0	0	0	34	1	2	96.3
38	M V-3		C-GII 4	0	0	0.066	0.033	0.033	0	0	0	0	0	0	0	20	0	3	97.1
39	M V-5		C-GII 5	0	0.033	1	0.066	0.033	0	0	0	0.033	0	0	0	13	0	3	98.2
40	M V-2		C-GII 6	0	0.033	1	0.066	0.066	0	0	0	0.033	0	0	0	12	1	1	99.2
41	M VII-3		P-RI 1	0	0	0	0	0	0	0.066	0.1	0	0.1	0	14	13	1	2	91.3
42	M VIII-2		P-RI 2	0	0	0	0	0	0	0.066	0.1	0	0.1	0	7	22	2	4	96.3
43	M VIII-3		P-RI 3	0	0	0	0	0	0	1	0.1	0	0.1	0	8	5	0	2	99.2
44	M IX-3		P-RI 4	0	0	0	0	0	0	0.066	0.1	0	0.066	0	35	0	0	3	94.3
45	M XXXII-2		P-RI 5	0	0	0	0	0	0	0.066	0.1	0	0.1	0	20	9	0	5	82.3
46	M XXXII-5L		P-RI 6	0	0	0	0	0	0	0.066	0.1	0	0.1	0	21	7	1	1	92.3
47	FSSA V-4L		P-RI 7	0	0	0	0	0	0	0.066	0.1	0	0.1	0	29	18	1	4	95.3
48	FSSA V-7D		P-RI 8	0	0	0	0	0	0	0.066	0.1	0	0.1	0	45	0	1	3	96.4
49	FSSA V-7U		P-RI 9	0	0	0	0	0	0	0.066	0.1	0	0.066	0	20	0	1	4	98.3
50	FSSA VII-3		P-RI 10	0	0	0	0	0	0	0.066	0.066	0	0.1	0	21	0	3	1	92.2
51	FSSA VII-4		P-RI 11	0	0	0	0	0	0	0.066	0.1	0	0.1	0	14	4	2	0	93.3
52	FSSA VII-6		P-RI 12	0	0	0	0	0	0	0	0.1	0	0.1	0	20	17	0	3	96.3
53	IPFUB JR/1992	M. mega holot	P-RI 13	0	0	0	0	0	0	0	0.1	0	0.033	0	39	12	3	0	94.1
54	IPFUB JR/1989	M kazm holot.	P-RI 14	0	0	0	0	0	0	0.033	0.1	0	0.1	0	26	16	0	3	99.2
55	M X-5		M-M 1	0	0	0	0	0	0	0	0	0	0	0	3	1	0	5	94.0
56	M X-8		M-M 2	0	0	0	0	0	0	0	0	0	0	0	5	2	0	10	99.0
57	M X-2L		M-M 3	0	0	0	0	0	0	0	0	0	0	0	6	1	0	5	98.0
58	M X-2R		M-M 4	0	0	0	0	0	0	0	0	0	0	0	5	0	0	8	95.0
59	MX-6		M-M 5	0	0	0	0	0	0	0	0	0	0	0	5	0	0	15	100.0
60	JR III-76		P-RII 1	0	0	0	0	0	0	0.1	0.066	0	0.066	0	21	3	0	0	99.3
61	JR III-25		P-RII 2	0	0	0	0	0	0	0.1	0.066	0	0.066	0	16	5	0	0	98.2
62	JR III-4		P-RII 3	0	0	0	0	0	0	0.1	0.066	0	0	0	7	6	1	0	100.2
63	JR III-11		P-RII 4	0	0	0	0	0	0	0.066	0.066	0	0.066	0	39	12	1	2	99.2
64	JR III-70		P-RII 5	0	0	0	0	0	0	0.1	0.1	0	0.066	0	7	1	0	1	99.3
65	JR III-121		P-RIII 1	0	0	0	0	0	0.1	0.033	0.033	0	0.066	0	17	13	0	0	98.2
66	JR III-29		P-RIII 2	0	0	0	0	0	0.033	0.1	0.033	0	0.066	0	26	14	0	4	96.2
67	JR III-14		P-RIII 3	0	0	0	0	0	0.033	0.1	0.033	0	0.066	0	23	16	0	3	97.2
68	JR III-20		P-RIII 4	0	0	0	0	0	0	0.1	0.033	0	0.033	0	24	9	0	8	98.2
69	FSSA XXV 1		C-m 1	0	0.033	0.033	0	0	0	0	0.066	0	0.066	0	29	1	0	0	96.3
70	FSSA XXV-7		C-m 2	0	0	0.033	0	0	0	0	0.066	0	0.066	0	39	1	0	0	95.2
71	FSSA XXV-3L		C-m 3	0	0	0.033	0	0	0	0	0.066	0	0.066	0	30	1	0	0	98.2
72	FSSA XXV-2L		C-m 4	0	0	0.033	0	0	0	0	0.066	0	0.066	0	57	4	0	0	98.2
73	FSSA XXV-6		C-m 5	0	0.033	0	0	0	0	0	0.1	0	0.066	0	26	0	0	0	90.2
74	FSSA XXV-4		C-m 6	0	0	0.033	0	0	0	0	0.066	0	0.066	0	15	8	0	0	97.2
75	FSSA XXV-8		C-m 7	0	0.033	0.033	0	0	0	0	0.033	0	0.066	0	30	4	0	0	92.2
76	FSSA XXV-11		C-m 8	0	0	0.033	0	0	0	0	0.066	0	0.066	0	22	2	0	0	93.2
77	FSSA XXV-9		C-m 9	0	0	0	0	0	0	0	0.066	0	0.066	0	30	0	0	0	97.2
78	JR Cas 27		C-m 10	0	0	0.033	0	0	0	0	0.066	0	0.033	0	27	6	0	0	94.2
79	JR II-2		A-M 1	0.033	0	0.066	0.033	0.033	0.033	0	0.033	0	0.033	0	21	1	0	2	99.3
80	CGI-1		C-GI 1	0	0	0.033	0.066	0.01	0.033	0	0.066	0	0.066	0	11	3	0	0	99.3
81	CGI-2		C-GI 2	0	0	0.033	0.066	0.01	0.033	0	0.066	0	0.033	0	3	4	0	3	99.3
82	JR Cas 22		C-GI 3	0	0	0.033	0.066	0.01	0.033	0	0.066	0.06	0.033	0	1	2	1	4	99.3
83	CGI-4		C-GI 4	0	0	0.033	0.033	0.01	0.033	0	0.066	0	0.066	0	11	3	0	1	98.3
84	CGI-5		C-GI 5	0	0	0.066	0.033	0.01	0.033	0	0.066	0.03	0.066	0	4	4	1	3	99.3
85	JR Cas 14		C-GI 6	0	0	0.066	0.066	0.01	0.033	0	0.066	0	0.066	0	2	2	0	2	98.4
86	JR Cas 21		C-GI 7	0	0	0.033	0.033	0.01	0.033	0	0.066	0	0.066	0	2	1	2	4	99.2
87	CGI-8		C-GI 8	0	0	0.033	0.033	0.01	0.066	0	0.066	0.03	0.066	0	13	2	1	2	98.3
88	JR Cas 13		C-GI 9	0	0	0.066	0.033	0.01	0.066	0	0.033	0	0.066	0	8	0	1	1	95.3
89	CGI-10		C-GI 10	0	0	0.033	0.033	0.01	0.033	0	0.066	0	0.033	0	6	3	0	0	100.2
90	JR. Cas 7		C-GI 11	0	0	0.033	0.033	0.01	0.033	0	0.066	0	0.033	0	2	8	0	2	98.2
91	CGI-12		C-GI 12	0	0	0.033	0.066	0.01	0.033	0	0.066	0	0.033	0	17	1	0	1	97.2
92	CGI-13		C-GI 13	0	0	0.033	0.033	0.01	0.033	0	0.066	0	0.066	0	3	3	0	6	99.3
93	CGI-14		C-GI 14	0	0	0.033	0.033	0.01	0.033	0	0.033	0	0.033	0	4	0	0	6	97.2
94	CGI-15		C-GI 15	0	0	0.033	0.033	0.01	0.033	0	0.033	0	0.033	0	2	3	0	7	99.2
95	CGI-16		C-GI 16	0	0	0.033	0.033	0.01	0.033	0	0.033	0.033	0.033	0	2	0	0	0	95.2
96	CGI-17		C-GI 17	0	0	0.033	0.033	0.01	0.033	0	0.033	0	0.033	0	1	0	0	1	100.2
97	JR II-5		C-GI 18	0	0	0.033	0.066	0.01	0.066	0	0.066	0	0.033	0	13	7	1	3	99.3
98	CGI-19		C-GI 19	0	0	0.033	0.066	0.01	0.066	0	0.066	0	0.033	0	3	1	1	2	99.3
99	CGI-20		C-GI 20	0	0	0.033	0.066	0.01	0.066	0	0.066	0	0.066	0	6	7	1	1	98.3
100	JR/IPFUB 87-1	C.zardinii Holot.	C-GI 21	0	0	0.066	0.033	0.01	0.033	0	0.066	0	0.066	0	12	11	1	0	98.3
101	CGI-22		C-GI 22	0	0	0.066	0.033	0.01	0.033	0	0.033	0	0.033	0	18	13	1	3	99.2
102	CGI-23		C-GI 23	0	0	0.066	0.033	0.01	0.033	0	0.033	0	0.066	0	4	11	1	0	97.2
103	JR II-15		C-GI 24	0	0	0.033	0.033	0.01	0	0	0.033	0	0.066	0	22	0	1	3	100.3
104	M XL-1		M-MII 1	0	0	0.01	0	0	0	0	0	0	0	0	2	3	0	11	100.0
105	M XL-2		M-MII 2	0	0	0.01	0	0	0	0	0	0	0	0	1	0	0	9	100.0
106	M XL-3		M-MII 3	0	0	0.01	0	0	0	0	0	0	0	2	1	1	0	23	98.0
107	M XL-4		M-MII 4	0	0	0.01	0	0	0	0	0	0	0	0	1	1	0	19	99.0
108	M XVII-5R		M-MII 5	0	0	0.01	0	0	0	0	0	0	0	0	1	0	0	6	99.0
109	M XXI-1		M-MII 6	0	0	0.066	0	0	0	0	0	0	0	0	0	0	0	5	97.1
110	M XXI-2		M-MII 7	0	0	0.01	0	0	0	0	0	0	0	0	0	0	0	5	99.0
111	M XXI-3		M-MII 8	0	0	0.03	0	0	0	0	0	0	0	0	0	10	0	7	97.0
112	M XXI-4		M-MII 9	0	0	0.03	0	0	0	0	0	0	0	0	0	13	0	4	93.0

Appendix AII

Key to each feature/ Taxon in Cluster Analysis from Appendix AI

MIC Microbialite
Dart *Dendronella articulate*
HEX Hexactinellid sponges
Cbr *Ceratoporella breviacanthostyla*
Htr *Hispidopetra triassica*
St-1 Stromatoporoid 1
St-2 Stromatoporoid 2
C -1 Chaetetid sponge 1
Col *Colospongia* sp
Pst *Petrosistroma stearnii*
Srb *Sestrostomella robusta*
Prc *Precorynella* sp
Mes *Mesophyllum* sp
Ccip *Cladogirvanella cipitensis*
P-1 Porostromate 1
Scas *Solenopora cassiana*
S1 *Solenopora* sp 1
Czit *Cryptocoelia zitteli*
Astr *Amblisyphonella strobiliformis*
Disj Disjectoporids
Mkaz *Murania kazmierczakii*
Mmeg *Murania megaspiculata*
LITH Lithistid sponge
Sram *Spongiomorpha ramosa*
Cass *Cassianothalamia zardinii*
Tcas *Thaumastocoelia cassiana*
Zard *Zardinia* sp
Epol *Eudea polymorpha*
Thec *Thecosmilia* sp
Mgp *Margarophylia* sp
Mgs *Margarosmilia* sp
Bal *Balatonia* sp
Ves *Vesicocaulis* sp
C-ch Branched ceratoporellid chaetetid
Sph-C Sphaerulitic chaetetid
Br-1 Bryozoan 1
Th-B Thecideid brachiopods
Meg *Megalodon* sp
Cor *Corynella* sp
Ch-2 Chaetetid sponge 2
Amed *Atrochaetetes medius*
Ecc 1 Encrusting coralline sponge 1
Ecc 2 Encrusting coralline sponge 2
Ecc 3 Encrusting coralline sponge 3
Uv *Uvanella* like thalamides
Srp 1 Serpullid worm tube 1
Srp 2 Serpullid worm tube 2
Srp 3 Serpullid worm tube 3
Aul *Aulotortus* sp

Plex *Plexoramea cerebriformis*
Plv *Planiinvoluta* sp
Mcom *Microtubus communis*
Aprf *Alpinophragmium perforatum*
Ter *Terebella* cf *lapilloides*
Tub *Tubiphytes* cf. *Obscurus*
Bacf *Baccanella floriformis*
Rct *Reptonoditrypa cautica*
Lpor *Ladinella porata*
Girv *Girvanella* sp
Aka *Aka* cf. *Cassianensis*
Ks *Koskinobullina socialis*
ISB *In situ* undetermined bivalves
Alloct Allochthonous sediment
UDTD Undetermined framework building fossils
MESP Microsparite
CEM Cements

Appendix AIII

UPGMA – Jaccard Phenogram for the 112 thin section samples. Brackets from the left show assumed associations before clustering; right brackets show obtained associations.
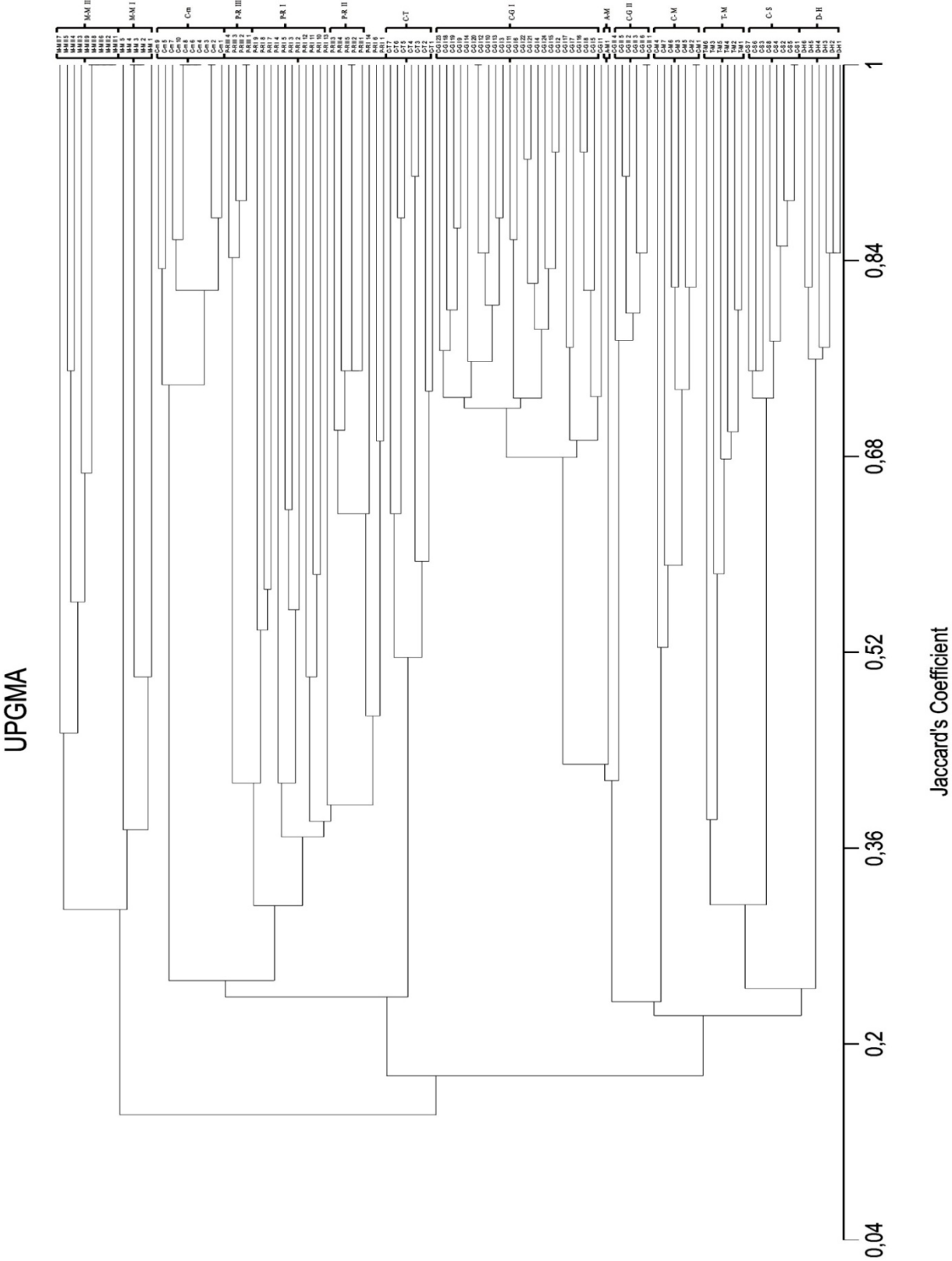
Appendix AIV

WPGMA – Jaccard Phenogram for the 112 thin section samples. Brackets from the left show assumed associations before clustering; right brackets show obtained associations.
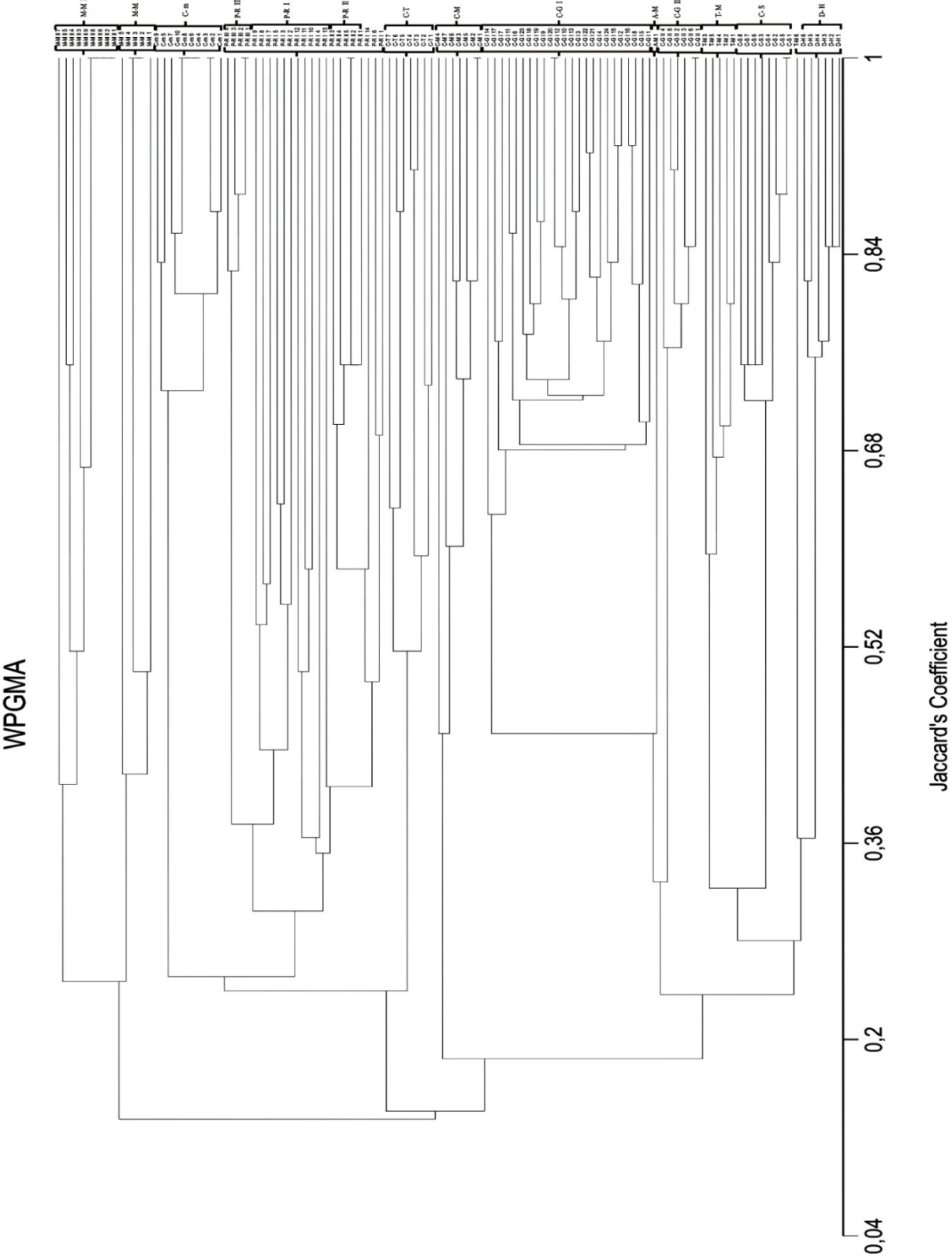
Appendix AV

Single Neighbor – Jaccard Phenogram for the 112 thin section samples. Brackets from the left show assumed associations before clustering; right brackets show obtained associations.
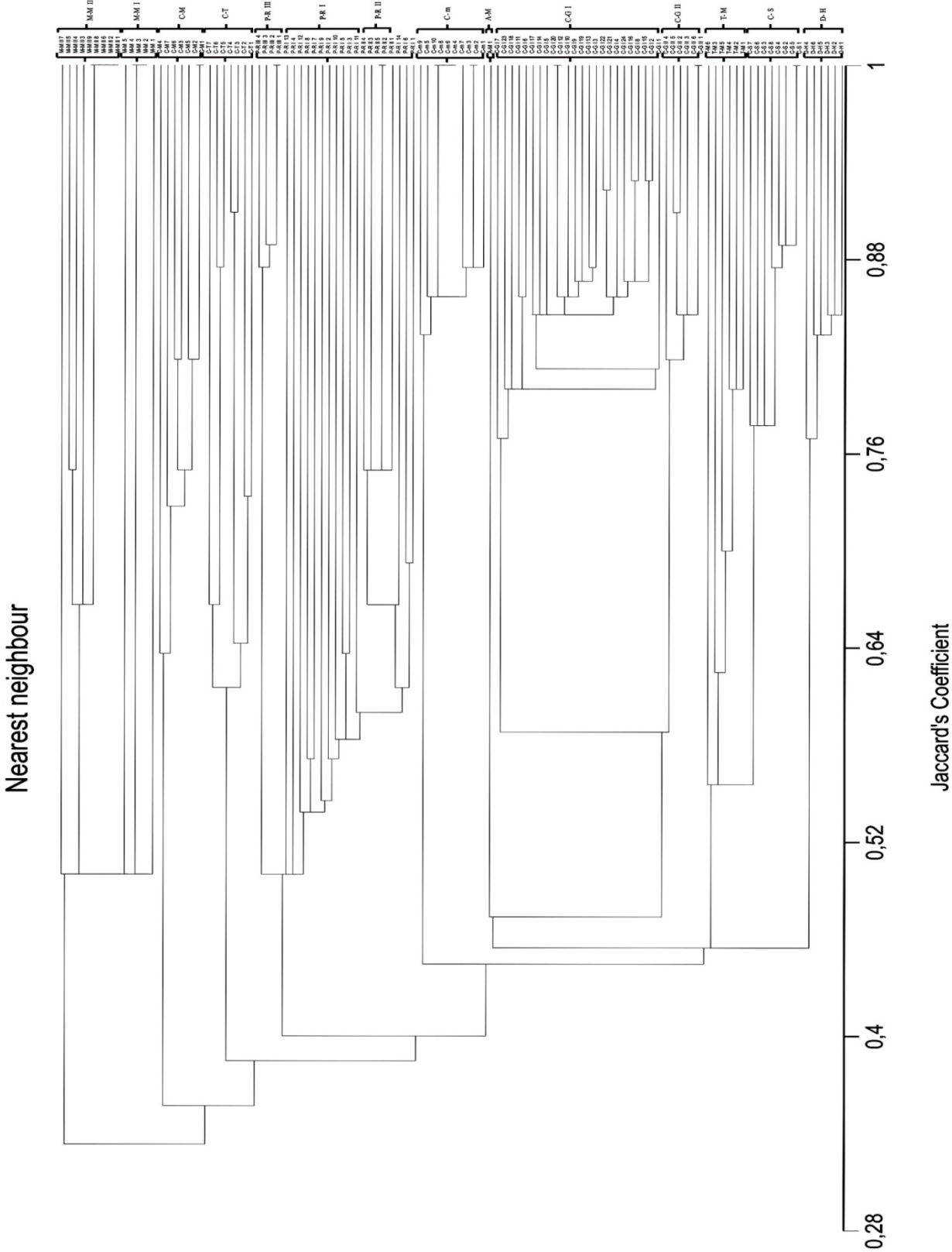
Appendix AVI

WPGMA – Bray Curtis Phenogram for the 112 thin section samples. Brackets from the right show obtained associations. All communities rich in microbialite -and poor in metazoans- (at least 50% of microbialitic content) are grouped in a single phenon.

x
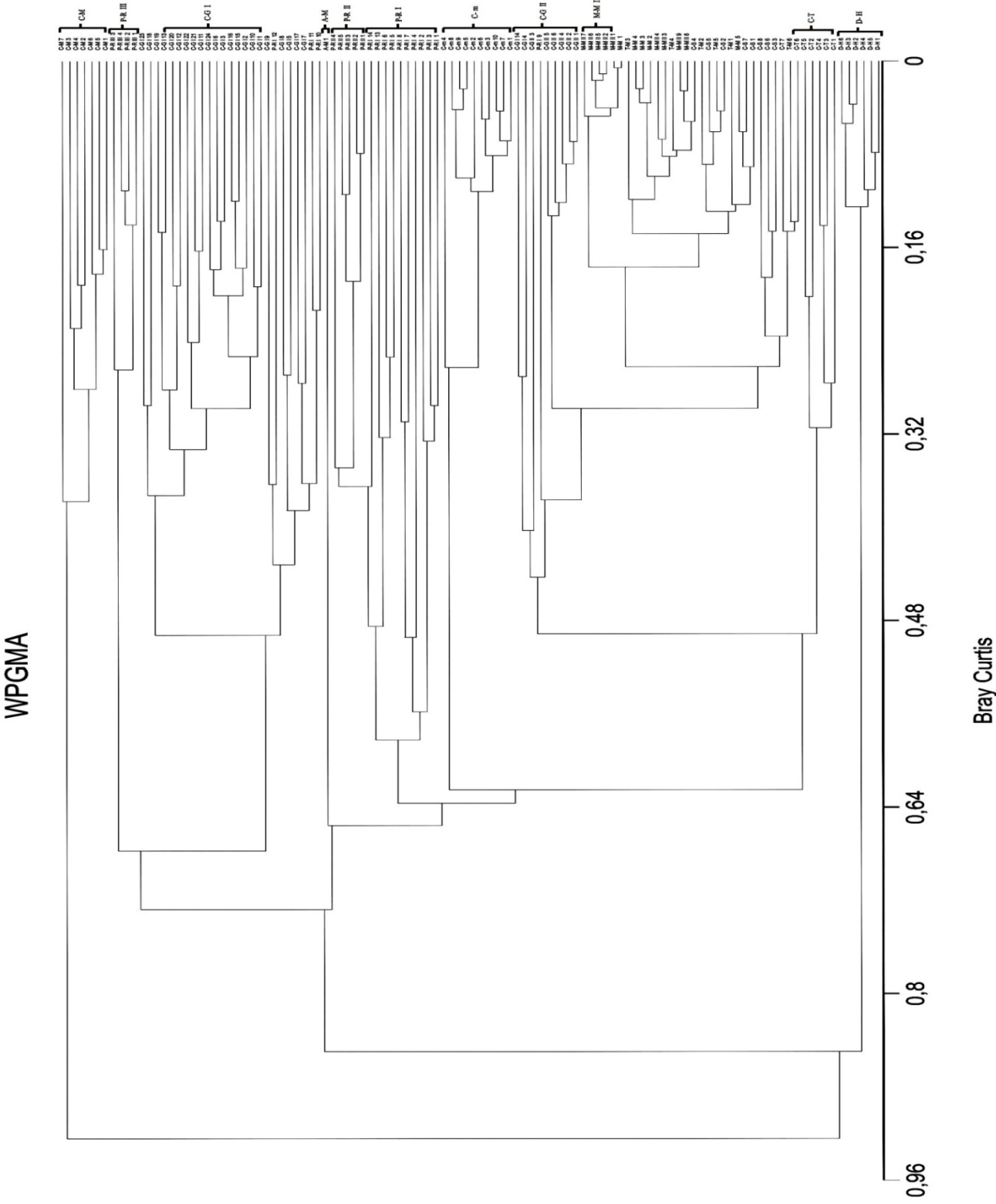
Appendix AVII

Raman spectra for a coral (a), a chaetetid aragonitic sponge (b) and a high Mg-calcite thrombolite (c). In the coral and the sponge signatures, peaks linked to the effects of lattice vibrations, the detection of ν4 in the plane bending mode and of ν1 symmetric mode of the carbonate ion indicate that an original aragonite mineralogy is still present. In the microbialitic signature, numerous peaks can be identified, like those related to symmetric and antisymmetric stretchings of the carbonate ion, but also C=C stretching and 2x ν2 overtone related peaks could be observed. In particular, antisymmetric stretching peak at 710 and 715 cm^{-1} suggests the existence of high Mg-calcite. From Sánchez-Beristain et al. (accepted).
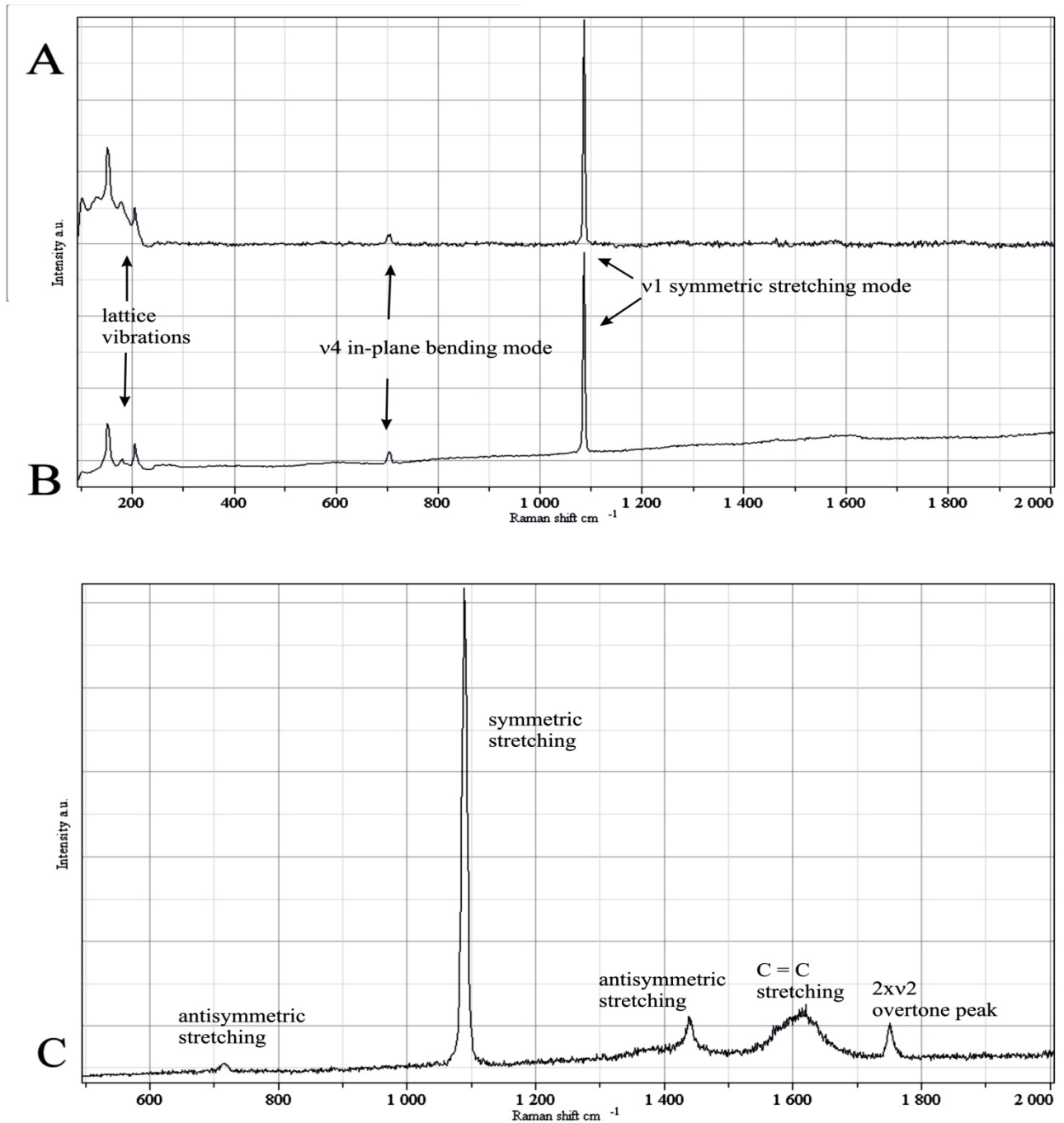
Appendix AVIII

LA-ICP-MS results for selected microbialites and associated facies. Concentrations are expressed in ppm.

MICROBIALITES	Mg24	Al27	Si29	P31	S34	Ti47	V51	Cr53	Mn55	Fe57	Co59	Ni60	Cu63	Zn66	Rb85
Cas12M1	13078.51	728.06	1531.44	568.13	418.53	45.39	3.87	5.07	323.01	4254.87	0.90	7.48	4.95	5.43	1.04
Cas12M2	12620.07	1612.41	3924.30	467.78	566.30	126.19	10.53	4.85	516.89	5525.90	1.75	13.49	5.01	4.39	2.42
Cas12M3	13188.30	1647.08	4423.47	399.61	645.88	90.11	5.96	7.17	500.99	3987.63	1.39	15.37	4.75	12.39	2.67
Cas12M4	17714.55	1785.89	4465.31	215.03	1174.16	120.37	3.42	6.91	219.99	4672.47	4.96	38.24	4.76	5.03	2.86
FSSA001- M1	15438.29	1657.19	4119.00	258.92	1113.00	102.86	3.57	7.41	348.31	4001.56	4.86	37.89	4.93	14.08	2.45
FSSA001- M2	13556.99	355.39	823.59	169.66	967.30	33.68	1.40	3.79	410.69	4864.01	3.40	33.57	4.14	2.16	0.42
FSSA001- M3	12983.30	1004.62	2346.31	172.54	993.69	51.93	2.78	5.07	649.84	5898.35	5.87	44.39	5.11	2.23	1.25
FSSA001- M4	14889.99	1610.47	3566.39	240.26	881.84	93.17	2.96	5.47	370.54	5772.85	4.77	35.45	4.64	10.14	2.15
FS-SA58 M1	17846.81	3030.08	6768.05	2710.11	1009.29	150.50	6.20	15.13	493.20	5927.11	1.27	6.58	4.46	8.28	3.55
FS-SA58 M2	15170.28	369.82	1008.55	141.69	1296.41	23.28	2.88	9.26	490.78	8409.54	1.01	8.26	4.74	7.26	0.61
MI 6 - M1	20636.37	1817.00	3507.22	101.31	2062.36	111.05	1.29	6.35	369.50	4934.80	0.49	7.20	4.39	1.38	1.24
MI 6- M2	20611.76	2415.49	4685.52	108.18	2022.27	132.29	2.11	5.66	366.27	5214.71	0.90	4.77	4.35	1.22	1.64
MX-2	16197.06	2010.38	3903.85	164.89	1024.76	120.65	1.99	5.01	530.87	6012.55	0.54	4.26	4.13	1.96	2.02
MXXI - M1	18511.74	1126.90	2622.93	169.40	268.00	55.01	1.84	3.08	1744.61	15529.31	0.23	1.96	3.68	1.77	1.31
MV3 - M1	21320.54	1161.82	3434.18	108.97	1710.51	88.09	1.86	7.07	255.89	2986.60	0.21	3.25	4.77	1.54	1.22
MV3 - M2	22473.68	2612.88	7591.33	154.48	1418.86	187.09	3.36	9.52	202.77	3428.29	0.80	6.02	4.85	1.59	3.67
MXXXII - M1	22460.78	1385.71	2658.62	148.07	1648.77	57.92	1.76	4.92	504.26	4108.81	0.32	2.22	3.91	1.22	1.41
r2 (Si-element)	**0.19**	**0.89**	**1.00**	**0.18**	**0.04**	**0.90**	**0.11**	**0.37**	**0.06**	**0.07**	**0.01**	**0.03**	**0.02**	**0.01**	**0.85**
r2 (Al-element)	**0.20**	**1.00**	**0.89**	**0.23**	**0.08**	**0.86**	**0.07**	**0.30**	**0.04**	**0.05**	**0.02**	**0.05**	**0.00**	**0.00**	**0.70**
ALLOCHTHONOUS MICRITE															
Cas 12- A1	95113.98	1800.27	4178.92	1499.32	591.97	124.50	8.83	15.05	984.27	9448.26	3.71	19.30	1.64	26.19	3.94
Cas 12- A2	73473.05	1947.10	4913.84	1538.20	854.38	117.84	7.24	11.93	1001.44	7903.67	2.70	15.01	1.98	23.49	4.09
FSSA58 -A1	49234.56	2828.16	6878.54	789.48	962.16	182.63	7.85	11.35	1301.45	11637.93	1.68	15.75	2.39	12.74	4.92
MXXXII - A1	71295.90	1916.01	3619.20	1085.41	575.29		6.59	7.54	1248.80	15784.51	3.24	12.79	0.49	1.49	1.52
OTHER FACIES TYPES															
Cas 12- S1 (Chaetetid sponge)	592.44	6.06	474.83	35.69	288.84	4.31	1.17	8.68	34.58	78.52	0.49	3.01	1.59	4.31	0.24
FSSA58 - K1 (Margarosmilia)	269.05	19.13	233.16	24.76	358.07	1.92	0.77	5.83	96.78	246.32	0.35	2.17	1.12	5.13	0.16
Cas 12 -Z1 (sparry cement)	4817.96	6.62	446.64	180.59	464.16	44.54	1.01	5.91	915.28	7011.54	0.99	7.35	1.98	4.99	1.16
MXXI -Z1 (sparry cement)	2068.66	3.15	168.22	54.44	227.72	38.43	0.87	3.76	1077.22	6061.33	0.03	1.36	1.96	6.33	1.24
MXXXII - 1 (Brachiopod)	1598.85	10.50	145.36	116.78	502.36	35.09	0.06	3.11	10.69	250.59	0.11	1.83	1.80	2.05	0.46
M XXXII - 2 (Brachiopod)	1170.59	0.00	72.11	5.06	452.47	12.64	0.02	3.32	11.27	68.26	0.05	1.01	0.20	0.00	0.01
M XXXII - 3 (Coral)	403.49	10.23	79.51	8.92	834.85	13.07	0.59	1.72	45.11	356.44	0.04	1.05	0.40	0.00	0.04
MXXXII - S1 (Celyphia)	568.14	37.51	173.63	78.63	323.31	41.56	0.75	2.93	841.90	6348.51	0.18	1.01	1.68	0.95	0.12
MXXXII - Z1 (sparry cement)	2640.74	32.09	157.06	45.37	104.27	30.12	0.73	2.40	1046.65	5456.01	0.09	0.99	2.99	3.04	1.17

Appendix AVIII (continued)

LA-ICP-MS results for selected microbialites and associated facies. Concentrations are expressed in ppm.

MICROBIALITES	Sr88	Y89	Zr90	Nb93	Mo95	Sn120	Sb121	La139	Ce140	Hf178	Ta181	Th232	U238	Th/U
Cas12M1	603.18	19.45	2.47	0.20	1.04	0.67	6.85	15.43	22.18	0.03		0.13	8.84	0.02
Cas12M2	725.87	4.01	3.91	0.37	1.17	0.47	0.48	3.50	5.26	0.26		0.26	35.92	0.01
Cas12M3	1087.91	5.15	3.08	0.32	1.05	2.12	0.44	4.44	7.10	0.08		0.36	24.04	0.02
Cas12M4	1224.44	5.59	3.38	0.45	1.18	0.57	0.41	5.30	8.27	0.41		0.28	1.31	0.21
FSSA001- M1	966.16	4.09	3.06	0.39	1.29	0.39	0.32	3.52	5.23	0.07	0.00	0.19	1.75	0.11
FSSA001- M2	850.21	7.01	1.06	0.09	1.21	0.34	0.16	3.45	4.83	0.11	0.00	0.12	0.58	0.21
FSSA001- M3	875.25	4.11	1.57	0.16	1.50	0.31	0.19	3.89	6.07	0.14	0.00	0.12	1.47	0.08
FSSA001- M4	809.88	3.62	2.40	0.26	1.42	0.38	0.32	3.15	4.79	0.21	0.00	0.20	1.08	0.18
FS-SA58 M1	1113.56	2.02	4.59	0.41	1.27	0.58	0.66	1.30	2.03	0.60		0.31	2.51	0.12
FS-SA58 M2	1649.41	3.18	0.87	0.20	1.20	0.60	3.19	3.13	3.94	0.40		0.16	4.96	0.03
MI 6 - M1	960.67		2.30	0.66	1.06	0.16	0.14			0.47		0.19	1.43	0.13
MI 6- M2	983.61		3.18	0.71	1.18	0.20	0.24			0.51		0.28	5.10	0.06
MX-2	802.66		3.09	0.58	1.49	0.32	0.52			0.46		0.23	4.08	0.06
MXXI - M1	583.56		3.01	0.19	1.09	0.17	0.10			0.16		0.11	1.22	0.09
MV3 - M1	811.02		1.38	0.25	0.96	0.13	0.05			0.20		0.21	0.92	0.22
MV3 - M2	649.71		7.03	0.89	1.02	0.26	0.12			0.71		0.62	3.50	0.18
MXXXII - M1	1293.40		2.14	0.21	1.35	0.17	0.06			0.19		0.19	1.60	0.12
r2 (Si-element)	**0.02**	**0.19**	**0.78**	**0.58**	**0.02**	**0.01**	**0.16**	**0.15**	**0.12**	**0.45**	**0.00**	**0.73**	**0.01**	
r2 (Al-element)	**0.01**	**0.17**	**0.63**	**0.61**	**0.00**	**0.00**	**0.16**	**0.13**	**0.11**	**0.50**	**0.00**	**0.50**	**0.00**	
ALLOCHTHONOUS MICRITE														
Cas 12- A1	984.19	30.49	4.51	0.37	0.36	1.68	1.58	27.38	41.73	0.11		0.56	1.73	0.32
Cas 12- A2	1124.66	30.92	7.53	0.43	0.23	0.98	0.87	28.83	48.85	0.13		0.67	2.00	0.34
FSSA58 -A1	911.62	6.21	5.37	0.53	0.32	0.71	0.75	4.70	6.93	0.51		0.48	1.83	0.26
MXXXII - A1	946.48		8.29	0.61	0.05	0.92	1.02			0.14		0.51	1.27	0.40
OTHER FACIES TYPES														
Cas 12- S1 (Chaetetid sponge)	8736.41	0.48	0.07	0.22	0.98	0.71	0.84	1.02	1.16	0.02		0.21	5.79	0.04
FSSA58 - K1 (Margarosmilia)	8491.12	0.14	0.44	0.16	0.81	0.47	0.34	0.14	0.15	0.52		0.21	3.20	0.07
Cas 12 -Z1 (sparry cement)	164.66	2.96	0.23	0.73	5.02	0.71	0.77	2.42	2.10	2.95		2.53	0.28	9.04
MXXI -Z1 (sparry cement)	239.49		0.81	0.92	1.04	0.65	0.57			2.12		1.27	0.92	1.38
MXXXII - 1 (Brachiopod)	574.20		0.35	0.23	0.23	0.90	0.95			0.00		0.00	0.04	0.04
M XXXII - 2 (Brachiopod)	436.92		0.00	0.01	0.01	0.93	0.92			0.00		0.00	0.00	0.16
M XXXII - 3 (Coral)	5851.87		0.02	0.21	0.02	0.13	0.02			0.46		0.17	1.72	0.10
MXXXII - S1 (Celyphia)	4063.48		0.79	0.23	0.41	0.61	0.70			0.01		0.15	1.69	0.09
MXXXII - Z1 (sparry cement)	384.61		0.32	0.88	0.93	0.32	0.09			1.64		1.01	0.13	7.94

Appendix AIX

Electron microprobe results for selected microbialites and associated facies. Concentrations are expressed in ppm, except where specified (% Wt.)

Sample		SrO [Wt %]	MgO [Wt %]	CaO [Wt %]	MnO [Wt %]	FeO [Wt %]	SiO$_2$ [Wt %]	SO$_3$ [Wt %]	Al$_2$O$_3$ [Wt %]	Sr	Mg	Ca	Mn	Fe	Si	S	Al	Wt-total
Cas12	*Margarosmilia* septum	0.81	0.05	52.98	0.00	0.02	0.01	0.37	0.01	6926	318	376140	0	139	48	1471	78	100
	Margarosmilia epitheca	0.86	0.06	54.77	0.01	0.01	0.03	0.34	0.01	7319	371	388895	71	112	158	1340	40	100
	Margarosmilia septum	0.86	0.03	54.89	0.00	0.00	0.01	0.33	0.01	7296	178	389735	0	0	64	1310	33	100
	Chaetetid sphaerulite center	0.10	1.37	55.13	0.09	0.50	0.02	0.11	0.01	864	8231	391429	664	3922	71	428	49	100
	Chaetetid sphaerulite mid-section	0.86	0.00	55.95	0.00	0.00	0.01	0.26	0.00	7293	10	397278	0	30	66	1045	0	100
	Chaetetid sphaerulite periphery	1.01	0.00	55.24	0.00	0.03	0.00	0.28	0.00	8605	0	392188	0	228	0	1108	5	100
	thrombolite	0.10	3.66	52.37	0.04	0.24	0.03	0.32	0.02	836	21986	371801	291	1836	142	1293	89	100
	thrombolite	0.15	4.07	49.99	0.08	0.64	1.12	0.55	0.48	1295	24440	354947	648	4993	5259	2214	2520	100
	thrombolite	0.12	3.94	50.60	0.04	0.52	0.44	0.42	0.18	983	23662	359254	296	4044	2060	1698	958	100
	thrombolite	0.34	2.33	52.73	0.15	0.47	0.47	0.15	0.18	2853	13987	374383	1147	3676	2209	614	976	100
	thrombolite	0.12	4.32	51.25	0.00	0.16	0.15	0.53	0.06	1057	25946	363864	7	1284	696	2107	317	100
	thrombolite	0.12	3.98	51.52	0.06	0.25	0.33	0.53	0.11	1039	23905	365784	449	1945	1539	2132	564	100
	sparry cement	0.04	1.02	55.46	0.05	0.32	0.02	0.14	0.00	335	6110	393746	420	2504	72	545	0	100
	thrombolite	0.10	2.19	53.10	0.00	0.13	0.31	0.33	0.11	834	13142	377024	7	984	1456	1309	574	100
	Chaetetid sphaerulite center	0.99	0.02	55.61	0.00	0.00	0.00	0.24	0.00	8452	103	394840	0	0	0	942	0	100
	Chaetetid sphaerulite mid-section	0.95	0.02	55.59	0.00	0.00	0.00	0.28	0.00	8094	148	394656	19	0	0	1126	14	100
	Chaetetid sphaerulite periphery	0.95	0.04	55.09	0.01	0.01	0.00	0.25	0.02	8109	220	391140	104	102	0	990	89	100
	Chaetetid sphaerulite center	0.90	0.02	55.84	0.00	0.00	0.00	0.23	0.00	7676	94	396433	10	0	0	917	0	100
	Chaetetid sphaerulite periphery	0.91	0.01	55.79	0.00	0.00	0.00	0.23	0.00	7765	86	396113	0	0	0	931	16	100
	sparry cement	0.04	1.05	54.93	0.09	0.48	0.04	0.15	0.00	341	6303	390017	703	3717	175	602	25	100
	sparry cement	0.04	0.99	54.82	0.08	0.46	0.01	0.15	0.00	314	5922	389220	631	3607	30	591	0	100
	cement	0.08	3.51	51.46	0.03	0.33	0.23	0.30	0.09	694	21072	365361	230	2577	1103	1219	494	100

Appendix AIX (continued)

Electron microprobe results for selected microbialites and associated facies. Concentrations are expressed in ppm, except where specified (% Wt.)

Sample		SrO [Wt %]	MgO [Wt %]	CaO [Wt %]	MnO [Wt %]	FeO [Wt %]	SiO$_2$ [Wt %]	SO$_3$ [Wt %]	Al$_2$O$_3$ [Wt %]	Sr	Mg	Ca	Mn	Fe	Si	S	Al	Wt-total
	allomicrite	0.13	3.65	49.66	0.03	1.07	0.73	0.47	0.29	1138	21916	352571	196	8327	3420	1886	1559	100
	allomicrite	0.11	3.90	50.15	0.03	0.76	0.82	0.41	0.33	940	23390	356084	264	5941	3848	1636	1726	100
	allomicrite	0.12	3.59	49.77	0.03	0.67	0.78	0.43	0.33	1009	21546	353376	206	5264	3666	1704	1757	100
	primary cement	0.26	2.32	52.20	0.04	0.59	0.45	0.38	0.20	2248	13924	370638	276	4595	2123	1500	1035	100
	thrombolite	0.08	4.20	50.98	0.06	0.66	0.63	0.29	0.24	652	25193	361956	489	5169	2974	1154	1287	100
	thrombolite	0.14	3.67	52.86	0.03	0.11	0.14	0.39	0.09	1166	22011	375340	206	888	664	1550	472	100
	thrombolite	0.65	0.64	54.05	0.05	0.21	0.00	0.12	0.00	5503	3812	380834	366	1655	0	485	0	100
	thrombolite	0.14	3.59	49.80	0.01	0.68	1.56	0.63	0.62	1208	21518	353598	109	5335	7337	2531	3303	100
	thrombolite	0.08	3.09	51.07	0.05	0.75	0.70	0.34	0.30	682	18538	362630	417	5887	3294	1358	1597	100
	thrombolite	0.10	3.82	52.38	0.04	0.11	0.02	0.27	0.03	836	22901	371865	330	885	112	1096	169	100
FSSA 001	thrombolite	0.12	3.66	49.59	0.04	0.61	0.98	0.71	0.39	978	21980	352076	273	4739	4604	2827	2086	100
	sparry cement	0.04	5.38	48.29	0.10	1.27	0.54	0.11	0.21	377	32300	342875	733	9932	2537	432	1111	100
	allomicrite	0.13	3.33	49.54	0.05	0.68	1.30	0.43	0.51	1092	19979	351712	405	5311	6106	1718	2682	100
	thrombolite	0.11	4.01	52.71	0.02	0.17	0.03	0.39	0.01	900	24074	374267	175	1310	144	1547	46	100
	thrombolite	0.14	2.92	45.64	0.04	0.44	7.55	0.34	2.37	1190	17511	324021	329	3395	35473	1349	12584	100
	thrombolite	0.10	3.81	51.03	0.11	0.60	0.34	0.35	0.14	837	22867	362329	837	4673	1606	1396	753	100
	thrombolite	0.14	3.60	52.17	0.00	0.20	0.09	0.39	0.02	1193	21578	370439	34	1583	423	1564	123	100
	thrombolite	0.12	3.91	48.90	0.01	1.29	0.53	0.38	0.19	1012	23438	347191	95	10056	2481	1527	1012	100
	thrombolite	0.09	3.45	50.40	0.03	0.50	0.54	0.42	0.24	772	20673	357841	263	3891	2544	1684	1252	100
	thrombolite	0.09	3.35	51.37	0.01	0.26	0.09	0.41	0.04	742	20095	364717	82	2051	426	1622	234	100
	thrombolite	0.10	2.91	50.49	0.02	1.53	0.18	0.40	0.07	870	17477	358463	189	11904	825	1617	374	100
	thrombolite	0.10	3.40	52.26	0.01	0.21	0.04	0.37	0.00	817	20427	371072	99	1632	171	1485	19	100
	sphaerulite	0.92	0.02	55.85	0.03	0.02	0.00	0.24	0.00	7834	127	396562	229	152	0	945	0	100
Cas 26	sphaerulite mid-	0.91	0.01	55.98	0.00	0.00	0.00	0.26	0.01	7715	76	397444	0	0	0	1028	28	100
	sphaerulite	0.97	0.08	56.05	0.02	0.04	0.00	0.24	0.00	8208	473	397971	166	322	0	970	19	100
	septum	0.11	1.88	54.45	0.08	0.03	0.12	0.03	0.03	895	11283	386591	615	218	577	122	139	100
	sphaerulite	0.89	0.03	55.52	0.01	0.01	0.01	0.27	0.00	7527	183	394202	68	85	29	1100	0	100
	sphaerulite	0.90	0.00	55.18	0.01	0.02	0.00	0.30	0.00	7681	14	391776	59	176	0	1215	0	100

Appendix AX

LA-ICP-MS results for microbialitic sample FSSA 001-M2. Concentrations in the first and second rows are expressed in ppm

	La139	Ce140	Pr141	Nd143	Sm147	Eu151	Gd157	Tb159	Dy163	Y89	Ho165	Er166	Tm169	Yb172	Lu175
FSSA 001 M2	11.57	12.05	0.68	3.93	0.76	0.23	1.60	0.24	0.73	0.32	0.32	0.75	0.18	1.22	0.19
PAAS	38.20	79.60	8.83	33.90	5.55	1.08	4.66	0.77	4.68	27.00	0.99	2.85	0.41	2.82	0.43
FSSA 001 M2/PAAS	0.30	0.15	0.08	0.12	0.14	0.21	0.34	0.31	0.16	0.01	0.32	0.26	0.45	0.43	0.44

Appendix AXI

Results from C and O isotope analyses. Samples whose obtained temperature data were not used for paleoenvironmental interpretation are shown with dark grey background filling.

SAMPLE	$\delta^{13}C$ (PDB) [‰]	$\delta^{18}O$ (V_{SMOW}) [‰]	$\delta18O$ (PDB) [‰]	T[°C]
FSSA XI-ht 1	4.43	27.06	-3.69	35.43
FSSA XI-ht 3	4.73	27.88	-2.90	31.29
FSSA XI-ht 4	4.65	27.98	-2.79	30.76
FSSA XI-ht 5	4.61	27.86	-2.92	31.40
FSSA XI-ht 6	4.56	27.76	-3.01	31.87
FSSA XI-ht 7	4.23	27.60	-3.16	32.67
FSSA XI-ht 8	4.76	27.88	-2.89	31.27
FSSA XI-ht 9	4.65	27.33	-3.43	34.04
FSSA XI-ht 10	4.35	26.86	-3.88	36.46
FSSA XI-ht 11	3.99	26.31	-4.42	39.35
FSSA XI-ht 12	4.19	26.74	-4.00	37.07
FSSA XI-ht 13	4.22	25.81	-4.90	41.99
FSSA XI-ht 14	2.70	26.08	-4.64	40.52
FSSA XI-ht 15	2.61	25.85	-4.86	41.78
FSSA XXX 4b 1	3.19	27.204	-3.55	34.70
FSSA XXX 4b 2	4.661	27.799	-2.97	31.69
FSSA XXX 4b 3	4.133	26.549	-4.19	38.08
FSSA XXX 4b 4	4.606	27.786	-2.99	31.75
FSSA XXX 4b 5	4.857	27.709	-3.06	32.14
FSSA XXX 4b 6	4.581	27.932	-2.84	31.02
FSSA XXX 4b 7	4.517	27.562	-3.20	32.88
FSSA XXX 4b 8	4.483	27.674	-3.09	32.32
FSSA XXX 4b 9	4.536	27.901	-2.87	31.18
FSSA XXX 4b 10	4.815	27.667	-3.10	32.35
FSSA XXX 4b 11	4.751	28.061	-2.72	30.38
FSSA XXX 4b 12	4.814	27.739	-3.03	31.99
FSSA XXX 4b 13	3.668	27.702	-3.07	32.17
FSSA XXX 4b 14	3.55	27.818	-2.95	31.59
FSSA XXX 4b 15	4.667	27.677	-3.09	32.30
FSSA XXX 4b 16	4.69	27.412	-3.35	33.64
FSSA XXX 4b 17	4.594	27.64	-3.13	32.49
FSSA XXX 4b 18	4.433	27.489	-3.27	33.25
FSSA XXX 4b 19	4.607	27.742	-3.03	31.97
FSSA XXX 4b 20	4.45	27.23	-3.53	34.56
FSSA XXX 4b 21	3.165	26.114	-4.61	40.37
FSSA XXX 4b 22	3.704	28.08	-2.70	30.29
FSSA XXX 4b 23	2.942	27.938	-2.84	30.99
FSSA XXX 1b 1	3.591	26.874	-3.87	36.39
FSSA XXX 1b 2	4.031	26.845	-3.9	36.54
FSSA XXX 1b 3	4.055	27.141	-3.61	35.02
FSSA XXX 1b 4	1.751	27.85	-2.92	31.43
FSSA XXX 1b 5	2.263	28.222	-2.56	29.59
FSSA XXX 1b 6	2.862	27.948	-2.83	30.94
FSSA XXX 1b 7	4.15	26.964	-3.78	35.93
FSSA XXX 1b 8	3.876	27.656	-3.11	32.41
FSSA XXX 1b 9	3.163	26.192	-4.53	39.95
FSSA XXX 1b 10	-2.179	20.245	-10.3	75.02
FSSA XXX 1b 11	3.607	27.167	-3.59	34.88
FSSA XXX 1b 12	3.713	27.188	-3.57	34.78
FSSA XXX 1b 13	4.016	27.108	-3.64	35.19
MX strom 6	2.56	28.574	-2.22	28.22
MX strom 7	2.654	28.704	-2.10	27.58
MX strom 8	2.716	28.688	-2.11	27.66
MX strom 9	2.48	28.765	-2.04	27.29
MX strom 10	2.672	28.705	-2.09	27.58
MX strom 11	2.594	28.745	-2.06	27.38
MX strom 12	2.43	28.818	-1.98	27.03
MX strom 13	2.282	28.661	-2.14	27.79
MX strom 14	1.974	28.812	-1.99	27.06
MX strom 15	1.166	28.831	-1.97	26.97

Publications

The following papers and abstracts are part of this study and are already published or prepared for publishing:

Sánchez Beristain, J. Francisco & Reitner, J. 2008. Association diversity among sponge boundstones from the Lower Carnian Cassian Formation (Dolomites, Northern Italy). *In:* Löffler, S.-B. & Freiwald, A. (eds). Erlanger Geol. Abh. Sonderband 6. 78. Jahrestagung der Paläontologischen Gesellschaft. 8.10. September 2008. Erlangen: 54 [Oral presentation].

Sánchez Beristain, J. Francisco & Reitner, J. 2008. Microbialites from the Cassian Formation: An insight. *In:* Reitner, J., Quéric, N.V. & Reich, M. (eds). Geobiology of stromatolites. International Kalkowsky Symposium. Göttingen, October 4-11, 2008. Abstract Volume and Field Guide to Excursions: 116-117. Universitätsdrucke Göttingen. [Oral presentation].

Sánchez Beristain, J. Francisco & Reitner, J. 2009. Neue Funde und Palökologie von inkrustierenden „korallinen" Schwämmen aus der Cipit Kalken der Cassian Formation (Unterkarn, Obertrias, Dolomiten, Norditalien). *In:* Martin, T. & Kaiser, S.I. (eds). Terra Nostra 2009 (3). 79. Jahrestagung der Paläontologischen Gesellschaft. 5.-7.Oktober 2009. Bonn: 99. [Oral presentation].

Sánchez Beristain, J. Francisco & Reitner, J. 2009. Der erste Hinweis auf die Bryozoe *Reptonoditrypa* aus den Cipit Kalken der Cassian Formation und seine paläoökologische Bedeutung). *In:* Martin, T. & Kaiser, S.I. (eds). Terra Nostra 2009 (3). 79. Jahrestagung der Paläontologischen Gesellschaft. 5.-7.Oktober 2009. Bonn: 99. [Poster presentation].

Sánchez Beristain, J. Francisco, Germer, J., Thiel, V. & Reitner, J. 2010. Neue Ergebnisse zur Geo- und Biogeochemie ausgewählter Karbonatfazies aus der Cassian Formation. *In:* Reichenbacher, B. & Dotzler, N. (eds). Zitteliana B29: Paläontologie im Blickpunkt. 80. Jahrestagung der Paläontologischen Gesellschaft. 5.-8.Oktober 2010. München: 89 [Oral presentation].

Sánchez Beristain, J. Francisco 2010. Palökologische Analyse ausgewählter Schwamm-Mikroinkrustierer-Gemeinschaften aus den Cipit-Kalken der Cassian Formation (Unterkarn, Obertrias) anhand statistischer Methoden. *In:* Reichenbacher, B. & Dotzler, N. (eds). Zitteliana B29: Paläontologie im Blickpunkt. 80. Jahrestagung der Paläontologischen Gesellschaft. 5.-8.Oktober 2010. München: 89 [Oral presentation].

Sánchez-Beristain, F., Schäfer, N., Simon, K. & Reitner, J. (accepted) New geochemical method to characterise microbialites from the St. Cassian Formaion, Dolomites, Northeastern Italy. Lecture Notes in Earth Sciences 131: 411-427 [Paper].

Sánchez-Beristain, J.F. & Reitner, J. New occurrence of encrusting "coralline" sponges in selected erratic blocks from two localities at the Cassian Formation (Lower Carnian, Upper Triassic, Dolomites, Northern Italy) and their relation to associated microencrusters. Paläont. Z. *in preparation* [Paper].

Acknowledgements

Curriculum vitae

05.07.1979	Geboren in Mexiko Stadt, Mexiko
Staatsangehörigkeit	Mexikanisch
September 1985- Juni 1991	Francés Hidalgo Grundschule in Mexico Stadt, Mexiko
September 1991- Juni1994	Francés Hidalgo Mittelschule in Mexico Stadt, Mexiko
August 1994 – Mai 1997	Francés Hidalgo Oberschule in Mexico Stadt, Mexiko (Schwerpunkt in Chemie und Biologie)
August 1997 – April 1999 und April 2000 – Dezember 2002	Studiengang „Biologie" an der „Freien Nationalen Universität Mexiko" (U.N.A.M)
März 2003	Bachelor of Science (B.Sc.)
August 2003- Juni 2005	Studiengang „Master of Sciences (Systematics)" an der "Freien Nationalen Universität Mexiko" (U.N.A.M.)
Februar 2004 – März 2007	Lehrbeauftragter für Paläobiologie für den Studiengang „Biologie" an der "Freien Nationalen Universität Mexiko" (U.N.A.M.)
August 2005 – Juni 2006	Lehrbeauftragter für Erdwissenschaften im Studiengang „Biologie" an der "Freien Nationalen Universität Mexiko" (U.N.A.M.)
Dezember 2005	Master of Science (M.Sc.) mit Auszeichnung.
Oktober 2007 – Dezember 2010	Stipendiat des Deutschen Akademischen Austauschdienstes (DAAD - A/07/94459) für die Promotion am Geowissenschaftlichen Zentrum der Georg-August-Universität Göttingen.